Università degli Studi di Bergamo

School of Engineering

DEPARTMENT OF ENGINEERING AND APPLIED SCIENCES

DOCTORAL PROGRAMME IN ENGINEERING AND APPLIED SCIENCES

Study of green fluids and lubricants for industry and electrochemical synthesis of hydrocarbons from renewable sources

Doctoral Dissertation of:
Haroon Ahmad

Supervisor:

Prof. Isabella NATALI SORA

XXXVII Cycle – January 2022

To my Mom, whose unwavering sacrifices and prayers have been the foundation of my strength and perseverance throughout this journey. Her constant encouragement and support have constantly fueled my energy and enthusiasm, making me able to complete this journey.

To my brothers and sisters, whose financial, moral, and ethical support has never let me divert my attention to anything else that might lead me astray somewhere far away from where I am standing today. I have always been thankful to them for their supporting behavior throughout my academic carrier even when I was quite young having a limited domain of knowledge. They paved my way to excellence through their prayers, enlightened thoughts, and broader vision that they had gained with time.
To Fathma, Ali, Safwan, Hamdan, Aiza, Uzair, Taimoor and all my nephews (lot of love for your laughters, thank you for always reminding me love and family)

Abstract

This thesis focused on the electrochemical process of synthesizing hydrocarbons and formulation of fully green bio-lubricants in light of the increasing concern for green industrial fluids.

With increasing concern about environmental degradation and resources depletion, the urgency for sustainable industrial processes and materials are very crucial. Traditionally, petroleum-based fuels and lubricants are used across industries and are a major contributor to greenhouse gas emission, pollution and dependence on limited resources. The need to shift to sustainable, renewable resources in the industrial applications is more pressing with rising concern with the environment and availability of resources of the petroleum derived products. Therefore, these challenges need to be overcome through the generation of renewable resources, such as bio-based products and sustainable material.

The United States Department of Agriculture (USDA) BioPerferred and European Union (EU) Ecolabel catalogs lists bio-lubricants as biodegradable and must be derived from renewable sources e.g. renewable hydrocarbon based bio-lubricants [1]. Hydrocarbons and their lubricants derived from renewable feedstocks have the advantages of biodegradability and high flash points, thus reducing the risk of toxicity to the environment and risk of fires in machinery [2]. Long chain hydrocarbons, especially have vital importance for the applications in lubricants, where their molecular structure improves thermal stability and viscosity, necessary for their efficiency and durability [3].

Currently, the production of bio-based hydrocarbons by many known methods has been limited due to high energy demand, high-cost feedstocks, and the complexity of the process. A sustainable alternative is provided by Kolbe electrolysis (KE), a process that is known for hydrocarbons production from fatty acids using electrochemical energy.

Despite extensive study of Kolbe electrolysis (KE) by using single fatty acids, its application to mixed fatty acids, especially those from complex sources such as vegetable oils, remains largely unexplored. The reason for this gap is mainly due to the complex molecular structure of vegetable oils, which consist of various saturated and unsaturated fatty acids, different chain lengths and functional groups, complicating their electrochemical conversion. Kolbe electrolysis with mixed fatty acids is important to explore, since real world applications of Kolbe electrolysis involve complex mixtures rather than pure compounds. The successful

application in such scenarios could make Kolbe electrolysis a more versatile tool in renewable energy and bio-lubricant production.

This research presents a foundational study of the electrochemical conversion of complex mixture of saturated and unsaturated fatty acids obtained directly from coconut oil, via Kolbe electrolysis. The study started from the KE electrolysis of lauric acid ($C_{12}H_{24}O_2$), palmitic acid ($C_{16}H_{32}O_2$) and their mixtures, advancing the process to the production of a wider range of hydrocarbons and other useful products. Both the fatty acids are very common in many vegetable oils. In this section, different reaction parameters, such as electrode material, current intensity, supporting electrolytes, solvent environments and electrolysis time were investigated to establish a basis for future studies with more complex fatty acid mixtures.

To further proceed the research for hydrocarbon synthesis from renewable sources, the alkaline hydrolysis (saponification) of coconut oil was conducted, isolating series of individual fatty acids such as caprylic ($C_8H_{16}O_2$), capric ($C_{10}H_{20}O_2$), lauric ($C_{12}H_{24}O_2$), myristic ($C_{14}H_{28}O_2$), palmitic ($C_{16}H_{32}O_2$) and oleic acids ($C_{18}H_{36}O_2$). These mixtures of saturated and unsaturated fatty acids were then subjected to Kolbe electrolysis to produce a wider range of hydrocarbons and other useful products. The adaptability of Kolbe electrolysis in converting mixture of fatty acids profiles to useful products is emphasized in this phase.

In addition, the thesis describes the synthesis of fatty acid methyl esters (FAME) or biodiesel using transesterification and electrolysis. A dual approach was used to enable a comprehensive comparison of yield and process efficiency. The key factors, including alcohol to oil ratio, reaction temperature, catalyst amount and voltage intensity were optimized to achieve maximum FAME production. The produced FAME and coconut oil was then used as a base oil for formulating bio-lubricants, blended with natural thickener, i.e., beeswax, to meet lubrication standards. Viscosity, thermal stability, lubricity and other critical parameters of the synthesized lubricants were detailed characterized.

The industrial collaborative project was also part of the research to formulate biodegradable bentonite-based greases. In this phase, the first part of this study involved an extensive analytical study of different commercially available greases, after which a series of bentonite and lithium-based greasess were formulated. The physical and chemical properties of the bentonite-based lubricants were compared, and it was shown that the bentonite-based lubricants not only met, but in some cases exceeded, the performance of lithium-based lubricants, making them viable and sustainable alternatives. Finally, these greases were scaled to a 1 kg production level via a colloidal milling process for marketing purposes.

In conclusion, this work is a contribution to the application of Kolbe electrolysis to synthesize hydrocarbons from complex renewable resources. Despite the progress made, future work should concentrate on further improvement of electrode materials designed for the complex fatty acid mixtures, process parameter optimization, and techniques to increase yield and selectivity. This process needs to be further explored to see how scalable it is, especially in integrating mixed and industrial grade feedstocks, in order to make Kolbe electrolysis a realistic, sustainable fuel and lubricant production process.

Acknowledgement

This thesis would not have been possible without the guidance and support of many important people, who have continuously been a source of courage and inspiration to accomplish this work.

First of all, I would like to thank my supervisor, Prof. Isabella NATALI SORA, that with her passion for research inspired me to become a curious (and hopefully better) researcher. Her guidance has not only fostered my curiosity but also shaped me into a more capable and thoughtful researcher. She also helped me out learning the real way how an early career researcher should take a step forward. The way she always ensured I never felt discouraged about my research is truly unforgettable. She provided me with invaluable support during my Ph.D. studies, and I am incredibly grateful to have shared with her an immense amount of time discussing about research work. I am thankful to her for the mistakes she has pointed out, which have been a source of continuous and quick learning for me during these days.

I extend my heartfelt gratitude to Prof. Francesca Fontana, who has been more than a co-supervisor to me, providing unwavering support and guidance. Her generosity in granting me full access to the lab and instruments was instrumental in advancing my research.

I sincerely thank Dr. Renato Pelosato for his invaluable guidance and mentorship throughout this journey. His expertise, constructive feedback, and (off course more importantly) his friendly behavior significantly enhanced my research skills.

I am deeply grateful to Dr. Andrea Cavallaro and Dr. Benedetta Bertolotti, for their invaluable support, attending numerous meetings with me and offering insightful suggestions. Their guidance and constructive feedback have been instrumental in shaping my work. I truly appreciate their dedication and generosity in sharing their expertise.

I would like to express my sincere gratitude to Bellini S.P.A Company, where I had the privilege to spend six months for conducting research. This experience was invaluable in enhancing my skills and knowledge. A special thanks to Simone Pota, who was not only a great friend but also an exceptional teacher, guiding me with patience and expertise throughout my time there.

I am also deeply thankful to my dearest friend M. Uzair, a Ph.D. scholar at the University of Palermo, for his constant motivation and encouragement throughout my journey. His positive words and support have been a great source of strength for me during challenging times. I truly value his friendship and his belief in my abilities.

I would also like to mention all friends I met in Bergamo, that made me always feel at home, especially Asad Ullah khan and Umair Shahb, M. Waleed the time I spent with them, the delicious foods and cherished trips is unforgettable.

Thank you All

Haroon Ahmad

Table of Contents

ABSTRACT ..... **III**

CHAPTER 1 INTRODUCTION **1**

1.1 PROBLEM DEFINITION: 3
1.2 CONTRIBUTIONS: 3

CHAPTER 2 BIBLIOGRAPHIC RESEARCH **5**

2.1 GREEN FLUIDS 5
2.2 BIOFUELS 7
2.2.1 Synthesis of Biofuels 8
2.2.2 Transesterification 8
2.2.3 Electrolysis 10
2.2.4 Sources of Biofuels 11
2.3 BIO-BASED LUBRICANTS 13
2.3.1 Sources of bio-based lubricants 14
2.3.2 Synthesis of bio-lubricants 16
2.3.3 Commercial synthetic bio-lubricants 18
2.3.4 Hydrocarbon based bio-lubricants 18
2.4 KOLBE ELECTROLYSIS 19
2.4.1 Factors effecting Kolbe electrolysis 20
2.4.2 Electrode material 21
2.4.3 Current intensity/Voltage 23
2.4.4 Solvent Environment 25
2.4.5 Electrolysis time 26
2.4.6 Supporting electrolytes 27

CHAPTER 3 MATERIALS AND CHARACTERIZATIONS **30**

3.1 MATERIALS 30
3.1.1 Kolbe electrolysis of a single fatty acid and mixture of two fatty acids 30
3.1.2 Kolbe electrolysis of a complex mixture of derived from from coconut oil 30
3.1.3 Kolbe electrolysis of a complex mixture of derived from from palm oil 31
3.1.4 Formulation of lubricants from coconut oil and fatty acid methyl esters (FAME) 31
3.1.5 Formulation of bentonite and lithium-based lubricants 31
3.2 CHARACTERIZATIONS 31
3.2.1 Gass Chromatography Mass Spectrometry (GC/MS) 31
3.2.2 Scanning Electron Microscopy 31
3.2.3 Consistency measurement (Penetrometer): 32
3.2.4 RSSOT (Rapid Small Scale Oxidation Test) 32
3.2.5 Rheology and viscoelastic properties of lubricants (Rheometer) 32
3.2.6 X-Ray Fluorescence Spectroscopy (XRF) 33
3.2.7 Atomic Emission Spectroscopy (AES): 33
3.2.8 Tribometer test 33

CHAPTER 4 KOLBE ELECTROLYSIS OF SINGLE AND MIXTURE OF FATTY ACIDS **34**

4.1 HIGHLIGHTS OF RESEARCH ACTIVITIES: 34
4.2 INTRODUCTION: 34
4.3 EXPERIMENTAL PART: 36
4.3.1 Experimental setup: 36
4.3.2 Experimental procedure: 37
4.4 RESULTS AND DISCUSSION: 38
4.4.1 X-ray Fluorescence Spectroscopy (XRF) assay of Pt-coated-Cu electrode and non-commercial platinum electrode 38
4.4.3 Scanning Electron Microscopy (SEM) of Pt-coated-Cu electrode and non-commercial platinum electrodes 39

4.4.4 Kolbe electrolysis of lauric acid on platinum-coated copper electrodes 40
4.4.5 X-ray diffraction (XRD) 42
4.4.6 Kolbe electrolysis of lauric acid using Au-coated copper electrode 43
4.4.7 Kolbe electrolysis of lauric acid using non-commercial platinum electrode 46
4.4.8 Kolbe electrolysis of palmitic acid: 49
4.4.9 Kolbe Electrolysis of Mixture of lauric and palmitic acids: 52
4.4.10 Effect of time on the electrolysis of mixture of acids: 55
4.5 CONCLUSION: 59

CHAPTER 5 ELECTROLYSIS OF MIXTURE OF FATTY ACIDS, DERIVED FROM COCONUT AND PALM OIL 60

5.1 HIGHLIGHTS OF RESEARCH ACTIVITIES 60
5.2 INTRODUCTION 60
5.3 EXPERIMENTAL PART 62
5.3.1 Base hydrolysis of coconut and palm oil 62
5.3.2 Kolbe elctrolysis on the mixture of fatty acids derived from oil (Experimental setup) 62
5.3.3 Preparation of electrolyte solution for Kolbe electrolysis 63
5.4 RESULTS AND DISCUSSION 64
5.4.1 Analysis of coconut oil and palm oil by Gass Chromatography/Flame Ionization detector (GC/FID) 64
5.4.2 Fatty acid methyl esters (FAME) profile 64
5.4.3 Sterols profile of coconut and palm oil 68
5.4.4 Glyceride profile of coconut and palm oil 69
5.4.5 Base hydrolysis of coconut oil analyzed by gas chromatography/mass spectrometry (GC/MS) 70
5.4.6 Base hydrolysis of palm oil analyzed by GC/MS 72
5.4.7 Kolbe electrolysis of mixture of fatty acids obtained from coconut oil 73
5.4.8 Kolbe electrolysis of mixture of fatty acids obtained from palm oil 81
5.5 CONCLUSION 86

CHAPTER 6 SYNTHESIS OF FAME FROM COCONUT OIL AND THEIR APPLICATION IN LUBRICANTS FORMULATION 87

6.1 RESEARCH HIGHLIGHTS 87
6.2 INTRODUCTION 87
6.3 METHODOLOGY 89
6.3.1 Preparation of FAME by transesterification method 89
6.3.2 Preparation of FAME using electrolysis method 91
6.3.3 Formulation of lubricants using FAME and Beeswax 92
6.4 RESULTS AND DISCUSSION 93
6.4.1 GC/MS analysis of FAME formed through transesterification 93
6.4.2 Effect of experimental parameters 94
6.4.3 Effect of MeOH/oil ratio 94
6.4.4 Impact of KOH amount on transesterification reaction 95
6.4.5 Impact of temperature on transesterification reaction 96
6.4.6 Synthesis of FAME through electrolysis technique (GC/MS analysis) 97
6.4.7 Effect of experimental parameters 99
6.4.8 Impact of current intensity 99
6.4.9 Effect of MeOH/oil ratio 100
6.4.10 Physiochemical characterization of lubricants 101
6.4.11 Penetrometer test 101
6.4.12 Rheometer tests 103
6.4.13 Viscosity vs temperature 103
6.4.14 Tack test 104
6.4.15 Flow test 105
6.4.16 Shear rate vs shear stress 105
6.4.17 Viscosity vs Shear rate 106
6.4.18 Storage modulus (G')/loss modulus (G") vs shear stress 107
6.5 CONCLUSION 109

CHAPTER 7 FORMULATION OF BENTONITE-BASED GREASES 110

6.1 HIGHLIGHTS OF RESEARCH ACTIVITIES 110

6.2 EXPERIMENTAL PART: 111
6.2.1 Preparation of bentonite-based grease (BBG) 111
6.2.2 Preparation of lithium-based grease (LBG) 112
6.3 RESULTS AND DISCUSSION 113
6.3.1 Analysis and comparison of CG and BBG 113
6.3.2 Rapid Small Scale Oxidation Test (RSSOT) 113
6.3.3 X-ray florescence (XRF) and atomic emission spectrometer (AES) 114
6.3.4 Rheometer tests 117
6.3.5 Viscosity vs temperature test of CG and BBG 117
6.3.6 Tack test 120
6.3.7 Storage modulus (G')/loss modulus (G") vs shear stress 121
6.3.8 Shear stress vs Shear rate 123
6.3.9 Viscosity vs Shear rate 125
6.4 COLLOIDAL MILL FOR THE PRODUCTION OF GREASES 127
6.5 PREPARATION OF LITHIUM-BASED GREASE AND FIXING NLGI 2 129
6.6 CONCLUSION 133
CONCLUSION AND FUTURE PERSPECTIVE 134
REFERENCES 137

List of figures

Figure 2-1: The uses of Green Fluids in different industries 6

Figure 2-2: A step wise process of transesterification for Biofuel production from waste cooking oil 9

Figure 2-3: A general representation of electrolysis process for biofuel production.....10

Figure 2-4: Different renewable sources for biofuel production 12

Figure 2-5: Structure of Triglycerides formed from glycerol and 3 fatty acids.....14

Figure 2-6: General representation of Kolbe electrolysis cell 21

Figure 2-7: a) Pt electrode surface during Kolbe electrolysis of acetic acid (passivation) b) Platinized titania (modified Pt) and nickel as anode in Kolbe electrolysis.....23

Figure 4-1: Electrochemical decarboxylation-dimerization of carboxylic acids, where R = methyl group.....35

Figure 4-2: (a) ElectraSyn 2.0, (b) Pt-coated copper electrode (c) Au-coated copper electrode and (d) Two non-commercial platinum electrodes 37

Figure 4-3: SEM images of Pt-coated Copper electrode surface at magnifications of (a) 50 X (b) 2500 X, (c) 10000 X and non-commercial Pt-electrode at magnifications of (d) 50 X (e) 2500 X, (f) 10000 X.....40

Figure 4-4: Mechanism of Kolbe electrolysis of lauric acid.....41

Figure 4-5: Pt-coated copper electrode: (a) black particles appeared during electrolysis (entry 4), (b) corrosion effects after 24 h of electrolysis (the black particles were removed), (c) fresh Pt-coated copper electrode.....42

Figure 4-6: X-ray diffraction (XRD) patterns of fresh (black) and damaged (red) Pt-coated copper electrode....43

Figure 4-7: Au-coated copper electrodes: (a) XRD of black particles appeared during electrolysis (No. 5), (b) corrosion effects after 23 h of electrolysis 45

Figure 4-8: Performance of electrodes after 6 and 29 hours (entries 1 and 8 in table 3), 17 and 31 hours (entries 5 and 9 in table 3) of usage. The values of Docosane% is on the top of each histogram. 45

Figure 4-9: Kolbe electrolysis of lauric acid investigating the effect of different parameters (a) effect of current intensity (0.7 mmol lauric acid, 0.4 eq. of KOH, MeOH as the solvent, and 6 h for electrolysis), (b) effect of KOH (0.7 mmol acid, 70 mA of current intensity (AP=30 min), MeOH as the solvent, and a 6h electrolysis time), (c) effect of time (0.4 eq. of KOH, MeOH as solvent and current intensity of 70 mA (AP=30 min)), (d) effect of solvent environment (0.7 mmol acid, a constant current intensity of 70 mA (AP=30 min), and an electrolysis duration of 6 h).....47

Figure 4-10: GC/MS result of electrolysis of lauric acid in Hexane:EtOH:Water (38.89:38.89:22.22%) and MeOH:EtOH: Water (16.67:16.67:66.67%) solvent systems.....49

Figure 4-11: Product distribution of electrolysis of palmitic acid using different solvent environments. The experimental conditions for each entry are as follows, Time = 6 hours, current intensity = 70 mA, 1.5 eq. of KOH for EtOH:MeOH:H2O and Hexane:EtOH:H2O while.....50

Figure 4-12: GC/MS spectra pf the product distribution after electrolysis of palmitic acid in EtOH:MeOH:H2O, Hexane:EtOH:H2O and EtOH:H2O solvent systems.....51

Figure 4-13: Representation of the formation of dimers as a result of homocoupling and hetero-coupling of radicals of lauric and palmitic acid mixture.....52

Figure 4-14: Product distribution of electrolysis of mixture of lauric and palmitic acid (1:1) using different solvent environments 53

Figure 4-15: GC/MS spectra pf the product distribution after electrolysis of mixture of lauric acid and palmitic acid in EtOH:MeOH:H2O, Hexane:EtOH:H2O and EtOH:H2O solvent systems.....55

Figure 4-16: Product distribution of the electrolysis of mixture of acids with time of electrolysis, Other HC are hydrocarbons other than dimers.....56

Figure 4-17: GC/MS spectra of the product distribution after different time of electrolysis 58

Figure 5-1: GC/FID spectra of FAME profile of coconut oil at different retention times.....67

Figure 5-2: GC/FID spectra of FAMEs profile of palm oil at different retention times.....68

Figure 5-3: GC/MS spectra of fatty acids derived after based hydrolysis of coconut oil 72

Figure 5-4: GC/MS spectra of fatty acids derived after based hydrolysis of palm oil 73

Figure 5-5: Kolbe electrolysis result of mixture of fatty acids obtained from coconut oil with a total mass of 1 g in different solvents environments; error bars represent the standard deviation of the doublet experiments 76

Figure 5-6: GC/MS spectra of the product distribution after electrolysis of mixture of coconut oil based fatty acids in different solvent systems 77

Figure 5-7: Hydrocarbons spectrum from electrolysis of mixture of fatty acids derived from coconut oil in solvent MeOH:EtOH:H2O (16.67:16.67:66.67%) system; *alkenes and dienes from C18:1, and the error bars represent the standard deviation of the doublet experiments 78

Figure 5-8: Hydrocarbons spectrum from electrolysis of mixture of fatty acids derived from coconut oil in solvent MeOH:EtOH:H2O (33.33 :33.33 :33.33%) system; *alkenes and dienes from C18:1 and the error bars represent the standard deviation of the doublet experiments 79

Figure 5-9: Hydrocarbons spectrum from electrolysis of mixture of fatty acids derived from coconut oil in solvent MeOH:EtOH:H2O (41.66 :41.66 :16.67) system; *alkenes and dienes from C18:1 and the error bars represent the standard deviation of the doublet experiments 79

Figure 5-10: Hydrocarbons spectrum from electrolysis of mixture of fatty acids derived from coconut oil in solvent EtOH:H2O (75:25%) system; *alkenes and dienes from C18:1 and the error bars represent the standard deviation of the doublet experiments 80

Figure 5-11: Hydrocarbons spectrum from electrolysis of mixture of fatty acids derived from coconut oil in solvent MeOH:H2O (75:25%) system; *alkenes and dienes from C18:1 and the error bars represent the standard deviation of the doublet experiments 80

Figure 5-12: Kolbe electrolysis result of mixture of fatty acids obtained from palm oil with a total mass of 1 g in different solvents environments; error bars represent the standard deviation of the doublet experiments 83

Figure 6-1: Representation of fatty acid methyl ester (FAME) and glycerol after transesterification reaction 91

Figure 6-2: GC/MS chromatogram of FAME obtained after transesterification reaction 93

Figure 6-3: Effect of MeOH/oil molar ratio on the FAME yield from coconut oil through transesterification reaction, the other parameters were as follows: KOH = 1% of oil wt., temperature = 50 °C 95

Figure 6-4: Effect of KOH concentration on the FAME yield from coconut oil through transesterification reaction, the other parameters were as follows: MeOH/oil ratio = 6:1, temperature = 50 °C 96

Figure 6-5: Effect of reaction temperature on the FAME yield from coconut oil through transesterification reaction, the other parameters were as follows: MeOH/oil ratio = 6:1, KOH = 1 wt.% of oil 97

Figure 6-6: GC/MS chromatogram of FAME obtained after electrolysis reaction 98

Figure 6-7: Effect of current intensity on the FAME yield from coconut through electrolysis reaction, the other parameters were as follows: MeOH/oil ratio = 6:1, KOH = 1 wt.% of oil 100

Figure 6-8: Effect of MeOH/oil molar ratio on the FAME yield from coconut through electrolysis reaction, the other parameters were as follows: current intensity = 70 mA, KOH = 1 wt.% of oil 101

Figure 6-9: Viscosity vs temperature profile of lubricants, the temperature range was 0-80 °C 104

Figure 6-10: Result of tack test of 6 samples of lubricants 105

Figure 6-11: Shear rate vs shear stress profile of all the lubricant samples 106

Figure 6-12: Viscosity vs shear rate profile of all the lubricant samples 107

Figure 6-13: Storage modulus (G') and loss modulus (G'') versus shear stress profile of all the lubricant samples 108

Figure 7-1: Viscosity vs temperature profile of different commercial greases. The temperature range was from 0-80 °C 118

Figure 7-2: Viscosity vs temperature profile of BBG, Arvina MB2 and Arvina EH2 119

Figure 7-3: Tack test result of different commercial greases 120

Figure 7-4: Result of tack test of four BBG 121

Figure 7-5: Storage modulus (G')/loss modulus (G") vs shear stress of different commercial greases 122
Figure 7-6: Storage modulus (G')/loss modulus (G") vs shear stress of bentonite-based greases 123
Figure 7-7: Flow test (shear stress vs shear rate) test of different commercial grease 124
Figure 7-8: Flow test (shear stress vs shear rate) test of BBG, Arvina MB2 and Arvina EH2 125
Figure 7-9: Flow test (Viscosity vs Shear rate) of different commercial greases 126
Figure 7-10: Flow test (Viscosity vs Shear rate) profile of BBG, Arvina MB2 and Arvina EH2 126
Figure 7-11: Schematic representation of Ball on plate tribometer tests 131
Figure 7-12: Images of scar diameters of (a) Bellini Lithium grease NLGI 2 (200 rpm), (b) Bellini Lithium grease NLGI 2 (500 rpm), (c) Bellini Lithium grease NLGI 2 + 5% (S-EP) additive (200 rpm), (d) Bellini Lithium grease NLGI 2 + 5% (S-EP) additive (500 rpm), (e) Bellini Lithium grease NLGI 0 (200 rpm), (f) Bellini Lithium grease NLGI 0 (500 rpm), (g) Divinol Lithogrease 7000 (200 rpm), and (h) Divinol Lithogrease 7000 (500 rpm).....132

List of tables

Table 2-1: Physiochemical properties of different oils used in bio-lubricants 15

Table 4-1: XRF result of Pt-coated-Cu electrode and non-commercial platinum electrode.....39

Table 4-2: Experimental parameters and results of Kolbe electrolysis of lauric acid using Pt-coated-Cu electrode, 12 ml MeOH was used in all the experiments, *AP = Alternate polarity every 30 minutes, a % mmol respect to the initial amount of starting material, Experiments of entry 4 and entry 10 were carried out under the same conditions, but entry 10 is the experiment of entry 4 after the electrodes had been utilized for 48 hours ...40

Table 4-3: Experimental conditions and results of Kolbe electrolysis experiments for the decarboxylation of lauric acid using Au-coated copper electrodes, AP* = Alternate polarity after each 20 minutes, a % mmol respect to the initial amount of starting material.....44

Table 4-4: Reaction conditions and resulting dimers percentage for investigating the effect of solvent nature on the electrolysis of lauric acid.....48

Table 4-5: Experimental conditions for the electrolysis of palmitic acid 49

Table 4-6: Summery of products observed from the electrolysis of palmitic acid 51

Table 4-7: Reaction conditions for the electrolysis of mixture of acids C12:C16 (1:1), $mmol_{total}$ is the combine molar amount of both acids (0.35 mmol each) 52

Table 4-8: Summery of product observed from the electrolysis of mixture of lauric and palmitic acids 54

Table 4-9: Product distribution of mixture of acids (1:1) and their percentage with respect to electrolysis time .57

Table 5-1: FAME profile with formulas showing saturated and unsaturated nature and their percentages, of coconut analyzed by GC/FID.....65

Table 5-2: FAME profile with formulas showing saturated and unsaturated nature and their percentages, of palm oil analyzed by GC/FID 66

Table 5-3: Sterol profile and their percentages of coconut and palm oil analyzed by GC/FID.....69

Table 5-4: Glycerides profile and their percentages of coconut and palm oil analyzed by GC/FID 70

Table 5-5: Mixture of fatty acids profile and their percentages at different retention times, derived after base hydrolysis of coconut oil, analyzed by GC/MS 71

Table 5-6: Mixture of fatty acids profile and their percentages at different retention times, derived after base hydrolysis of palm oil, analyzed by GC/MS.....72

Table 5-7: Reaction conditions for the electrolysis of mixture of 6 fatty acids derived after base hydrolysis of coconut oil, KOH addition was according to 100 % neutralizations of fatty acids, considering a stoichiometric reaction with all acid molecules in the.....74

Table 5-8: Physical properties of three polar protic solvents used in the Kolbe electrolysis 75

Table 5-9: Types of alcohols and aldehydes formed after the electrolysis of mixture of fatty acids derived from base hydrolysis of coconut oil in different solvent environments.....81

Table 5-10: Reaction conditions for the electrolysis of mixture of fatty acids derived after base hydrolysis of palm oil, KOH addition was according to 100 % neutralizations of fatty acids, considering a stoichiometric reaction with all acid molecules in the mixture 82

Table 5-11: Hydrocarbons spectrum from electrolysis of mixture of fatty acids derived from palm oil in different solvent environments; *alkenes and dienes from C18:1.....84

Table 5-12: Types of alcohols and aldehydes formed after the electrolysis of mixture of fatty acids derived from base hydrolysis of coconut oil in different solvent environments.....85

Table 6-1: Result of FAME profile analyzed by GC/MS, their percentages and retention times after transesterification reaction 94

Table 6-2: Result of FAME profile analyzed by GC/MS, their percentages and retention times after electrolysis reaction.....99

Table 6-3: ASTM standard NLGI classification system based on lubricants consistency 102

Table 6-4: The result of penetrometer test, including penetration values of doublet trails, their average, and NLGI value of each sample (compared with ASTM grade NLGI standards) 102

Table 7-1: Optimized concentrations of components for the formulation of bentonite-based greases with NLGI 2 112

Table 7-2: Oxidation stability of CG greases and BBG.....114

Table 7-3: Atomic emission spectroscopy (AES) results of four commercial greases.....115

Table 7-4: XRF results of four commercial greases 116

Table 7-5: Experimental conditions and parameters of different formulations 129

Table 7-6: Formulation of lithium-based greases using different concentration of components, addition of Sulphurized EP additive and their NLGI and Brugger values 130

Table 7-7: Results of ball on plate tribometer test of different grease samples, using two rotation speeds (200, 500 rpm), values of coefficient of friction and scare diameter after test 132

List of Schemes

Scheme 2-1: Representation of different pathways of Kolbe electrolysis of palmitic acid ($C_{16}H_{32}O_2$) 20

Scheme 6-1: Schematic representation of synthesis of FAME from coconut oil 90

Scheme 6-2: Schematic representation of formulation of lubricants using coconut oil and their FAME as base oil, and beeswax as thickener.....92

Scheme 7-1: Schematic representation of formulation of lubricants using coconut oil and their FAME as base oil, and beeswax as thickener.....111

Scheme 7-2: Schematic representation of formulation of lubricants using coconut oil and their FAME as base oil, and beeswax as thickener.....113

Scheme 7-3: Schematic representation of preparation of bentonite-based greases using colloidal mill 128

Abbreviations

RQ	Research question
RO	Research Objective
FAME	Fatty acid methyl ester
Pt-coated	Platinum coated
Au-coated	Gold coated
BW	Beeswax
WCO	Waste cooking oil
KOH	Potasium hydroxide
MeOH	Methanol
EtOH	Ethanol
GC/MS	Gass chramatography/Mass spectrometry
GC/FID	Gass chramatography/Flame ionization detector
SEM	Scanning electron microscopy
Xrd	X-ray diffraction
XRF	X-ray fluorescence
AES	Atomic emission spectroscopy
NLGI	National lubricating grease Institute
RSSOT	Rapid small scale oxidation test
BBG	Bentonite based lubricants
CG	Commercial lubricants
LBG	lithium based lubricants
°C	Degree centigrade

Chapter 1 Introduction

With the industrial revolution of the 18th century and advancements in machinery, there was a need for improved fuels and lubricants, and thus industries became dependent on oil-based products. Along with many applications, the petroleum-based liquids have been identified as a large source of greenhouse gas emissions and environmental pollution and their use likely contributes to global climate change and risk of ecological destruction [4]. With the geopolitical tensions, environmental concerns and fluctuation of oil prices, conventional fluid has been replaced by industries in the search for secure and sustainable alternatives. The concern for the environment and the exhaustion of fossil resources have revived the interest in bio-based fluids. In recent years, chemical engineering advancements have further facilitated the modification of bio-oils to enhance the performance and applications, especially in lubricants industry to be used in high temperature and high-pressure scenarios [5].

In the late 19th century, the mineral oils obtained from crude oil were used as lubricants because of their better performance under high temperature conditions. At the same time, the synthesis of hydrocarbons also started with the crude oil distillation, from which fuels such as kerosene and gasoline emerged and revolutionized transportation and industrial processes. With the passage of time, catalytic reforming and thermal cracking further enhanced the refining process which also enhance the production of hydrocarbon fuels and petrochemicals. Such developments in the hydrocarbon production increases their applications in the various fields like energy, plastic creation, synthetic fibers and pharmaceuticals [6].

The hydrocarbon-based lubricants then mark a shift towards its use on industrial level because of their superior performance. Hydrocarbons having stable carbon-hydrogen bonds, high energy density and low chemical reactivity allowing them to undergo controlled combustion and synthetic transformations. Hydrocarbons specifically alkanes and iso-alkanes, provide the best viscosity, oxidative stability and thermal resistance for lubricants which are necessary to reduce friction, wear and thermal degradation in high performance applications. Because of better performance and consideration of environmental impacts, it was important to synthesize hydrocarbons from renewable sources rather than petroleum-based sources [7].

For hydrocarbon production, a variety of techniques have been used, although each faces trade-offs in efficiency, cost, and environmental impacts. For example, catalytic cracking breaks larger molecules into small chain hydrocarbons using lower energy but requires relatively

expensive catalysts. Hydrocracking involves adding hydrogen to the process, forming high quality fuels, but the process becomes very costly due to high pressure and high temperature demand [8]. Fischer–Tropsch synthesis converts syngas into liquid hydrocarbons, but the process is complex and capital intensive. Pyrolysis process converts organic waste into hydrocarbons but results in a variety of unwanted byproducts [9]. The Kolbe electrolysis among them is the most versatile bio-based technique, converting fatty acids into hydrocarbons, relies on bio-based feedstocks derived from animal and vegetable oils.

Kolbe electrolysis discovered by Hermann Kolbe in 1849, for the formation of alkanes by the electrochemical decarboxylation of carboxylic acids. Early experiments were limited to low yields and restricting the method to small aliphatic acids. From the middle of the 20th century, the advancements in the process starts with focusing on electrode materials and controlled electrolytes for improving yields and efficiency. By the 1970s, various catalysts and electrolyte compositions were explored by researchers to better control the reaction and to scale up [10]. Interest in Kolbe electrolysis as a bio-based hydrocarbon production route was revived in the early 2000s with the rise of green chemistry principles [11]. Currently, Kolbe electrolysis is regarded as a potential way and the research continues to explore ways to increase efficiency and yield.

Besides all these improvements, still there are several obstacles in making Kolbe electrolysis commercially viable. Anodic passivation, where side products accumulate on the anode causing increased voltage needs and energy consumption [12]. Further, techno economic analysis is also needed to evaluate the potential to produce both Kolbe and non-Kolbe products, such as diesel like compounds. Efficient cell design and spacing of electrodes will be needed to facilitate the continuous process rather than batch processing [13]. Additionally, Kolbe electrolysis is shown to leverage excess renewable energy to maximize environmental and economic benefits. Finally, the application of KE to real feedstocks such as complex vegetable oils and biomass necessitates the choice of suitable solvents to overcome the problems presented by their structural complexity and solubility [14].

This thesis has the objectives to apply KE on the complex saturated and non-saturated fatty acids system from renewable source for the synthesis of long chain hydrocarbons. It also explores the synthesis of fatty acid methyl esters (FAME) from vegetable oils and their suitability as base oil for the synthesis of bio-lubricants. Additionally, the thesis also explores the formulation of economic and fully biodegradable lubricants from renewable raw materials, fulfilling green chemistry principles.

1.1 Problem definition:

The main research questions (RQ) that we tackle in this thesis is formulated as follows:
RQ1: How to apply Kolbe electrolysis on the complex saturated and unsaturated fatty acid mixtures, obtained directly from renewable source to synthesize hydrocarbons.
RQ2: How to use vegetable oil as a renewable source in the formulation of lubricants.
RQ3: How to formulate the biodegradable and fully green bio-lubricants to obtain similar properties like commercially available synthetic lubricants.

Based on these research questions, we identify the following research objectives (RO):
RO1: Kolbe electrolysis of a single fatty acid (lauric acid) and mixture of two fatty acids (lauric acid and palmitic acid)
RO2: Kolbe electrolysis of a complex mixture of saturated and unsaturated fatty acids (caprylic, capric, lauric, myristic, palmitic and oleic acids), obtained directly from coconut oil
RO3: Electrolysis and transesterifications techniques for the synthesis of FAME
RO4: Coconut oil and their FAMEs as a base oils and beeswax as a thickener for the formulation of lubricants
RO5: Formulation of bentonite based fully green bio-lubricants; an alternative to the lithium-based lubricants at industrial level
Each RO is explained shortly in the contributions section below while detailed explanation is given in **chapter 4-7**:

1.2 Contributions:

By fulfilling the research objectives, the thesis presents the following four major contributions:
Outcomes of RO1: In this part, lauric acid, palmitic acid and their mixtures were used as a substrate fatty acid for the Kolbe electrolysis. Both lauric and palmitic acids constitutes a major part of many vegetable oils. Different experimental conditions such as electrolysis time, current intensity, KOH as a supporting electrolyte, solvent environment and nature of electrodes were used to investigate the product yield%. Two types of electrodes were used i.e., commercial (Pt-coated-copper, Au-coated-copper electrodes) and non-commercial Pt electrodes. During initial experiments on lauric acid, the degradation of commercial electrodes was observed and therefore, further all the experiments were conducted using non-commercial Pt-electrodes.

Using non-commercial Pt electrodes, the Kolbe electrolysis of individual lauric acid, individual palmitic acid and mixture of both fatty acids were conducted in order to optimize the best experimental conditions. The detail explanation of RO1 is given in chapter 4.

Outcomes of RO2: Once the best experimental conditions were optimized from RO1, the process was continued to apply the Kolbe electrolysis on the complex mixture of saturated and unsaturated mixture of fatty acids obtained from renewable source. The purpose of this work was to open a pathway to apply directly the Kolbe electrolysis on the renewable source. For this purpose, coconut oil was used as a source to obtain the mixture of fatty acids as it is famous vegetable oil containing broad range of saturated and unsaturated fatty acids. In this part, first the base hydrolysis of oil was conducted to isolate the fatty acids. After isolation of fatty acids, the Kolbe electrolysis with different experimental conditions was conducted on the mixture of fatty acids to optimize best conditions. The experimental conditions obtained from RO1 were applied here to investigate the product distribution and dissociation of all the reactant fatty acids. The detail explanation of RO2 is given in chapter 5.

Outcomes of RO3: In this part bio-lubricants are prepared from using coconut oil and their FAME as a base oil in combination with beeswax (BW) as a thickener. Initially the FAME was prepared through transesterification and electrolysis technique. The effect of oil/methanol ratio, reaction temperature, and current intensity was optimized to investigate higher yield and comparison. The prepared FAME was then used as a based oil with beeswax as a thickener to prepare bio-lubricants. Viscosity, thermal stability, lubricity and other critical parameters of the synthesized lubricants were then detailed characterized. The detail explanation of RO3 is given in chapter 6.

Outcomes of RO4: This part of the research is the industrial collaborative part. In this part the bentonite-based lubricants are prepared as environmentally friendly alternatives to lithium-based lubricants that are commonly used but environmentally taxing. Initially, a series of commercially available lithium-based lubricants were analyzed by different analytical techniques to collect extensive data. In the second step the bentonite-based lubricants and our own lithium-based lubricants were prepared and optimized different parameters. The physical and chemical properties of the bentonite-based lubricants were compared with the commercial lubricants. Finally, these lubricants were scaled to a 1 kg production level via a colloidal milling process for marketing purpose. The detail explanation of RO4 is given in chapter 7.

Chapter 2 Bibliographic Research

2.1 Green Fluids

Green fluids are eco-friendly liquids formulated to minimize environmental impact while offering enhanced performance over traditional petroleum-based fluids. These are fluids derived from biological sources and are recognized for their environmentally friendly properties [15]. Green fluids signify a significant progress in both commercial and sustainable industrial practices. Traditional industrial fluids, particularly those derived from petroleum, have demonstrated considerable environmental risks, including the release of toxins, soil contamination, and water pollution. Consequently, the emergence of eco-friendly fluids began in the late 20th century, emphasizing sustainability and environmental issues [16].

There are numerous uses for green fluids, and they play a significant role in protecting the environment by reducing pollution. Efficiency, safety, environmental preservation, and innovation in the sector are all areas in which they have made significant contributions, making them equally vital. **Figure 2-1** shows many businesses that rely on green fluids due to their distinctive properties and practical uses. Green fluids, such as hydraulic oil and coolants, help to locate leakage. This observable identification allows for faster problem detection, which in turn minimizes damage and downtime. Also, by revealing subcellular or sub tissue structures in response to light, green fluorescent proteins (GFP) and associated markers contribute to the advancement of genetic and cell biology research [17].

Green fluids exhibit a variety of types depending on their specific applications. The literature categorizes them into sustainable coolants, green solvents, industrial process fluids, and bio-based lubricants [18]. The sustainable coolants can be categorized into bio-based antifreeze coolants and natural refrigerants. Bio-based antifreeze coolants are sustainable and eco-friendly solutions derived from renewable sources such as plant glycols [19]. The components can include glycerin, organic additives, propylene glycol, and various natural corrosion inhibitors. The antifreeze solutions present multiple benefits, such as lower toxicity and enhanced biodegradability, rendering them appropriate for a range of applications. Dynalene BioGlycol serves as a non-toxic antifreeze coolant, being derived from corn, in contrast to ethylene glycol, a conventional coolant known for its high toxicity [19].

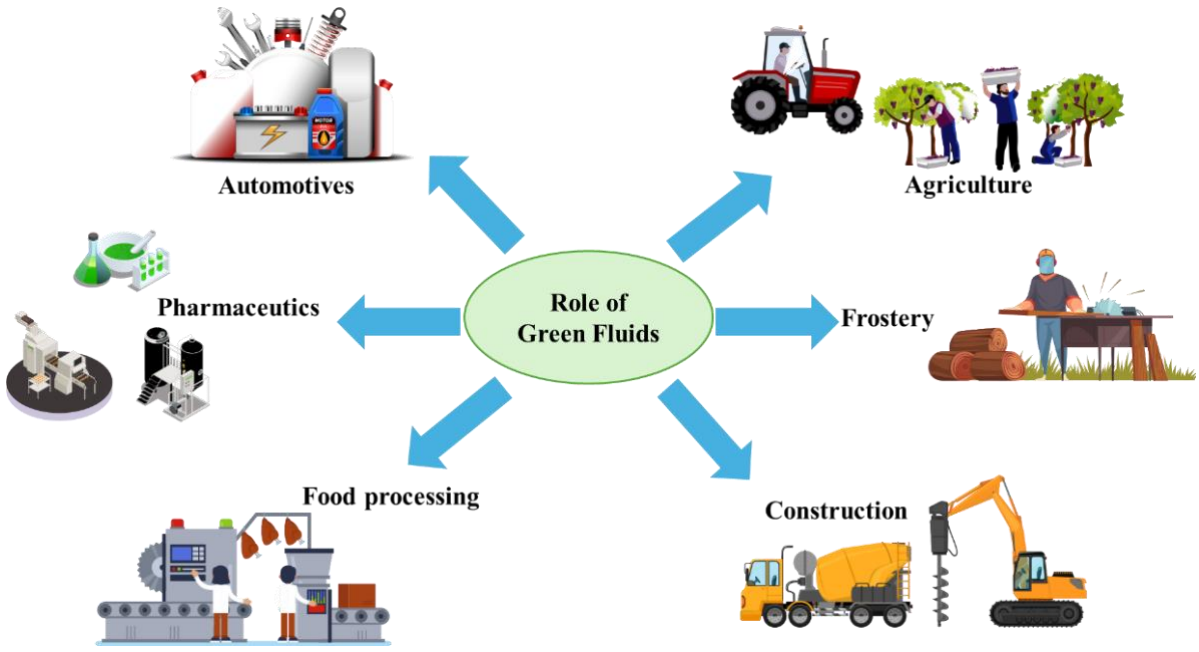


Figure 2-1: The uses of Green Fluids in different industries

These coolants safeguard the cooling systems against corrosion and damage, hence extending their lifespan. These coolants are utilized in HVAC systems, automobile systems, industrial heat exchangers, and process cooling [20]. Natural refrigerants are inherently occurring chemicals utilized in refrigeration applications. They are significant because of their minimal detrimental effects on global warming. The prevalent varieties of these eco-friendly refrigerants are carbon dioxide (R-744), hydrocarbons (Propane R-290, Isobutane R-600a), water-based systems (R-718), and ammonia (R-717) [21].

In contrast to traditional petroleum-based solvents, bio-alcohols such as bioethanol and biobutanol exhibit a reduced environmental impact and are renewable, hence gaining recognition as effective green solvents [22]. Their categories may encompass ethanol, butanol, propanol, and various mixed alcohols. Owing to their superior solubilities, they are utilized in industrial applications like adhesives, coatings, and paints. Bio-alcohols serve as solvents for many therapeutic formulations in the pharmaceutical and cosmetic industries [23].

Industrial process fluids encompass metalworking fluids and hydraulic fluids. The term metalworking fluid refers to the category of liquids and oils utilized for lubricating metallic materials, such as machinery [24]. These oils and lubricants diminish heat and friction between the workpiece and cutting instruments, thereby preventing damage to the machinery. These oils also assist in eliminating swarf, chips, and fines from the tools, hence enhancing the quality

of the machined workpiece. Straight oils, synthetic fluids, semi-synthetic fluids, and soluble oils represent several categories of these lubricants [25].

Hydraulic fluids represent the second category of industrial lubricants. These substances serve multiple purposes, including energy transmission, acting as sealants, lubricants, and coolants, while also facilitating the removal of contaminants. Hydraulics encompasses two main branches: hydrostatics and hydrodynamics. According to this classification, the oils utilized for hydrodynamic applications are referred to as energy gearbox oils [26]. The oils utilized for hydrostatic applications are classified as hydraulic oils. Hydraulic oils exhibit non-compressible characteristics, attributed to their high pressures and low flow rates. Following engine oils, hydraulic oils represent the next most important category of lubricants. Stationary, mobile, and aircraft hydraulics represent the three primary subfields of hydraulics, indicating that each application necessitates a distinct hydraulic medium that meets its operational requirements [27]. Hydraulic oils enhance maintenance schedules and extend the lifespan of machinery by minimizing wear on equipment and components, while also conserving energy when utilized correctly. Examples of hydraulic oils include synthetic esters, triglycerides, polyglycol, and poly-alkylene glycol. The final category of lubricants is bio-based lubricants, which are considered to be the most efficient among all types [28].

2.2 Biofuels

Biofuel refers to liquid fuels and blended components derived from biomass, such as feedstocks. These fuels may encompass methane generated from biogas, hydrogen gas, and landfill gas derived from renewable sources [29]. Biofuels serve as a source for electricity generation and heating applications in the transportation sector. Consequently, they are referred to as transportation fuels [30]. These fuels serve as alternatives to fossil fuels. Biodiesel and bioethanol are the prevalent forms of biofuels. These substances are utilized in engines and are frequently blended with fossil fuels to reduce carbon emissions [31]. Nonetheless, it is commonly utilized as diesel to reduce the concentrations of hydrocarbons, particulate matter, and carbon monoxide in diesel vehicles. Conversely, bioethanol is generated through the fermentation of carbohydrates. Carbohydrates can be derived from starch crops such as sugarcane and maize. Cellulose biomass derived from trees and grass serves as a valuable feedstock for ethanol production [32].

Bioethanol can be utilized in its pure form for vehicles; however, it is predominantly blended with gasoline to improve the vehicle emissions. Biofuels hold significant importance and are categorized as green fluids due to their potential to lower greenhouse gas emissions [33]. Their role in the adsorption of CO_2 is significant, contributing to the maintenance of CO_2 balance in the environment. In contrast to fossil fuels, biofuels generate fewer harmful gas emissions into the atmosphere. These can be conveniently utilized in vessels, aircraft, and both light and heavy-duty trucks. These fuels do not contain sulfur or other harmful aromatic compounds [34].

2.2.1 Synthesis of Biofuels

There are variety of methods explained in literature to produce biofuels like thermal cracking, pyrolysis, microalgae, electrolysis and transesterification. Thermal cracking is a process which involves thermochemical conversion via gasification [35]. Gasification is the incomplete combustion of feedstock and biomass in limited supply of air. Which consequently results in the formation of gaseous biofuel [36]. Pyrolysis involves the decomposition of biomass and feedstock at relatively high temperatures in an inert environment. This method results in the production of biofuel, and solid products. The solid product is known as biochar [37]. Microalgae process can also be used to produce biofuels which can have same properties as vegetable oils. The microalgae can adsorb the excess CO_2 which is produced in the combustion process of biodiesel [38]. Transesterification involves the conversion of lipids into glycerol and biofuel [39]. Fermentation involves the use of metabolic activity of different microorganisms to produce biofuel [40]. Most of the biofuel is produced by using the transesterification process because it is the most economical method which requires low temperatures and pressures and can achieve about 98% conversion [29].

2.2.2 Transesterification

Biofuel production requires the use of oils or fats along with alcohol. In certain instances, catalysts are also present. Esterification and transesterification reactions can be utilized to produce biofuels, contingent upon the quality of oils and feedstock [39], [41]. The process of transesterification involves the use of a catalyst. This approach proves to be effective when the moisture, fatty acids, and phosphorus content of oils is below 0.1%. Potassium hydroxide (KOH), sodium methoxide (CH_3ONa), and sodium hydroxide (NaOH) are the most frequently utilized catalysts in the transesterification process. Sodium methoxide stands out as a more

useful and effective catalyst; however, it comes with a higher cost. Methanol is the prevalent alcohol utilized for the conversion of oils and fats. It is flammable; therefore, it necessitates appropriate safety measures and handling procedures. The transesterification process necessitates an excess of methanol to shift the equilibrium, as it is a reversible reaction [42]. A general procedure as an example of biodiesel production process from waste cooking oil involves five key steps as shown in **Figure 2-2.** First, waste cooking oil (WCO) is filtered to remove impurities, followed by moisture removal to ensure proper processing. Free fatty acids are reduced, and the oil undergoes acid or base-catalyzed transesterification, resulting in the production of biodiesel [43].

Malabadi et al. highlighted that the process of transesterification for biofuel production is essential for producing biodiesel, a renewable energy source that has the potential to reduce reliance on fossil fuels and lessen environmental pollution. This chemical reaction entails the transformation of oils or fats into fatty acid methyl esters (FAME) through their interaction with alcohol, usually methanol or ethanol, facilitated by a catalyst. The effectiveness of this process is affected by the catalyst employed, which may be homogeneous, heterogeneous, or enzymatic in nature. Additionally, the process of producing biodiesel through transesterification entails the reaction of oil and alcohol with a catalyst, leading to the formation of fatty acid methyl esters (FAME). This approach improves yield and efficiency, tackling issues related to fossil fuel depletion and environmental pollution [44].

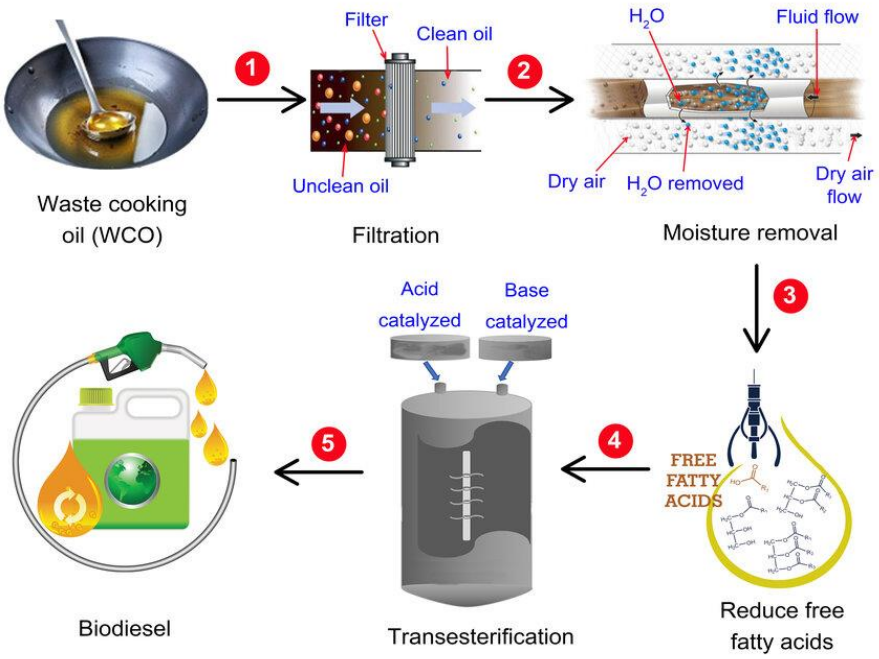


Figure 2-2: A step wise process of transesterification for Biofuel production from waste cooking oil

2.2.3 Electrolysis

The biodiesel production process via electrolysis involves the use of a reactor where vegetable oil and methanol are combined with a suitable catalyst. A DC power supply generates an electric current between electrodes to drive the chemical reactions. The process ensures efficient mixing and reaction completion, leading to the production of biodiesel as shown in **Figure 2-3**.

The production of biofuels via electrolysis represents a cutting-edge method that utilizes electrochemical processes to create biodiesel and various other biofuels from renewable sources. This approach has aroused interest because of its ability to improve yield and efficiency relative to conventional techniques. Recent studies indicate that the application of alkaline hydroxides and methoxides as catalysts can result in significant biodiesel production rates, reaching efficiencies of up to 97.11%. Electrolysis presents a promising approach to produce biofuels, particularly fatty acid methyl esters (FAME), utilizing alkaline hydroxides and methoxides as catalysts.

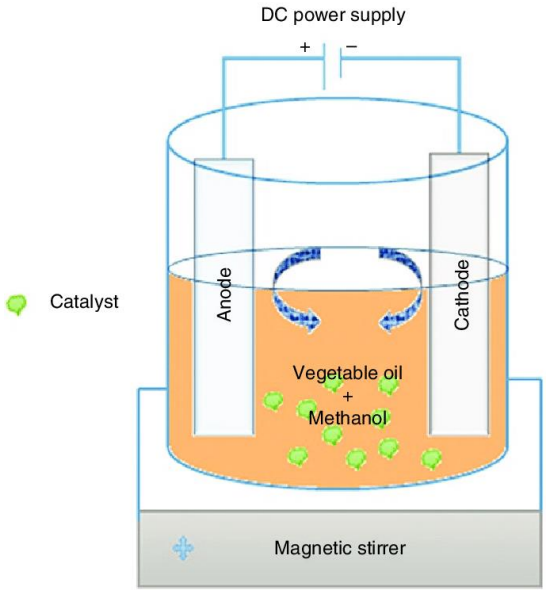


Figure 2-3: A general representation of electrolysis process for biofuel production

This method can attain significant biodiesel yields without the use of electrolytes, presenting a viable alternative to traditional transesterification techniques [46]. The author showcased electrolysis as a viable approach for biodiesel production, employing ionic liquids such as 1-ethyl-3-methylimidazolium chloride to improve electrical conductivity. The investigation resulted in a peak biodiesel yield of 97.76% under optimized conditions, showcasing an effective and environmentally friendly production process [47].

Dhafir et al. detailed that the production of biodiesel through electrolysis encompasses esterification-transesterification processes utilizing alcohol and acid/base catalysts, while the use of platinum electrodes contributes to improved yield. The investigation revealed the highest biodiesel yield at 6 V (88.67%), with diverse physicochemical properties affected by varying voltages throughout the electrolysis process. He also studied investigates biodiesel production from palm oil and waste cooking oil via electrolysis, highlighting that electro-catalysts significantly enhance yields, achieving approximately 87% from waste cooking oil and 90% from palm oil, while meeting ASTM standards for quality [48].

2.2.4 Sources of Biofuels

Biodiesel feedstocks are categorized into three generations based on their origin and sustainability. First-generation sources come from edible materials, which may compete with food resources. Second-generation sources utilize non-edible materials, offering a more sustainable alternative without impacting the food supply. Third-generation sources focus on advanced and eco-friendly options, including waste materials and innovative biological sources, ensuring minimal environmental impact **(Figure 2-4).**

The production of bioethanol entails the fermentation process of sugarcane and sugar beet. The process may additionally encompass the hydrolysis and fermentation of starchy crops. In 2012, the production of bioethanol derived from corn crops reached nearly 60 billion liters in the United States, establishing a significant presence in the global market [49]. The second dominant bioethanol is derived from sugarcane, with production reaching nearly 20 billion liters in Brazil in 2013. Various feedstocks have been evaluated for the production of bioethanol and biodiesel. For instance, sugar beet is utilized in the EU, while maize is employed in China, the US, and Brazil. In a similar vein, cassava has been utilized in Nigeria, Brazil, Indonesia, and Thailand for biofuel production. Oil crops serve as a valuable resource for biofuel production. The production involves the combination of oil extracts derived from seeds and oil-rich nuts via the transesterification process. In the United States, soybean oil is the most prevalent, while in the European Union, rapeseed oil takes precedence. Meanwhile, Malaysia and Indonesia are known for their production of palm and coconut oil [50].

A study indicates that the oil content is 21% in soybean and 35% in rapeseed [51]. The elevated oil content of 40% in palm oil has produced the greatest quantity of biofuel, nearing 5 tons per hectare, in comparison to other oils. For instance, soybean produced 0.52 tons and rapeseed

produced 1 ton per hectare [29]. Common sources of biofuels include sugarcane, animal fats, rice, canola oil, rapeseed oil, sunflower oil, soybean oil, corn oil, and palm oil [52].

Vegetable oils represent a viable feedstock for biofuel production, motivated by the demand for sustainable energy solutions in light of fossil fuel depletion and environmental issues. Their biodegradability, renewability, and advantageous physicochemical properties position them as viable alternatives to conventional fossil fuels. Although edible oils are prevalent in biofuel production, there is a growing interest in non-edible oils because they present reduced competition for food resources and are more cost-effective [53]. Ghosh et al. reported that vegetable oil, especially pumpkin seed oil, serves as a viable alternative to diesel fuel. The trans-esterification process for refining vegetable oil is emphasized, while also considering potential engine-related complications that may arise from its unrestricted use [54].

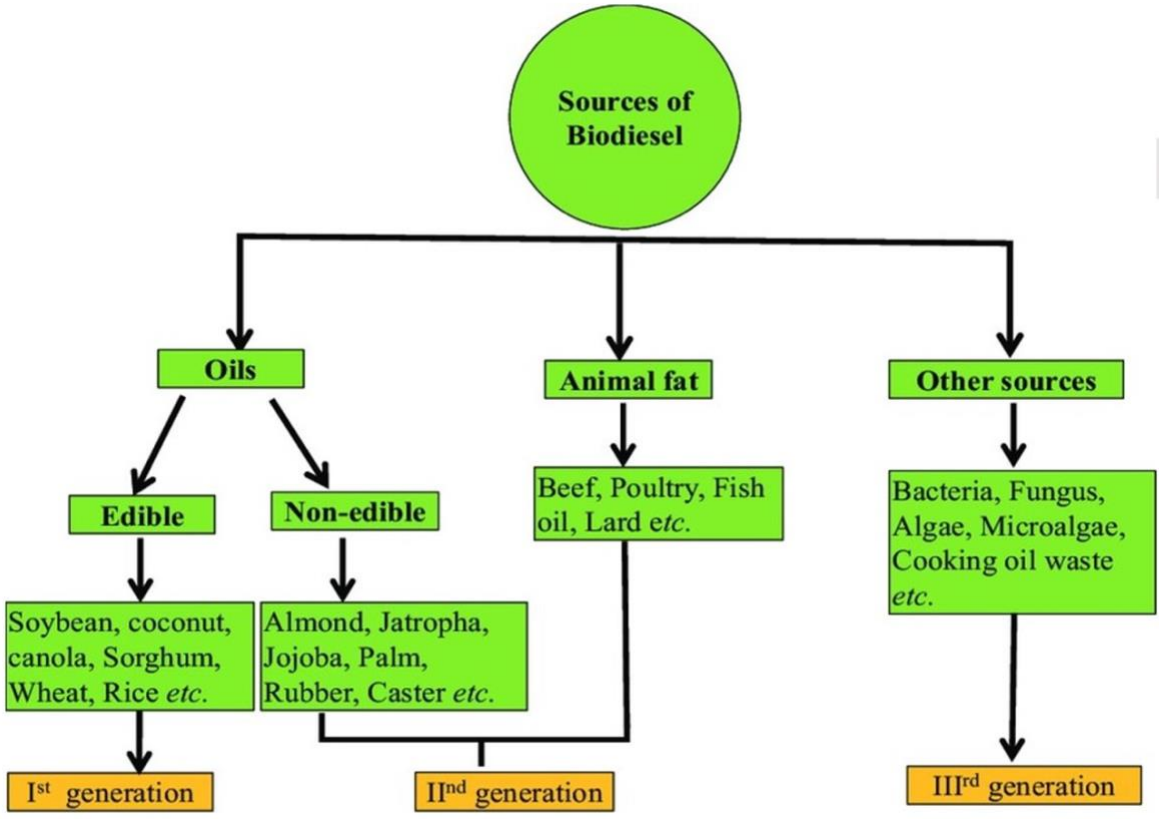


Figure 2-4: Different renewable sources for biofuel production

Singh et al. reported a study on biofuel oil that discusses biodiesel production from vegetable oils derived from biomass vegetative tissues, highlighting their potential as renewable energy sources. This study explores different methods of oil extraction, the characteristics of these oils, and the advantages of utilizing vegetable oils for the production of sustainable biofuels [56]. Boas et al. examined the transesterification of vegetable oils, emphasizing their

application in biodiesel production. The focus is on the difficulties posed by elevated raw material costs and investigates non-edible sources as potential alternatives to lower production expenses without compromising the quality of biodiesel [57].

2.3 Bio-based lubricants

Lubricants derived from bio-based raw materials, such vegetable oils, animal fats, or other environmentally benign, are designated as "bio-based lubricants" or "bio-lubricants". The manufacture of these lubricants yields numerous advantages, including enhanced health and environmental benefits, along with superior performance relative to traditional petroleum-based lubricants. The initial biodegradable lubricants were effectively synthesized in the early 1980s using neopentyl polyol esters as base fluids. This represented a significant alteration in the oil's structure by transforming it into an ester referred to as polyol ester [58], [59].

In contrast to mineral oils, bio-based lubricants demonstrate enhanced lubricity, elevated flash points, a high viscosity index, and robust shear resistance, while also being readily biodegradable and renewable. Nonetheless, not all lubricants derived from biological sources exhibit biodegradability. The degree of biodegradability is entirely contingent upon the materials utilized in synthesis and their specific formulation . The increasing demand for environmentally friendly and sustainable options across various applications is propelling the shift towards bio-based solutions. Bio-based lubricants are utilized in various applications, including machine tools, gear oils, metal forming, and chain lubricants .

Bio-based lubricants furthermore comprise modified natural oils. Vegetable oils that have been altered physically or chemically to enhance their lubricating characteristics are referred to as modified natural oils. These modifications aim to improve specific attributes such as oxidative stability, viscosity, and low-temperature performance, so rendering them more suitable for industrial applications. The prevalent varieties of these oils comprise hydrogenated oils, trans-esterified oils, and epoxide oils [60]. These lubricants provide enhanced stability and oxidation resistance. They demonstrate characteristics such as enhanced lubricity and elevated viscosity. High oleic soybean oil, derived from improved oilseeds, has superior oxidative and viscosity stability. They often biodegrade up to 70% within 28 days, enhancing their applicability for diverse uses, in contrast to petroleum-based oils, which degrade 15-35% over the same period [61]. These oils have numerous applications in pharmaceuticals, agriculture, and food processing owing to their diminished toxicity. Furthermore, they are more economical [62].

2.3.1 Sources of bio-based lubricants

Vegetable oils serve as a valuable resource for the synthesis of bio-lubricants. The global production of vegetable oil has seen a positive rise in recent years, coinciding with advancements in agriculture. Triglyceride molecules constitute the molecular structure of all vegetable oils, which are fundamentally similar [63]. A triglyceride molecule typically comprises two primary components, a glycerol and fatty acids as shown in **Figure 2-5.** The glycerol component consists of three interconnected hydroxyl groups, whereas the fatty acids portion is made up of long-chain saturated fatty acids that are linked to each hydroxyl group. In natural fatty acids, the hydrocarbon chain, with rare exceptions such as isovaleric acid, has an odd number of carbon atoms and thus naturally occurring fatty acids have an even total number of carbon atoms, usually between 12 and 22 [26]. Vegetable oils consist of three distinct types of natural fatty acids: polyunsaturated, monounsaturated, and saturated fatty acids. The primary fatty acids found in the oil composition influence the saturation level of vegetable oils. The presence of unsaturated fatty acids in these oils leads to suboptimal oxidation and thermal characteristics. Consequently, processes such as epoxidation, hydrogenation, and transesterification are implemented to reduce the level of unsaturation [60], [64].

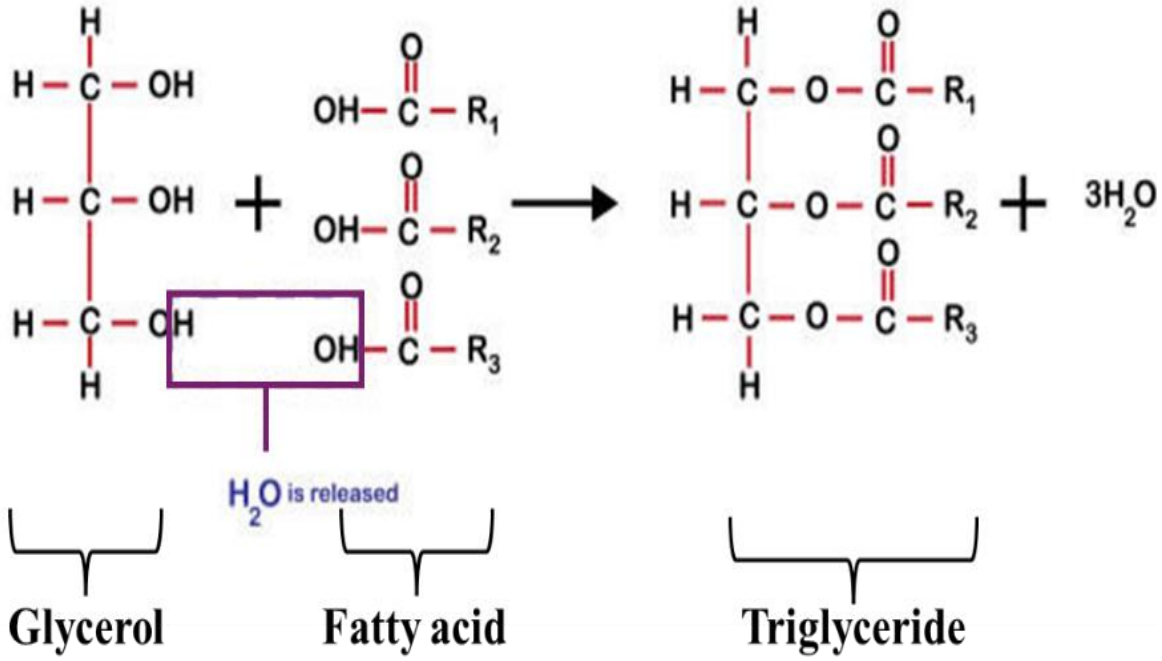


Figure 2-5: Structure of Triglycerides formed from glycerol and 3 fatty acids

Common sources of bio-lubricants derived from vegetable oils include sunflower oil, castor oil, canola oil, palm oil, and soybean oil [65]. The physiochemical properties of different oil sources for lubricants are presented in **Table 2-1**.

Oil	Viscosity Index	Pour point °C	Flash point °C	Reference
Palm oil	186	-5	263	[66]
Coconut oil	159	22	320	[67]
Sunflower oil	176	-18	332	[68]
Jatropha	205	-6	186	[69]
Rapeseed oil	220	--	234	[70]
Castor oil	220	-27	250	[71]

Table 2-1: Physiochemical properties of different oils used in bio-lubricants

Sunflower oil is derived from the seeds of Helianthus annuus. These seeds are prevalent in North America, where the moderate climate provides an ideal environment for sunflower cultivation. Sunflower oil exhibits a yellow hue and has a documented density of 0.934 kg/m3 [28]. This oil consists of oleic acid (30-50%), linoleic acid (60-70%), palmitic acid (5-10%), and stearic acid (6-8%). Sunflower oil exhibits a significant viscosity attributed to elevated oleic acid content, an unsaturated fatty acid, while containing lower amounts of linoleic acids, which are inherently polyunsaturated fatty acids. This high-oleic sunflower oil demonstrates excellent thermal stability when exposed to elevated temperatures. This oil demonstrates effective lubrication and oxidative stability [72].

Castor oil serves as a significant source of bio-based lubricants, derived from castor beans (Ricinius plant) [28]. The transesterification of castor oil yields innovative bio-based lubricants. This transesterification employs trimethylolpropane alongside lipase as biocatalysts. Castor oil is composed of 5.35% oleic acid, 82.48% ricinoleic acid, 7.01% linoleic acid, and 1.51% linolenic acid [73]. It exhibits lubricity at elevated temperatures and viscosity at reduced temperatures, rendering it ideal for racing engines and jets. Additionally, it finds use in various industries such as ink, coatings, and paints [74]. The canola oil plant is classified as a variety of rape seed plant. It has a low erucic acid content and a high nutritional profile.

Jatropha oil is derived from Jatropha Curcas, known for its high seed production rate and utilized in the synthesis of lubricants because of its high fatty acid content [28], [75]. Coconut oil is characterized by a significant presence of saturated fatty acids (90-95%), which exhibit

slow oxidation processes. The derivatives have applications as a lubricant for transformers [76]. Palm oil is characterized by a significant presence of palmitic acid (60-70%) in addition to oleic acid (20-25%). The formation of lubricants leads to an impressive load carrying capacity [77]. The incorporation of soybean oil has the potential to enhance the flash points of lubricants, contributing to an extended lifespan of transformers. This renders it optimal for dielectric fluids [28].

2.3.2 Synthesis of bio-lubricants

Five technologies are widely employed for the synthesis of bio-lubricants. These techniques may encompass transesterification, estolides synthesis, epoxidation, hydrolysis and hydrogenation. The specifics of each strategy are provided below.

The initial approach is the two stage transesterification, described as the extraction of saturated fatty acids from vegetable oils [78]. In the first stage, triglycerides react with alcohol such as methanol or ethanol to produce another fatty acid methyl/ethyl esters (FAME/FAEE), also called biodiesel. Methanol is most preferred because of easy solubility of catalyst NaOH or KOH and fast reaction with triglycerides. The second step is the reaction of methyl esters with polyols to produce tri-esters, which are biolubricants. Heikal et al. employed a two-stage transesterification process to synthesize bio-lubricant from palm oil and Jatropha oil [79]. Initially, they generated biodiesel from palm oil and Jatropha oil. Methanol and potassium hydroxide were utilized as catalyst and alcohol in the first stage. In the second stage, biodiesel is permitted to react with trimethyl propane in the presence of a catalyst. Sodium methoxide serves as a catalyst for the conversion into bio-lubricant (trimethylolpropane ester). The experiment yielded 97.8% of palm oil-based bio-lubricant. The yield recorded for Jatropha oil bio-lubricant was 98.2% [79].

The second technique involves the synthesis of estolides for the preparation of bio-lubricants, through the oligomerization of unsaturated fatty acids, where the alkene group reacts with the carboxylic group to form an ester bond. These estolides based lubricants offer enhanced performance and environmental benefits because of their biodegradable nature. This process involves the use of acidic catalysts, such as H_2SO_4 or $HClO_4$. The use of $HClO_4$ can result in superior effectiveness in reducing carboxylic acid content and enhancing the stability of the resulting estolides [80]. The transformation of natural oil based fatty acids into estolides improves the oxidative stability and low-temperature performance of bio-lubricants.

Additionally, reaction conditions, including catalyst and reaction time, play an important role in the final properties. For instance, a higher estolides number contributes to improved oxidation stability and viscosity index, while shorter fatty acid chains enhance the pour point, making them suitable for diverse applications [81].

The third technique is the utilization of epoxide groups in the preparation of bio-lubricants through the epoxidation process, which involves the reaction between a per-oxy acid and an alkene group. This process relies on various catalysts and reactants to enhance efficiency and performance [64]. For example, Somidi et al. utilized a MoO_3/Alumina catalyst to synthesize bio-lubricants from canola oil, with epoxidation requiring one hour for canola oil and thirty minutes for canola biodiesel [83]. Different catalysts, including lipase, clay, sodium ethoxide, and formic acid, have been employed to improve production rates and achieve better tribological properties in bio-lubricants. Among these, heterogeneous catalysts have proven more effective than homogeneous catalysts in bio-lubricant production, offering higher efficiency and improved outcomes [84].

The fourth technique is the hydrolysis, which can be used for the formulation of bio-lubricants by enhancing the chemical and physical properties of vegetable oils. This process involves two main steps. First, water is added along with an appropriate enzyme, such as lipase, to initiate the reaction. In the second step, water, ester, and glycerol are separated through esterification, resulting in the production of fatty acids and other components [85]. Hydrolysis of triglycerides in castor oil produces ricinoleate and glycerol, while crude palm kernel oil undergoes hydrolysis to yield a higher proportion of free fatty acids. These fatty acids, such as oleic acid, palmitic acid, linoleic acid, stearic acid, and erucic acid, are key components of waste cooking oils and other feedstocks [86], [87]. For instance, the hydrolyzed product from palm kernel fatty acids demonstrates excellent properties, including a flash point of 320°C and a viscosity index of 154, making it suitable for bio-lubricant applications [88].

Hydrogenation can be used for the formulation of bio-lubricants by enhancing the oxidative stability and modifying the fatty acid composition of vegetable oils. This process involves incorporating hydrogen into oil using a catalyst, which increases the saturation of fatty acids while reducing the levels of unsaturated fatty acids [89]. In the hydrogenation process, linoleic acid is converted into cis-oleic acid, which is further transformed into oleic acid, contributing to the formation of fatty acids. Additionally, the transformation of cis-oleic acid into transforms and the conversion of cis-linoleic acid into trans configurations are observed during the process

[90]. Hydrogenation of vegetable oils such as sunflower and canola oil, using a palladium catalyst, results in the formation of monoene's. This modification improves the physical and chemical properties of the oils, making them suitable for bio-lubricant applications [91].

2.3.3 Commercial synthetic bio-lubricants

The catalogues of the United States Department of Agriculture (USDA) BioPreferred® and the European Union (EU) Ecolabel feature a limited selection of commercial bio-lubricants. For inclusion in bio-lubricants, a product must be both biodegradable and sourced from renewable materials, such as hydrocarbon-based bio-lubricants [92].

2.3.4 Hydrocarbon based bio-lubricants

Multiple pathways exist to produce lubricants derived from vegetable oils, commonly referred to as hydrocarbon-based bio-lubricants. Comprehensive mechanisms regarding the synthesis of bio-lubricants utilizing these strategies are documented in the literature. The primary methods for producing hydrocarbon-based bio lubricants are hydrotreatment and electrochemical decarboxylation via Kolbe electrolysis, which are widely recognized and utilized [93].

Hydrocarbon bio-lubricants represent a sustainable alternative, originating from vegetable oil feedstocks. These materials exhibit greater biodegradability, thereby minimizing the potential for pollution. These materials originate from renewable sources, thereby minimizing their environmental impact. Their elevated lubricity can significantly improve machinery performance [93]. The elevated flash points of HBL serve to reduce the potential for fire hazards within industrial environments. The flash point of soybean is approximately 322 °C, which exceeds that of mineral oils [94].

Alternative methods for olefin production, including metathesis and the dehydration of fatty alcohols, are currently under investigation. Iso-alkanes within the C24–C50 range serve as examples of bio-based hydrocarbon lubricants. The molecular structure of iso-alkanes exhibits notable characteristics that render them appropriate for use as bio-lubricants. The absence of unsaturation sites and ester linkages leads to (1) remarkable stability; (2) outstanding cold flow properties due to alkyl branches; and (3) superior compatibility and interchangeability when compared to traditional petroleum-based lubrication systems, attributed to the absence of polar functional groups [95].

Organizations such as RSC Bio Solutions (United states) and Total (France) (BioLife Isane, Berylane) promote hydrocarbon bio-lubricants while not clearly disclosing the specific substances they include. Other businesses, such as Eni and Renewable Energy Group, Italy, have created technology for generating hydrocarbon bio-lubricants, but they are currently concentrating on the production of renewable diesel from vegetable oils. The production of hydrocarbons-based bio-lubricants and renewable diesel within an integrated biorefinery could prove advantageous moving forward. Hydrocarbon-based bio-lubricants are present in engine oils, gearbox fluids, hydraulic oils, greases and metalworking fluids [96].

2.4 Kolbe electrolysis

Kolbe electrolysis is the most promising route due to its minimal operating conditions, low hydrogen consumption, and fewer steps compared to the hydrodeoxygenation (hydrotreatment) process. Kolbe electrolysis transforms fatty acids into alkanes, resulting in the production of CO_2, with hydrogen generated as a byproduct. The process initiates with the hydrolysis of vegetable oil, yielding free fatty acids that are subsequently dissolved in suitable solvent, mostly the mixture of alcohol and water to produce hydrocarbons.

Kolbe electrolysis represents a sustainable approach for producing hydrocarbon-based bio-lubricants, utilizing carboxylic acids derived from biomass. In comparison to conventional methods, this process produces less harmful byproducts, thus helps to reduce the environmental effects. A diverse range of hydrocarbons can be generated, including those suitable for bio-lubricants. These are gaining popularity due to their reduced environmental impact compared to synthetic lubricants and their biodegradable nature [97].

The formulation of the electrolyte entails dissolving sodium and potassium salts derived from carboxylic acid. This salt is essential for the electrochemical process to occur smoothly. The electrolytic cell serves as the apparatus for conducting the electrolysis process. The process's selectivity and efficiency necessitate a meticulous choice of electrode material, such as carbon or platinum. At the anode, carboxylate ions undergo oxidation through the application of electric current, resulting in the formation of alkyl radicals. These radicals subsequently combine to form hydrocarbons [92].

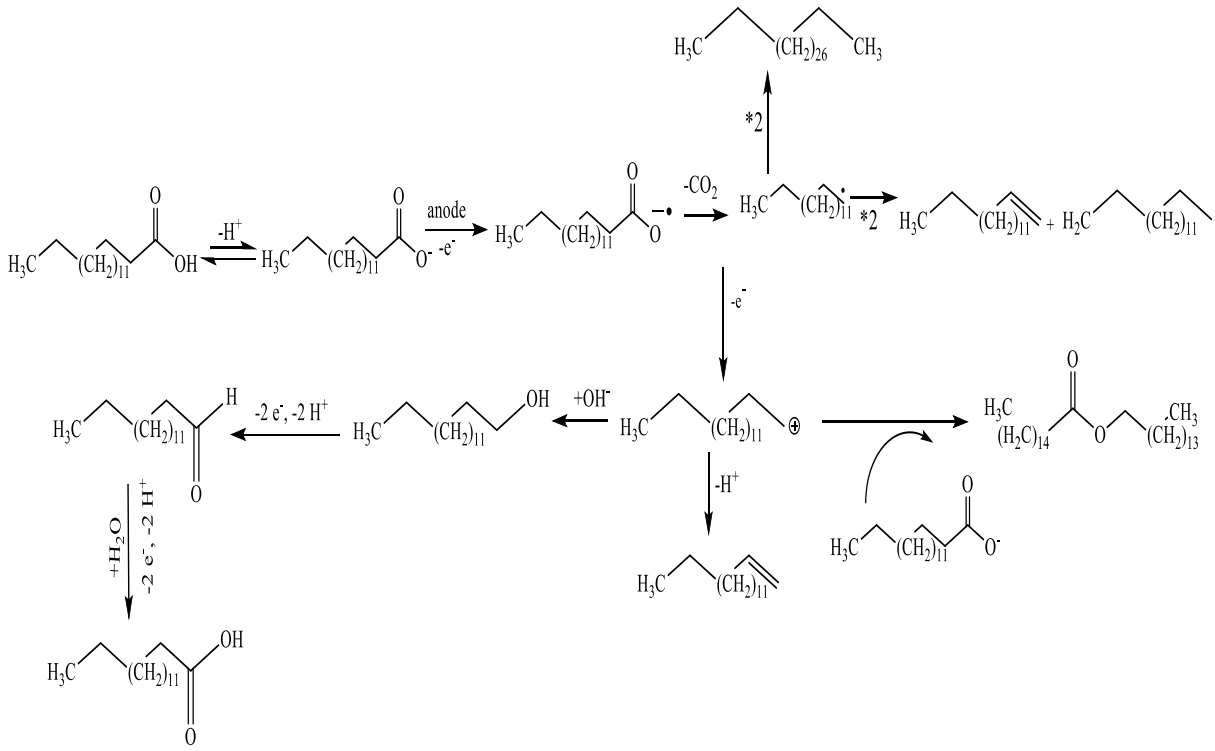
Kolbe electrolysis can follow various reaction pathways [98].

Pathway I. The primary mechanism for generating symmetrical alkanes involves the dimerization of alkyl radicals. The example of Kolbe electrolysis of palmitic acid is shown in **Scheme 2-1,** representing all product formation through different pathways.

Pathway II. The second way involves the disproportionation of radicals resulting in the formation of alkanes and alkenes.

Pathway III. Alkyl radicals may occasionally undergo rearrangement to generate carbenium ions, which can subsequently react with nucleophiles, resulting in the formation of esters and alcohols (non-Kolbe product). This pathway may lead to the generation of olefins through alkyl radicals.

Pathway IV. Radical coupling entails the interaction of diverse alkyl radicals. This pathway results in the creation of non-symmetrical alkanes.



Scheme 2-1: Representation of different pathways of Kolbe electrolysis of palmitic acid ($C_{16}H_{32}O_2$)

2.4.1 Factors effecting Kolbe electrolysis

A general Kolbe cell design is shown in **Figure 2-6**. Various factors may be responsible for the Kolbe electrolysis method. These factors can impact selectivity, effectiveness and results of the reaction. Details of these factors are given below:

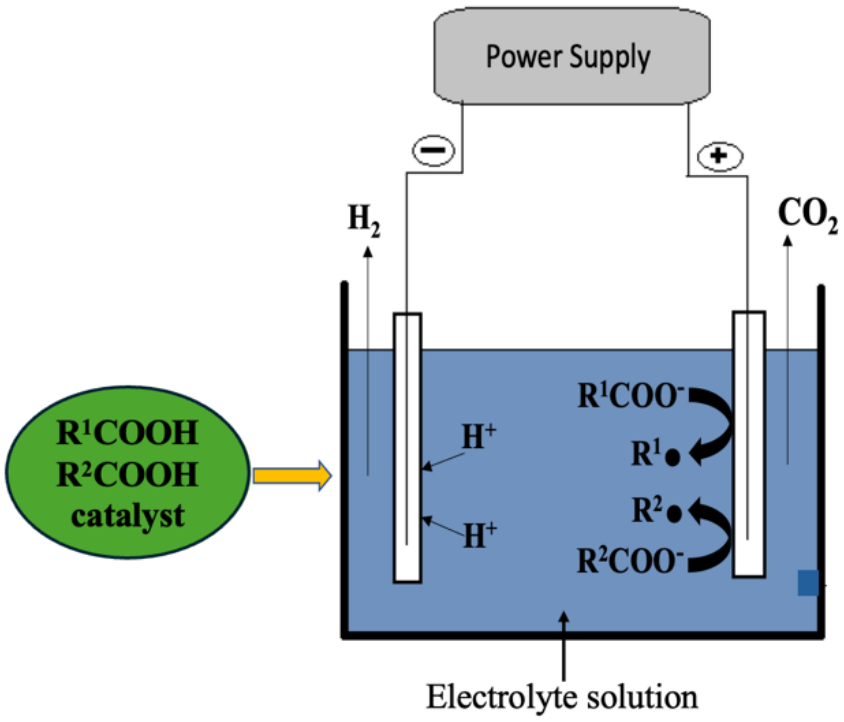


Figure 2-6: General representation of Kolbe electrolysis cell

2.4.2 Electrode material

Electrodes play a crucial role in the Kolbe electrolysis process. They enable the transformation of carboxylic acid into hydrocarbons. The choice of electrode material can influence the selectivity and efficiency of the process. The oxidation process generates alkyl radicals on electrodes derived from carboxylate ions. The catalytic activity of an electrode is influenced by the material which is composed of; for instance, platinum electrodes are predominantly utilized because of their high redox potential and chemical stability. The products' selectivity is influenced by the electrode material [99], [100]. For instance, the behavior of alkyl radicals can vary, leading to dimerization or disproportionation, contingent upon the specific electrode employed. In a similar manner, the surface roughness of the electrode can either enhance or reduce the adsorption of reactants and intermediates, thereby influencing the reaction rates.

During Kolbe reaction, the issue of passivation can occur in electrode materials which could arise from various factors. The application of coatings on products or other materials on the electrode can lead to passivation, consequently diminishing the electrodes' activity. In the process of oxidation during electrolysis, there is a possibility for the oxide layer to accumulate on the electrode material when subjected to elevated potentials. This fills the active sites and consequently diminishes the electrode's activity. Occasionally, by-products and other impurities can accumulate, leading to passivation. Furthermore, as time progresses, the

electrode material may experience degradation from corrosion and chemical processes, resulting in passivation and diminished activity of the electrode material [101].

Different types of electrode materials, specifically platinum, platinized titanium (modified), graphite, and carbon-based electrodes, have been utilized in the Kolbe reaction. Olde Nordkamp et al. reported on platinum electrodes that enhance Kolbe electrolysis by suppressing oxygen evolution and promoting anodic decarboxylation. However, these electrodes may dissolve under high anodic potentials, which could impact their economic viability [100]. Furthermore, they reported an association between in situ and ex situ surface techniques, indicating that acetate ions restrict the formation of passive oxide layers (passivation of the electrode at elevated anodic potential and in an aqueous electrolyte) on the electrode surface (in this instance, platinum was used as the electrode). The issue at hand was the dissolution of Pt; to address this, both active and alternative materials are necessary.

In another study, Zhang et al. investigated the most common electrodes used in the Kolbe reaction, specifically platinum and graphite. Both electrodes demonstrated effectiveness in the reaction, albeit through different pathways and kinetics, attributed to their distinct preference mechanisms in Kolbe electrolysis. Research indicates that Pt demonstrates superior efficiency and facilitates decarboxylation more effectively on its surface compared to graphite [102]. Neubert et al. investigated the platinization of titanium, achieving a high CE percentage of 93.1% for n-hexanoic degradation. The study indicated that the modified electrode material demonstrates enhanced performance in the Kolbe reaction, nearing the performance levels of pure Pt electrodes [103]. Liu et al. reported on the use of a Pt electrode for Kolbe electrolysis of acetic acid (Pt anode), noting that the passivation of the Pt surface through oxidation reduces the adsorption of species involved in the Kolbe reaction. The decarboxylation step demonstrates the activity of the Kolbe product while inhibiting the oxygen evolution reaction [98].

Liu et al. investigated on the amorphous RuO_2 catalyst material in the context of the Kolbe reaction. The hydrothermally synthesized amorphous RuO_2 catalyst demonstrated significant efficacy in the decarboxylation of hexanoic acid, facilitating both oxidation and alkane dimerization. Notably, this process on the electrode surface yields the Kolbe product [104]. Neubert and colleagues investigated the use of platinized titania and nickel as anodes for the electrolysis of acetic acid. The study compares platinized titania and nickel electrodes with pure Pt foil electrodes, revealing that electrode performance is substrate specific and requires high selectivity for the Kolbe reaction [103]. Layers of electrode passivation and platinized titania along with nickel electrodes are referenced in **Figure 4** [100]**.** This illustrates the

mechanism and passivation effect of acetate on the electrode surface, along with a comparison of modified platinum and nickel electrodes in electrolysis.

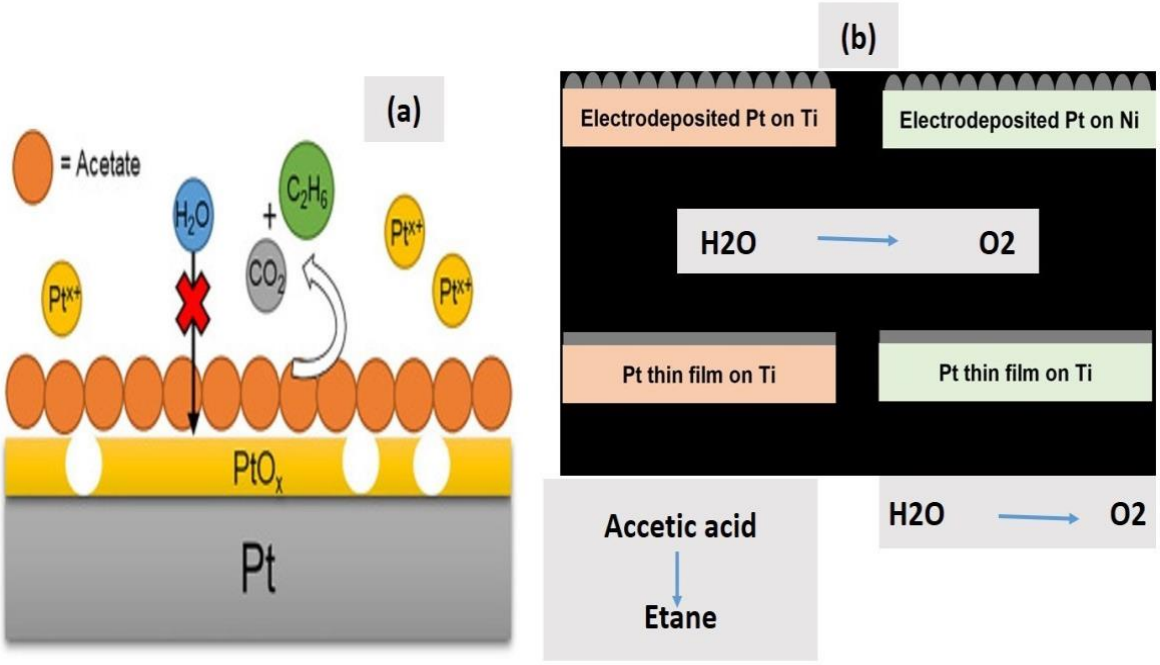


Figure 2-7: a) Pt electrode surface during Kolbe electrolysis of acetic acid (passivation) b) Platinized titania (modified Pt) and nickel as anode in Kolbe electrolysis

2.4.3 Current intensity/Voltage

The effectiveness and precision of the electrochemical process are influenced by the measurements of current intensity and voltage. Modifying these parameters can influence the Kolbe electrochemical process [103]. For instance, a high intensity of current can ultimately accelerate the oxidation rate at the anode and the reduction at the cathode, thereby enhancing the flow of electrons, which leads to the rapid formation of hydrocarbon bio-lubricants. The rapid formation of the product subsequently results in substantial product yields. Nonetheless, elevated current intensity can lead to side reactions that may compromise the selectivity of the intended product. In a similar manner, elevated voltage can enhance the generation of specific products. High voltage can lead to the occurrence of undesired side reactions. The influence of high voltage extends to the overall reaction kinetics and the dispersion of products.

The influence of current density and potential on Kolbe electrolysis is significant, affecting several parameters including product distribution, efficiency, and reaction pathways. The electrochemical environment for reaction is directed by current density and potential, which in turn influences the specificity and selectivity of the involved reactions. The variation of current

density indicates that lower current densities, such as 25 mA/cm², promote the formation of Kolbe products [104].

Liu et al. reported a study indicating that high anodic potentials result in large Tafel slopes and inflection zones, whereas low potentials may enhance the adsorption strength of carboxylic species. This may significantly influence Kolbe product formation [96]. Ze Sun et al. investigated magnesium electrolysis, showing that an increase in current intensity has minimal effect on voltage, whereas structural constraints significantly affect resistance voltage. The study does not specifically address Kolbe electrolysis. Furthermore, a linear relationship exists between the voltage and the thicknesses of the electrodes (both anode and cathode). The working height of the anode and cathode significantly influences the voltage [105].

Halford et al. discussed in their own study the advancements in Kolbe electrolysis. High current intensity generates robust oxidizing conditions that can potentially eliminate various functional groups. Conversely, recent studies indicate that low current intensity facilitates a more subtle and practical method for the coupling of carboxylates [106]. Furthermore, the elevated current density in Kolbe electrolysis, aimed at producing the desired product under specific conditions, resulted in amorphous carbon-based electrode passivation due to the formation of an oxide layer, ultimately leading to diminished selectivity. Low current intensity offers flexibility for enhanced substrate (not passivated) and significantly improved chemo-selectivity, particularly with the reverse alternate polarity waveform [107]. A subsequent investigation demonstrated that varying current and voltage intensities in Kolbe electrolysis influence reaction efficiency and selectivity, with rapid alternating polarity enhancing chemo-selectivity and accommodating a broader spectrum of functional groups [107]. Moreover, Forschner et al. presented findings on the electrolysis study, highlighting that in Kolbe electrolysis, the current density significantly impacts the reaction rate and the formation of final products, whereas the actual voltage primarily influences electrolyte resistance. This study demonstrates that the application of an external potential difference between two electrodes results in a voltage drop across an ion-conducting electrolyte. This decline is primarily significant in poorly conducting electrolytes and under high current conditions. The estimation of electrolytic potential is pertinent in the field of electrochemistry, including areas such as bipolar electrochemistry, ohmic microscopy, and contact glow discharge electrolysis [108].

2.4.4 Solvent Environment

The solvent environment significantly influences the overall selectivity and efficiency of the Kolbe reactions. To enhance the solubility of the reactants and products, the traditional Kolbe method utilizes organic solvent [109]. Nonetheless, these solvents present both financial and toxicological challenges, complicating the product separation process. The recent developments eliminate the necessity for organic solvents in Kolbe's method. Currently, Kolbe electrolysis can occur in aqueous conditions [110]. The conductivity of the solvent is a crucial factor in electrolysis. Superior conductivity during electrolysis results in enhanced reaction rates and boosts the overall efficiency of the process. Solvent environments can also exert an influence on reaction pathways. The presence of water can lead to the formation of hydroxyl radicals. These radicals have the potential to initiate side reactions that can affect the overall productivity of the reaction, leading to the generation of intermediates. Hydrocarbons can be readily separated into aqueous solvents instead of organic solvents, aligning with the principles of green chemistry [111].

The influence of solvent on Kolbe electrolysis is significant, potentially impacting product selectivity, efficiency, and the overall results of the reaction. Recent studies have explored the impact of various solvents on the electrochemical performance and product delivery in the Kolbe electrolysis process. The integration of Kolbe electrolysis with microbial processes in solvents like isopropanol resulted in elevated carbon and Coulombic efficiencies, underscoring the significance of the solvent in enhancing the overall performance of the method [112].

Chichina et al. published a report examining various solvent environments, highlighting the significant influence of solvents on the reactivity and polarization curves in Kolbe electrolysis using non-aqueous solvents. Non-aqueous solvents favored dimerization and influenced the adsorption of species on electrode surfaces. The Kolbe synthesis with two per-fluorinated oxa acids, perfluoro-3,7-dioxa-2-methyloctanoic and perfluoro tetrahydro-α-furylacetic, was studied volta-metrically on bare platinum (Pt) and glassy carbon anodes in water/acetonitrile and methanol/acetonitrile solvent system. The influence exerted on the process by the concentration of acid, degree of neutralization, and the solvent was examined. The solvent-anode system demonstrates a segregating influence on the reactivity of perfluorinated acids during the Kolbe electrolysis synthesis process [113].

Stanescu et al. conducted a study that revealed solvents with low dielectric constants promote carbonation in the Kolbe–Schmitt reaction, thereby stabilizing reactive species and enhancing yields. Nonetheless, polar solvents play a crucial role in influencing thermodynamic properties

and solvation energies, which in turn affect reaction rates and equilibrium behavior. In a similar way, certain solvents promote uniformity in the reaction mixture and may enhance the reaction rate of the Kolbe–Schmitt reaction. This study aims to connect empirical observations with an in-silico analysis of the Kolbe–Schmitt reaction mechanism through density functional methods and to explore the solvent effects on this reaction [114].

Additionally, Waldvogel et al. discussed various solvents in Kolbe electrolysis, highlighting their impact on parameters like product selectivity and reaction pathways, as noted in previous reports. Protic solvents enhance Kolbe dimerization, whereas dipolar/aprotic solvents support non-Kolbe processes. The characteristics of the solvent, including its acidity and dielectric constant, significantly influence the electrochemical results. The role of solvent control in electro-organic conversions is often undervalued in preparation-scale electrolysis. This straightforward electrolytic approach in fluorinated solvents facilitates the adjustment of the substrate's nucleophilicity and the stabilization of both the intermediates and the final product against over-oxidation [115].

Hioki et al. reported in their work the role of acetone as an unconventional reaction solvent in Kolbe electrolysis, which mitigates restrictions by altering the local pH around the electrodes, hence boosting the reaction's efficiency and functional compatibility. Acetone plays a crucial role in the efficacy of the reaction, especially regarding the recently introduced waveform-controlled electrosynthesis. The authors propose that the selection of solvent may affect the local pH surrounding the electrodes during electrolysis. The control of pH is essential as it influences the decarboxylative oxidation process, which is fundamental to the Kolbe reaction. The solvent effect is related to the overall compatibility of different functional groups in the Kolbe reaction. Acetone's capacity to stabilize certain intermediates or transition states may facilitate the utilization of a broader array of substrates without experiencing competing oxidation, a prevalent challenge in conventional Kolbe electrolysis [107].

2.4.5 Electrolysis time

Another significant aspect is the duration of electrolysis, which can influence the Kolbe electrolysis method. Extended electrolysis can lead to the generation of targeted products. Extended oxidation of carboxylate ions leads to an increased yield of the desired products. Nevertheless, it is essential to maintain balance, as excessive duration can frequently lead to the generation of byproducts [95].

The duration of electrolysis can influence the properties of the electrode material. Extended durations may lead to the degradation of the electrode surface, particularly under high current intensities. This decline subsequently results in the passivation of the electrode material. The number of radicals is also influenced by the duration of electrolysis. Prolonged exposure leads to the generation of additional alkyl radicals, thereby enhancing the likelihood of dimerization to form higher hydrocarbons. Determining the optimal duration of electrolysis is essential for enhancing product output while minimizing side effects and electrode degradation [116].

The duration of electrolysis plays a crucial role in Kolbe electrolysis, affecting multiple aspects such as the distribution of Kolbe products, the selectivity of the process, and overall efficiency. Recent reports suggest that adjusting electrolysis time could improve the conversion of carboxylic acids into hydrocarbon products, with specific parameters affecting the outcomes. Increasing current densities (up to 0.6 A/cm^2) could enhance the reaction rate, while extended electrolysis durations might result in diminishing returns in product yield due to side reactions. Nordkamp et al. observed that prolonged electrolysis of acetate at basic pH led to a decrease in faradaic effectiveness towards ethane, which was offset by the production of alcohols like methanol. This indicates that the duration of electrolysis significantly influences product selectivity in Kolbe electrolysis. The duration of electrolysis influenced the faradaic efficiency of the Kolbe electrolysis reaction. The prolonged electrolysis of acetate under basic pH conditions results in a reduction in the efficiency of ethane production. This can be linked to the generation of methanol as a compensatory byproduct, suggesting a change in selectivity as time progresses. The surface of the platinum (Pt) electrode undergoes alterations during extended electrolysis. An oxidized Pt surface exhibits distinct interactions with the electrolyte, potentially impacting the selectivity of the reaction. The presence of bicarbonate and carbonate ions on the oxidized surface modifies the reaction pathways, resulting in varied product distributions over time [117]

2.4.6 Supporting electrolytes

Enhancing conductivity is a fundamental aspect of Kolbe electrolysis, achievable using supporting electrolytes. Supporting electrolytes may increase the ion transport thus increasing the conductivity [117]. The allocation of products is influenced by the density of auxiliary materials. For instance, investigations have shown that employing sodium sulfate as a supporting electrolyte could improve the yield, while utilizing potassium nitrate might decrease the columbic efficiency and elevate the energy demand. The use of supporting electrolytes to

stabilize intermediates has the potential to enhance reaction kinetics [118]. In a similar way, supporting electrolytes may occasionally impede the formation of unwanted products. This has the potential to enhance the selectivity of the reaction [109].

The presence of supporting electrolytes is crucial in electrochemical reactions, such as Kolbe electrolysis. These electrolytes facilitate the preservation of electrical conductivity within the solution. Their provision of ions facilitates charge movement, which is essential for the efficient occurrence of electrochemical processes. The impact of supporting electrolytes on Kolbe electrolysis is significant, as it can affect the distribution of reaction products, the efficiency of the reaction, and the overall electrochemical activity. Numerous investigations underscore the critical significance of this aspect, where the type and concentration of supporting electrolytes can influence the reaction dynamics, especially through the interaction of cations with the electrode surface.

Stang and Harnisch released a report that examines the advantages and disadvantages of different supporting electrolytes. For instance, KNO_3 was found to reduce CE, while Na_2SO_4 was shown to enhance time yields. The findings indicate that the choice of electrolytes can be customized according to objectives in the electro-organic synthesis process. The supporting electrolyte influences both the efficiency, and the composition of the products generated during the electrolysis process. Variations in electrolytes can result in diverse product outcomes, which is crucial for enhancing the desired results in electro-organic synthesis.

Ahmadpour et al. employed multivariate curve resolution alternative least squares for current deconvolution, utilizing various types of supporting electrolytes including KCl, NaCl, KF, NaF, KBr, NaBr, KOH, NaOH, KNO_3, and $NaNO_3$, among others. The investigation further examines the impact of the type and concentration of supporting electrolytes on charging currents in electrochemical processes, including Kolbe electrolysis. It affects reaction efficiency and product distribution by altering ionic strength and conductivity within the electrochemical cell [119].

Different alkali metal cations (Li^+, Na^+, K^+, Cs^+) exhibit distinct influences on Kolbe electrolysis, with K^+ demonstrating the most advantageous outcomes regarding product selectivity and electrochemical activity. The findings suggest that the selectivity of Kolbe electrolysis is affected by multiple factors, such as the choice of supporting electrolyte. The presence of alkali metal cations specifically influences product distribution and overall electrochemical activity during the electrooxidation of acetic acid. Supporting electrolytes are crucial in Kolbe electrolysis as they affect reaction conditions, product distribution, and the overall electrochemical activity through their interactions with alkali metal cations [104].

Ashraf et al. investigated the influence of supporting electrolytes, particularly monovalent alkali cations, and evaluated their performance with platinum (Pt) electrodes in the context of Kolbe electrolysis of acetic acid. The findings indicate a significant importance of electrochemical performance related to the type of alkali cation utilized as a supporting electrolyte. The analyzed trend was $Li^+ < Na^+ < K^+ \sim Cs^+$, indicating that each alkali cation affects the efficiency of the electrolysis process over a wide pH range. The presence of Li^+ and Na^+ alkali cations significantly promote the oxygen evolution reaction (OER), which competes with the favored Kolbe oxidation. The observed competition diminishes the selectivity of the Kolbe reaction, indicating that selecting the appropriate supporting electrolyte is essential for enhancing the targeted electrochemical reaction. Another observation indicates that Li^+ may improve the dissolution of electrodes (Pt), potentially influencing the performance of the electrodes. This aspect emphasizes the significance of comprehending the interactions between various cations and the electrode material [120].

Chapter 3 Materials and Characterizations

In this chapter it is presented the materials and instrumentations employed for the physical and chemical characterizations of the vegetable oils, the products obtained after Kolbe electrolysis and all the commercial and synthesized lubricants. It is important to mention that methodology and experimental setup of each process is explained in the specific chapter.
The **section 3.1** is divided in subparagraphs, each one presenting a list of the materials used for the studies developed during the Ph.D. research. Furthermore, the characterization techniques applied for all research are described in detail at **section 3.2.**

3.1 Materials

In the following subparagraphs a list of all materials used in this thesis is reported. These materials were divided according to the study they were employed. All chemicals reported here were used as received, without further purifications.

3.1.1 Kolbe electrolysis of a single fatty acid and mixture of two fatty acids

Lauric acid (*n*-dodecanoic acid, $C_{12}H_{24}O_2$, 97 %, white powder), palmitic acid (hexadecanoic acid, $C_{16}H_{32}O_2$, 97 %, white scales), potassium hydroxide (KOH, 97 %), ethyl acetate (99.5%) methanol (MeOH, 99.5%), ethanol (EtOH, 99.5%), hexane (n-hexane, 99.5%) and hydrochloric acid (HCl, 39%) were used as purchased (Sigma-Aldrich). Distilled water was used in all the experiments.

3.1.2 Kolbe electrolysis of a complex mixture of derived from from coconut oil

Coconut oil (purchased from OLDFOOD S.r.l, Italy), potassium hydroxide (KOH, 97%), ethyl acetate (99.5%) methanol (MeOH, 99.5%), ethanol (EtOH, 99.5%), hydrochloric acid (HCl, 39%), were used as purchased (Sigma-Aldrich). Distilled water was used in all the experiments.

3.1.3 Kolbe electrolysis of a complex mixture of derived from from palm oil

Palm oil (purchased from OLDFOOD S.r.l, Italy), potassium hydroxide (KOH, 97%), ethyl acetate (99.5%) methanol (MeOH, 99.5%), ethanol (EtOH, 99.5%), hydrochloric acid (HCl, 39%), were used as purchased (Sigma-Aldrich). Distilled water was used in all the experiments.

3.1.4 Formulation of lubricants from coconut oil and fatty acid methyl esters (FAME)

Coconut oil (purchased from OLDFOOD S.r.l, Italy), beeswax (purchased from Tooget S.r.l 99%), potassium hydroxide (KOH, 97%), ethanol (EtOH, 99.5%) and methanol (MeOH, 99.5%) were used as purchased (Sigma-Aldrich).

3.1.5 Formulation of bentonite and lithium-based lubricants

This part is related to the research activities performed in company (Bellini S. P. A). Bentonite clays, unsaturated vegetable oil, propylene carbonate, 12-hydroxystearic acid (12-HSA), azelaic acid, lithium hydroxide (LiOH) was used as purchased. Distilled water was used in all the experiments.

3.2 Characterizations

In the following subparagraphs all the characterizations used for the analysis of all the samples and products are discussed.

3.2.1 Gass Chromatography Mass Spectrometry (GC/MS)

The GC/MS analysis was performed to investigate the product distribution and their percentages after the electrolysis experiments. The analysis was performed on an Agilent 6850 chromatography instrument equipped with an Agilent 5975N mass spectrometer.

3.2.2 Scanning Electron Microscopy

The morphology of the commercial and non-commercial electrodes was studied using an EVO 15 scanning electron microscope (SEM) from Zeiss (Oberkochen, Germany), coupled with an Ultim Max 40 energy dispersive X-ray (EDX) microanalyzer by Oxford Instruments (High Wycombe, UK). The samples were analysed using a secondary electron detector, with energy

set at 20.00 kV, at different four different magnifications (250 X, 1000 X, 2500 X and 10000 X).

3.2.3 Consistency measurement (Penetrometer):

The consistency or hardness of lubricants were determined by using penetrometer. The consistency was measured by determining the penetration depth of a standardized cone (mass and geometry defined by ASTM D217) into the grease sample at room temperature. The cone was released for 5 seconds, and the penetration depth was recorded in 0.1 mm unit using a digital readout to measure the consistency of materials. The penetration value was then related to National Lubricating Grease Institute (NLGI) levels to determine the hardness of the grease.

3.2.4 RSSOT (Rapid Small Scale Oxidation Test)

The oxidation stability of all the lubricants were determined by using Rapid Small Scale Oxidation test (RSSOT). The oxidative stability of the sample was determined by exposing it to pure oxygen at a pressure of 700kPa and target temperature of 140°C starting at 25°C in a closed vessel. The sample container was equipped with pressure sensitive transducer to monitor consumption of oxygen. The stopping criteria of the test was 10% pressure drop as per ASTM D7525, and the cooling temperature of the system was 30°C.

3.2.5 Rheology and viscoelastic properties of lubricants (Rheometer)

Anton-Par Rheometer instruments was used for determining the rheological, viscoelastic properties and flow behaviour of all lubricants. Following four types of tests were conducted using rheometer instrument: (a) Viscosity vs temperature, (b) storage modulus/loss modulus vs shear stress, (c) flow test (shear stress vs shear rate, viscosity vs shear rate) and (d) tack test. For viscosity vs temperature test the samples were tested at a temperature range of 0°C to 80°C. For flow behaviour test two different sizes cone-plates (25 and 50 mm diameter) were used to measure shear force. Different instrumental conditions were applied like torque sensors (0.5 nNm to 230 mNm) by varying shear rates and normal force with a range of -50 N to +50 N to investigate viscoelastic behaviour, yield stress determination, flow behaviour and thixotropy, temperature sensitivity and performance. Tack test was conducted to investigate the ability of grease to adhere to surfaces under separation, where motion can cause lubricant displacement.

The normal force required to separate surfaces with a consistent layer of grease was measured against the increasing gap, providing insights into the adhesive properties of the tested greases.

3.2.6 X-Ray Fluorescence Spectroscopy (XRF)

The Thermo Fisher Scientific XRF instrument was used for determining the elemental composition of the electrodes used in the electrolysis experiments and commercial lubricants to gain an insight study. The X-ray source used was operated at a 40 kV voltage and a 50mA of current. A silicon drift detector operated with an energy resolution of 125eV was used to catch the emitted X-rays. The instrument was configured to analyze 10% lubricant liquid solution samples.

3.2.7 Atomic Emission Spectroscopy (AES):

Atomic emission spectroscopy (AES, AES Spectrometer, Perkin Elmer, Waltham, MA, USA) was used to determine elemental composition of commercial lubricants. The measurements were performed at 251.611 nm.

3.2.8 Tribometer test

Ball-on-plate tribometer tests (a type of tribological test) was used to investigate the friction and wear characteristics of lubricating materials. In these tests a spherical ball is brought into contact with a flat plate, providing the sliding contact between two surfaces typically under controlled conditions of force, speed, and temperature. In our experiments, the samples were checked under specified condition including steel plate, test run of 1 hour, an applied force of 23 N, rotation of 200 and 500 rpm and a temperature of 75°C. After completion of the tribometer tests, the coefficient of friction vs time and scar diameter was analysed. The scar diameter was analysed by using optical microscope

Chapter 4 Kolbe electrolysis of single and mixture of fatty acids

In this chapter, the Kolbe electrolysis of lauric acid, palmitic acid and the mixture of both lauric and palmitic acid in (1:1) are presented, aiming to investigate the effect of different experimental parameters like current intensity, supporting electrolyte, solvent environment, electrolysis time and nature of electrode on the product formation. Before the description of the experimental part and discussion of the main results, short highlights of the research activities and an introduction about the Kolbe electrolysis is presented. Materials and instrumentations for characterization were reported in the previous chapter.

4.1 Highlights of research activities:

This chapter contains the following research activities.

(a) Kolbe electrolysis of lauric acid using commercial platinum-coated-copper (Pt-coated-Cu) electrode and gold-coated-copper (Au-coated-Cu) electrode
(b) Investigation of degradation platinum-coated-copper electrode and gold-coated-copper electrode during electrolysis experiments
(c) Kolbe electrolysis of individual lauric acid and palmitic acid using non-commercial platinum electrode and optimization of experimental parameters
(d) Kolbe electrolysis of mixture of lauric acid and palmitic acid (1:1) and investigation of the products trends

4.2 Introduction:

In 1849 Adolf Wilhelm Hermann Kolbe (frequently shortened to H. Kolbe) first obtained the synthesis of hydrocarbons by electrolysis [121]. He proposed the synthesis of ethane from acetic acid through electrolysis as shown in **Figure 4-1**, offering an alternative to traditional production methods. The process involves the anodic oxidation of carboxylate to form a radical, commonly referred to as the "Kolbe reaction" or "Kolbe electrolysis" [122].

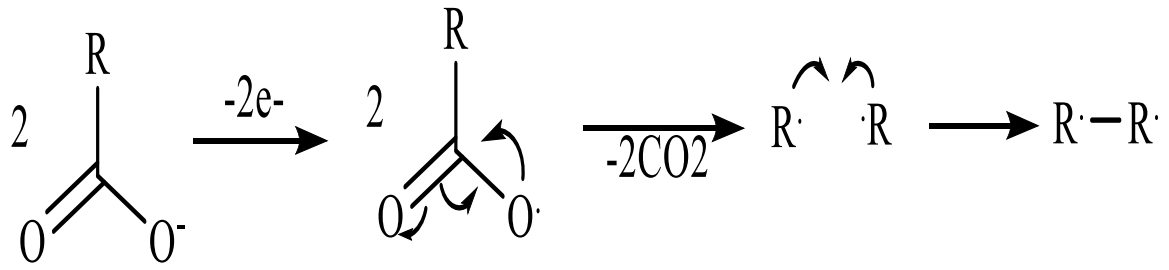


Figure 4-1: Electrochemical decarboxylation-dimerization of carboxylic acids, where R = methyl group

With the further improvements by many researchers, the Kolbe electrolysis now considered as an environmentally friendly pathway to produce alkanes because it can be conducted in aqueous solutions and at room temperature. Until now, many studies on the experimental conditions of the Kolbe electrolysis reaction have been carried out for tuning the yield and selectivity of the specific reaction pathway. The concentration of fatty acid, current density, electrode material, temperature, solvent nature and pH value are found to have a broad effect on the selectivity of the products.

Many researchers utilize the Kolbe electrolysis for many different applications, especially on the electrolysis of bio-resources into chemicals. For example, T. R. dos Santos investigated the conversion of fatty acids and triglycerides in organic and aqueous solvents into ether and olefins [123]. Meyers et al., investigated the Kolbe electrolysis of 3-hydroxy-decanoic acid into diesel like fuels [124]. Joschka Holzhäuser investigated the direct electrocatalytic conversion of lignocellulose biomass for fuel production [125]. Nilges et al., used two-step electrochemical conversion to produce octane as a fuel from levulinic acid through valeric acid [126].

Despite significant advancements in Kolbe electrolysis, certain aspects still require further improvements. A common limitation in the electrochemical conversion of biomass feedstock into useful products is the challenge of their solubility. Therefore, a recent trend in the Kolbe electrolysis is to use the process in combination with biological, chemical or thermal pretreatment processes for the conversion of biomass into useful chemicals and biofuels. Recently, C. Urban *et al* successfully proved the conversion of corn beer to a hydrocarbon mixture as a drop-in-fuel by using combined microbial and electrolysis methods [127]. The second challenge for the direct electrochemical conversion of biomass is its complex structure and understanding of their electrolysis mechanism. Therefore, it is important to ensure and understand the contact between substrate and electrode for the efficient conversion. A very important work for understanding the mechanism of homo- and hetero-coupling of bio-based

mixture of fatty acids providing full detail of electrons transfers and product formation is done by K. Neubert [128].

This study describes the Kolbe electrolysis of single long-chain carboxylic acids (lauric and palmitic acids) that are the essential parts of different vegetable oils. Lauric acid is the main constituent of coconut oil (45,4 g/100 g $f.a._{tot}$, where $f.a._{tot}$ is the total of fatty acids) and of palm-kernel oil (46,9 g/100 g $f.a._{tot}$). Palmitic acid constitutes 40,1 g/100 g $f.a._{tot}$ of palm oil [129]. These acids are commonly obtained from vegetable oils through different techniques, and thereof the electrolysis on the mixture of these carboxylic acids is also performed and explained. Hence, using the mixture of carboxylic acids can be a representative for the implementation of Kolbe electrolysis on complex fatty acid system. The electrolysis of single and mixture of carboxylic acids were conducted to produce long chain hydrocarbons as a result of homo- and hetero-coupling of radicals, which have many industrial applications like diesel and heavy fuel production, waxes and lubricants, pharmaceutical and agrochemicals etc. The effect of different parameters on the electrolysis of single/mixture of carboxylic acids and their product distribution were investigated.

4.3 Experimental Part:

4.3.1 Experimental setup:

All the Kolbe electrolysis experiments were performed using a commercially available ElectraSyn 2.0 (IKA®) system (purchased from Germany), operated under galvanostatic or potentiostatic control **(Figure 4-2a)**. The instrument specifications included a maximum current input of 1500 mA, electrode voltage output of 30/10 V, electrode current output of 100 mA and permissible ambient temperature range of 5-50 °C. The stirring speed range was 50-1500 rpm, compatible with stirring bars 8-16 mm in length, and the instrument weighed 3.72 kg. All the experiments were conducted in a 20 mL vial provided with the instrument, with stirring carried out before electrolysis for 5-10 minutes at 500 rpm using a magnetic stirrer. The electrodes included two types of commercially available with instrument, (a) Pt-coated copper **(Figure 4-2b)** and (b) Au-coated copper **(Figure 4-2c)**, each with dimensions of 0.8 x 5.25 x 0.2 cm^3 and a layer thickness of 400-600 µm, with a 5 mm gap between the electrodes facing each other. Two non-commercial platinum electrodes was used, with dimensions of 0.7 x 5.3 x 0.04 cm^3 and a total geometrical surface area of 7.9 cm^2, also maintaining a 5 mm electrode gap (custom-adjusted in the instrument electrode holder) **(Figure 4-2d)**. The

elemental composition and morphology of the commercial Pt-coated-Cu and non-commercial platinum electrodes were investigated using XRF and SEM analysis (discussed in results and discussion section). After each experiment, electrodes were thoroughly cleaned using distilled water and acetone.

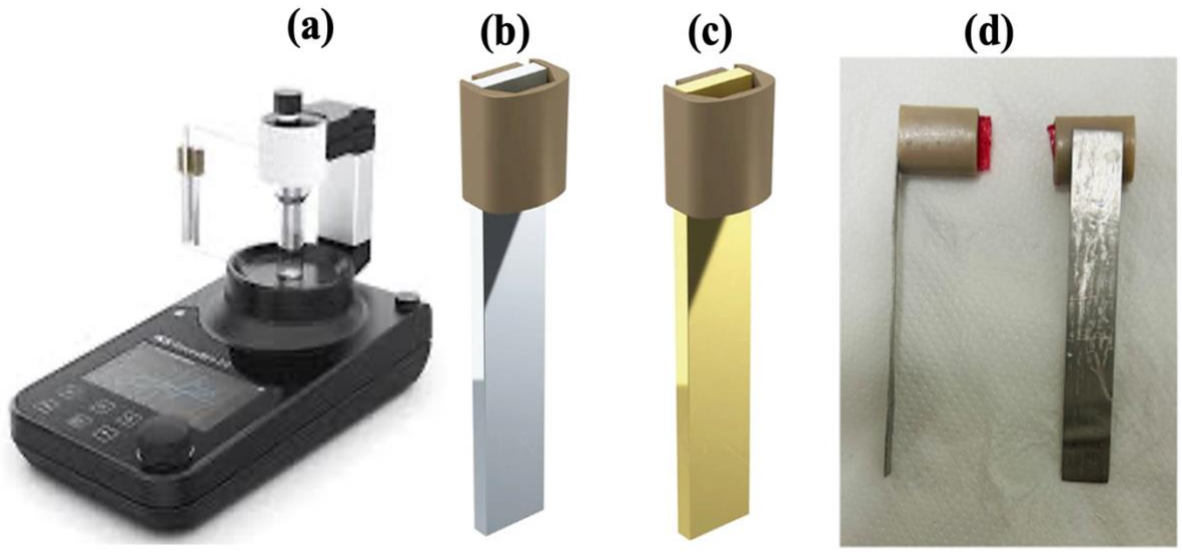


Figure 4-2: (a) ElectraSyn 2.0, (b) Pt-coated copper electrode (c) Au-coated copper electrode and (d) Two non-commercial platinum electrodes

4.3.2 Experimental procedure:

All the Kolbe electrolysis experiments were conducted on lauric acid, palmitic acid, and a mixture of lauric and palmitic acids. Initially, the electrolysis of lauric acid was performed using two commercial electrodes in methanol (MeOH) as the solvent. KOH was used as the supporting electrolyte in all experiments at different equivalent levels. For explanation, when 0.7 mmol of lauric acid was used, the 1 eq. of KOH corresponds to 0.7 mmol or 39.27 mg (molar mass of KOH: 56.1056 g/mol), while 0.4 equivalent (eq.) corresponds to 0.28 mmol or 15.71 mg. KOH was added directly to the solvent and acid/acids solution and was stirred using hot plate for 5-10 minutes at 500 rpm until the solution becomes fully homogeneous. Further investigations were conducted on the electrolysis of lauric acid, palmitic acid, and their 1:1 mixture using a non-commercial electrode. In the mixture experiments, both acids were combined in equal molar proportions; for example, a total of 0.7 mmol of acids consisted of 0.35 mmol each of lauric acid and palmitic acid. This corresponded to masses of 70.105 mg (molar mass of lauric acid: 200.31876 g/mol) and 89.99 mg (molar mass of palmitic acid: 257.42656 g/mol), respectively. When 1.5 eq. of KOH was used for this mixture, it corresponded to 1.05 mmol or 58.91 mg. The mixture was dissolved in various solvents, and

KOH was added according to the equivalent level to investigate its effect on the electrolysis. Next, the vial was connected with the ElectraSyn 2.0 setup, and the experiment was carried out at room temperature with the stirring at 600 rpm at different current intensities. After completion, the mixture was transferred quantitively to a round-bottom flask, and the solvent was evaporated by rotary evaporator. The residues were then treated with acidified water in the separatory funnel to transform carboxylate salts back into corresponding acids and the organic layer was extracted with ethyl acetate. The acetate phase with organic residues was then treated with distilled water until the pH reaches to 7.0. The organic phase was then separated and dried with sodium sulfate and then analysed by gas chromatography-mass spectrometry (GC/MS) to determine the product distribution. The detailed explanation and reaction conditions for each experiment are mentioned in the following part of this chapter. All the experiments were conducted at room temperature in a duplicate trail and the final value was taken as an average.

4.4 Results and discussion:

In these paragraphs, results and discussion of characterization analyses are provided and divided depending on the chemical-physical technique employed.

4.4.1 X-ray Fluorescence Spectroscopy (XRF) assay of Pt-coated-Cu electrode and non-commercial platinum electrode

The commercial Pt-coated-Cu electrode analyzed exhibits a complex composition, comprising a diverse range of elements. Significant constituents include platinum (25.6 mass %), gold (21 mass %), and copper (26.3 mass %). Additionally, the electrode contains notable amounts of phosphorus (17.2 mass %) and nickel (7.31 mass %). Smaller quantities of aluminum, sulfur, zinc, tantalum, thallium, bismuth, and chlorine are also present. The non-commercial electrode was composed of highest mass percentage of 77.5% and phosporus with 19.1%. Smaller amount of electrodes' composition includes aluminum, sulfur, iron, nickel, copper, rhodium, palladium, and tungsten, mercury, calcium, and chlorine. Tabulated results of the components with mass percentage obtained from XRF examination are shown in the **table 4-1.**

Pt-coated-Cu electrode		**Non-commercial platinum electrode**	
Component	**Mass%**	**Component**	**Mass%**
Al	0,734	Al	0,753
S	1,150	S	1,805
Ni	**8,831**	Fe	0,051
Cu	**31,771**	Ni	0,013
Zn	0,067	Cu	0,336
Ta	0,672	Rh	0,054
Pt	**30,926**	Pd	0,025
Au	**25,369**	W	0,528
Tl	0,055	**Pt**	**95,809**
Bi	0,098	Hg	0,037
Cl	0,208	Ca	0,383
-	-	Cl	0,156

Table 4-1: XRF result of Pt-coated-Cu electrode and non-commercial platinum electrode

4.4.3 Scanning Electron Microscopy (SEM) of Pt-coated-Cu electrode and non-commercial platinum electrodes

The SEM analysis provide a comprehensive examination of the surface morphology of the Pt-coated-Cu electrode and non-commercial Pt electrode as shown in **figure 4-3.** The Pt coating has a rather uniform appearance, with slight discrepancies in thickness and roughness. The surface has a granular texture, indicating its polycrystalline nature, with discernible grain boundaries **figure 4-3a-c.** For non-commercial Pt electrodes as shown in **figure 4-3d-f**, at lower magnification, the surface has uniform parallel grooves. At 2.5k X magnification, the grooves are more proper with no visible damage. At high magnification, the surface has smoother layer and fine appearance. Increasing the roughness of the electrode surface and stepped sites leads to an increase in the number of reaction sites. Stepped sites are high surface gradient sites.

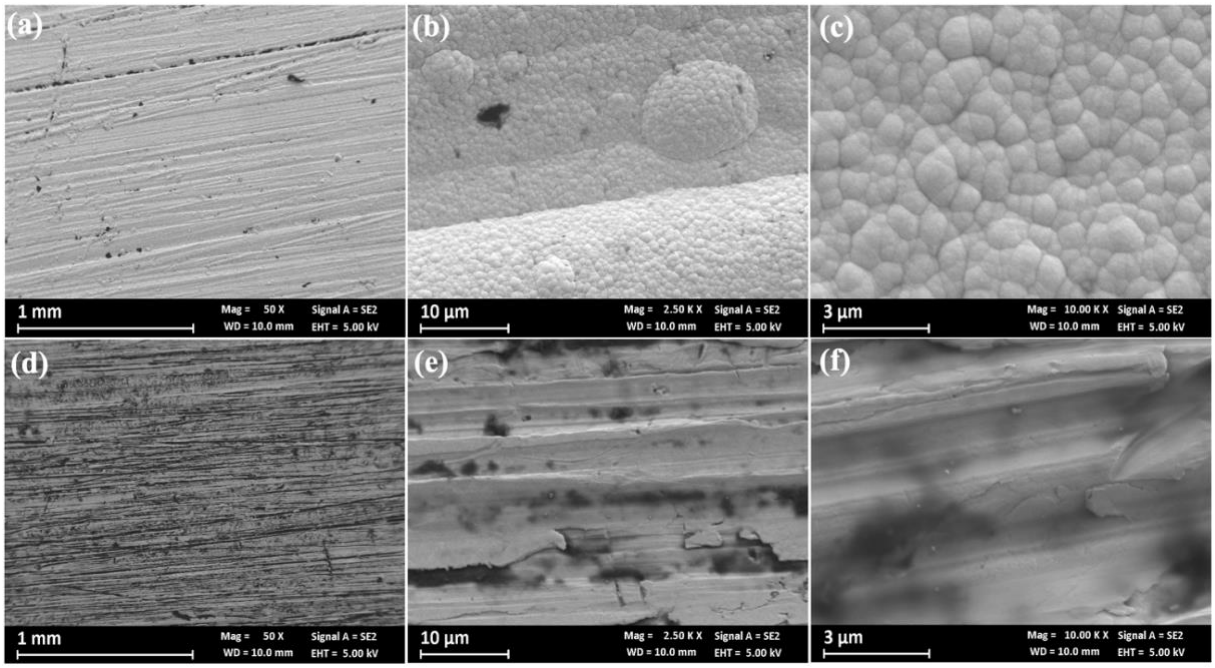


Figure 4-3: SEM images of Pt-coated Copper electrode surface at magnifications of (a) 50 X (b) 2500 X, (c) 10000 X and non-commercial Pt-electrode at magnifications of (d) 50 X (e) 2500 X, (f) 10000 X

4.4.4 Kolbe electrolysis of lauric acid on platinum-coated copper electrodes

A set of experiments was carried out utilizing Pt-coated-Cu electrodes for the decarboxylation of lauric acid, as shown in **table 4-2.**

Entry	Lauric acid	KOH	Current (mA)	Time (h)	Docosane %[a]
1	0.7	1.5	20	3	1
2	0.7	1.5	20	3 AP	4
3	0.4	1.5	20	6 AP	4
4	0.4	1.5	85	6 AP	45
5	0.4	1.5	85	6	4
6	0.7	0.4	85	6 AP	21
7	0.7	0.8	85	6 AP	19
8	0.7	1.0	85	6 AP	14
9	0.7	1.3	85	6 AP	3
10	0.4	1.5	85	6 AP	10

Table 4-2: Experimental parameters and results of Kolbe electrolysis of lauric acid using Pt-coated-Cu electrode, 12 ml MeOH was used in all the experiments, *AP = Alternate polarity every

30 minutes, a % mmol respect to the initial amount of starting material, Experiments of entry 4 and entry 10 were carried out under the same conditions, but entry 10 is the experiment of entry 4 after the electrodes had been utilized for 48 hours

The experiments were carried out with 0.4 or 0.7 mmol of lauric acid in methanol (12 mL) as solvent for 3 or 6 hours, with or without alternate polarity (AP). The amount of desired product was minimal in all the experiments conducted with a lower current, i.e. 20 mA and, as shown in entries 1-3, the unreacted starting material was almost completely recovered. The best result (45%) was obtained when the current was increased to 85 mA by alternating polarity every 30 minutes (entry 4), a much higher yield than without AP (entry 5). Under these conditions the major product obtained was "one electron" Kolbe dimer *n*-Docosane $CH_3(CH_2)_{20}CH_3$ as shown in **figure 4-4.** From these experiments, it was concluded that higher current intensities show effective conversion of lauric acid into Docosane. During the experiment of entry 4, black particles began to appear inside the solution, due to the dissolution of the electrode, as shown in **Figure 4-5 a**. After reaction completion, the colour of the electrode was changed from its original metallic grey as shown in **Figure 4-5 b-c**. The passivation of the electrodes inside the solution during electrolysis experiments provide a proof that electrodes with thin layer of platinum coated on copper might not be useful in high current intensities experiments.

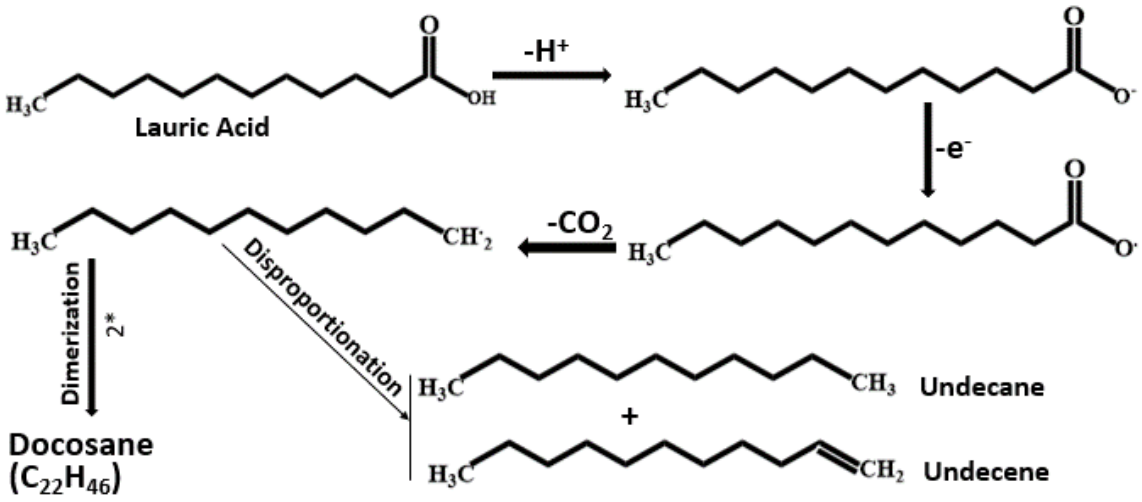


Figure 4-4: Mechanism of Kolbe electrolysis of lauric acid

Once selected the optimal current conditions, the effects of increasing amount of KOH were investigated. Varying amounts of KOH, i.e., 0.4, 0.8, 1 and 1.3 eq. were examined while setting other conditions as follows: lauric acid 0.7 mmol, current: 85 mA and time 6 hours (entries 6-9). As the amount of supporting electrolyte was increased, a downward trend in product yield

(21, 19, 14 and 4 % of Docosane) was observed. Since an increase in electrolyte concentration causes an increase in the current through the cell, it is possible to attribute the slight decrease in product yield to the corrosion of the Pt coating. Moreover, the formation of a substantial amount of several side products was observed. In order to gain information about the performance of the electrodes, the experiment of entry 4 was repeated after the electrodes had been utilized for 48 hours (**Table 4-2, entry 10**). The product yield decreased from 45 % to 10 %, as shown in **Table 4-2.** After 54 hours of electrolysis time, the colour of electrode was totally changed into black.

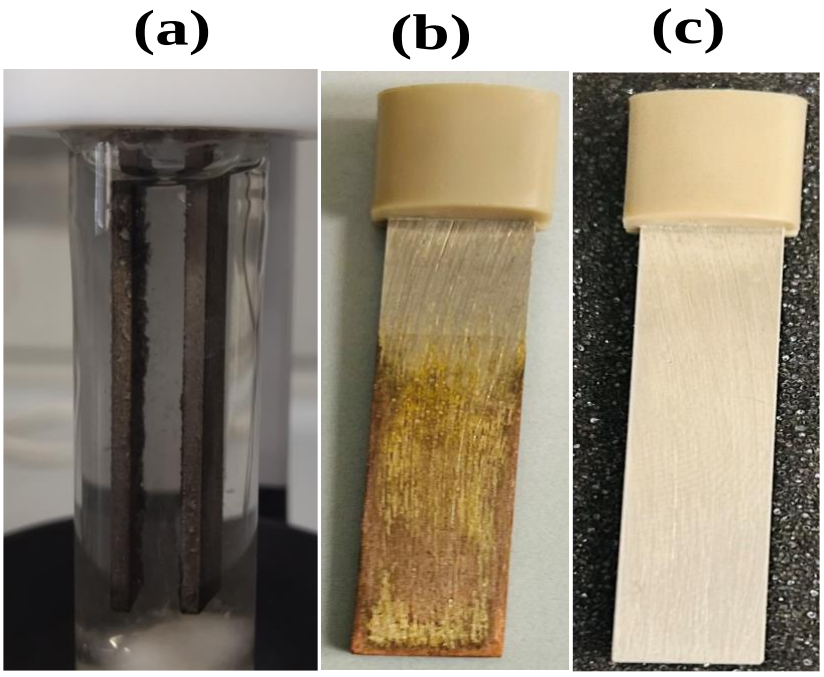


Figure 4-5: Pt-coated copper electrode: (a) black particles appeared during electrolysis (entry 4), (b) corrosion effects after 24 h of electrolysis (the black particles were removed), (c) fresh Pt-coated copper electrode

4.4.5 X-ray diffraction (XRD)

The XRD analysis was performed for the confirmation of the corrosion of electrode. The XRD patterns in **Figure 4-6** refer to used (red) and fresh (black) Pt-coated copper electrodes. The pattern shows the diffraction peaks of platinum at 39.6° and 46.1°, of copper at 43.1° and 50°, and of gold at 38°, 42° and 64.4° 2θ. Surprisingly, a coating of gold is sandwiched between the copper substrate and the platinum coating. These results are in agreement with XRF analysis (**Table 4-1**). The XRD analysis indicates the stability of these commercial Pt-coated copper electrodes was decreased significantly due to electrode dissolution during the electrolysis.

Recently, Ranninger et al., associated the anodic damaging to direct dissolution of Pt in the form of Pt ions [130].

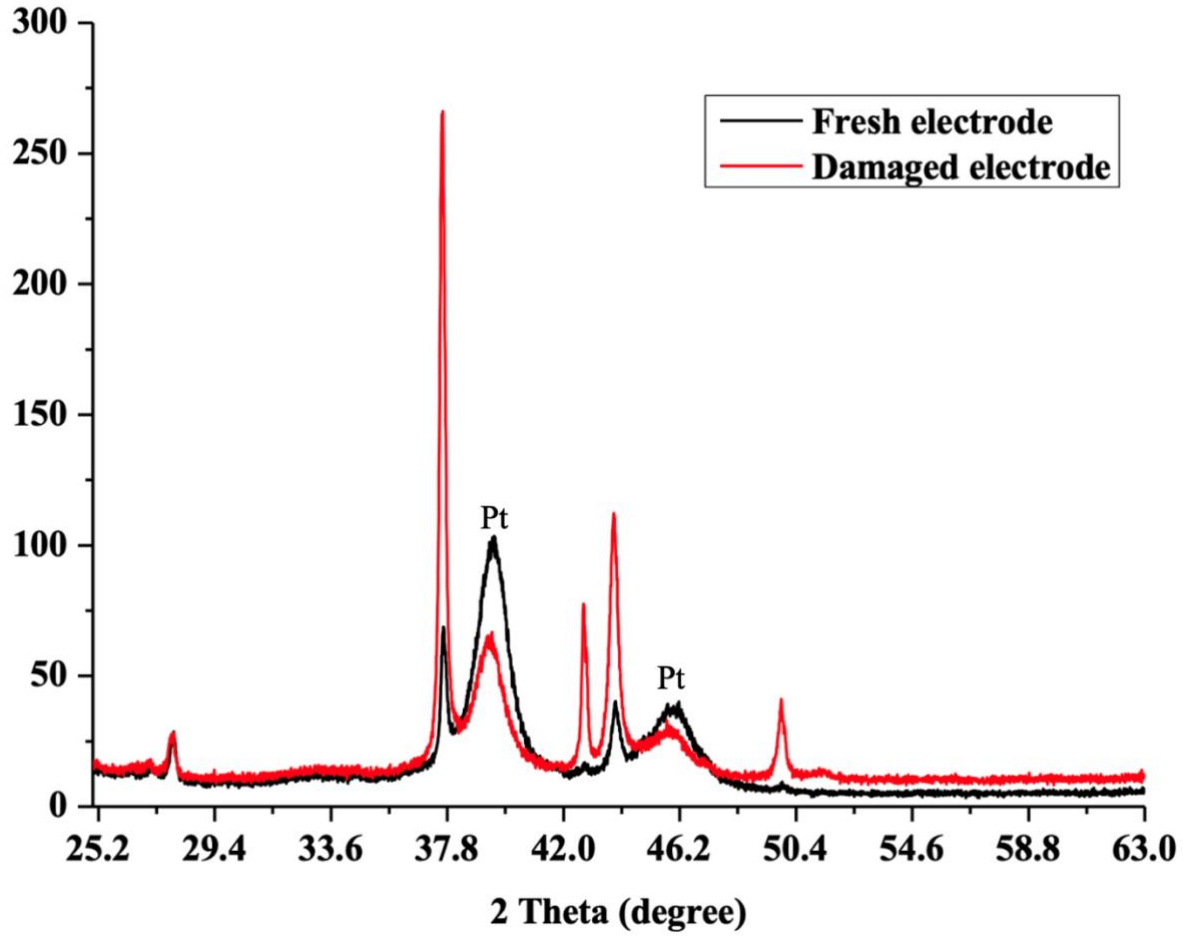


Figure 4-6: X-ray diffraction (XRD) patterns of fresh (black) and damaged (red) Pt-coated copper electrode

4.4.6 Kolbe electrolysis of lauric acid using Au-coated copper electrode

Multiple experiments were carried out to examine the impact of Au-coated copper electrode on the electrolysis of lauric acid, as shown in **table 4-3.**

All the experiments were conducted with either 0.4 or 0.7 mmol of lauric acid and 1.5 eq. of KOH as supporting electrolyte. In the first test, high values of the experimental parameters were used, including a constant current intensity of 85 mA for 6 hours of electrolysis, alternating polarity every 30 minutes. After completion of the experiment, 16 % of *n*-Docosane was formed (entry 1). As expected, no Kolbe product was observed when the current was then reduced below 85 mA to 10 and 20 mA for 3 hours (No. 2-3 and 4).

No	Acid (mmol)	Solvent (12 mL)	Current (mA)	Time (h)	Docosane % [a]
1	0.7	MeOH	85	6 AP	16
2	0.4	MeOH	10	3 AP	0
3	0.4	MeOH	20	3 AP	0
4	0.4	MeOH	20	3 AP	0
5	0.4	MeOH	85	2 AP	6
6	0.4	MeOH	85	2	2
7	0.4	MeOH	85	4 AP	0
8	0.7	MeOH	85	6 AP	4
9	0.4	MeOH	85	2 AP	5

Table 4-3: Experimental conditions and results of Kolbe electrolysis experiments for the decarboxylation of lauric acid using Au-coated copper electrodes, AP* = Alternate polarity after each 20 minutes, a % mmol respect to the initial amount of starting material

When electrolysis was carried out for 2 hours with and without AP, only 6 % and 2 % of yield along with side products were formed (entries 5-6). Worse products yield % was obtained with the Au-coated electrodes compared with Pt-coated electrodes. The result is consistent with observations in the literature on electrooxidation of carboxylic acids suggesting that parasitic Faradaic processes on Au electrodes are easier than on Pt, and, as a consequence, the Faradaic efficiency of gold anode is much lower than that of platinum [131].

In entry 5, black particles appear in the solution, indicating that the anodic dissolution of gold is likely to occur. After completion of the experiments, the particles were collected through filter paper and then analysed through XRD as shown in **Figure 4-7a**. The XRD pattern obtained indicates the presence of gold and copper particles.

The impact of operation time with current intensity of 85 mA was then studied. After using the same electrodes continuously for 23 hours, the performance was noticeably reduced, and the electrode colour completely changed from golden to dark, as shown in **Figure 4-7b**. The experiments 1 and 5 were repeated with the deteriorated electrode, and the yield decreased from 16 % to 4 % and from 6 % to 5 % (entries 8-9). The yield of *n*-Docosane progressively decreased with usage of the electrode. The comparison of the performance of Au-coated electrodes after different time of usage are shown in **Figure 4-8.**

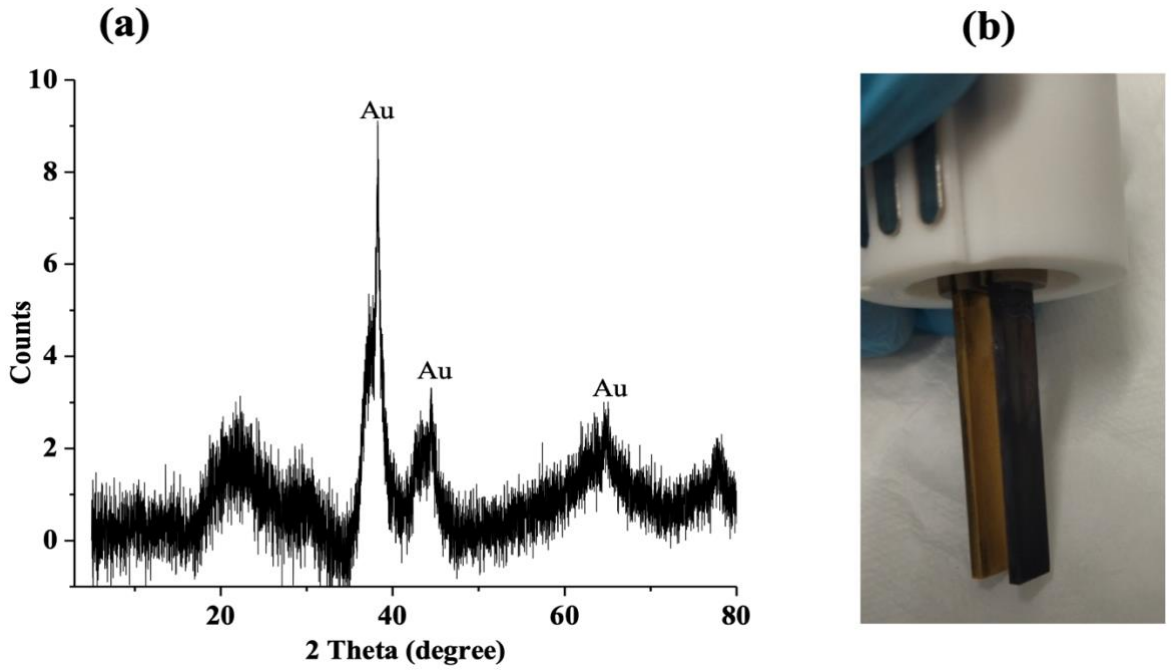


Figure 4-7: Au-coated copper electrodes: (a) XRD of black particles appeared during electrolysis (No. 5), (b) corrosion effects after 23 h of electrolysis

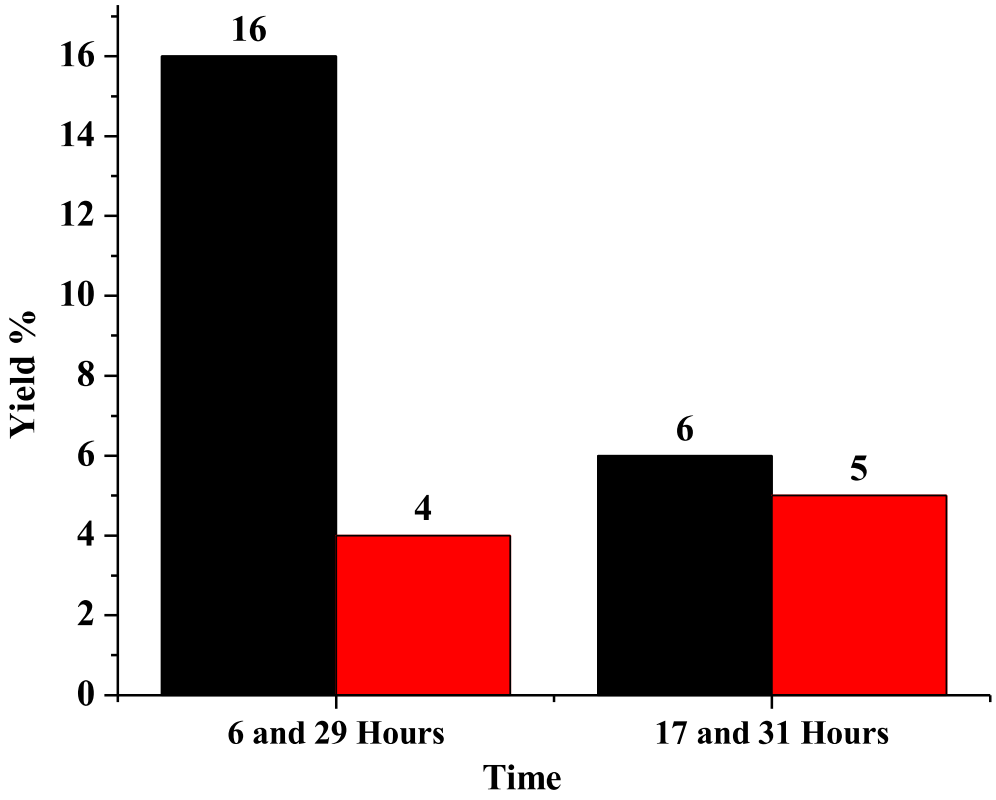


Figure 4-8: Performance of electrodes after 6 and 29 hours (entries 1 and 8 in table 3), 17 and 31 hours (entries 5 and 9 in table 3) of usage. The values of Docosane% is on the top of each histogram.

4.4.7 Kolbe electrolysis of lauric acid using non-commercial platinum electrode

After the corrosion of commercial electrodes, the non-commercial Pt-electrodes were used for all subsequent experiments. Four factors (electrolysis conditions and reaction parameters) were studied for the electrolysis of lauric acid: (1) current intensity; (2) KOH loading; (3) electrolysis duration; and (4) the nature of the solvent. The first set of tests examined the impact of constant current intensity within the range of 10 mA to 100 mA with an alternate polarity (AP) after each 30 minutes. The remaining parameters remained constant, with the following values: 0.7 mmol lauric acid, 0.4 eq. of KOH, MeOH as the solvent, and 6 h for electrolysis. **Figure 4-9 a,** displays a product spectrum that includes the formation of Docosane as a dimer, undecane and undecene as "other hydrocarbons" resulting from the disproportionation of radicals, undecanol as alcohol, and undecanal as aldehydes. Alkene and ester formation is presumably caused by a small degree of carbocation generation known as non-Kolbe or Hofer-Moest reaction. Because a significant quantity of unreacted lauric acid was detected in the product distribution, it was determined that, when employing MeOH as the solvent system at 0.4 eq. of KOH, there was a small conversion rate of lauric acid even at higher current intensities. A small portion of the peaks that were undetected by GC/MS in the trials with current intensities of 70 mA and 85 mA emerged and are named as undetected peaks.

The impact of KOH loading (0.4, 0.7, 1, 1.3, and 1.5 eq.) was then examined while keeping constant the remaining parameters as 0.7 mmol acid, 70 mA of current intensity (AP=30 min), MeOH as the solvent, and a 6h electrolysis time. **Figure 4-9 b** illustrates that using 0.4 eq. of KOH results in a greater dimer yield (19%); nonetheless, overall, the conversion rate was low, with almost 80% of the unreacted acid remaining visible in all experiments. Aldehydes, alcohol, and a lower quantity of other hydrocarbons were also produced.

The next series of experiments were to investigate the effect of electrolysis time from 2-18 h and other conditions were constant like 0.4 eq. of KOH, MeOH as solvent and current intensity of 70 mA (AP=30 min). As shown in **Figure 4-9 c**, using MeOH as a solvent and 0.4 eq. of KOH, the conversion rate was very modest after 8 h or more of electrolysis. Therefore, the impact of different solvent types was investigated in an effort to boost the conversion rate.

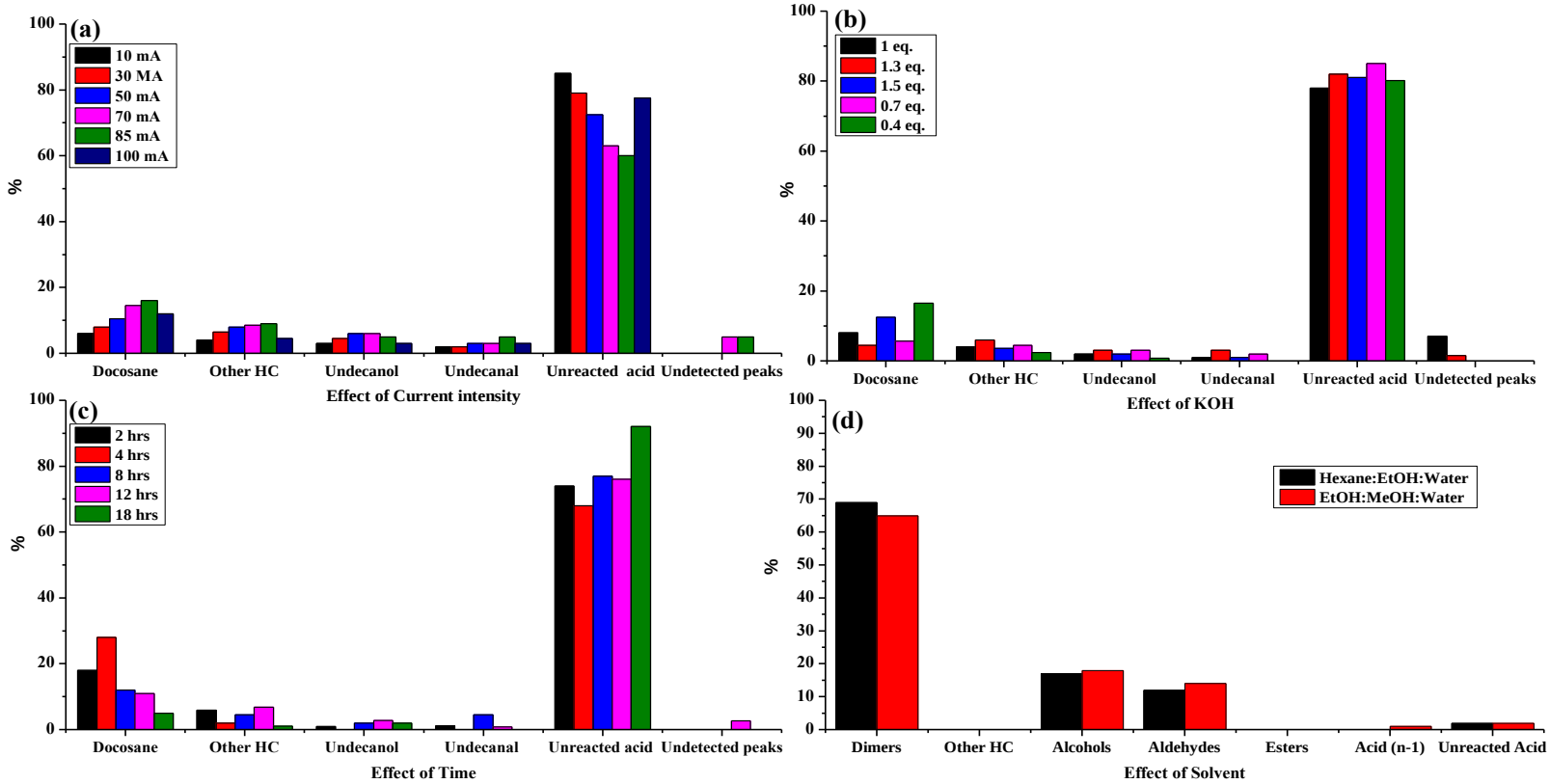


Figure 4-9: Kolbe electrolysis of lauric acid investigating the effect of different parameters (a) effect of current intensity (0.7 mmol lauric acid, 0.4 eq. of KOH, MeOH as the solvent, and 6 h for electrolysis), (b) effect of KOH (0.7 mmol acid, 70 mA of current intensity (AP=30 min), MeOH as the solvent, and a 6h electrolysis time), (c) effect of time (0.4 eq. of KOH, MeOH as solvent and current intensity of 70 mA (AP=30 min)), (d) effect of solvent environment (0.7 mmol acid, a constant current intensity of 70 mA (AP=30 min), and an electrolysis duration of 6 h)

Table 4-4 displays the specifics of each experiment's solvent type, KOH amount, and dimer yield percentage. These studies were all carried out with an acid content of 0.7 mmol, a constant current intensity of 70 mA (AP=30 min), and an electrolysis duration of 6 h. As shown in **Figure 4-9d**, the best results, with the highest dimer yield of 69% and 65%, as well as the highest degree of acid dissociation, were produced using Hexane:EtOH:Water and EtOH:MeOH:Water as solvents, respectively **(table 4-4, entries 8, 9).** The solvent system Hexane:EtOH:Water produces mostly dimers (n-Docosane), accounting for 69% of the product; alcohol (undecanol) accounts for 17%; aldehydes (undecanal) accounts for 12%; and unreacted acids make up a very small percentage. Comparably, larger levels of dimer (n-Docosane) at 65%, alcohols (undecanol) at 18%, aldehydes (undecanal) at 14%, acids (n-1) (undecanoic acid) at 1%, and very few unreacted acids were formed in the EtOH:MeOH:Water solvent system. These results imply that both of these mixtures of solvents are highly efficient in electrolyzing lauric acid, and that the solvents' chemical makeup has a significant impact on the number and diversity of products that are produced.

Entry	Mole	Solvent and proportion %	KOH eq.	Docosane %
1	0.7	MeOH	0.4	25
2	0.7	EtOH	0.4	30
3	0.7	MeOH:EtOH (50:50)	0.4	28
4	0.7	MeOH:EtOH (33.33:66.6)	0.4	25
5	0.7	MeOH:EtOH (25:75)	0.4	27
6	0.7	MeOH:EtOH (75:25)	0.4	29
7	0.7	MeOH:EtOH:H_2O (38.89:38.89:22.22)	0.4	17
8	0.7	MeOH:EtOH:H_2O (16.67:16.67:66.67)	1.5	65
9	0.7	Hexane:EtOH:H_2O (38.89:38.89:22.22)	1.5	69

Table 4-4: Reaction conditions and resulting dimers percentage for investigating the effect of solvent nature on the electrolysis of lauric acid

Figure 4-10 shows the GC/MS result of electrolysis of lauric acid in Hexane:EtOH:Water (38.89:38.89:22.22%) and MeOH:EtOH: Water (16.67:16.67:66.67%) solvent systems. For Hexane:EtOH:Water system, the retention times 4.820, 5.178 and 8.732 shows undecanal, undecanol and Docosane respectively. For EtOH:MeOH:Water system, the retention times 4.809, 5.169 and 8.742 shows undecanal, undecanol and Docosane respectively. The retention

times are automatically generated by OriginPro software and little peaks for lauric acid at 6.220 and for undecanoic acid at 8.410 cannot be detected.

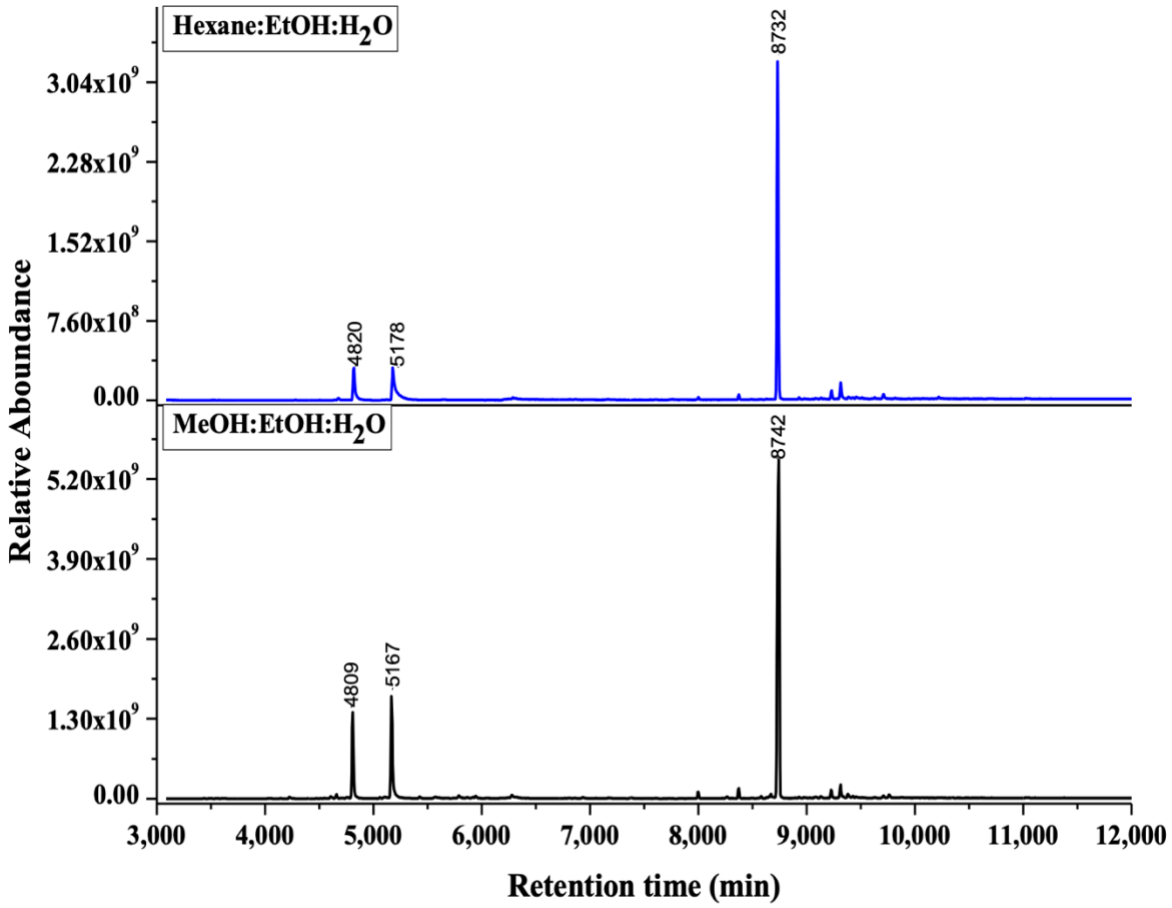


Figure 4-10: GC/MS result of electrolysis of lauric acid in Hexane:EtOH:Water (38.89:38.89:22.22%) and MeOH:EtOH: Water (16.67:16.67:66.67%) solvent systems

4.4.8 Kolbe electrolysis of palmitic acid:

Once the reaction conditions were fixed from the electrolysis of lauric acid, the same parameters were applied to the electrolysis of palmitic acid. **Table 4-5** displays the specifics of the reaction conditions for the electrolysis of palmitic acid.

Entry	Mole	Solvent%	KOH eq.
1	0.7	EtOH:MeOH:H_2O (16.67:16.67:66.67)	1.5
2	0.7	Hexane:EtOH:H_2O (38.89:38.89:22.22)	1.5
3	0.7	EtOH:H_2O (66.67:33.33)	1.7

Table 4-5: Experimental conditions for the electrolysis of palmitic acid

Figure 4-11 displays the product distribution formed after an electrolysis of palmitic acid. Dimers make up the majority of the product in the MeOH:EtOH:Water solvent system, with

23%, followed by "other hydrocarbons" (19.5%) and alcohols (18%). The Hexane:EtOH:Water system produces 15% of dimers and 30% of other hydrocarbons. The larger percentages of dimers (9%), alcohol (20%), and aldehydes (21.79%) are produced in the EtOH:Water solvent environment. Since the solution was not homogenous, as indicated in **Table 4-5** (entry 3), the quantity of KOH was raised from 1.5 eq. to 1.7 eq. These results led to the conclusion that the selectivity and distribution of a particular product are significantly influenced by the nature of the solvent. Zhang et al. investigated the electrolysis of palmitic acid using platinum foil electrodes and biphasic solvent system (H_2O:MeOH:petroleum ether) with 1.5 eq. of KOH achieved 27% of dimers yield [132].

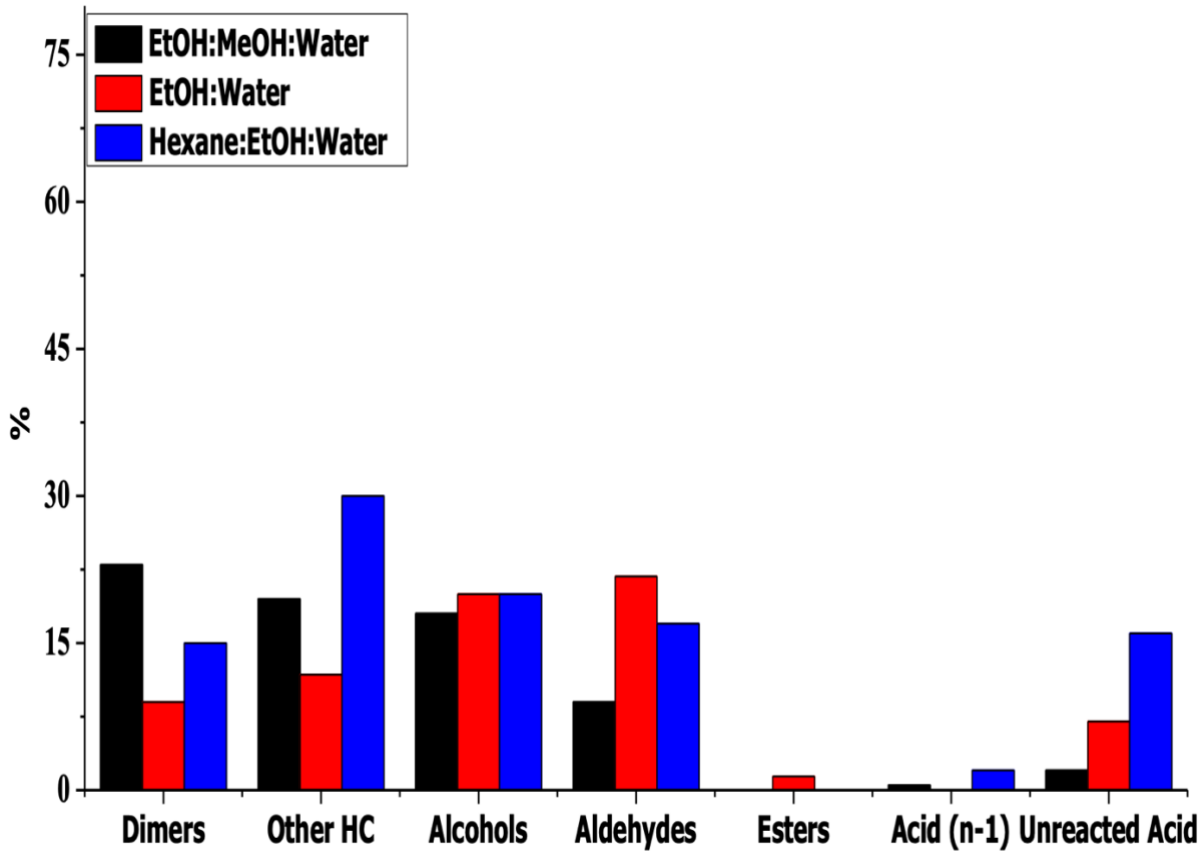


Figure 4-11: Product distribution of electrolysis of palmitic acid using different solvent environments. The experimental conditions for each entry are as follows, Time = 6 hours, current intensity = 70 mA, 1.5 eq. of KOH for EtOH:MeOH:H_2O and Hexane:EtOH:H_2O while 1.7 eq. for EtOH:H_2O solvent system

A solvent system with a greater water content and a lower alcohol content produces a larger percentage of dimers, whereas a solvent system with a high alcohol content and a low water content produces a higher concentration of alcohol and aldehyde. The details of the observed products analysed by GC/MS and their retention times are shown in **Table 4-6 (Figure 4-12).**

Product	Product name (Retention time)	Chemical Formula
Dimer	Triacontane (12.59)	$C_{30}H_{62}$
Other Hydrocarbon	Pentadecene (5.774)	$C_{15}H_{30}$
Other Hydrocarbon	Pentadecane (5.811)	$C_{15}H_{32}$
Other Hydrocarbon	Hexadecane (6.298)	$C_{16}H_{34}$
Other Hydrocarbon	Tetradecane (6.01)	$C_{14}H_{30}$
Alcohol	Pentadecanol (5.81)	$C_{15}H_{32}O$
Alcohol	Hexadecanol (6.85)	$C_{16}H_{34}O$
Unreacted acid	Palmitic acid (7.88)	$C_{16}H_{32}O_2$
Aldehyde	Pentadecanal (7.13)	$C_{15}H_{30}O$
Aldehyde	Hexadecanal (6.65)	$C_{16}H_{32}O$
Esters	Pentadecanoic acid, methyl ester (7.58)	$C_{16}H_{32}O_2$
Acid (n-1)	Pentadecanoic acid (7.43)	$C_{15}H_{30}O_2$

Table 4-6: Summery of products observed from the electrolysis of palmitic acid

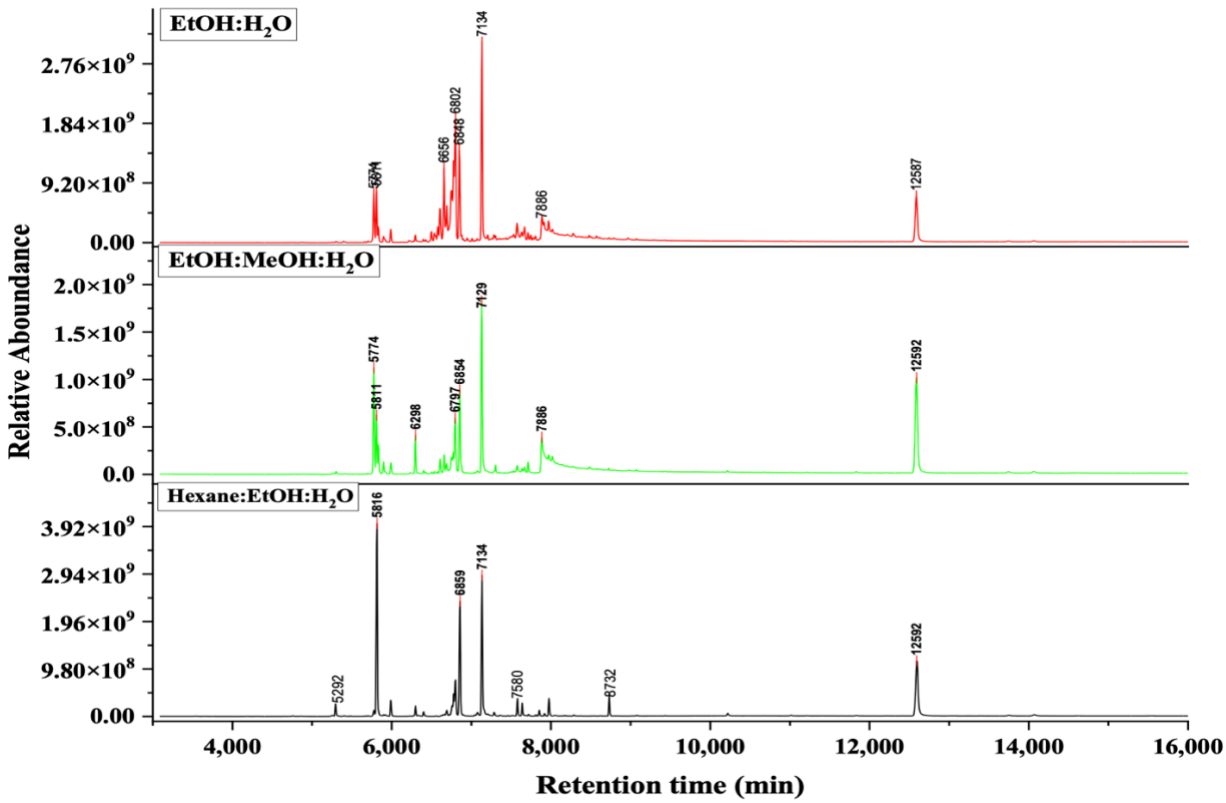


Figure 4-12: GC/MS spectra pf the product distribution after electrolysis of palmitic acid in EtOH:MeOH:H2O, Hexane:EtOH:H2O and EtOH:H2O solvent systems

4.4.9 Kolbe Electrolysis of Mixture of lauric and palmitic acids:

Following the conclusion of the lauric acid and palmitic acid electrolysis tests, the two acids were mixed ratio (1:1) to examine the distribution trend of the products, particularly the formation of dimers. **Table 4-7** displays the experimental parameters as well as the dimer yield (%) of Docosane, triacontane and Hexacosane.

Entry	$mmol_{total}$	Solvent%	KOH eq.	Current mA	Dimer %
1	0.7	Hexane:EtOH:H_2O (38.89:38.89:22.22)	1.5	70	32.2
2	0.7	MeOH:EtOH:H_2O (16.67:16.67:66.67)	1.5	70	45
3	0.7	EtOH:H_2O (66.67:33.33)	1.7	70	10.4

Table 4-7: Reaction conditions for the electrolysis of mixture of acids C12:C16 (1:1), $mmol_{total}$ is the combine molar amount of both acids (0.35 mmol each)

As expected, a broad spectrum of product distribution was observed when using a mixture of acids as compared to single acid electrolysis because of the higher possible combination of formed radicals. When using the mixture of acids, the dimers were formed either by homocoupling i.e., a combination of radicals of the same chain length or by hetero-coupling i.e., a combination of radicals of two different chain lengths. The dimers Docosane ($C_{22}H_{46}$) and triacontane ($C_{30}H_{62}$) were formed by the combination homocoupling of $C_{11}H_{23}^{\bullet}$ and $C_{15}H_{31}^{\bullet}$ radicals, respectively, and Hexacosane was formed by hetero-coupling of $C_{11}H_{23}^{\bullet}$ and $C_{15}H_{31}^{\bullet}$ radicals as shown in **figure 4-13.**

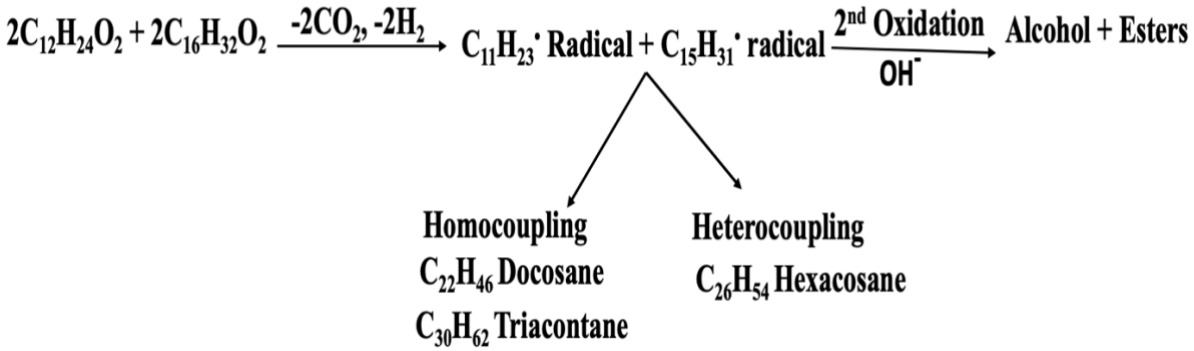


Figure 4-13: Representation of the formation of dimers as a result of homocoupling and hetero-coupling of radicals of lauric and palmitic acid mixture

The product formation and their percentage are shown in **Figure 4-14**. In the EtOH:MeOH:Water solvent system, a notably high percentage 45% of dimers were produced

followed by alcohols at 19.6%, other hydrocarbons at 17.7% and aldehydes at 10%. A very little percentage of esters and acids (n-1) were also formed. On the other hand, in the EtOH:Water system, alcohols were the most dominant with 31.4% and a lower number of dimers at 10.4%. This might suggest that the absence of MeOH discourages dimer formation and leads to the higher formation of alcohols and aldehydes. Lastly, the Hexane:EtOH:Water system leads to the substantial formation of dimers 32.2% and also a significant number of alcohols 25.4%. Based on these observations, the MeOH:EtOH:Water solvent system is the most efficient choice for dimers production from the mixture (1:1) of lauric and palmitic acids. Neubert et al., findings show that using artificial mixture of acids (butyric acid: hexanoic acid: octanoic acid) in 3:8:1 molar ratio at 150 mA/cm^2 of current density gives alkane production of 55 + 10% and acid degradation with columbic efficiency of around 82% [133]. Therefore, understanding these variations in experimental conditions is important in optimizing the electrolysis process to explore reaction scalability and potential for industrial applications. The details of the products observed from GC/MS analysis after the electrolysis of mixture of lauric, and palmitic acid are shown in **Table 4-8 (Figure 4-15).**

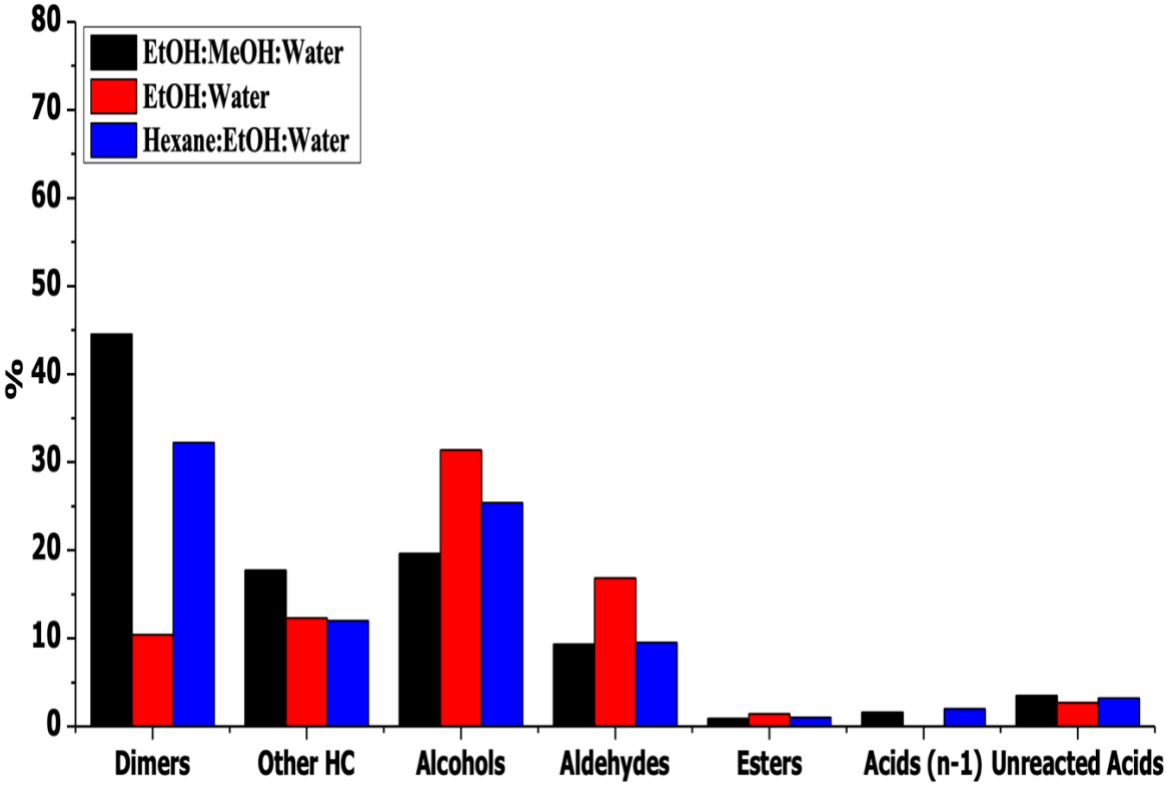


Figure 4-14: Product distribution of electrolysis of mixture of lauric and palmitic acid (1:1) using different solvent environments

Product	Product name (Retention time)	Chemical Formula
Dimers	Docosane (8.72)	$C_{22}H_{46}$
-	Triacontane (12.59)	$C_{30}H_{62}$
-	Hexacosane (10.21)	$C_{26}H_{54}$
Other hydrocarbon	Undecene (3.43)	$C_{11}H_{22}$
-	Undecane (3.45)	$C_{11}H_{24}$
-	Pentadecane (5.80)	$C_{15}H_{32}$
-	Pentadecene (5.77)	$C_{15}H_{30}$
-	Tetradecane (6.6)	$C_{14}H_{30}$
-	Hexadecane (5.9)	$C_{16}H_{34}$
Alcohols	Undecanol (4.75)	$C_{11}H_{24}O$
-	Pentadecanol (7.13)	$C_{15}H_{32}O$
-	Hexadecanol (6.5)	$C_{16}H_{34}O$
-	Tetradecanol (5.9)	$C_{14}H_{30}O$
-	Undecanal (4.8)	$C_{11}H_{22}O$
-	Pentadecanal (6.7)	$C_{15}H_{30}O$
Esters	Pentadecanoic acid-methyl ester (7.5)	$C_{16}H_{32}O_2$
-	Undecanoic acid methyl ester (6.6)	$C_{12}H_{24}O_2$
Acid (n-1)	Pentadecanoic acid (6.31)	$C_{15}H_{30}O_2$
-	Undecanoic acid (4.9)	$C_{11}H_{22}O_2$

Table 4-8: Summery of product observed from the electrolysis of mixture of lauric and palmitic acids

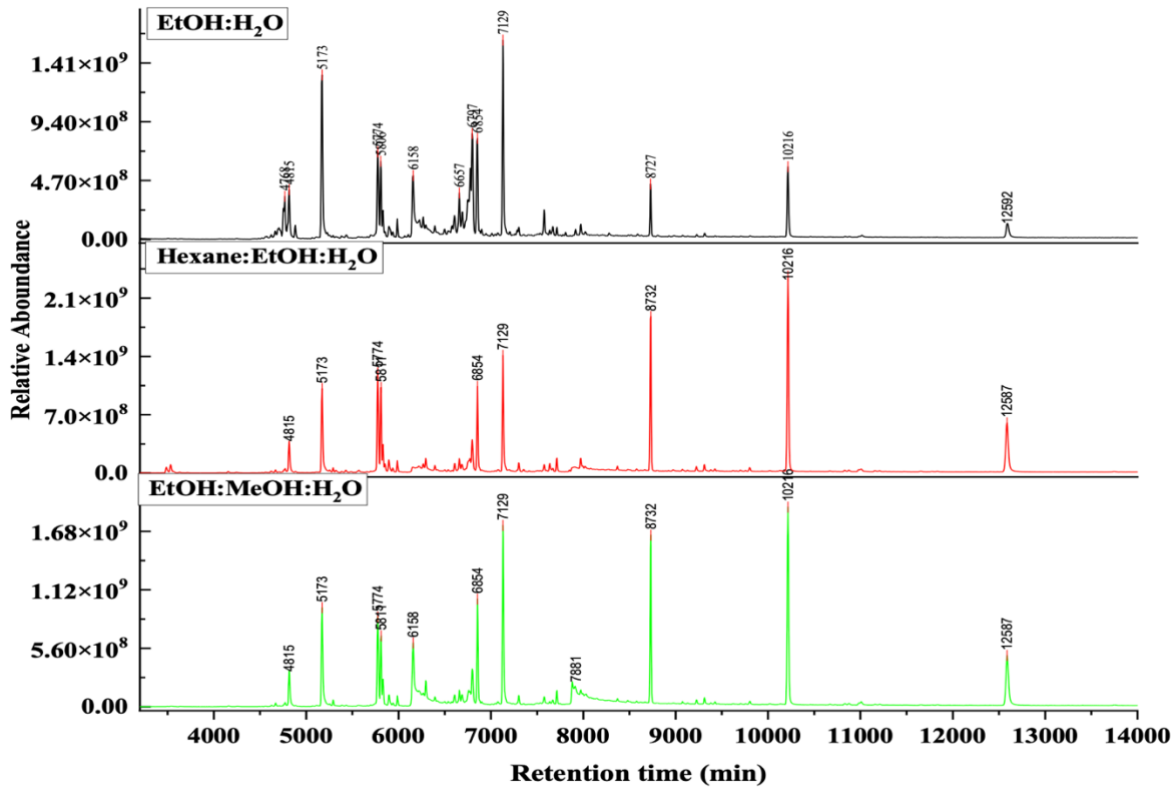


Figure 4-15: GC/MS spectra pf the product distribution after electrolysis of mixture of lauric acid and palmitic acid in EtOH:MeOH:H_2O, Hexane:EtOH:H_2O and EtOH:H_2O solvent systems

4.4.10 Effect of time on the electrolysis of mixture of acids:

The time study was conducted in order to investigate the trend of product formation from the starting time of electrolysis. All the experiments were conducted in MeOH:EtOH:H_2O (16.67:16.67:66.67%) solvent system. As shown in **Figure 4-16,** it can be observed that the product formation other than dimers appeared form the start of the reaction. It is shown that with the increase in time, the unreacted acid decreases from 89.2% to 3.5% after 6 hours of electrolysis, indicating the dissociation and progress of acids. Correspondingly, there is an increase in production of dimers, from 7.7% at 0.5 hours to 44.5% after 6 hours of electrolysis time. Other products like alcohols and aldehydes also shows an increasing trend with electrolysis time but lesser than dimers. The ester formation appears at 4 hours of electrolysis while acid (n-1) formation starts at 6 hours of electrolysis. All the products formation after different electrolysis duration are shown in **Table 4-9** and the GC/MS spectra of some experiments are shown in **Figure 14-7.**

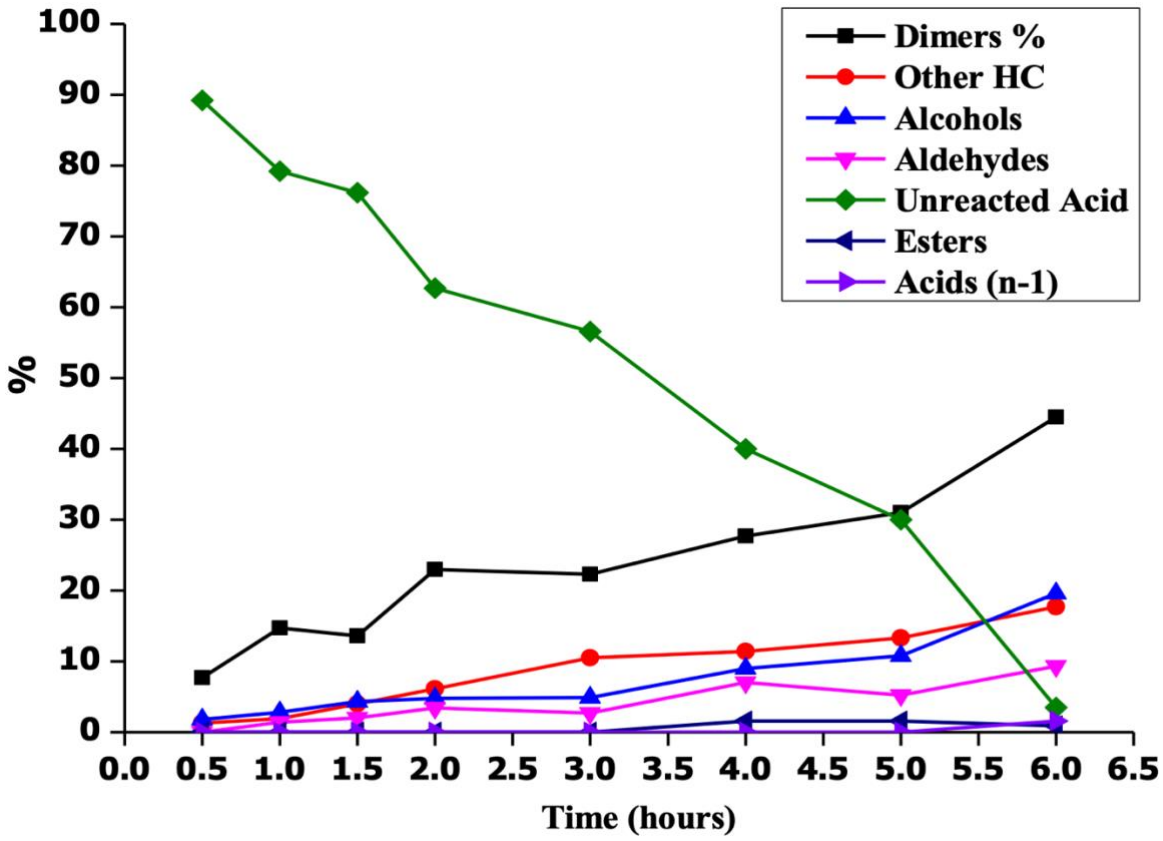


Figure 4-16: Product distribution of the electrolysis of mixture of acids with time of electrolysis, Other HC are hydrocarbons other than dimers

This trend suggests that as the time of electrolysis increases, a shift towards more complex products appears. This is because of the mix nature of acids, more radical's availability and electrochemical environment which favors certain products over others. The longer electrolysis time can lead to the higher yield of desired products such as dimers in this case, but at the same time, other products like aldehydes and alcohols formation also increases. Therefore, optimization of electrolysis time is very crucial for achieving the balance between selectivity, yield and efficiency

Product	Formula	Electrolysis time (hours)							
		0.5	1	1.5	2	2.5	3	4	5
Undecane/undecene	$C_{11}H_{24}$ / $C_{11}H_{22}$	-	0,5/0,6	1,3/0,9	-	0,6/0,6	-	0,7/0,7	0,5/0,5
Undecanal	$C_{11}H_{22}O$	-	-	0,5	0,9	1,4	1	3	1,5
Undecanol	$C_{11}H_{24}O$	0,6	0,9	1,8	0,9	4,2	2,5	4,2	4,4
Pentadecane	$C_{15}H_{32}$	0,7	0,3	0,8	3,2	5	1,9	5	6,6
Pentadecene	$C_{15}H_{30}$	0,6	0,5	1	2,9	5	2,8	5	5,7
Pentadecanal	$C_{15}H_{30}O$	-	1,4	1,5	2,5	2,4	1,7	4	3,7
Pentadecanol	$C_{15}H_{32}O$	-	1,9	2,5	3,9	5,1	2,4	4,8	6,4
Lauric acid	$C_{12}H_{24}O_2$	64,6	63,2	53,8	57,3	41	33,7	32	22
Palmitic acid	$C_{16}H_{32}O_2$	24,6	16	22,3	5,4	6,4	22,9	8	10
Docosane	$C_{22}H_{46}$	2,2	5,3	3,5	6,9	9,6	8	7,2	10
Hexacosane	$C_{26}H_{54}$	4,2	6,8	6,8	11,3	15,7	10,4	13,5	15
Triacontane	$C_{30}H_{62}$	1,3	2,6	3,3	4,8	7,3	3,9	7	6
Hexadecane	$C_{16}H_{34}$	-	-	-	-	-	5,8	-	-
Undecanoic acid, methyl ester	$C_{12}H_{24}O_2$	-	-	-	-	-	-	0,8	0,5
Pentadecanoic acid, methyl ester	$C_{16}H_{32}O_2$	-	-	-	-	-	-	0,8	0,6
Sum undetected peaks	-	-	-	-	-	1,7	3	3,3	6,6

Table 4-9: Product distribution of mixture of acids (1:1) and their percentage with respect to electrolysis time

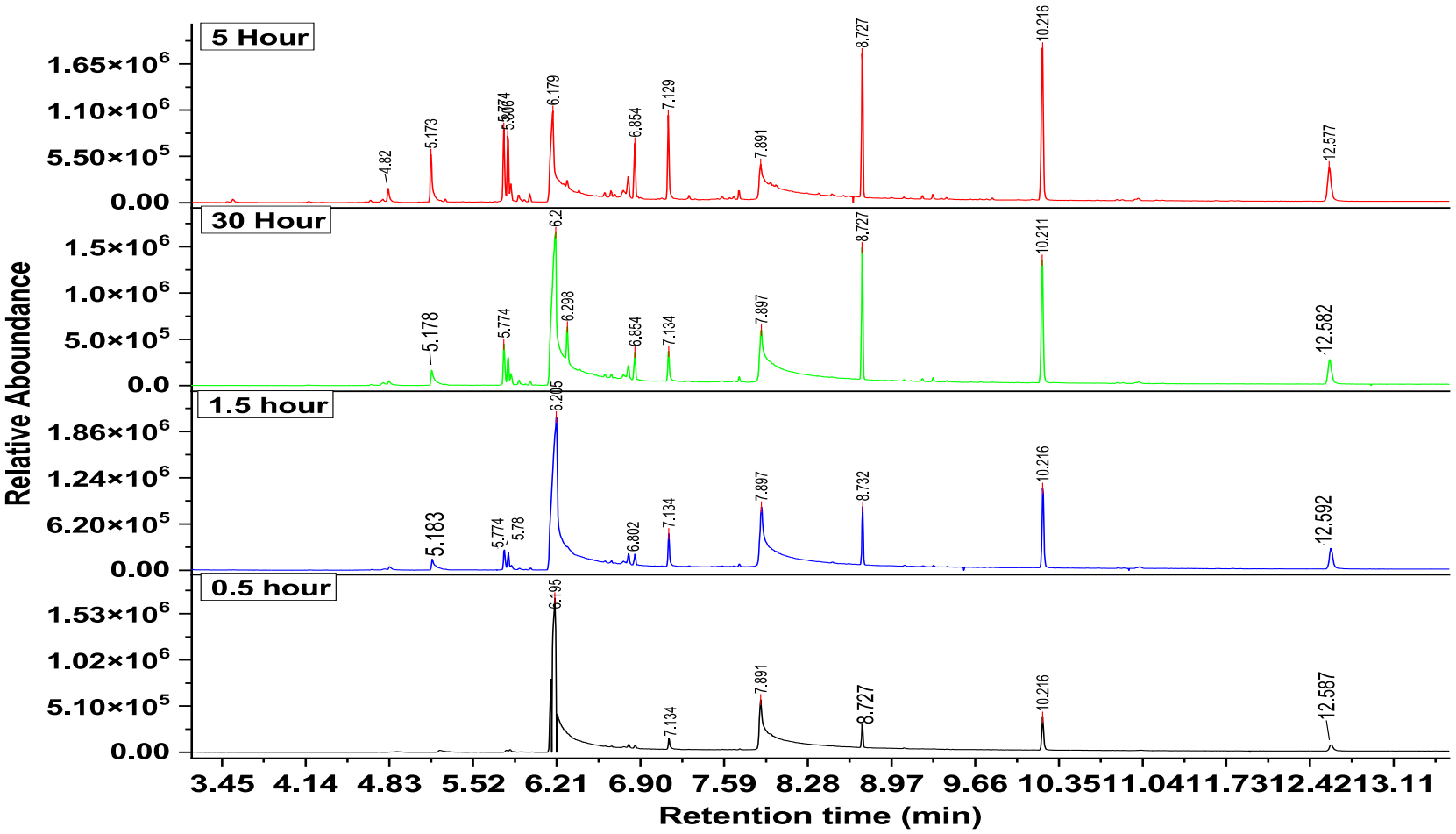


Figure 4-17: GC/MS spectra of the product distribution after different time of electrolysis

4.5 Conclusion:

This study demonstrated that an efficient process of electrochemical oxidation of lauric acid by Kolbe coupling reaction with 45% product yield of *n*-docosane can be conducted using Pt-coated copper electrodes. However, the service life of the Pt-coated copper electrode is short (< 30 h), because of surface corrosion effects. The performance for Au-coated copper electrodes was lower than that of Pt-coated electrodes. The study also shows that Pt-coated copper electrode and Au-coated copper electrodes with a layer thickness of 400-600 µm might not be useful for electrosynthesis experiments using high current intensities.

The study also shows a safe and green electrochemical approach for the production of useful chemical products using non-commercial Pt electrodes. The bio-based fatty acids lauric acid and palmitic acid are converted into hydrocarbons and other useful chemical products by electrochemical technique. The electrolysis of single lauric acid, palmitic acid, and a mixture of both acids through Kolbe electrolysis gives 65%, 23% and 45% of dimers hydrocarbons respectively. Using non-commercial platinum electrodes, the Kolbe electrolysis in MeOH:EtOH:H_2O (16.67:16.67:66.67) solvent system shows nearly full dissociation of the substrate acids into useful chemical products like alcohols, aldehydes, and other hydrocarbons with shorter chain then dimers.

Chapter 5 Electrolysis of mixture of fatty acids, derived from coconut and palm oil

In this chapter, the base hydrolysis of coconut oil for the collection of free fatty acids and their subjection to Kolbe electrolysis are presented. The series of fatty acids were collected after base hydrolysis of coconut and palm and then subjected to the Kolbe electrolysis to produce other chemical products. Different experimental parameters were applied to investigate the product trend especially the hydrocarbons formation. Before the description of the experimental part and discussion of the main results, short highlights of the research activities and an introduction about the Kolbe electrolysis is presented. Materials and instrumentations for characterization were reported in the chapter 3.

5.1 Highlights of research activities

This chapter contains the following research activities.

(a) Analysis of coconut oil using GC/FID to investigate the nature and composition of coconut and palm oils.
(b) Base hydrolysis of coconut and palm oil to isolate fatty acids.
(c) Kolbe electrolysis of a complex mixture of fatty acids derived after base hydrolysis of coconut and palm oil to produce hydrocarbons and other chemicals.

5.2 Introduction

Fossil fuel sources are limited, making a future mismatch between their availability and demand, particularly with the rising global population and living standards. To address these challenges, alternative energy technologies have already been developed and continue to be refined. These innovations rely on renewable resources such as biomass, which includes both solid and liquid biofuels and solar and wind power energies [134].

Beyond the energy sector, the production of chemicals is also transitioning from petrochemical-based processes to bio-based approaches to promote sustainable resource management. Established bio-based processes include the production of acetate, as well as the fermentation

of ethanol, n-butanol, and 2,3-butanediol, using biomass or syngas as substrates [135], [136], [137]. Currently, n-carboxylic acids and their salts (n-carboxylates) have been recognized as key components which are mainly obtained from vegetable oils or biomass. The n-carboxylic acids have potential applications as precursors for electrochemical hydrocarbon platform chemicals [138].

In recent years, the production of hydrocarbons from biomass, are referred as green diesel or renewable diesel. Several technical methods are used to convert vegetable oils or biomass into hydrocarbons directly or through coupling electrochemical methods. For example, Hydrotreatment typically occurs at temperatures between 300°C and 450°C under hydrogen pressures of 4 to 15 MPa, using sulfide or noble metal catalysts resulting in hydrocarbons primarily in the C_{15} to C_{18} range [139]. Catalytic cracking, on the other hand, operates at 350°C to 500°C under atmospheric pressure, using catalysts such as zeolite, Al_2O_3, and MgO producing hydrocarbons with a wide range of carbon chain lengths [140], [141], [142]. However, both methods face challenges that limit product yield and selectivity [143]. Other techniques which are used for the formation of carboxylic acids from biomass and then coupled with electrochemical methods to convert acids into hydrocarbons. For example, Hydrolysis of vegetable oil is carried out at high temperatures (200–250°C) with 1–5 MPa pressures, where triglycerides react with water to produce free fatty acids and glycerol. However, its applicability to vegetable oils and animal fats especially those containing multiple/conjugated double bonds and hydroxyl groups (castor oil and fish oil, for example) is limited because at high temperature they undergo undesired thermal decomposition [144]. Thermal cracking decomposes oils at elevated temperatures (350–500°C) and atmospheric pressure to produce a mixture composed of fatty acids and hydrocarbons [145]. Microbial fermentation utilizes specific bacteria or fungi to convert biomass into fatty acids under controlled conditions of temperature (30 - 40 °C) and pH (5.5–7.0) [146]. Saponification occurs under alkaline conditions (typically using NaOH or KOH) at temperatures around 80–100°C, breaking triglycerides into glycerol and fatty acid salts [147]. Saponification is a cost-effective and straightforward process that operates under mild conditions, reducing energy requirements. Additionally, it does not require expensive catalysts or high-pressure equipment, making it ideal for large-scale and economical fatty acid production [148].

This chapter discribes the investigation of coconut and palm oils through a detailed analysis of GC/FID to characterize their fatty acid methyl ester (FAME), sterols and di/triglycerides profiles, providing a baseline for further processing. The GC/FID analyses were performed at the Innohub laboratory in Milan, Italy. Subsequently, base hydrolysis was performed on both

oils to effectively convert the triglycerides into their respective free fatty acids. The resulting fatty acid mixtures were then subjected to Kolbe electrolysis, a key experimental procedure aimed at producing value-added hydrocarbons and green chemicals.

5.3 Experimental part

5.3.1 Base hydrolysis of coconut and palm oil

Base hydrolysis reaction was performed for converting oil into fatty acids. Before the base hydrolysis step, the nature and composition of the coconut and palm oil was analyzed using GC-FID. The purpose of GC-FID analysis was to get the baseline information and to identify the nature and major components of both oils, including fatty acid profile sterols, and mono-, di-, and triglycerides. For the base hydrolysis reaction, 25 g of coconut/palm oil was taken and melted at 50 ^{o}C for 5 minutes and then 10 mL of EtOH was added and mixed using magnetic stirrer. 11% w/v of KOH (5.5 g) in 50 mL aqueous solution was prepared and added to the oil. The hydrolysis reaction occurred under reflux at 600 rpm and 110 ^{o}C for 1.5 - 2 hours, following the reported methodology with little modifications [149]. After the hydrolysis reaction completes, the mixture (having KOH, EtOH, unsaponifiable and fatty acids salts) were cooled until the fatty acid salts were completely precipitated. Next, n-hexane (30 mL) was added, and the aqueous phase was separated. The aqueous phase was then acidified with 1 M (M=mol dm^{-3}) HCl (37 %) until the pH of the solution reached to 1.0 and then with distilled water to reach the pH to 7. The generated fatty acids mixture was then dried with the help of anhydrous sodium sulfate (Na_2HSO_4) and then filtered to isolate pure fatty acid mixture. The obtained fatty acids were then characterized by GC/MS. The fatty acids obtained from the coconut oil were (1) Octanoic acid ($C_8H_{16}O_2$), (2) Decanoic acid ($C_{10}H_{20}O_2$), (3) Dodecanoic acid ($C_{12}H_{24}O_2$), (4) Tetradecanoic acid ($C_{14}H_{28}O_2$), (5) Hexadecanoic acid ($C_{16}H_{32}O_2$) and (6) 9-Octadecanoic acid (E) ($C_{18}H_{34}O_2$) and from palm oil were (1) Hexadecanoic acid ($C_{16}H_{32}O_2$) and (2) 9-Octadecanoic acid (E) ($C_{18}H_{34}O_2$).

5.3.2 Kolbe elctrolysis on the mixture of fatty acids derived from oil (Experimental setup)

All Kolbe electrolysis experiments on the mixture of fatty acids obtained from both oils were performed using a commercially available ElectraSyn 2.0 (IKA®) system, as discussed in chapter 4. All the experiments were conducted at galvanostatic controlled system using three

electrode steup consisting of non-commercial platinum electrodes as working and counter electrode (5 mm costom adjusted electrode gap) and an an Ag/AgCl 3 M KCl reference electrode (available with instrument). The complete details of composition analysis by XRF and surface analysis by SEM of non-commercial electrodes are explained in chapter 4. All the experiments were conducted in duplicate trials and after each experiment, electrodes were thoroughly cleaned using distilled water and acetone.

5.3.3 Preparation of electrolyte solution for Kolbe electrolysis

The mixture of fatty acids system (derived from base hydrolysis of coconut and palm oil) were then subjected to Kolbe electrolysis to investigate to products formation trend. In a detailed procedure, 1 gram sample of the mixture of fatty acids system was taken in a 20 mL vial (available with the instrument) with different solvent systems. The molar amounts of each acid were calculated based on their percentage composition in the mixture known from the GC/MS results. For coconut oil, for example, decanoic acid, comprising 10.5% of the mixture, contributed 0.105 g, which was converted to moles using its molar mass (172.27g/mol), resulting in 0.000586 mol. Similarly, the molar amounts of all other acids were calculated in the same way. KOH as a supporting electrolyte was added according to 100% neutralization (0.236 g, 4.21 mmol, 0.2105 mol/L), considering a stoichiometric reaction with all acid molecules in the mixture. For palm oil, hexadecanoic acid, comprising 47.5% of the mixture, contributed 0.475 g, which was converted to moles using its molar mass (256.42 g/mol), resulting in 0.001852 mol. Similarly, the moles of 9-octadecanoic acid (E), comprising 52.5% of the mixture, were calculated to be 0.001859 mol. The total moles of acids were determined to be 0.003711 mol. To achieve 100% neutralization, 0.208 g of potassium hydroxide (KOH) was added, ensuring complete reaction with all acid molecules in the mixture. Then, the electrodes were inserted in the vial, which was closed with a cap, and the reaction mixture was stirred using hot plate for 5-10 minutes at 500 rpm until the solution becomes fully homogeneous. Next, the vial was connected with the ElectraSyn 2.0 setup, and the experiment was carried out at room temperature with the stirring at 600 rpm. All the experiments in this thesis were conducted in a duplicate trail and the final value was taken as an average. After completion, the mixture was transferred into a beaker, and the solvent was evaporated by using hot plate. The dried mixture was then mixed with ethyl acetate to extract the organic components in a separatory funnel. The sample was acidified using 1 M hydrochloric acid (HCl) on vigorous shaking. The aqueous phase was removed repeatedly until the pH of the

remaining organic layer reached neutral (pH 7). The organic phase was collected, dried using Na_2HSO_4 (anhydrous sodium sulfate) to eliminate any residual water, and then filtered. Finally. the prepared sample was injected into a GC-MS for product analysis.

5.4 Results and discussion

In these paragraphs, results and discussion of characterization analyses are provided and divided depending on the chemical-physical technique employed.

5.4.1 Analysis of coconut oil and palm oil by Gass Chromatography/Flame Ionization detector (GC/FID)

The purpose of GC-FID analysis was to identify the nature and major components of both oils, including fatty acid profile sterols, and mono-, di-, and triglycerides.

5.4.2 Fatty acid methyl esters (FAME) profile

The analysis provided data on the oil's components, including fatty acid methyl esters (FAME), the methylated forms of fatty acids profile including saturated and unsaturated fatty acids. The tabulated details of the fatty acids profile of both oils and their GC/FID spectra are shown in **Table 5-1, 5-2 (Figure 5-1, 5-2)**. For the coconut oil**,** lauric acid (C12:0) was the most abundant fatty acid, comprising 45.83%, followed by myristic acid (C14:0) at 18.97% and palmitic acid (C16:0) at 10.11%, medium-chain fatty acids, including caprylic acid (C8:0) and capric acid (C10:0), accounted for 6.64% and 5.50%**,** respectively. Unsaturated fatty acids were present in smaller proportions, with cis-oleic acid (C18:1 cis) at 7.35% and linoleic acid (C18:2) at 1.76%. Minor components, including stearic acid (C18:0) at 3.07%, and trace amounts of other fatty acids (e.g., caproic, behenic, and lignoceric acids), were detected, trans-isomers of linoleic and oleic acids were also present at negligible levels (<0.02%).

Coconut oil (FAME)	Formula	Percentage
Caproic acid	C6:0	0.49
Caprylic acid	**C8:0**	**6.64**
Capric acid	**C10:0**	**5.50**
Lauric acid	**C12:0**	**45.83**
Myristic acid	**C14:0**	**18.97**
Pentadecanoic acid	C15:0	0.01
Palmitic acid	**C16:0**	**10.11**
Palmitoleic acid	C16:1	0.02
Heptadecanoic acid	C17:0	< 0.01
Heptadecenoic acid	C17:1	< 0.01
Stearic acid	**C18:0**	**3.07**
Trans-isomer of Oleic acid	C18:1 trans	0.02
Cis-Oleic acid	**C18:1 cis**	**7.35**
Linoleic acid (omega-6)	C18:2	1.76
Arachidic acid	C20:0	0.09
Eicosenoic acid	C20:1	0.05
Alpha-linolenic acid (omega-3)	C18:3	0.01
Behenic acid	C22:0	0.02
Erucic acid	C22:1	< 0.01
Lignoceric acid	C24:0	0.04
Sum of trans isomers of linoleic acid	C18:2 trans	0.01

Table 5-1: FAME profile with formulas showing saturated and unsaturated nature and their percentages, of coconut analyzed by GC/FID

Palm oil (FAME)	Formula	Percentage
Caproic acid	C6:0	< 0.01
Caprylic acid	C8:0	0.02
Capric acid	C10:0	0.02
Lauric acid	C12:0	0.18
Myristic acid	C14:0	1.05
Pentadecanoic acid	C15:0	0.04
Palmitic acid	**C16:0**	**42.13**
Palmitoleic acid	C16:1	0.19
Heptadecanoic acid	C17:0	0.09
Heptadecenoic acid	C17:1	0.02
Stearic acid	**C18:0**	**4.46**
Trans-isomer of Oleic acid	C18:1 trans	0.05
Cis-Oleic acid	**C18:1 cis**	**41.33**
Linoleic acid (omega-6)	**C18:2**	**9.25**
Arachidic acid	C20:0	0.38
Eicosenoic acid	C20:1	0.16
Alpha-linolenic acid (omega-3)	C18:3	0.12
Behenic acid	C22:0	0.06
Erucic acid	C22:1	< 0.01
Lignoceric acid	C24:0	0.07
Sum of trans-isomers of linoleic acid	C18:2 trans	0.32
Sum of trans-isomers of linolenic acid	C18:3 trans	0.05

Table 5-2: FAME profile with formulas showing saturated and unsaturated nature and their percentages, of palm oil analyzed by GC/FID

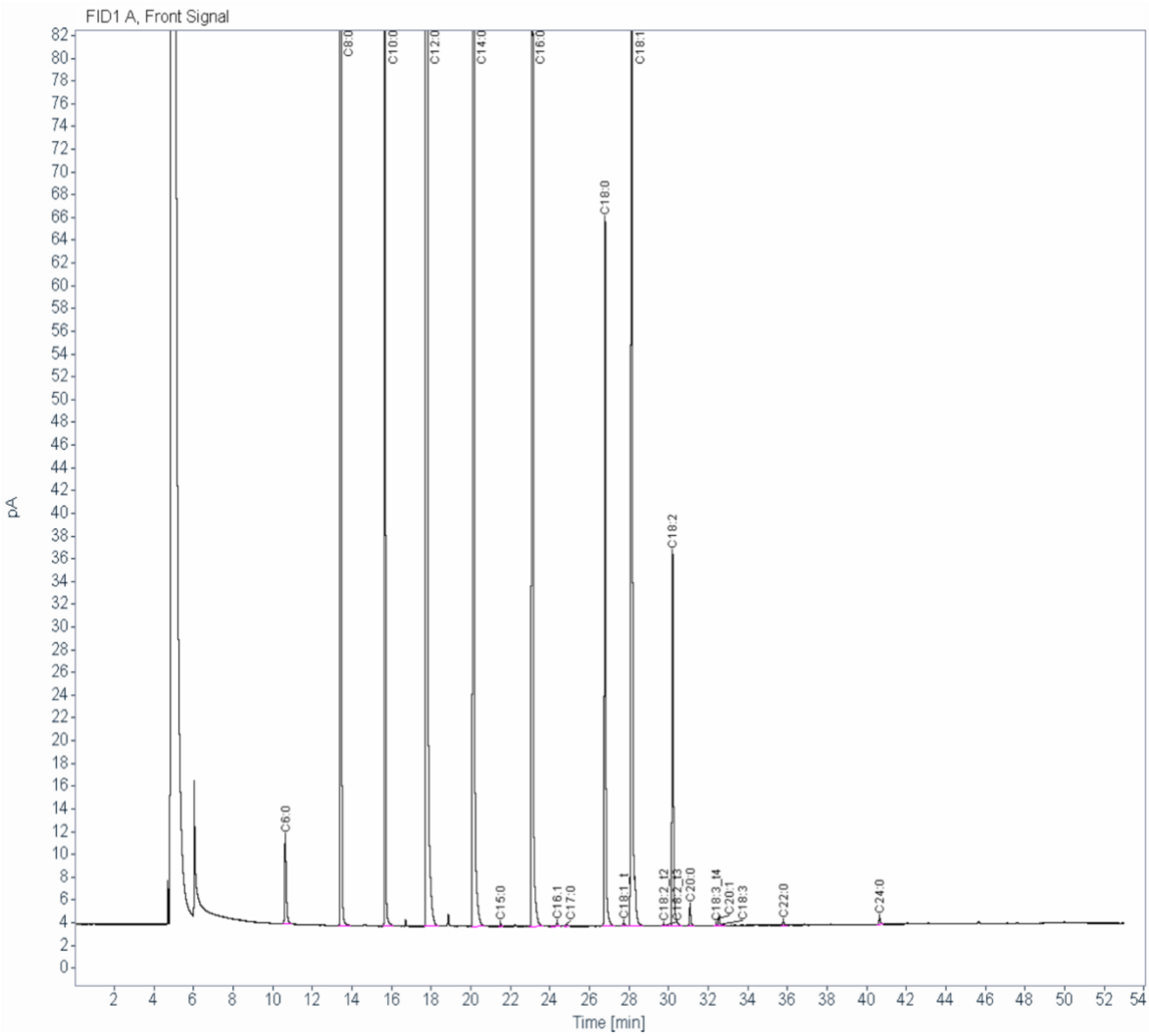


Figure 5-1: GC/FID spectra of FAME profile of coconut oil at different retention times

The GC/FID analysis of palm oil reveals a diverse fatty acid methyl ester (FAME) profile, with significant contributions from both saturated and unsaturated fatty acids. Palmitic acid (C16:0) and cis-oleic acid (C18:1 cis) dominate the composition, representing 42.13% and 41.33%, respectively. Linoleic acid (C18:2, omega-6) is the primary polyunsaturated fatty acid at 9.25%, while among the other components the main one is stearic acid (C18:0) at 4.46%. Minor FAMEs, including alpha-linolenic acid (C18:3, omega-3) at 0.12% and trace trans-isomers, collectively contribute less than 1%.

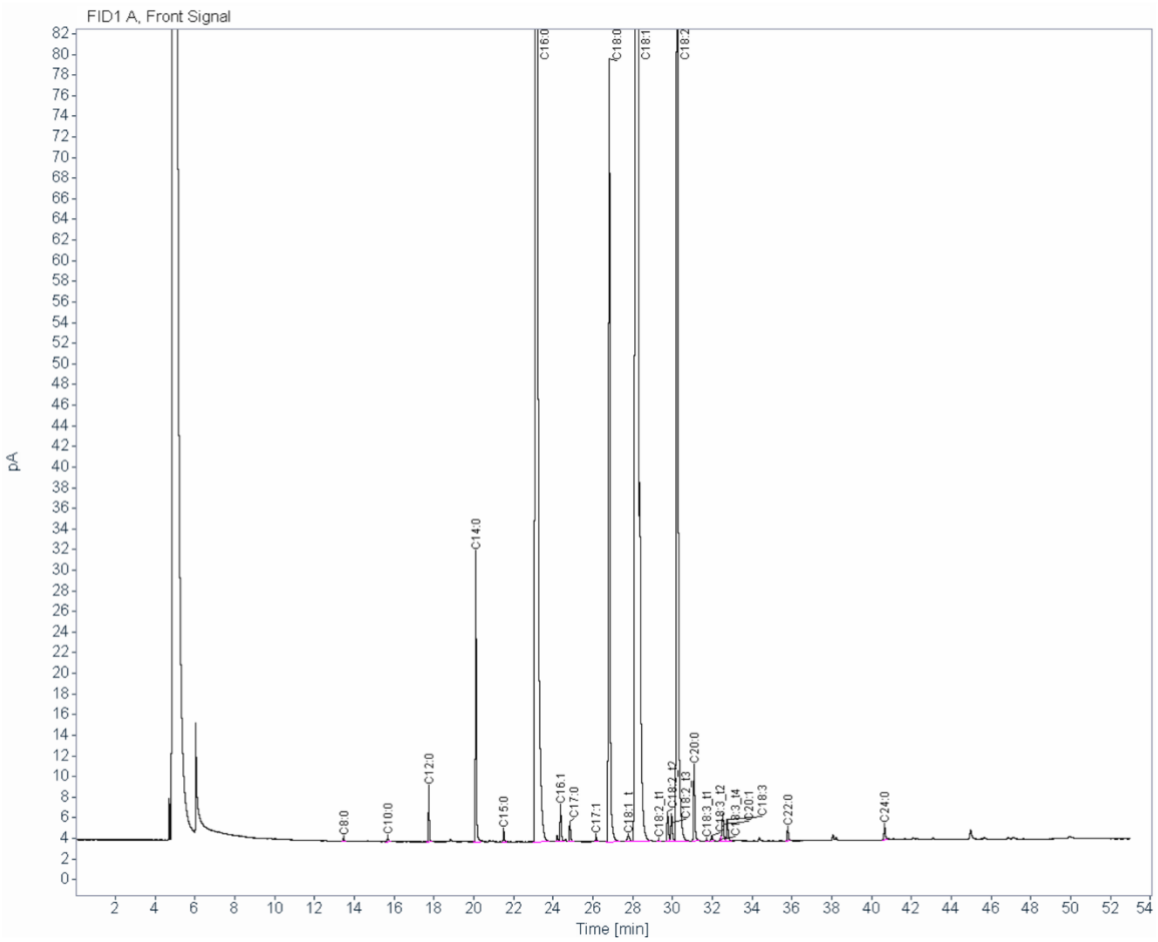


Figure 5-2: GC/FID spectra of FAMEs profile of palm oil at different retention times

5.4.3 Sterols profile of coconut and palm oil

The sterol profile of both oils is shown in **Table 5-3.** In coconut oil, the highest amount Beta sitosterol are consisting 73.7% of the total sterol amount. Other major sterols included Campesterol at 11.1%**,** Delta 5-avenasterol at 8.1%, and Stigmasterol at 2.7%**.** Smaller amount sterols such as Clerosterol (1.6%), 24 Methylenecholesterol (0.7%), Sitostanol (0.5%), and Delta 5.24-stigmastadienol (0.5%) are also present, while Cholesterol and Brassicasterol were present in minimal amounts (0.1%).

The palm oil sterol profile analysis reveals beta-sitosterol as the predominant sterol in sample, accounting for 56.8% of the total sterols, followed by campesterol at 23.7% and stigmasterol at 12.2%. These three sterols collectively constitute over 90% of the profile, emphasizing their significant role in the sterol composition. Other sterols, such as delta-5-avenasterol (1.9%), cholesterol (1.8%), and clerosterol (1.0%), are present in moderate amounts, while trace components like brassicasterol, delta-7-stigmastenol, and delta-7-avenasterol are detected in negligible concentrations (<0.1%).

Coconut oil		Palm oil	
Sterol	**Percentage**	**Sterol**	**Percentage**
Cholesterol	0.1	**Cholesterol**	**1.8**
Brassicasterol	0.1	Brassicasterol	< 0.1
24-Methylenecholesterol	0.7	24-Methylenecholesterol	0.8
Campesterol	**11.1**	**Campesterol**	**23.7**
Campestanol	0.3	Campestanol	0.2
Stigmasterol	**2.7**	**Stigmasterol**	**12.2**
Clerosterol	**1.6**	Delta-7-Campesterol	0.7
Beta-sitosterol	**73.7**	**Clerosterol**	**1.0**
Sitostanol	0.5	**Beta-Sitosterol**	**56.8**
Delta 5-avenasterol	**8.1**	Sitostanol	0.3
Delta 5,24-stigmastadienol	0.5	**Delta-5-Avenasterol**	**1.9**
Delta 7-stigmastenol	0.2	Delta-5,24-Stigmastadienol	0.4
Delta 7-avenasterol	0.4	Delta-7-Stigmastenol	< 0.1
-	-	Delta-7-Avenasterol	0.1

Table 5-3: Sterol profile and their percentages of coconut and palm oil analyzed by GC/FID

5.4.4 Glyceride profile of coconut and palm oil

The diglyceride and triacylglyceride (TAG) profile of both oils are shown in **Table 5-4**. **1**,3-Diglycerides accounted for the majority of the diglycerides at 69.2%, while 1,2-Diglycerides were 30.8%, with total diglycerides measured at 2.6%. Among the triglycerides, TAG C36 was the most abundant at 18.75%, followed by TAG C38 **(**17.13%**)**, TAG C34 **(**15.67%**)**, and TAG C32 **(**11.73%**)**. Medium-chain triglycerides, such as TAG C30 and TAG C28, contributed 2.89% and 0.63%, respectively. Long-chain triglycerides, including TAG C40 **(**11.18%**)** and TAG C42 **(**8.19%**)**, were also detected, with levels decreasing for higher chain lengths, such as TAG C54 **(**0.76%**)** and beyond.

The palm oil analysis of di- and triglycerides reveals a composition dominated by 1,3-diglycerides, which constitute 74.2% of the total diglycerides, compared to 25.8% for 1,2-diglycerides. In terms of triglycerides (TAGs), the most abundant species are TAG C50 and TAG C52, representing 39.62% and 40.53%, respectively, followed by TAG C54 at 11.85%. Minor TAGs, such as TAG C46 (0.77%), TAG C48 (5.61%), and trace amounts of TAG C42, C44, and higher carbon TAGs (C58, C60, C62), highlight the diversity of the lipid profile.

Coconut oil		Palm oil	
Name	**Percentage**	**Name**	**Percentage**
1.2-Diglycerides	**30.8**	**1.2-Diglycerides**	**25.8**
1.3-Diglycerides	**69.2**	**1.3-Diglycerides**	**74.2**
Total Diglycerides	**2.6**	**Total Diglycerides**	**7.4**
TAG C26	0.08	TAG C42	0.14
TAG C28	0.63	TAG C44	0.12
TAG C30	**2.89**	TAG C46	0.77
TAG C32	**11.73**	**TAG C48**	**5.61**
TAG C34	**15.67**	**TAG C50**	**39.62**
TAG C36	**18.75**	**TAG C52**	**40.53**
TAG C38	**17.13**	**TAG C54**	**11.85**
TAG C40	**11.18**	**TAG C56**	**1.19**
TAG C42	**8.19**	TAG C58	0.12
TAG C44	**4.73**	TAG C60	0.05
TAG C46	**2.8**	TAG C62	0.01
TAG C48	**2.37**	-	-
TAG C50	**1.71**	-	-
TAG C52	**1.32**	-	-
TAG C54	0.76	-	-
TAG C56	0.04	-	-
TAG C58	0.01	-	-
TAG C60	0.01	-	-
TAG C62	< 0.01	-	-

Table 5-4: Glycerides profile and their percentages of coconut and palm oil analyzed by GC/FID

5.4.5 Base hydrolysis of coconut oil analyzed by gas chromatography/mass spectrometry (GC/MS)

The base hydrolysis of coconut oil yielded a series of fatty acids, i.e., medium-chain, saturated and unsaturated, analyzed by GC/MS as shown in **Table 5-5 and Figure 5-3 (gc/ms spectra)**. The major fatty acids identified were dodecanoic acid (C12:0) at 46%, tetradecanoic acid (C14:0) at 18.5%, and octanoic acid (C8:0) at 12.5%. The percentage of decanoic acid (C10:0), hexadecanoic acid (C16:0), and 9-octadecenoic acid (C18:1, trans) are 10.5%, 7%, and 5.5%, respectively. The fatty acids profile of coconut oil are already reported by many researchers with different percentages [150].

Fatty acid	Percentage	Retention time
Octanoic acid ($C_8H_{16}O_2$)	12.5 %	4.259
Decanoic acid ($C_{10}H_{20}O_2$)	10.5 %	5.323
Dodecanoic acid ($C_{12}H_{24}O_2$)	46 %	6.475
Tetradecanoic acid ($C_{14}H_{28}O_2$)	18.5 %	7.258
Hexadecanoic acid ($C_{16}H_{32}O_2$)	7 %	7.990
9-Octadecanoic acid (E) ($C_{18}H_{34}O_2$)	5.5 %	8.639

Table 5-5: Mixture of fatty acids profile and their percentages at different retention times, derived after base hydrolysis of coconut oil, analyzed by GC/MS

The comparison of fatty acids percentages between GC/MS and GC/FID analyses highlights successful conversion of the base hydrolysis, with some minor variations. For example, caprylic acid (C8:0), which was 6.64% in the GC/FID analysis, increased to 12.5% as octanoic acid ($C_8H_{16}O_2$) in GC/MS. Similarly, capric acid (C10:0) increased from 5.50% to 10.5%. Additionally, some minor components identified in the GC/FID analysis, such as trace unsaturated fatty acids and trans-isomers, were not detected after hydrolysis and analyzed by GC/MS. These variations can be attributed to differences in the analytical methods, the possibility of their instability under alkaline conditions, leading to degradation or volatility and loss of trace components during processing after hydrolysis.

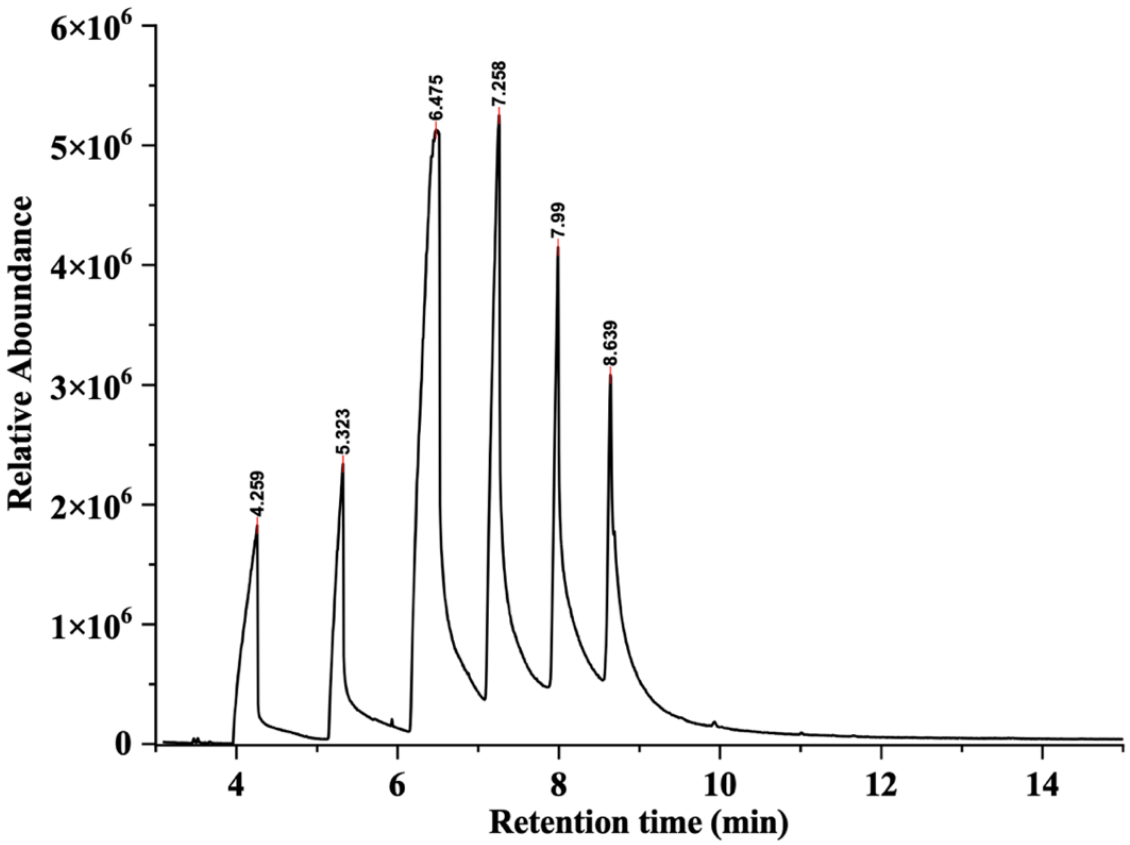


Figure 5-3: GC/MS spectra of fatty acids derived after based hydrolysis of coconut oil

5.4.6 Base hydrolysis of palm oil analyzed by GC/MS

The base hydrolysis of palm oil yielded two types of fatty acids, as shown in **Table 5-6 and Figure 5-4 (gc/ms spectra)**. The percentage of hexadecanoic acid (C16:0) and 9-octadecenoic acid (E) (C18:1, trans) are 47.5 % and 52.5 % respectively. The fatty acid profile of palm oil with highest percentage of hexadecanoic acid and octadecenoic acid are already reported [151].

Compound (fatty acid)	Percentage	Retention time
Hexadecanoic acid ($C_{16}H_{32}O_2$)	47.5%	7.959
9-Octadecanoic acid (E) ($C_{18}H_{34}O_2$)	52.5%	8.644

Table 5-6: Mixture of fatty acids profile and their percentages at different retention times, derived after base hydrolysis of palm oil, analyzed by GC/MS

The results indicate that the base hydrolysis of palm oil was successful, as the major FAMEs identified in the GC/FID analysis, namely palmitic acid (C16:0) and cis-oleic acid (C18:1), were effectively converted into their corresponding free fatty acids, hexadecanoic acid (C16:0) and 9-octadecenoic acid (C18:1), during the process. Only a few minor FAMEs were not

reflected in the GC/MS results after hydrolysis, which can be attributed to their trace presence in the original oil composition, potential degradation during the hydrolysis process, or loss during sample handling and processing.

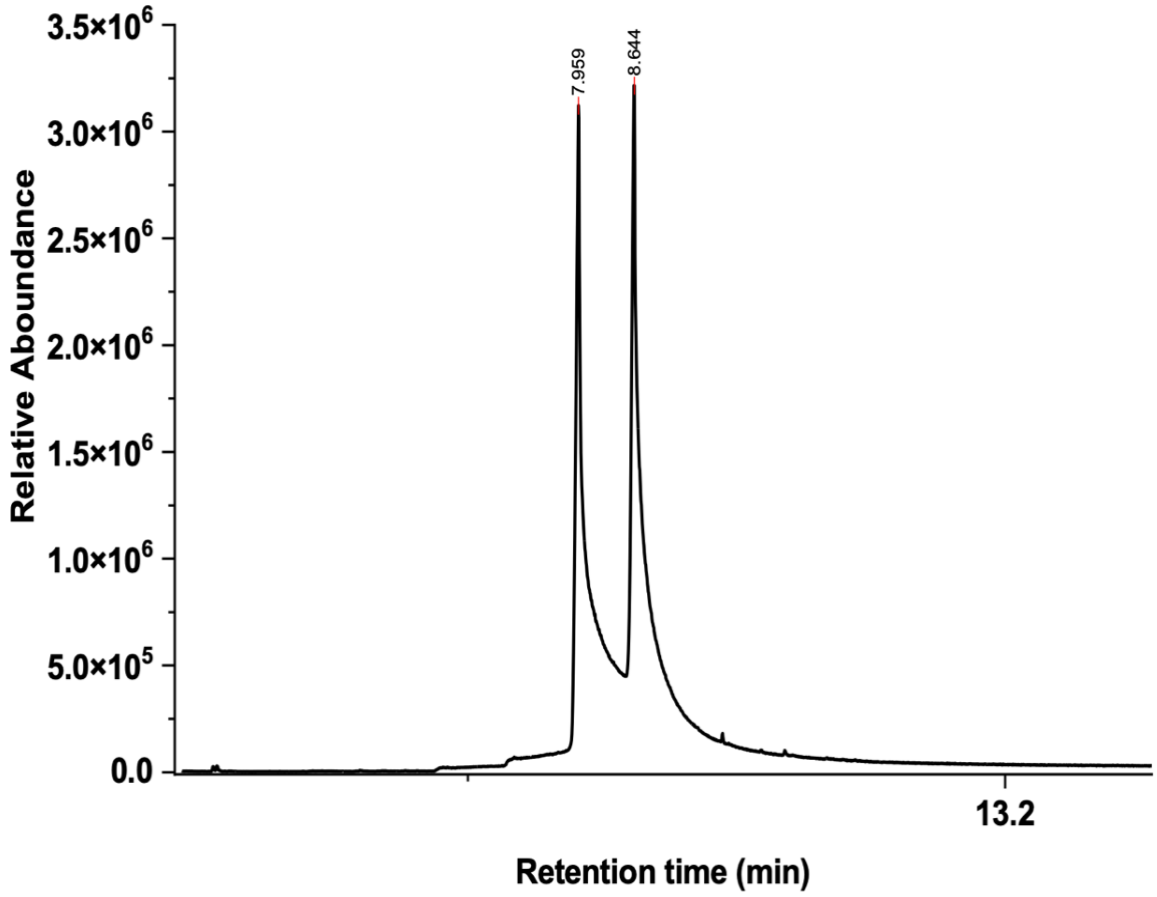


Figure 5-4: GC/MS spectra of fatty acids derived after based hydrolysis of palm oil

5.4.7 Kolbe electrolysis of mixture of fatty acids obtained from coconut oil

After collecting a mixture of fatty acids derived from the base hydrolysis of coconut oil, the mixture was subjected to Kolbe electrolysis under various solvent environments to thoroughly evaluate the influence of solvent composition on the distribution of reaction products. The solvents tested included combinations of methanol (MeOH), ethanol (EtOH), and water in varying proportions to determine their effects on the yields of products. **Table 5-7** displays the experimental parameters used for all the electrolysis experiments.

Solvent system (v/v) and %	Current intensity (mA)	KOH (mmol)	Time (hours)
MeOH:EtOH:water (1:1:4) (16.67 :16.67 :66.67%)	100	4.21	6
MeOH:EtOH:water (1:1:1) (33.33 :33.33 :33.33%)	100	4.21	6
MeOH:EtOH:water (5:5:2) (41.66 :41.66 :16.67%)	100	4.21	6
MeOH:Water (3:1) (75:25 %)	100	4.21	6
EtOH:Water (3:1) (75:25 %)	100	4.21	6

Table 5-7: Reaction conditions for the electrolysis of mixture of 6 fatty acids derived after base hydrolysis of coconut oil, KOH addition was according to 100 % neutralizations of fatty acids, considering a stoichiometric reaction with all acid molecules in the

The results of product formation following Kolbe electrolysis of a mixture of six fatty acids derived from the base hydrolysis of coconut oil are shown in **Figure 5-5.** In mixtures containing methanol, ethanol, and water in varying ratios, distinct trends in product distribution were observed. The solvent system with a composition of MeOH:EtOH:water (16.67:16.67:66.67%) resulted in the production of 68.3% total hydrocarbons, accompanied by 4.75% alcohol, 4.25% aldehyde, and 20.95% unreacted acid. Increasing the relative proportions of methanol and ethanol while decreasing water content, as in the MeOH:EtOH:water (33.33:33.33:33.33%) system, led to a slight increase in hydrocarbon yield (70.4%) and alcohol content (4.8%), while the aldehyde percentage increased to 5.5%, and the unreacted acid decreased to 18.55%. The solvent system with the highest proportion of organic solvents MeOH:EtOH:water (41.66:41.66:16.67%) yielded the maximum hydrocarbon production at 73.55%. This system also produces higher alcohol (5.5%) and aldehyde (5.25%) content and the lowest percentage of unreacted acid (12.5%). These results suggest that reducing the water content and increasing the proportion of organic solvents slightly promote the formation of hydrocarbons while minimizing the residual acid. The observed variations in product distribution during Kolbe electrolysis can be attributed to several factors related to solvent composition and properties **(Table 5-8**). Solvent polarity and dielectric constant significantly influence the reaction pathways. High water content in solvents, such as the MeOH:EtOH:water mixture at

16.67:16.67:66.67%, creates a polar environment that facilitates the ionization of fatty acids into carboxylate ions. However, this increased polarity may also stabilize reaction intermediates, reducing the efficiency of radical coupling and leading to lower hydrocarbon yields. This phenomenon is discussed in the context of solvent effects on electro-organic synthesis [152]. Furthermore, methanol in high amount, tends to stabilize intermediates like aldehydes and alcohols, resulting in higher production of these compounds. In contrast, ethanol's lower polarity and hydrogen-bonding capacity make it less effective at stabilizing such intermediates, thereby favoring hydrocarbon production [153].

In binary solvent systems, methanol and ethanol were combined with water in a 75:25 ratio to further explore their individual effects. The MeOH:Water (75:25%) system produced only 30.35% total hydrocarbons, accompanied by a significantly higher percentage of alcohol (14.25%) and aldehyde (13.25%), with 41.5% unreacted acid. This solvent environment was notably less efficient in driving hydrocarbon formation and instead facilitated higher alcohol and aldehyde production, likely due to altered reaction mechanisms or intermediate stabilization in the presence of methanol and water. On the other hand, the EtOH:Water (75:25%) system resulted in a hydrocarbon yield of 62.35%, with significantly lower alcohol and aldehyde content (3% each) and a residual acid percentage of 29.5%. These findings indicate that ethanol in higher proportions enhances hydrocarbon formation compared to methanol under similar conditions [154].

Solvent	**Dipole moment (μ)**	**Polarity index (P')**	**Dielectric constant (ε)**
H_2O	1.87 D at 20°C	10.2	80.10 at 20°C
MeOH	2.87 D at 20°C	5.1	32.70 at 25°C
EtOH	1.66 D at 20°C	4.3	24.55 at 25°C

Table 5-8: Physical properties of three polar protic solvents used in the Kolbe electrolysis

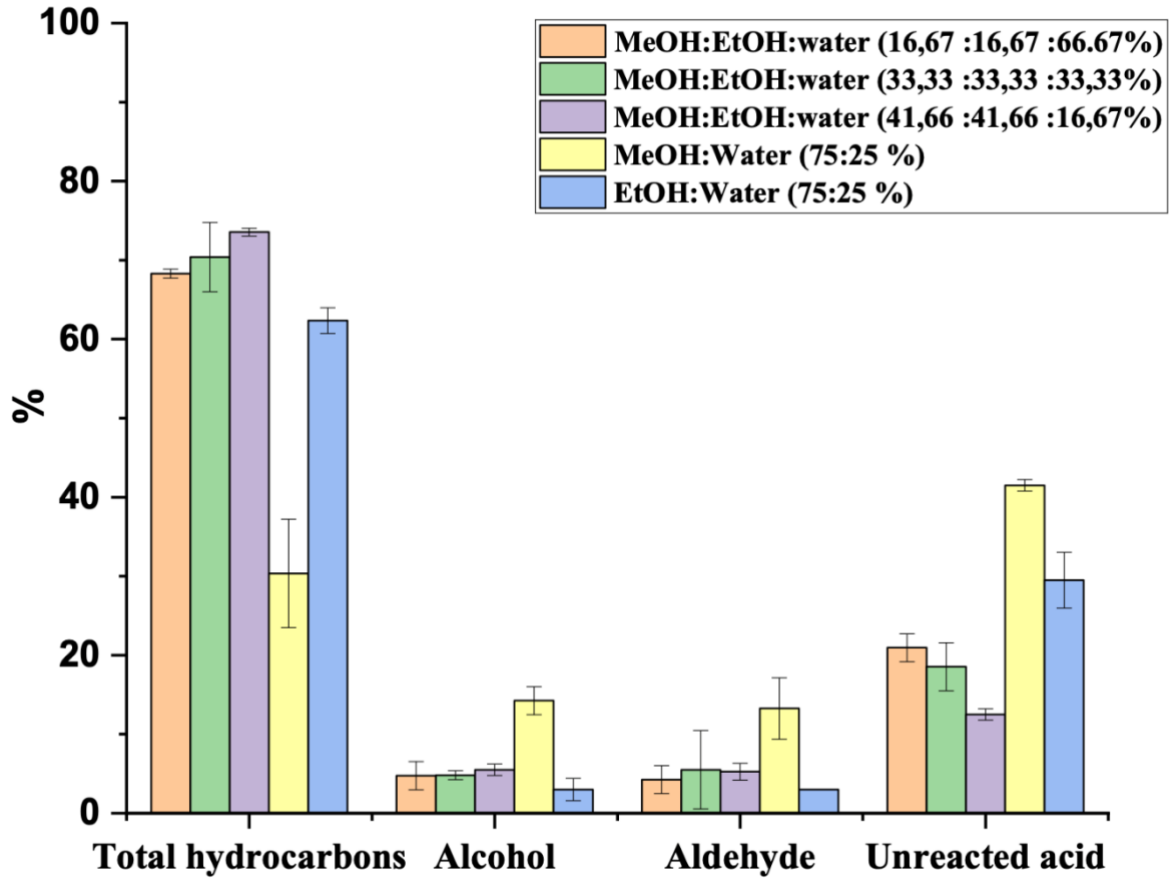


Figure 5-5: Kolbe electrolysis result of mixture of fatty acids obtained from coconut oil with a total mass of 1 g in different solvents environments; error bars represent the standard deviation of the doublet experiments

The GC/MS spectra of all experiments in different solvent environments are shown in **Figure 5-6.** The retention times at different peaks are automatically geneterated by Origin sofware and the majority of the smaller peaks are smaller peaks are undetected by software.

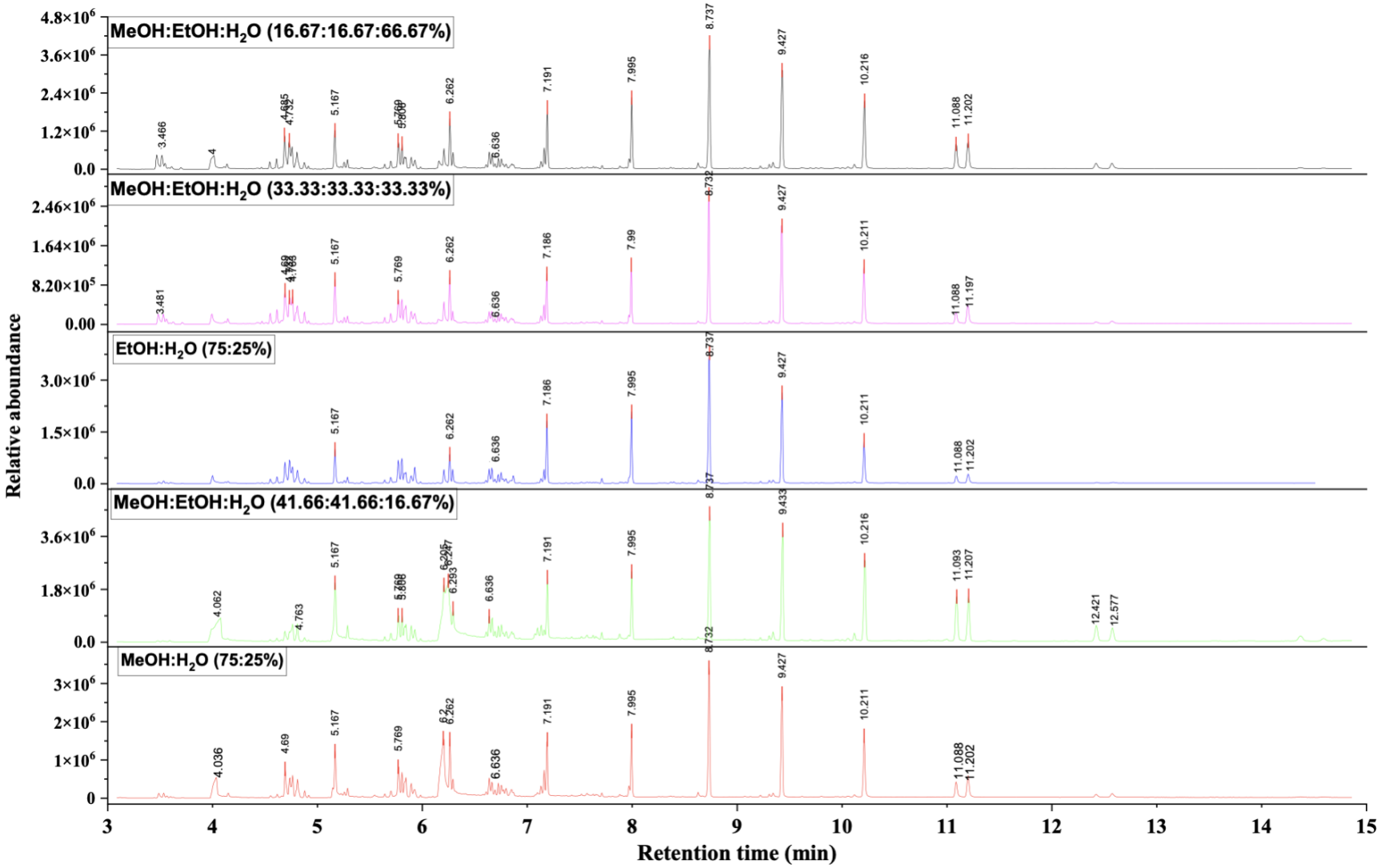


Figure 5-6: GC/MS spectra of the product distribution after electrolysis of mixture of coconut oil based fatty acids in different solvent systems

Overall, the results reveal that solvent composition significantly impacts the Kolbe electrolysis outcomes. Mixtures with higher organic solvent content, particularly MeOH and EtOH combined in approximately equal proportions with reduced water, yielded the highest hydrocarbon production. Conversely, solvent systems with higher water content or a dominance of methanol alone promoted the formation of alcohols and aldehydes and left a higher percentage of unreacted acid.

The GC/MS analysis revealed that the trend of hydrocarbon formation varied across experiments. This variation can be attributed to the complex mixture (fatty acids) and the influence of the solvent's nature. Due to the highly intricate composition of the solution and the extensive generation of radicals on the electrode surface, the pattern of product formation appeared inconsistent, further reflecting the dynamic nature of the electrolysis process under these conditions. The complete profile of hydrocarbons formed in each solvent environment and their percentages are shown in all separate **Figures 5-(7 - 11).**

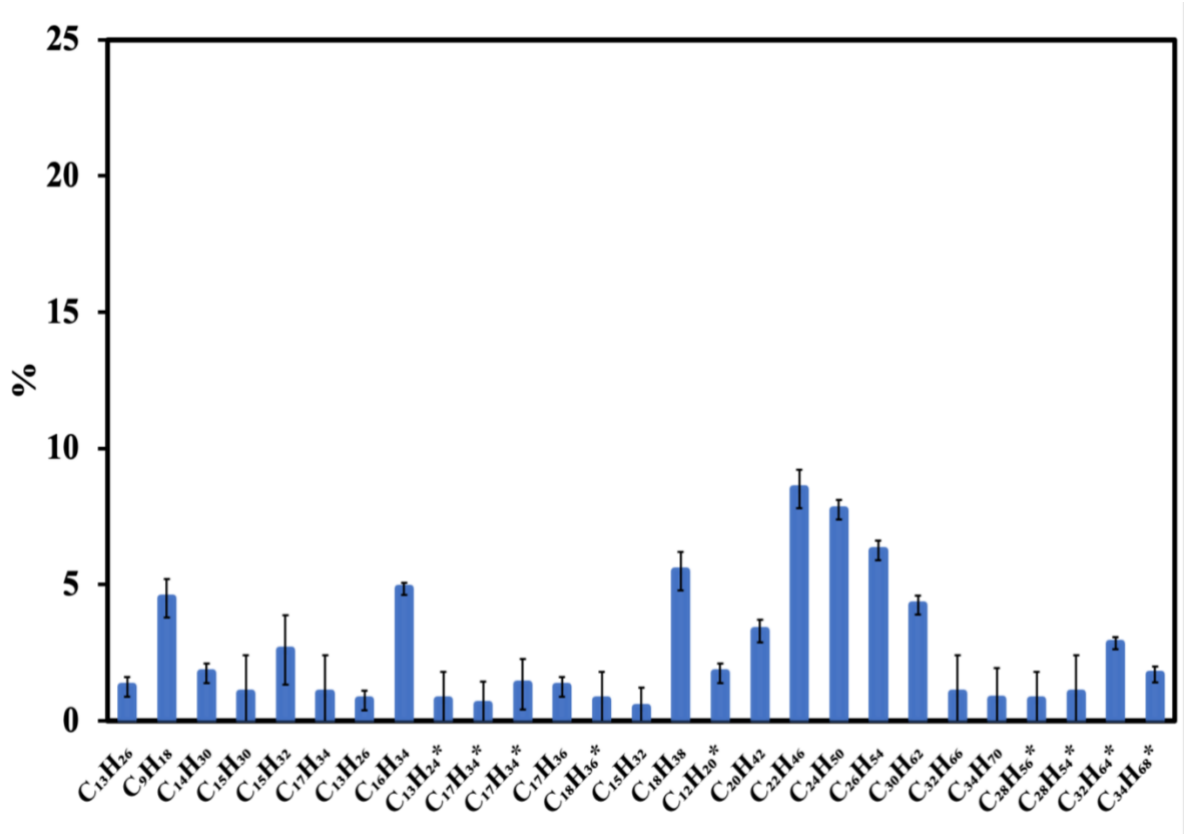


Figure 5-7: Hydrocarbons spectrum from electrolysis of mixture of fatty acids derived from coconut oil in solvent MeOH:EtOH:H2O (16.67:16.67:66.67%) system; *alkenes and dienes from C18:1, and the error bars represent the standard deviation of the doublet experiments

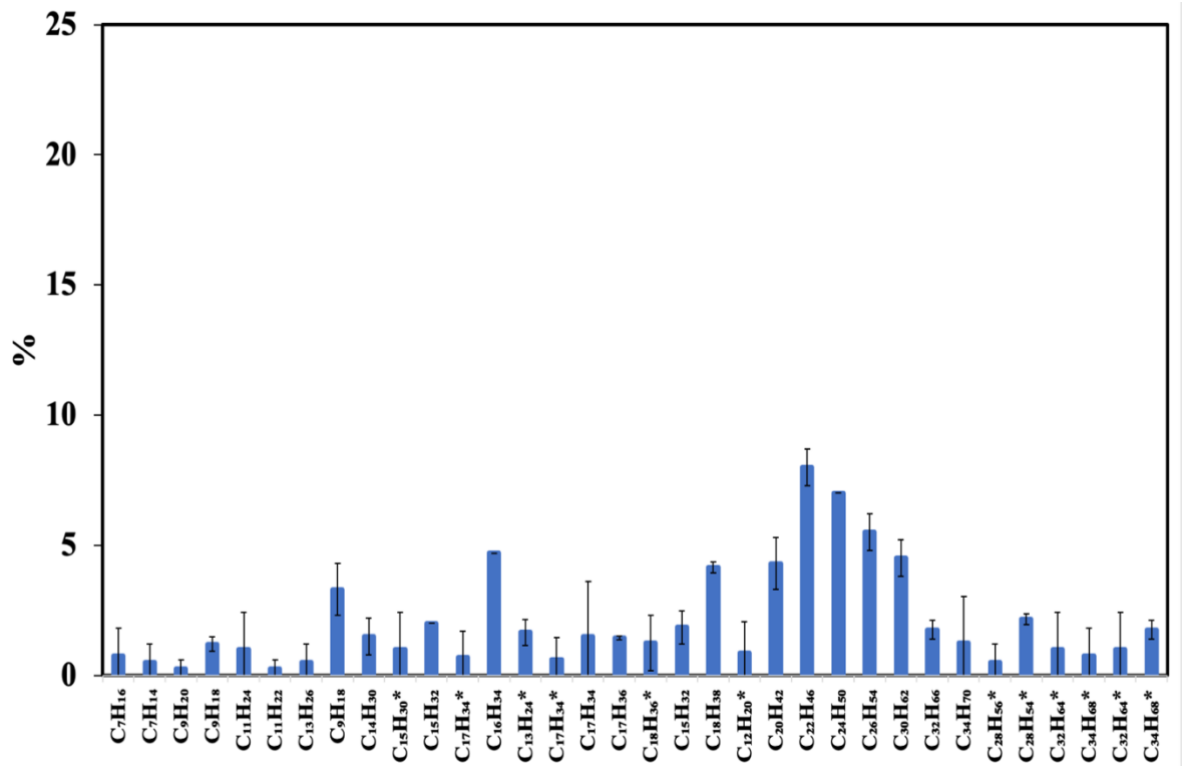


Figure 5-8: Hydrocarbons spectrum from electrolysis of mixture of fatty acids derived from coconut oil in solvent MeOH:EtOH:H2O (33.33 :33.33 :33.33%) system; *alkenes and dienes from C18:1 and the error bars represent the standard deviation of the doublet experiments

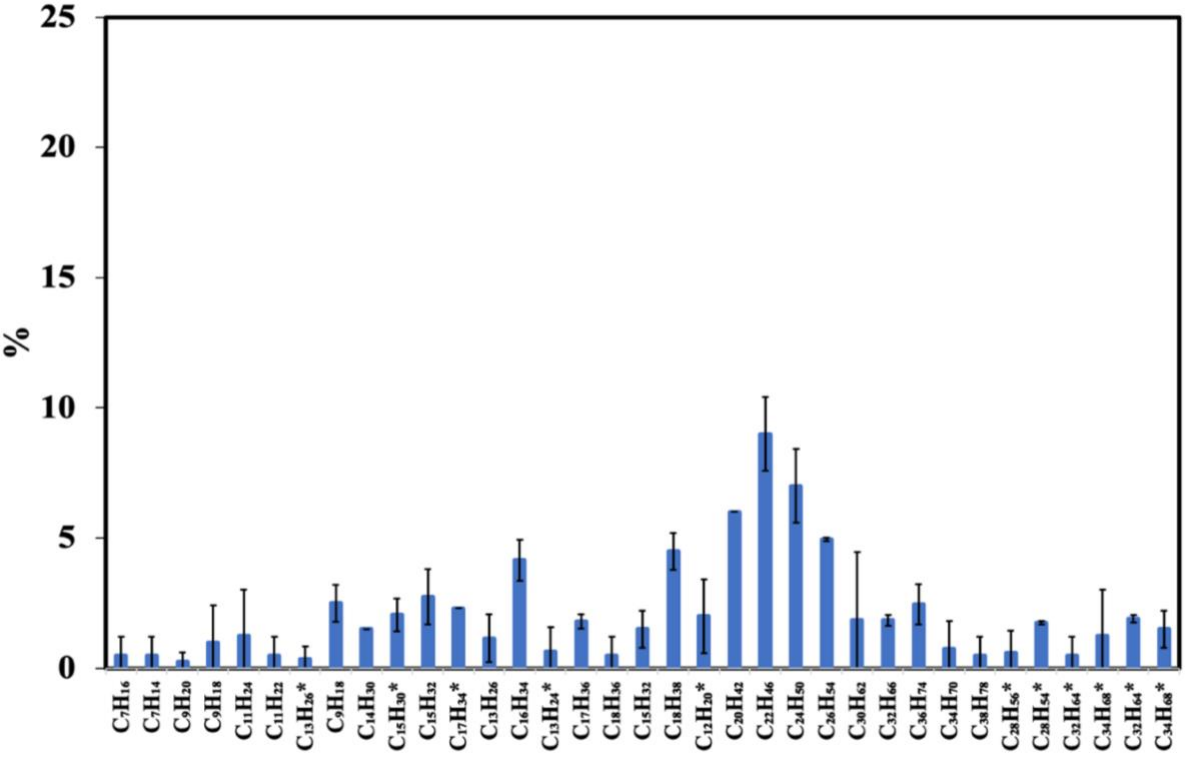


Figure 5-9: Hydrocarbons spectrum from electrolysis of mixture of fatty acids derived from coconut oil in solvent MeOH:EtOH:H2O (41.66 :41.66 :16.67) system; *alkenes and dienes from C18:1 and the error bars represent the standard deviation of the doublet experiments

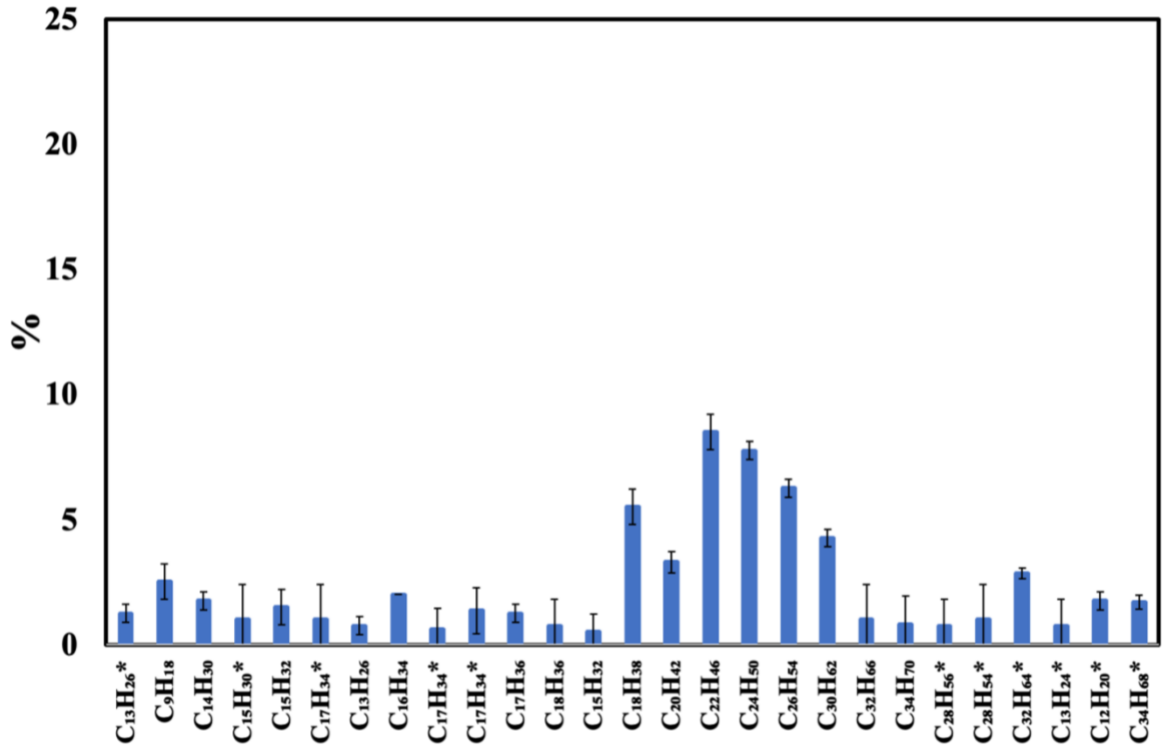


Figure 5-10: Hydrocarbons spectrum from electrolysis of mixture of fatty acids derived from coconut oil in solvent EtOH:H2O (75:25%) system; *alkenes and dienes from C18:1 and the error bars represent the standard deviation of the doublet experiments

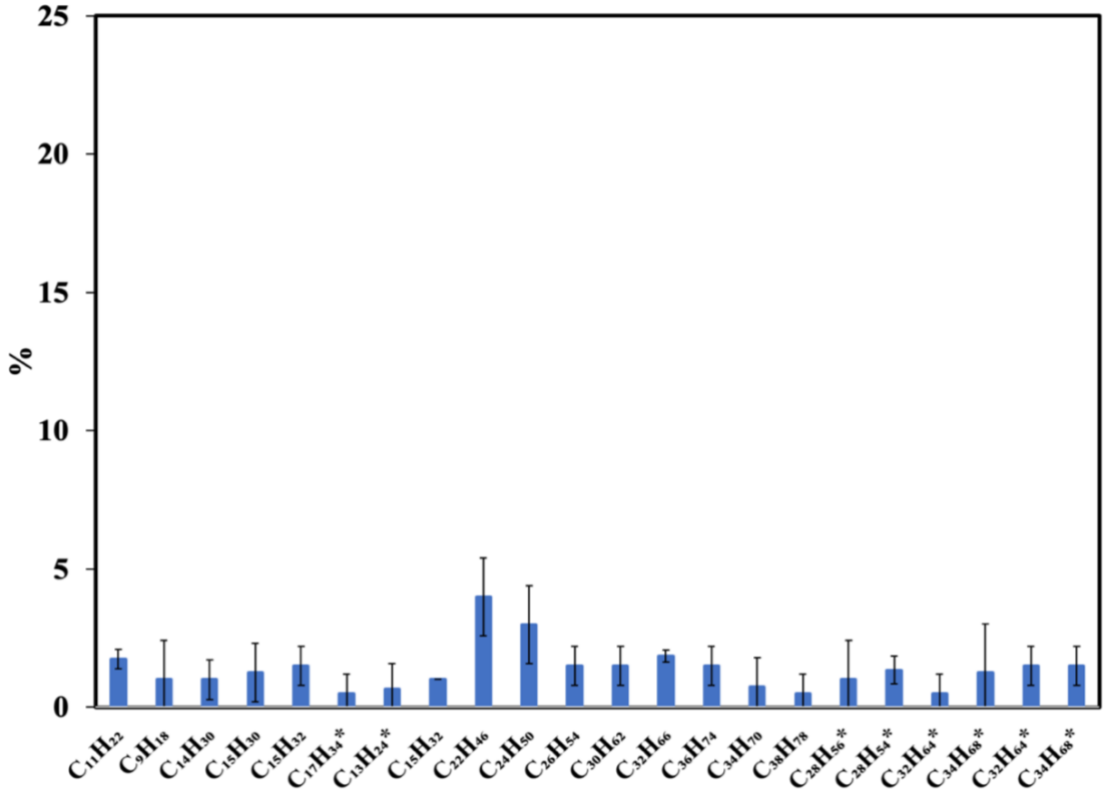


Figure 5-11: Hydrocarbons spectrum from electrolysis of mixture of fatty acids derived from coconut oil in solvent MeOH:H2O (75:25%) system; *alkenes and dienes from C18:1 and the error bars represent the standard deviation of the doublet experiments

The type of alcohols and aldehydes formed in each solvent environment are shown in **Table 5-9.** The different solvent compositions influence the diversity of alcohols and aldehydes. The product distribution varies with solvent polarity and composition, highlighting the influence of the solvent environment on the electrochemical cleavage and rearrangement of fatty acid-derived compounds.

Solvent System	Alcohol	Aldehyde
MeOH:EtOH:H_2O (16.67:16.67:66.67%)	1-Hexadecanol ($C_{16}H_{34}O$) 2-Heptadecanol ($C_{17}H_{36}O$)	Undecanal ($C_{11}H_{22}O$) Tetradecanal ($C_{14}H_{28}O$) 9-Octadecanal ($C_{18}H_{36}O$)
MeOH:EtOH:H_2O (33.33:33.33:33.33%)	1-Hexadecanol ($C_{16}H_{34}O$) Pentadecanol ($C_{15}H_{32}O$)	Undecanal ($C_{11}H_{22}O$) Dodecanal ($C_{12}H_{24}O$) Hexadecanal ($C_{16}H_{32}O$)
MeOH:EtOH:H_2O (41.66:41.66:16.67)	2-Hexadecanol ($C_{16}H_{34}O$) 1-Octadecanol ($C_{18}H_{38}O$)	Tridecanal ($C_{13}H_{26}O$) Tetradecanal ($C_{14}H_{28}O$) 9-Octadecanal ($C_{18}H_{36}O$)
EtOH:H_2O (75:25%)	1-Heptadecanol ($C_{17}H_{36}O$) Hexatadecanol ($C_{16}H_{34}O$)	Dodecanal ($C_{12}H_{24}O$) Pentadecanal ($C_{15}H_{32}O$) Tetradecanal ($C_{14}H_{28}O$)
MeOH:H_2O (75:25%)	1-Hexadecanol ($C_{16}H_{34}O$) Heptadecanol ($C_{17}H_{36}O$) Tridecanol ($C_{13}H_{28}O$) Pentadecanol ($C_{15}H_{32}O$)	Undecanal ($C_{11}H_{22}O$) Dodecanal ($C_{12}H_{24}O$) Tetradecanal ($C_{14}H_{28}O$) Tetradecanal ($C_{14}H_{28}O$) 2-Octadecanal ($C_{18}H_{36}O$)

Table 5-9: Types of alcohols and aldehydes formed after the electrolysis of mixture of fatty acids derived from base hydrolysis of coconut oil in different solvent environments

5.4.8 Kolbe electrolysis of mixture of fatty acids obtained from palm oil

After collecting a mixture of fatty acids derived from the base hydrolysis of palm oil, the mixture was subjected to Kolbe electrolysis under various solvent environments to thoroughly evaluate the influence of solvent composition on the distribution of reaction products. The solvents tested included combinations of methanol (MeOH), ethanol (EtOH), and water in varying proportions to determine their effects on the yields of products. **Table 5-10** displays the experimental parameters used for all the electrolysis experiments.

Solvents	Current intensity (mA)	KOH (mmol)	Time (hours)
MeOH:EtOH:water (41.66 :41.66 :16.67%)	100	0.371	6
MeOH:Water (75:25 %)	100	0.371	6
EtOH:Water (75:25 %)	100	0.371	6

Table 5-10: Reaction conditions for the electrolysis of mixture of fatty acids derived after base hydrolysis of palm oil, KOH addition was according to 100 % neutralizations of fatty acids, considering a stoichiometric reaction with all acid molecules in the mixture

The result of the product distribution of Kolbe electrolysis are shown in **Figure 5-12.** Under the MeOH:EtOH:Water solvent condition, the highest yield of total hydrocarbons, reaching 73.25% was observed. Alcohol formation accounted for 7.75%, while aldehydes and unreacted acids were measured at 4.85% and 13.5%, respectively. The MeOH:Water (75:25%) system, in contrast, resulted in hydrocarbon yield of 36.4%, alcohol at 8% and aldehyde formation at 3.3%. Notably, the unreacted acids increased substantially to 49.5%, indicating that this solvent environment was less effective in facilitating complete reaction. The EtOH:Water (75:25%) solvent condition yielded hydrocarbons formation at 46.3%, which was higher than in the MeOH:Water system but lower than in the MeOH:EtOH:Water environment. Alcohol and aldehyde production were 12.85% and 7.5%, respectively. The unreacted acids accounted for 32.5%, reflecting a moderate degree of reactant conversion compared to the other systems.

The complete profile of hydrocarbons and their average percentage of doublet trails are shown in **Table 5-11.** Dienes and some alkenes, e.g., 1,13-tetradecadiene and 17-pentatriacontene, are likely derived from 9-octadecanoic acid, which has an inherent double bond.

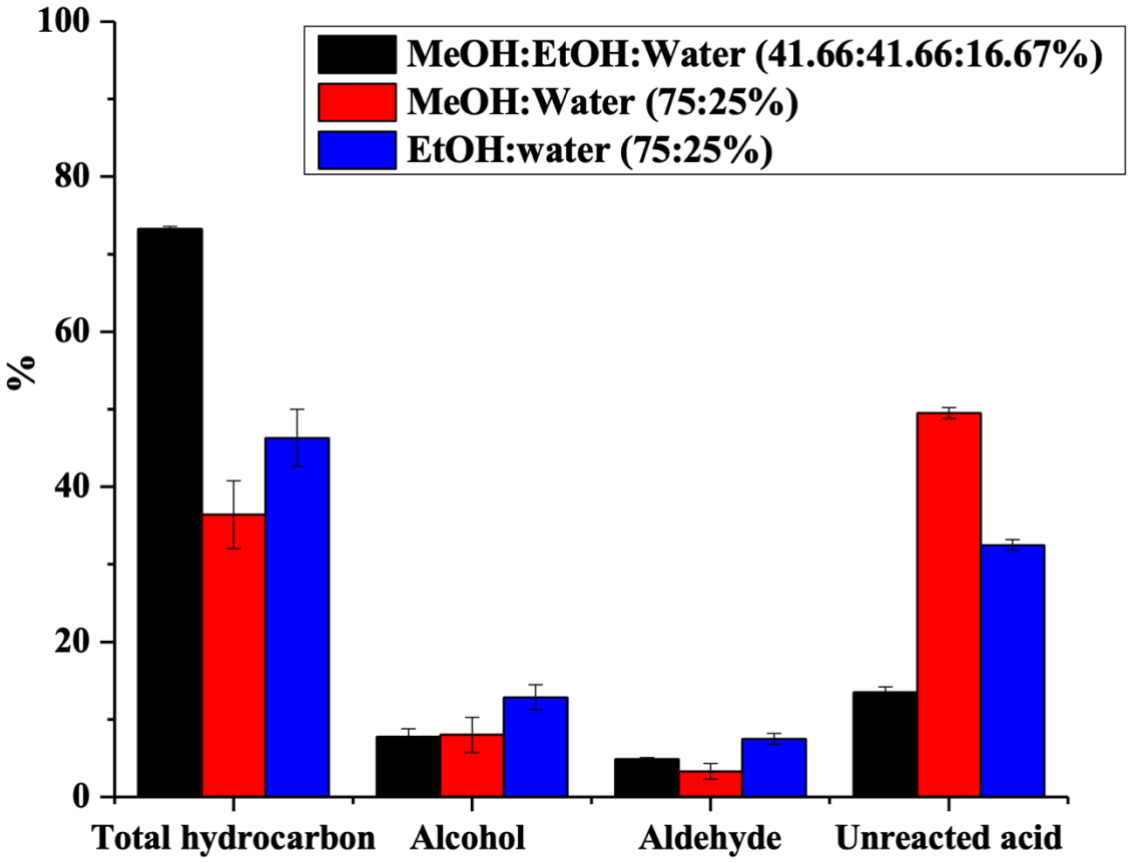


Figure 5-12: Kolbe electrolysis result of mixture of fatty acids obtained from palm oil with a total mass of 1 g in different solvents environments; error bars represent the standard deviation of the doublet experiments

The nearly same hydrocarbon yields (73.55% and 73.25%) for coconut oil and palm oil fatty acids in the same EtOH:MeOH:water (41.66:41.66:16.67%) solvent system indicate that solubility differences of carboxylate anions in water might not significantly influence Kolbe reaction. For instance, research has demonstrated efficient Kolbe electrolysis of water-insoluble long-chain fatty acid salts can result in substantial hydrocarbon production [155]. This suggests that the process efficiency is primarily governed by the electrochemical process itself, rather than the solubility of the carboxylates in the solvent system.

The type of alcohols and aldehydes formed in each solvent environment are shown in **Table 5-12.** The different solvent compositions influence the diversity of alcohols and aldehydes. The product distribution varies with solvent polarity and composition, highlighting the influence of the solvent environment on the electrochemical cleavage and rearrangement of fatty acid-derived compounds.

Formula	Hydrocarbons	Average %	Formula	Hydrocarbons	Average %	Formula	Hydrocarbons	Average %
$C_{15}H_{30}$	Pentadecene	2.15	$C_{15}H_{30}$	Pentadecene	4.5	$C_{15}H_{30}$	Pentadecene	7.5
$C_{15}H_{32}$	Pentadecane	1.5	$C_{15}H_{32}$	Pentadecane	3	$C_{15}H_{32}$	Pentadecane	3.5
$C_{18}H_{36}$	5-Octadecene	1	$C_{18}H_{38}$	Octadecane	1.75	$C_{18}H_{38}$	Octadecane	3.75
$C_{17}H_{34}$	1-Heptadecene	0.4	$C_{17}H_{34}$	1-Heptadecene	3	$C_{17}H_{34}$	1-Heptadecene	4.5
$C_{16}H_{34}$	Hexadecane	3.2	$C_{16}H_{34}$	Hexadecane	3.5	$C_{16}H_{34}$	Hexadecane	3.5
$C_{14}H_{24}$	1,13-tetradecadiene*	3	$C_{14}H_{24}$	1,13-tetradecadiene*	4	$C_{14}H_{24}$	1,13-tetradecadiene*	4
$C_{17}H_{34}$	8-Heptadecene	2.1	$C_{17}H_{36}$	Heptadecane	3.5	$C_{17}H_{36}$	Heptadecane	6.5
$C_{12}H_{24}$	dodecene	1.5	$C_{13}H_{28}$	tridecane	3	$C_{13}H_{28}$	tridecane	5.5
$C_{15}H_{30}$	1-Pentadecene	1.5	$C_{15}H_{30}$	3-Pentadecene	2	$C_{13}H_{26}$	3-tridecene	3
$C_{17}H_{36}$	Heptadecane	1.6	$C_{17}H_{36}$	Heptadecane	1.6	$C_{17}H_{36}$	Heptadecane	6
$C_{18}H_{34}$	9-Octadecene	1.25	$C_{18}H_{34}$	9-Octadecene	1.25	$C_{19}H_{38}$	3-nonadecene	3
$C_{15}H_{30}$	Pentadecene	3.2	$C_{15}H_{30}$	Pentadecene	3.2	$C_{20}H_{42}$	Eicosane	5
$C_{14}H_{26}$	1,13-tetradecadiene*	3	$C_{14}H_{26}$	1,13-tetradecadiene*	3	$C_{18}H_{32}$	3-octadecadiene*	3.5
$C_{30}H_{62}$	Triacontane	3	$C_{30}H_{62}$	Triacontane	3	$C_{30}H_{62}$	Triacontane	6.5
$C_{35}H_{68}$	17-Pentatriacontene*	5.5		Pentatriacontene*	3.5	$C_{34}H_{68}$	Tetratriacontene*	3.5
$C_{32}H_{64}$	Dotriacontane	2.5	$C_{32}H_{64}$	Dotriacontane	2.5	$C_{32}H_{64}$	Dotriacontane	4

Table 5-11: Hydrocarbons spectrum from electrolysis of mixture of fatty acids derived from palm oil in different solvent environments; *alkenes and dienes from C18:1

MeOH:Water (75:25)			EtOH:Water (75:25)			MeOH:EtOH:water (41.66 :41.66 :16.67%)		
Formula	**Alcohol**	**Average %**	**Formula**	**Alcohol**	**Average %**	**Formula**	**Alcohol**	**Average**
$C_{15}H_{31}OH$	Pentadecanol	0.8	$C_{15}H_{31}OH$	Pentadecanol	5.5	$C_{15}H_{31}OH$	Pentadecanol	2.5
$C_{16}H_{33}OH$	Hexadecanol	3	$C_{14}H_{29}OH$	Tetradecanol	3	$C_{14}H_{29}OH$	Tetradecanol	2.5
$C_{17}H_{35}OH$	Heptadecanol	4.2	$C_{17}H_{35}OH$	Heptadecanol	4.35	$C_{17}H_{35}OH$	Heptadecanol	2.75
Aldehydes								
Formula	**Aldehyde**	**Average %**	**Formula**	**Aldehyde**	**Average %**	**Formula**	**Aldehyde**	**Average**
$C_{16}H_{32}O$	Hexadecanal	1.8	$C_{15}H_{30}O$	Pentadecanal	3.5	$C_{15}H_{30}O$	Pentadecanal	3.5
$C_{18}H_{36}O$	Octadecanal	1.5	$C_{16}H_{32}O$	Hexadecanal	4	$C_{16}H_{32}O$	Hexadecanal	4

Table 5-12: Types of alcohols and aldehydes formed after the electrolysis of mixture of fatty acids derived from base hydrolysis of coconut oil in different solvent environments

5.5 Conclusion

In this study, a green electrochemical process is developed to produce bio-based hydrocarbons from vegetable oils using a low cost KOH as base and supporting electrolyte. The base hydrolysis described in this study can successfully convert triglycerides present in vegetable oils into fatty acids at a moderate temperature (110 ^{o}C) and non-toxic aqueous and ethanol solvents.

The study shows a green and safe electrochemical approach for the production of useful and bio-based chemicals like hydrocarbons, alcohols and aldehydes using non-commercial Pt electrodes. The Kolbe electrolysis of mixture of 6 fatty acids derived from coconut oil and 2 fatty acids derived from palm oil gives 73.55 % and 73.25 % of hydrocarbons in MeOH:EtOH:water (41.66 :41.66 :16.67%) solvent system, along with alcohols and aldehydes and with highest percentage of substrate acid dissociation. The nearly identical hydrocarbon yields (73.55% and 73.25%) for coconut oil and palm oil fatty acids in the same EtOH:MeOH:water solvent system indicate that the solubility of carboxylate anions does not significantly impact hydrocarbon yields in Kolbe electrolysis, and water-insoluble long-chain fatty acid salts, can also lead to the substantial hydrocarbon production.

The strategy works well that Kolbe electrolysis can be used as a green and low cost approach for the synthesis of hydrocarbons from renewable sources. However, further improvement in optimization of selectivity and mechanistic study of radicals formed on the electrodes surface needs to be studied in future.

Chapter 6 Synthesis of FAME from coconut oil and their application in lubricants formulation

In this chapter, the synthesis of fatty acid methyl ester (FAME) from coconut oil and their application as a base oil in comparison with coconut oil in lubricants formulation are presented. The FAME (also called biodiesel) was synthesized *via* both transesterification and electrolysis techniques. Different experimental parameters were applied to investigate the FAME yield. The lubricants were formulated by using coconut oil and their FAMEs as base oils, in combination with Beeswax (BW) as thickener. Before the description of the experimental part and discussion of the main results, short highlights of the research activities and an introduction is presented. Materials and instrumentations for characterizations were reported in the chapter 3.

6.1 Research Highlights

This chapter contains the following research activities.

(e) Formulation of FAME from coconut oil *via* transesterification and electrolysis techniques
(f) Effect of different experimental conditions on the FAME yield
(g) Application of coconut oil and FAME obtained from coconut oil, as a base oil for the formulation of lubricants in combination with beeswax as thickener

6.2 Introduction

The world's energy majorly sourced from fossil fuel which are scarce and will deplete soon due to high demand. An increase in the utilization of fossil fuels leads to increase in local air pollution and deterioration of global warming especially through release of CO_2 [156]. The demand for sustainable green lubricants are urgent for replacement of the fossil-based lubricants due to environmental effects and sustainability problems [157]. As the global climate continues to change, and oil continues to become scarcer, there is growing concern on

sustainable solutions to current practices [158]. Studies shows that in Europe, 5.2 million tons of lubricants are used annually, whose 20% is discharged into the environment [159].

A key approach to reducing dependance on fossil fuels is the use of biodegradable lubricants which offer environmental and health advantages over petroleum-based alternatives [160]. Many biolubricants are biodegradable, environment friendly with no risks to the users [161]. Biolubricants base oils can be obtained from renewable sources such as vegetable oils and animal fats which are safe for humans and ecosystem.

Vegetable oils for biolubricants are produced from plant seeds exhibiting excellent properties which can directly be used as a base oil or can be modified to improve their properties. Vegetable oils as a direct source of base oil are the most commonly used feedstock for biolubricants production due to their availability and convenience. These oils consist of triglycerides and three straight-chain fatty acids [162]. The high viscous properties of vegetable oils make them good candidate for many applications including lubrications. Many vegetable oils such as jojoba oil, crambe oil, soybean oil have many industrial applications like plastics, resins, detergents, lubricants, and solvents [163].

For the biolubricants production, the modification of vegetable involves a two-stage transesterification process. In the first stage, triglycerides react with alcohol such as methanol or ethanol to produce another fatty acid methyl/ethyl esters (FAME/FAEE), also called biodiesel, which can directly be used as a based oil for lubricants. Methanol is most preferred because of easy solubility of catalyst NaOH or KOH and fast reaction with triglycerides [164]. The second step is the reaction of methyl esters with polyols to produce tri-esters, which are biolubricants.

The esters including FAME/FAEE (biodiesel) are the widely used marketed bio-based lubricants [165], [166]. They can be derived by the transesterification or electrolysis of vegetable oils using monofunctional alcohols [167], [168]. One disadvantage of FAME/FAEE as a based oil are their low cold flow properties (CFPs) and for this purpose additives like pour point depressants are often used to improve their low CFPs [169].

Many factors impact the transesterification and electrolysis process for the poduction of FAMEs from vegetable oils. The first important factor is the molar ratio of alcohol/oil. The molar ratio of alcohol/oil influence the production cost, yield and conversion efficiency of the process [170]. To increase the contact between the triglyceride and alcohol molecules and to increase the solubility, it is essential to increase the molar ratio more than the stiochiometric ratio which is 3:1. Generally 4-6:1 or high are effective for efficient conversion [171]. The high amount of alcohol leads the breaking down of the bond between the glycerin and fatty acids in

the vegetable oils [172]. Patil et al., used acid catalyzed esterification reaction for the conversion of jatropha and karanja oils to esters at 80% to 95% respectivelly, at 6:1 molar ratio [173]. The next important factor is the reaction temperature. The reaction temperature effects the yield of FAME from vegetable oils. It is important to maintain the temperature below the boiling point of alcohols to avoid evaporation for the FAME synthesis through both transesterification and electrolysis processes [174]. It is evident from the Istiningrum et al. that increase in temperature below the boiling point of alcohol results in the increase FAME yield [175]. The nature of catalyst is also an important factor in the transesterificatio reaction. Catalyst amount or loading can broadly effect the FAME yiled in the transesterification or electrlysis reaction. Catalyst amount are normally taken in the weight % of oil amount. Hussein et al. investigation shows that by increasing the catalyst amount from 0.8% to 1.5% (w/w) results in in the conversion yield from 2% to 98% [176].

This chapter highlights the synthesis of FAME (biodiesel) from coconut oil *via* boht transesterification and electrolysis techniques. Different experimental parameters like alcohol/oil molar ratio, temperature, KOH amount and current intensity on the FAME yield were investigated and dicussed. The procedure and application of coconut oil and FAME from coconut oil, as a base oil in combination with natural beeswax (BW) as thickener for the formulation of lubricants are explained. The physiochemical properties like hardness, flow and viscour behavior of synthesized lubricants were also investigated and discussed.

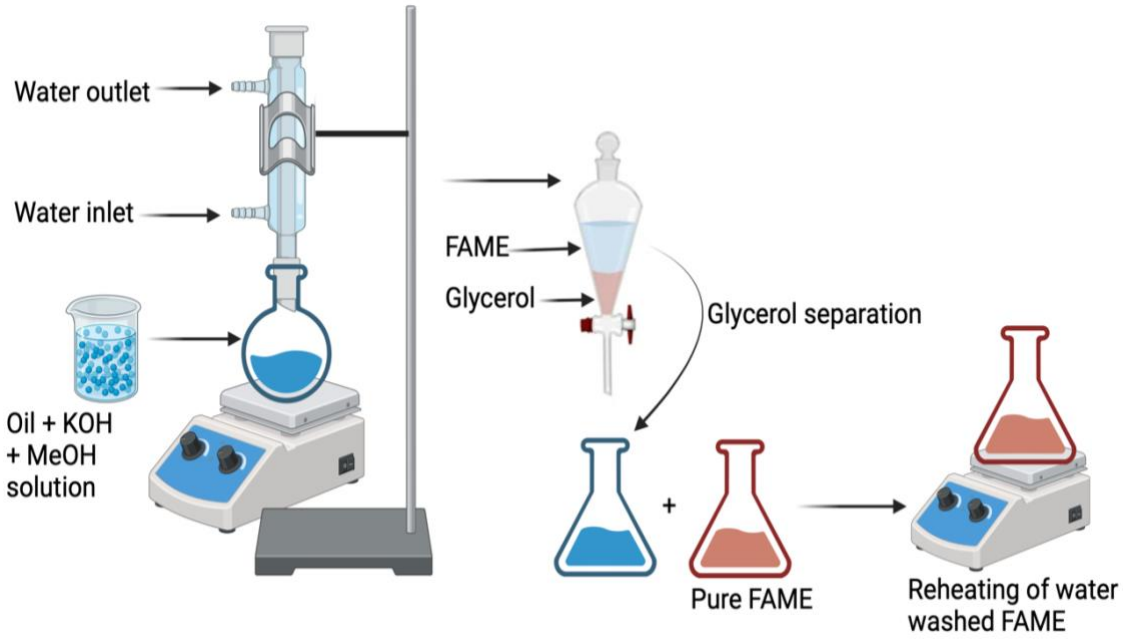
6.3 Methodology

6.3.1 Preparation of FAME by transesterification method

The transesterification and electrolysis reaction were performed for producing FAME from coconut oil. For the transesterification process, coconut oil was taken and mixed with KOH catalyst solution in MeOH as an alcohol (**Scheme 6-1**). The mixture was refluxed at different temperature ranges (25°C, 40°C, 50°C and 70°C) to investigate the FAME yield. Different molar ratios (3:1, 4:1, 6:1, 9:1 and 12:1) of MeOH/oil were tested. The KOH amount in varying proportions i.e., 0.5%, 1%, 1.5%, and 2% of the oil weight were tested. In detailed procedure, 10 g of coconut oil (average molar mass: 218 g/mol, the average molar mass was calculated based on the fatty acid profile, as discussed in chapter 4) was taken and melted at a temperature of 50–60 °C. A KOH catalyst solution was prepared by dissolving 0.1 g of KOH (1% of the oil weight) in 3.23 g of methanol (corresponding to a 6:1 molar ratio of MeOH to oil). The

prepared catalyst solution was then added to the melted oil, and the mixture was refluxed at 50°C for 1.5 hours with continuous stirring. The temperature was recorded using thermometer. After completion, the mixture was transferred into the separatory funnel and allowed to settle down the glycerol as shown in **Figure 6-1.** The upper layer was the fatty acid alkyl ester (biodiesel) which was collected by removing the lower glycerol and weighted. Before injecting into GC/MS, the FAME was further dried over anhydrous sodium sulfate. The yield percentage of fatty acid methyl ester was calculated by the following **equation 1:**

$$\text{FAME \% yield} = \frac{\text{Weight of FAME}}{\text{Weight of oil used}} * 100 \qquad \text{(Eq. 1)}$$



Scheme 6-1: Schematic representation of synthesis of FAME from coconut oil

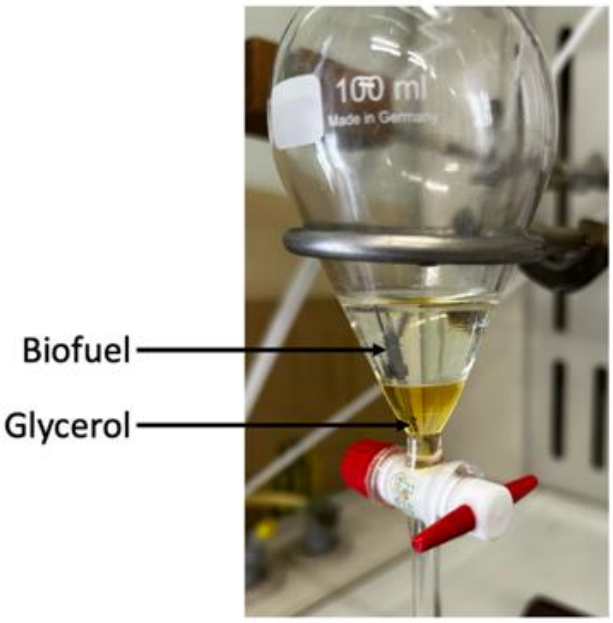


Figure 6-1: Representation of fatty acid methyl ester (FAME) and glycerol after transesterification reaction

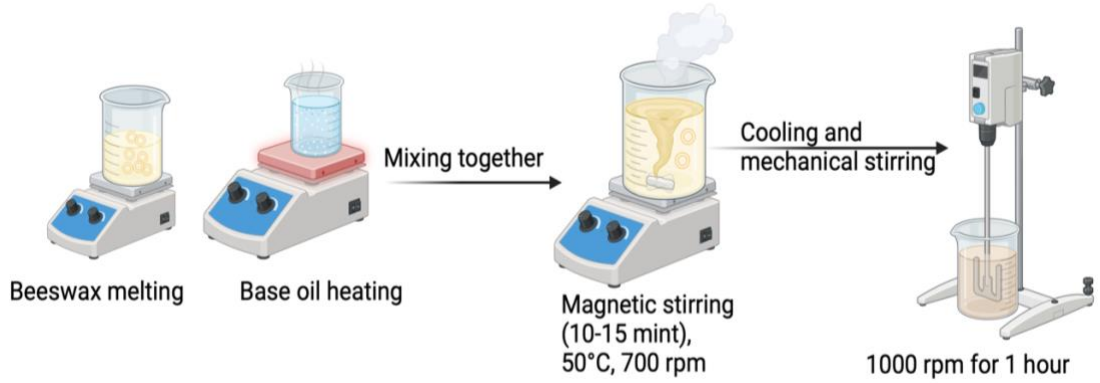
6.3.2 Preparation of FAME using electrolysis method

The ElectraSyn 2.0 cell (as discussed in chapter 3 and 4) was equipped with two non-commercial platinum electrodes. The 20 mL vial was filled with a mixture consisting of coconut oil, MeOH, KOH, and water. In detail procedure, 14 g of coconut oil (average molar mass: 218 g/mol) was mixed with 3.86 ml of MeOH with molar ratio of 6:1. Potassium hydroxide was added as a supporting electrolyte at 1 wt.% of the oil's weight, dissolved in 2 ml of distilled water. The electrolysis reaction was carried out at room temperature under a constant current of 70, 80 and 100 mA for 2 hours at 600 rpm using magnetic stirrer. The nature of Ika ElectraSyn 2.0 instrument, nature and arrangement of electrodes and further procedure were same as discussed in chapter 3 and 4. After completion, the product was transferred to separatory funnel and left for 10-20 minutes to allow the FAME and glycerol phases to separate. The glycerol phase was removed carefully, and FAME phase was washed with distilled water to remove residual including traces of potassium hydroxide and unreacted methanol to get pH of 7. The yield of FAME was calculated using formulas shown in Equation 1. Before injecting into GC/MS, the mixture was rewashed with distilled water and then heated at 80°C to ensure complete removal of impurities and contaminants and then treated with anhydrous sodium sulfate.

6.3.3 Formulation of lubricants using FAME and Beeswax

After preparation of FAME mixture from coconut oil by transesterification method, both FAME and coconut oil was used as a base oil in combination with beeswax (BW) as a thickener for the synthesis of lubricants. The lubricants were prepared according to the following procedure, as reported with little modifications [177]. The two types of base oil (coconut oil and FAME mixture of coconut oil) containing beeswax as a thickener (the BW concentrations were 20%, 25% and 35%) were heated in beakers separately at a temperature of 70 °C to ensure proper melting and homogenization. Afterwards, they were removed from hot-plate, mixed and mechanically stirred for 10-15 min with a magnetic stirrer at 700 rpm and 50 °C, until homogenizations occurred. Finally, the mixture was cooled and then mechanically stirred using VELP shaker at 1000 rpm for 1 hour with carefully mixing to avoid agglomeration **(Scheme 6-2)**. The formulations prepared in the experiments are presented below;

a. CO+35BW – Coconut oil (CO) base oil, mixed with 35% beeswax (35BW)
b. CO+25BW – Coconut oil (CO) base oil, mixed with 25% beeswax (35BW)
c. CO+20BW – Coconut oil (CO) base oil, mixed with 20% beeswax (35BW)
d. F-CO+35BW – FAME from coconut oil (F-CO) base oil, mixed with 35% beeswax (35BW)
e. F-CO+25BW – FAME from coconut oil (F-CO) base oil, mixed with 25% beeswax (35BW)
f. F-CO+20BW – FAME from coconut oil (F-CO) base oil, mixed with 20% beeswax (35BW)



Scheme 6-2: Schematic representation of formulation of lubricants using coconut oil and their FAME as base oil, and beeswax as thickener

6.4 Results and discussion

6.4.1 GC/MS analysis of FAME formed through transesterification

Gas chromatography/Mass spectrometry was used to investigate the contents and percentage of the product. The GC/MS chromatogram of FAME formed by transesterification of coconut oil **(Figure 6-2)** shows the type and percentage of fatty acid methyl esters present in biodiesel (**Table 6-1**).

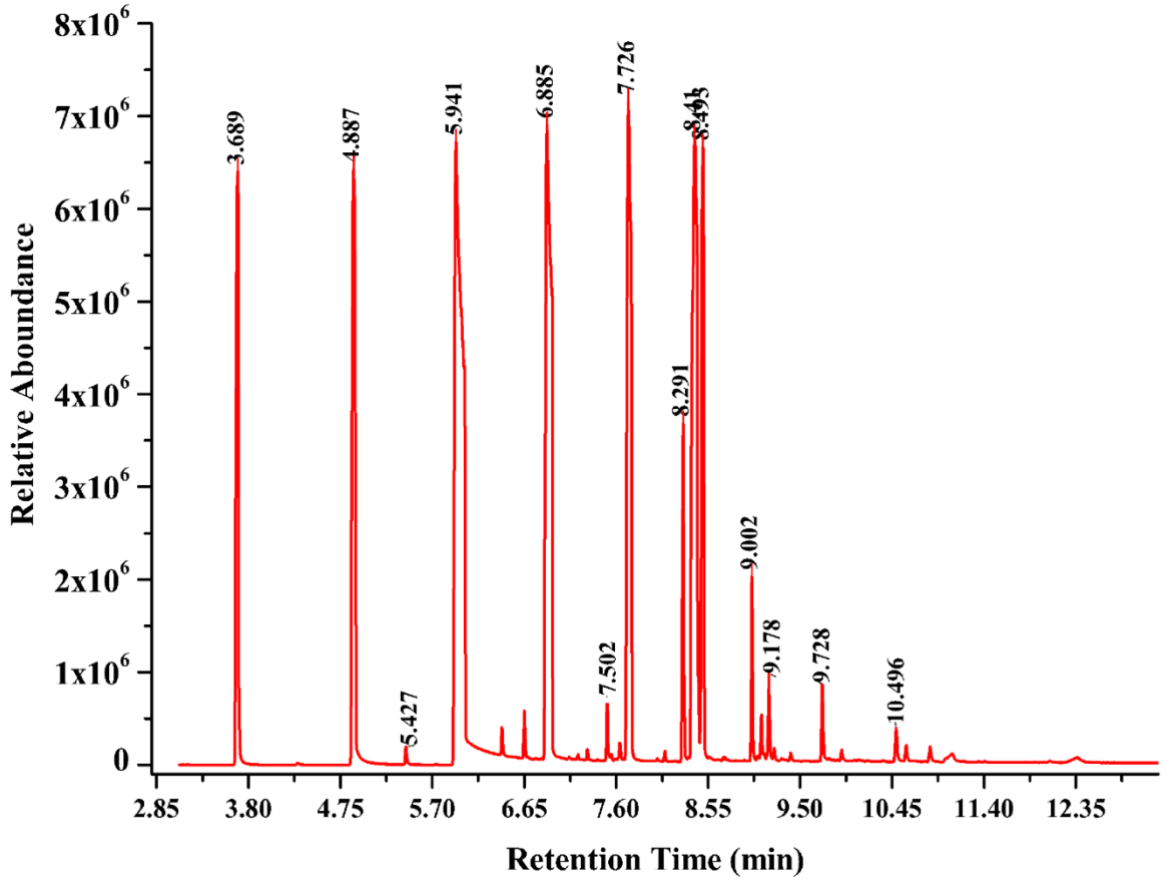


Figure 6-2: GC/MS chromatogram of FAME obtained after transesterification reaction

The FAME profile of the biodiesel obtained after transesterification was investigated by GC-MS, showing the composition of methyl esters. The lauric acid methyl ester (C12:0) with 33%, tetradecanoic acid methyl ester (C14:0) with 18.7%, and 13-octadecanoic acid methyl ester (C18:1) with 17.8%, combinedly constitute 69.5% of the FAME product. Other FAMEs are Hexadecanoic acid methyl ester (C16:0) at 16% and octadecanoic acid methyl ester (C18:0) at 7.4%. The other methyl esters including octanoic acid methyl ester (C8:0), decanoic acid methyl ester (C10:0), tridecanoic acid methyl ester (C13:0), and some long chain esters such

as eicosanoic acid methyl ester (C20:0), contribute minor percentages, ranging between 0.1% and 2.9%. A little percentage of 1.2% of total percentage were undetected by instrument (named undetected peaks) which might be because of unidentified components or impurities in the biodiesel.

Compound	Formula	Percentage %	Retention Time
Octanoic acid methyl ester	C8:0	2	3.689
Decanoic acid methyl ester	C10:0	2.9	4.887
Undecanoic acid methyl ester	C11:0	0.1	5.428
lauric acid methyl ester	C12:0	33	5.941
tridecanoic acid methyl ester	C13:0	0.6	6.422
tetradecanoic acid methyl ester	C14:0	18.7	6.885
Hexadecanoic acid methyl ester	C16:0	16	7.726
13-octadecanoic acid methyl ester	C18:1	17.8	8.413
octadecanoic acid methyl ester	C18:0	7.4	8.498
11-Eicosanoic acid methyl ester	C20:1	0.3	9.178
Eicosanoic acid methyl ester	C20:0	0.4	9.178
Undetected peaks		1.2	

Table 6-1: Result of FAME profile analyzed by GC/MS, their percentages and retention times after transesterification reaction

6.4.2 Effect of experimental parameters

Three experimental parameters i.e., MeOH/oil molar ratio, temperature and KOH amount was investigated to analyze the FAME yield through transesterification reaction.

6.4.3 Effect of MeOH/oil ratio

Figure 6-3 shows the impact of the MeOH/oil molar ratio on the FAME yield after transesterification. As the MeOH/oil ratio increases, the FAME yield also increases, showing a direct relation between methanol availability and product yield. At a 3:1 molar ratio, the FAME yield is 76%, which increases to 85.5% at a 4:1 ratio. The yield further increases to 87.65% at a 6:1 ratio, which is the optimal ratio in transesterification reactions. The yield further continues to increase till 89% at a 9:1 ratio and 93.5% at a 12:1 ratio. This trend

confirms that an excess amount of methanol promotes the conversion efficiency because the access amount of MeOH increase the solubility and helps in breaking the bonds between glycerin and fatty acids in triglycerides [178].

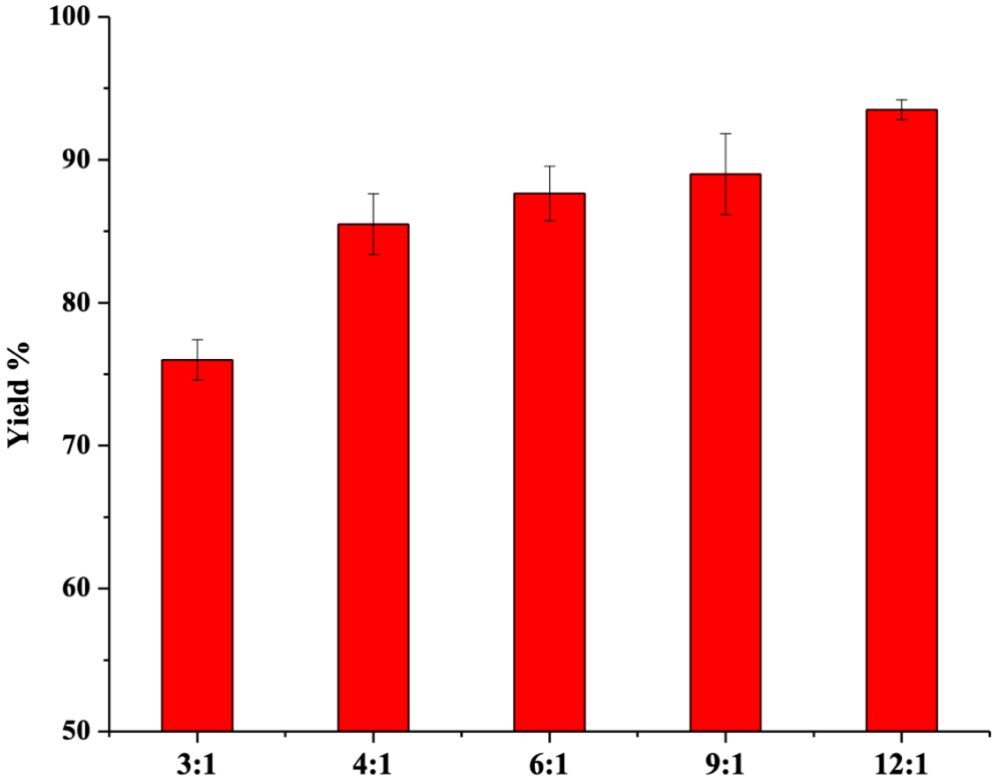


Figure 6-3: Effect of MeOH/oil molar ratio on the FAME yield from coconut oil through transesterification reaction, the other parameters were as follows: KOH = 1% of oil wt., temperature = 50 °C

6.4.4 Impact of KOH amount on transesterification reaction

The impact of varying KOH concentrations on the fatty acid methyl ester (FAME) yield was examined and the results are shown in **Figure 6-4.** At 0.5 wt.% KOH, the FAME yield was 85%. Increasing the KOH concentration to 1 wt.% resulted in a higher yield of 92%. However, 1.5 wt.% of KOH led to a little decrease in yield to 91%. Notably, at 2 wt.% KOH, the FAME yield further decreased to 84.5%. These results suggest that by increasing the KOH concentration generally increases FAME yield and with an optimal concentration beyond which the yield might be plateau or slightly decreased. The initial increase in FAME yield with increased KOH amount might be because of enhanced catalytic activity, which accelerates the transesterification process. The observed decrease in yield at 1.5 wt.% KOH may be because of the saponification reactions, where excess KOH reacts with free fatty acids to form soap,

and inhibiting ester formation. This phenomenon are in agreement with the results of O.J. Alamu et al. who present an optimal KOH concentration of 1 wt% for transesterification of palm kernel oil, beyond which yields decreases due to soap formation [179].

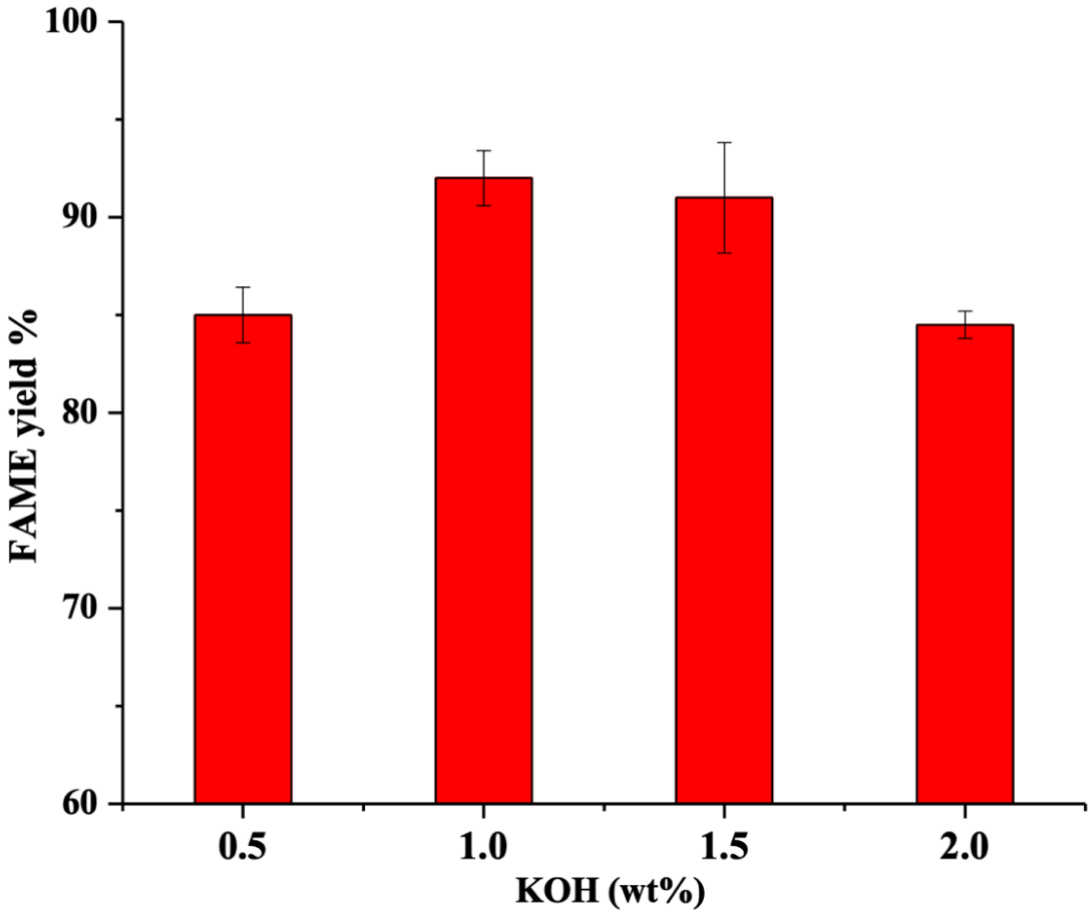


Figure 6-4: Effect of KOH concentration on the FAME yield from coconut oil through transesterification reaction, the other parameters were as follows: MeOH/oil ratio = 6:1, temperature = 50 °C

6.4.5 Impact of temperature on transesterification reaction

The impact of reaction temperature on FAME yield after transesterification are shown in **Figure 6-5.** The FAME yield was highest at 97.5% at 25°C, showing that the reaction was most efficient at this temperature. However, as the temperature increased, the FAME yield also decreased to 91.5% at 40°C, 89% at 50°C and to 84.5% at 70°C. These results demonstrate a negative correlation between reaction temperature and FAME yield beyond 25°C, indicating that elevated temperatures might disturb reaction equilibrium. The observed decline in FAME yield with increased temperatures can be attributed to several factors. Increased temperatures may accelerate side reactions, such as saponification reaction. Additionally, higher

temperatures can also increase methanol evaporation, decreasing its availability for the reaction. A recent study by Barboza et al. highlights the benefits of lower temperatures in biodiesel production, founded that conducting the transesterification process at 30 °C minimized acidity without compromising yield [180]. Similarly, Nwakuba et al. reported that increased temperature 65 °C could lead to methanol evaporation minimizing the FAME yield [181].

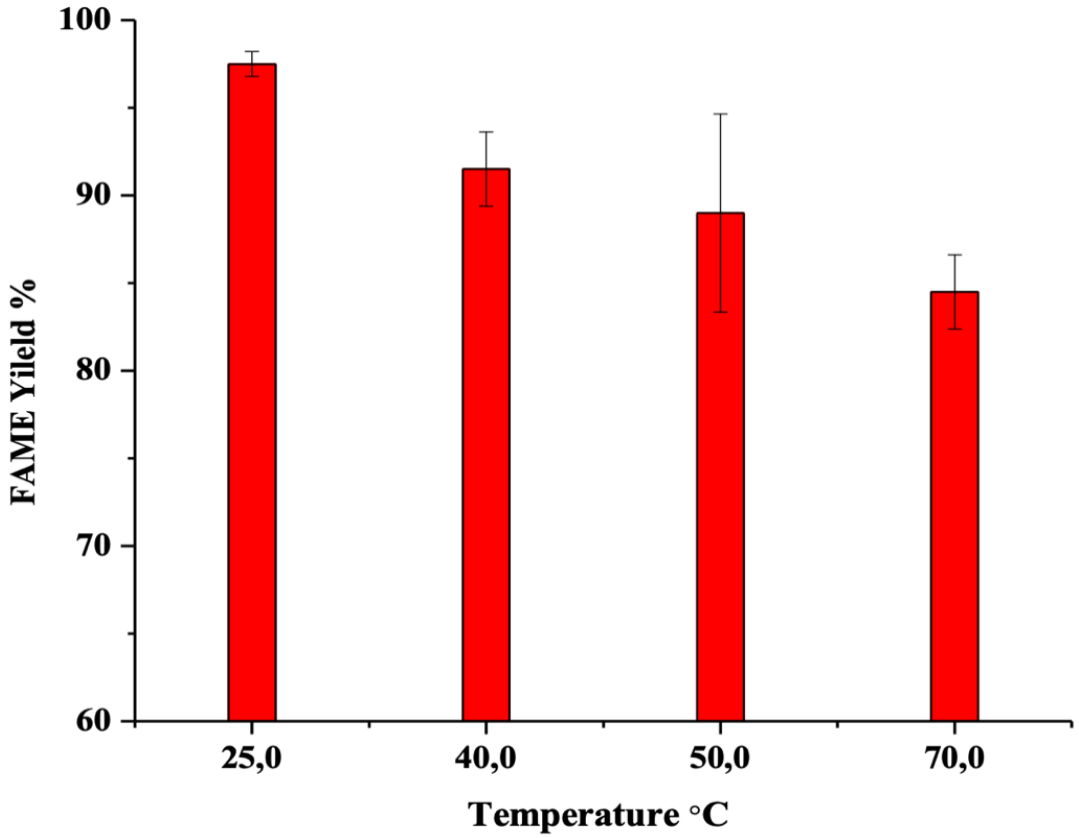


Figure 6-5: Effect of reaction temperature on the FAME yield from coconut oil through transesterification reaction, the other parameters were as follows: MeOH/oil ratio = 6:1, KOH = 1 wt.% of oil

6.4.6 Synthesis of FAME through electrolysis technique (GC/MS analysis)

Gas chromatography/Mass spectrometry was used to investigate the contents and percentage of the product after electrolysis technique. The GC/MS chromatogram of FAME **(Figure 6-6)** shows the type and percentage of fatty acid methyl esters profile present in biodiesel (**Table 6-2**).

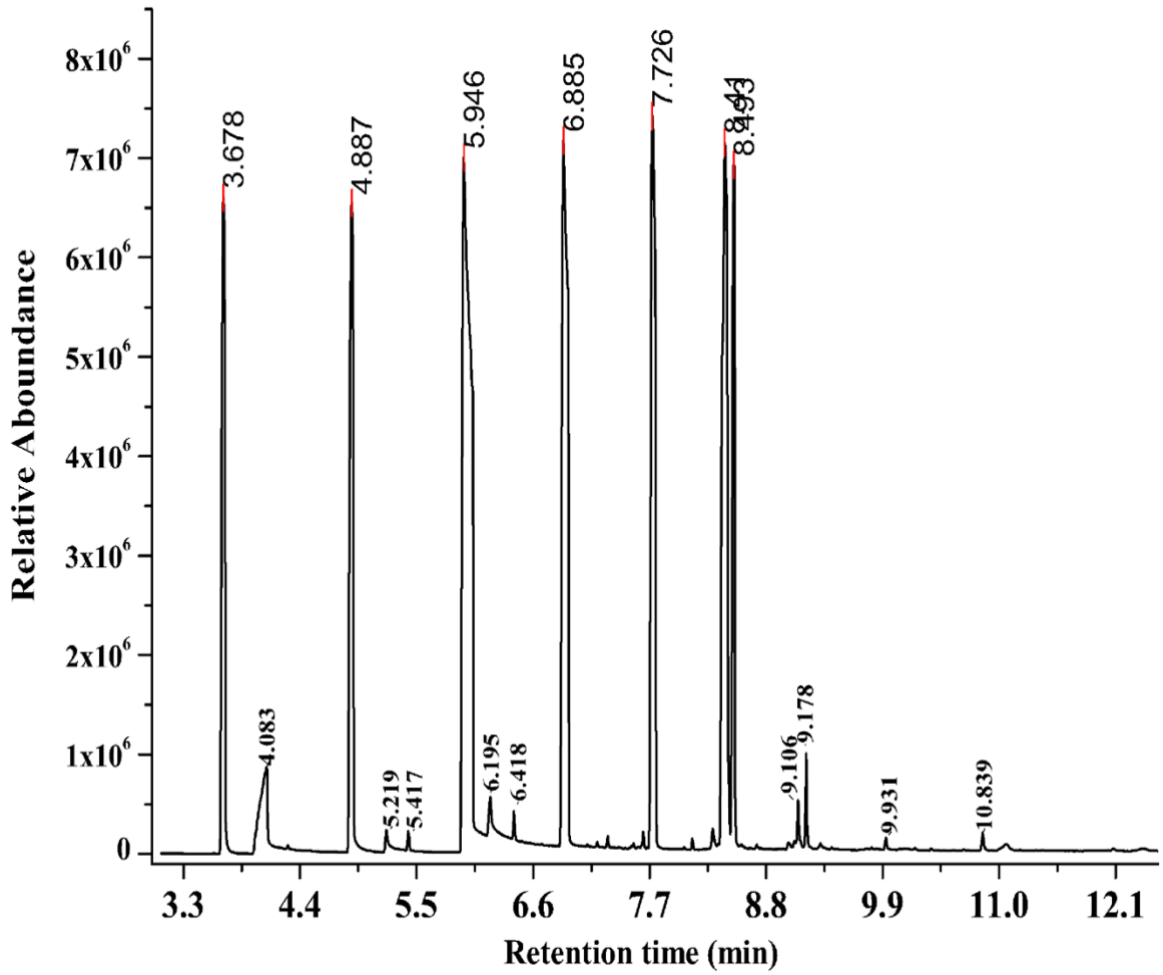


Figure 6-6: GC/MS chromatogram of FAME obtained after electrolysis reaction

The FAME profile of the biodiesel obtained after electrolysis experiment was investigated by GC-MS, showing the composition of methyl esters. Lauric acid methyl ester (C12:0) with the highest percentage at 29%, followed by tetradecanoic acid methyl ester (C14:0) and Hexadecanoic acid methyl ester (C16:0) at 25% and 18% respectively. Unsaturated 9-octadecanoic acid methyl ester (C18:1) constitutes 14% of the total. The octanoic acid methyl ester (C8:0), decanoic acid methyl ester (C10:0) and tridecanoic acid methyl ester (C13:0) are present in minor amount as 3%, 3.8% and 1.8% respectively. The number of peaks which are undetected by GC/MS are accounted for 1.9%.

Compound	Formula	Percentage %	Retention Time
Octanoic acid methyl ester	C8:0	3	3.678
Decanoic acid methyl ester	C10:0	3.8	4.887
lauric acid methyl ester	C12:0	28.4	5.946
tridecanoic acid methyl ester	C13:0	1.8	6.195
tetradecanoic acid methyl ester	C14:0	24	6.885
Hexadecanoic acid methyl ester	C16:0	16	7.726
9-octadecanoic acid methyl ester	C18:1	14	8.413
octadecanoic acid methyl ester	C18:0	6.7	8.433
Eicosanoic acid methyl ester	C20:0	1	9.178
Docosanoic acid methyl ester	C22:0	0.4	10.839
Sum of undetected peaks		1.9	

Table 6-2: Result of FAME profile analyzed by GC/MS, their percentages and retention times after electrolysis reaction

6.4.7 Effect of experimental parameters

Two experimental parameters i.e., current intensity and MeOH/oil molar ratio was investigated to analyze the FAME yield through electrolysis technique.

6.4.8 Impact of current intensity

The current intensity and applied potential have wider effect on the FAME yield. As shown in **Figure 6-7,** at 70 mA, the FAME yield was 88.5%, which was increased to 94% at 80 mA. The maximum FAME yield of 96.5% was observed at 100 mA. These results highlight that increasing current intensity also increases the efficiency of the electrolysis process, to a higher yield of FAME. The increase in FAME yield with increase current intensities are due to the increased rate of electrochemical reaction. The continues production of hydroxide ions at the cathode might react with available methanol and oil which can enhance the product yield [182].

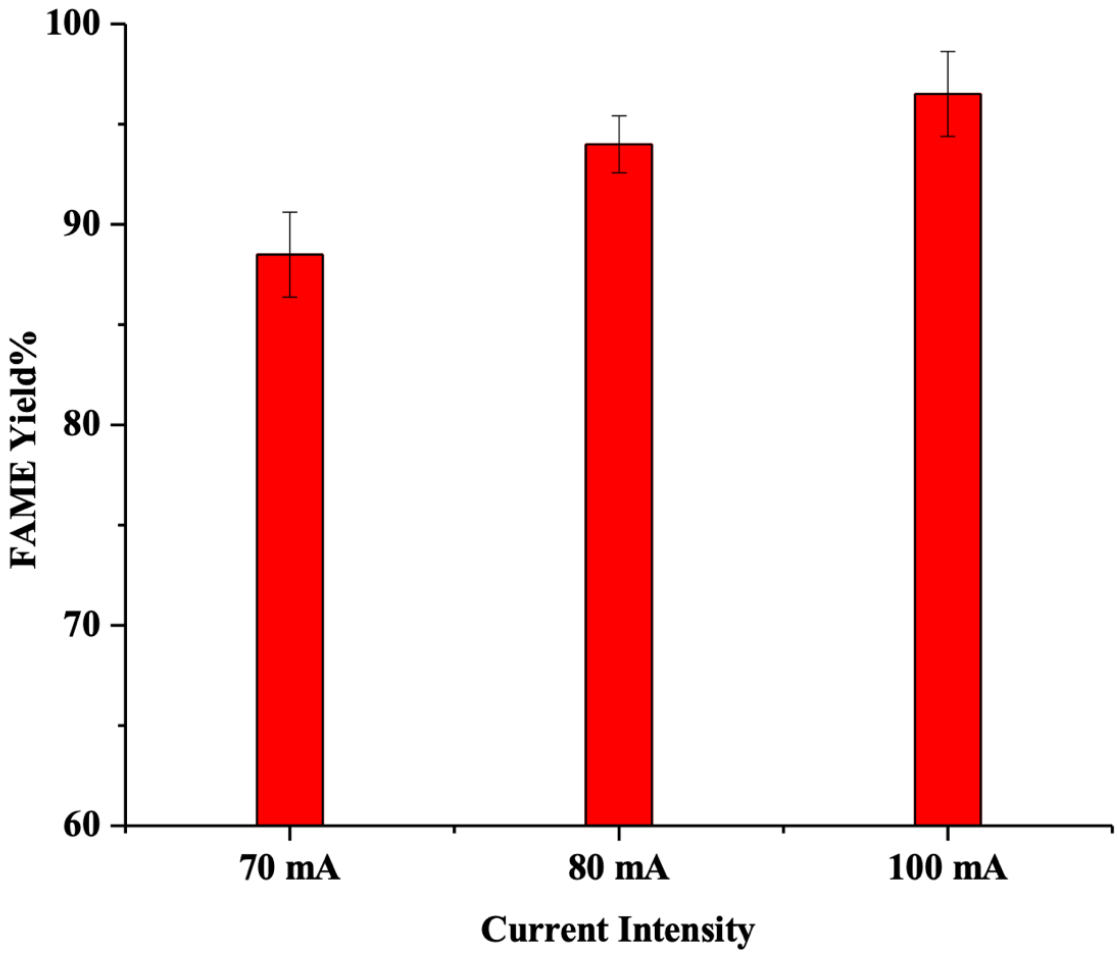


Figure 6-7: Effect of current intensity on the FAME yield from coconut through electrolysis reaction, the other parameters were as follows: MeOH/oil ratio = 6:1, KOH = 1 wt.% of oil

6.4.9 Effect of MeOH/oil ratio

Figure 6-8 shows the effect of different methanol/oil molar ratios on FAME yield during the electrolysis process. MeOH/oil in 3:1 yielded 81% of FAME. The highest yield 96% was observed when methanol/oil was used in 12:1 molar ratio. The trend shows a positive correlation between the MeOH/oil ratio and FAME yield, indicating the importance of enough methanol for efficient conversion. The reason can be attributed that the excess methanol ensures complete conversion of triglycerides, reducing the chances of incomplete reactions. This effect has been explained in studies where increasing the MeOH/oil ratio led to higher biodiesel yields [183].

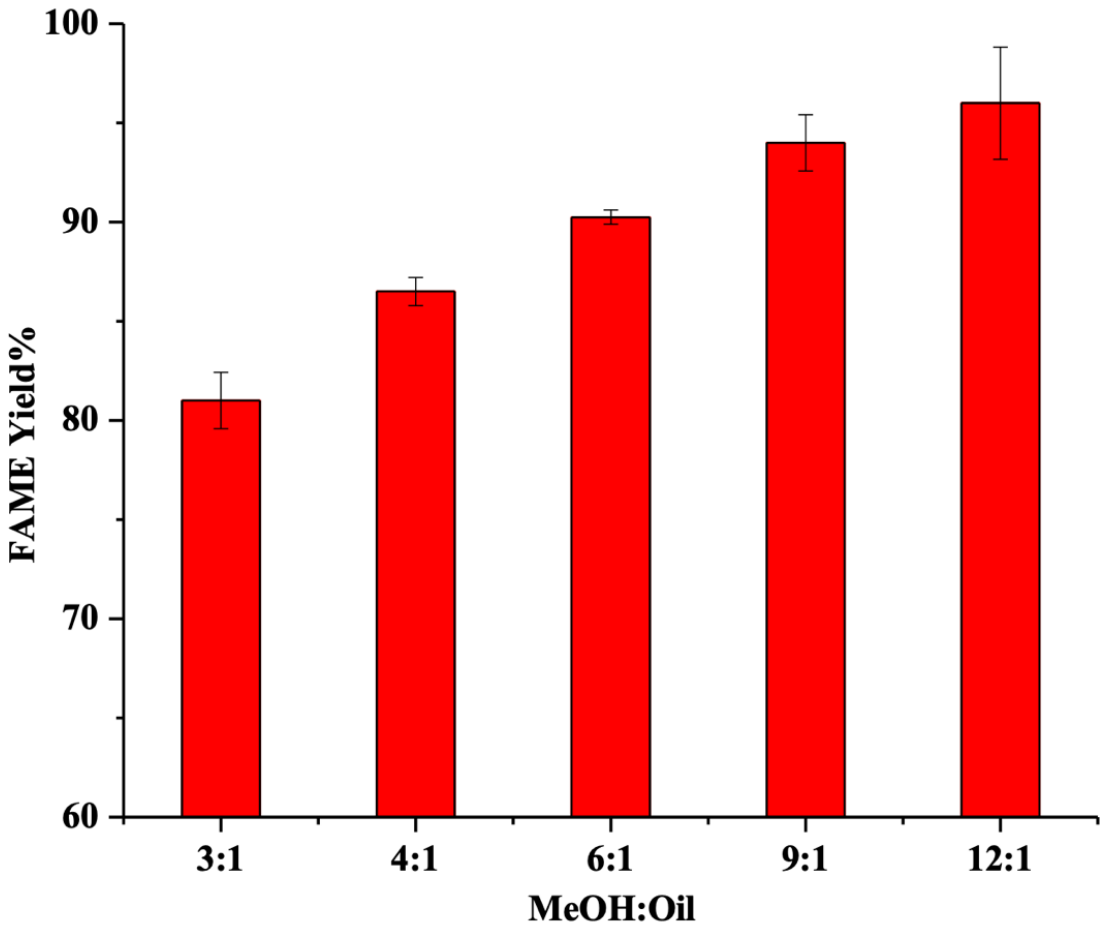


Figure 6-8: Effect of MeOH/oil molar ratio on the FAME yield from coconut through electrolysis reaction, the other parameters were as follows: current intensity = 70 mA, KOH = 1 wt.% of oil

6.4.10 Physiochemical characterization of lubricants

The formulated lubricants using FAME, coconut oil (as base oil) and beeswax (BW) was characterized by using penetrometer and rheometer tests to investigate their lubricity behavior. Details of each test are given below:

6.4.11 Penetrometer test

The consistency or hardness of lubricants were determined by using penetrometer. The consistency was measured by determining the penetration depth of a standardized cone into the lubricants sample at room temperature. The penetration value was then related to National Lubricating Grease Institute (NLGI) levels to determine the hardness of the grease as shown in **Table 6-3**.

NLGI Grade	Worked Penetration	Appearance
000	445-475	Fluid
00	400-430	Fluid
0	355-385	Very Soft
1	310-340	Soft
2	265-295	Moderately Soft
3	220-250	Semi-Fluid
4	175-205	Semi-Hard
5	130-160	Hard
6	85-115	Very Hard

Table 6-3: ASTM standard NLGI classification system based on lubricants consistency

The consistency of grease is an important property that determines the ability to provide lubrication and maintain mechanical integrity in various applications. The results of all the 6 lubricants samples are shown in **Table 6-4.** The penetration of each sample was determined two times using penetrometer and the average was compared with ASTM grade NLGI standards. It was concluded from the results that the BW increases the hardness of the lubricants, as 35% in both coconut oil based and FAME based lubricants shows NLGI of 4 and 2 respectively, which shows much hardness as compared to 25% and 20% of BW in both samples.

Sample	Penetrations	Average	NLGI
CO+35BW	181, 177	179	4
CO+25BW	289, 273	281	2
CO+20BW	305, 281	293	2
F-CO+35BW	285, 261	273	2
F-CO+25BW	329, 351	340	1
F-CO+20BW	360, 350	355	0

Table 6-4: The result of penetrometer test, including penetration values of doublet trails, their average, and NLGI value of each sample (compared with ASTM grade NLGI standards)

6.4.12 Rheometer tests

Rheometer tests was used for the deep analysis of lubricants, particularly for understanding the viscoelastic properties and flow behavior of lubricating materials. Three types of tests i.e., (1) viscosity vs temperature, (2) tack test, (3) flow test (a) shear rate vs shear stress, (b) viscosity vs shear rate and (c) storage modulus (G')/loss modulus (G'') vs shear stress was conducted to gain following information: viscoelastic behavior, yield stress determination, flow behavior and thixotropy, temperature sensitivity and performance under shear. The results of each test are shown below:

6.4.13 Viscosity vs temperature

The results of rheological study of 6 samples of coconut oil and their FAME based lubricants are shown in **Figure 6-9,** to evaluate their behavior of temperature dependent viscosity. The viscosity of all the lubricants samples decreases with increasing temperatures, which is a common behavior of lubricating substance under thermal conditions. In general, different samples show different behavior with increasing temperature. Overall, coconut oil-based formulations show higher viscosities at the same BW% compared to FAME based formulations. This might be because of larger triglyceride molecules with stronger intermolecular forces. At low temperatures (0°C to around 9°C), the coconut oil-based lubricants show an irregular viscosity trend which might be because of partial crystallization of the coconut oil with BW at low temperatures. The triglyceride structure tends to form a mixture of solid and liquid phases near freezing conditions. With the temperature rises to around 40°C - 50°C, viscosities of all samples drop sharply which might be because of melting behavior of both oil and BW. The possible reason for the inconsistency in the viscosity can be because of the inhomogeneity, thermal breakdown or evaporation.

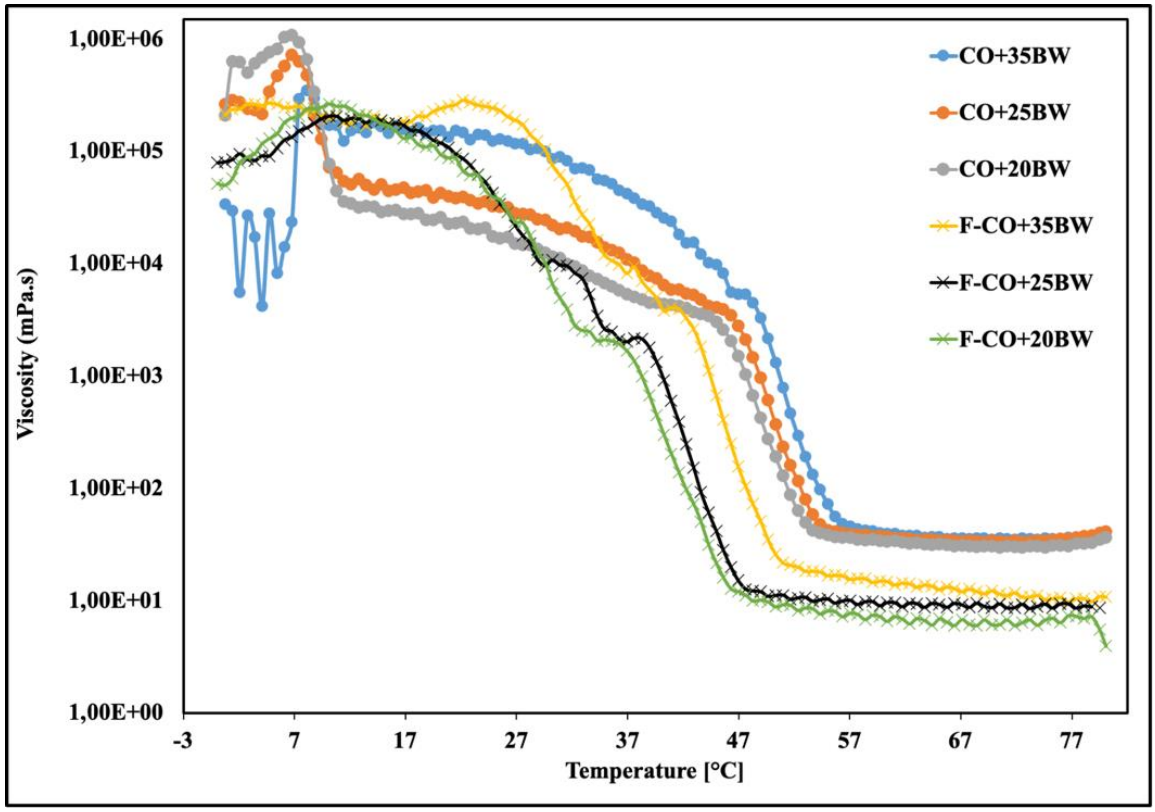


Figure 6-9: Viscosity vs temperature profile of lubricants, the temperature range was 0-80 °C

6.4.14 Tack test

The purpose of the tack test was to investigate the ability of lubricants to adhere to surfaces under separation, where motion can cause lubricant dis-attachment. During the test, the normal force required to separate two surfaces with a layer of lubricants between, was measured against the increasing gap. The result of the tack test of all samples are shown in **Figure 6-10,** showing that the coconut oil-based lubricants exhibit a sharp slope in tackiness, representing more sticky behavior because of triglyceride nature. All the samples having FAME as a base oil exhibit a gentle slope, showing minimum stickiness. In all samples, the higher beeswax concentration corelates with strong adhesive forces, for example CO-35BW sample shows the highest adhesive force at the smallest gap, showing a strong interaction due to the higher BW%. As the gap increases, the force rises toward equilibrium, and breakdown of the adhesive network.

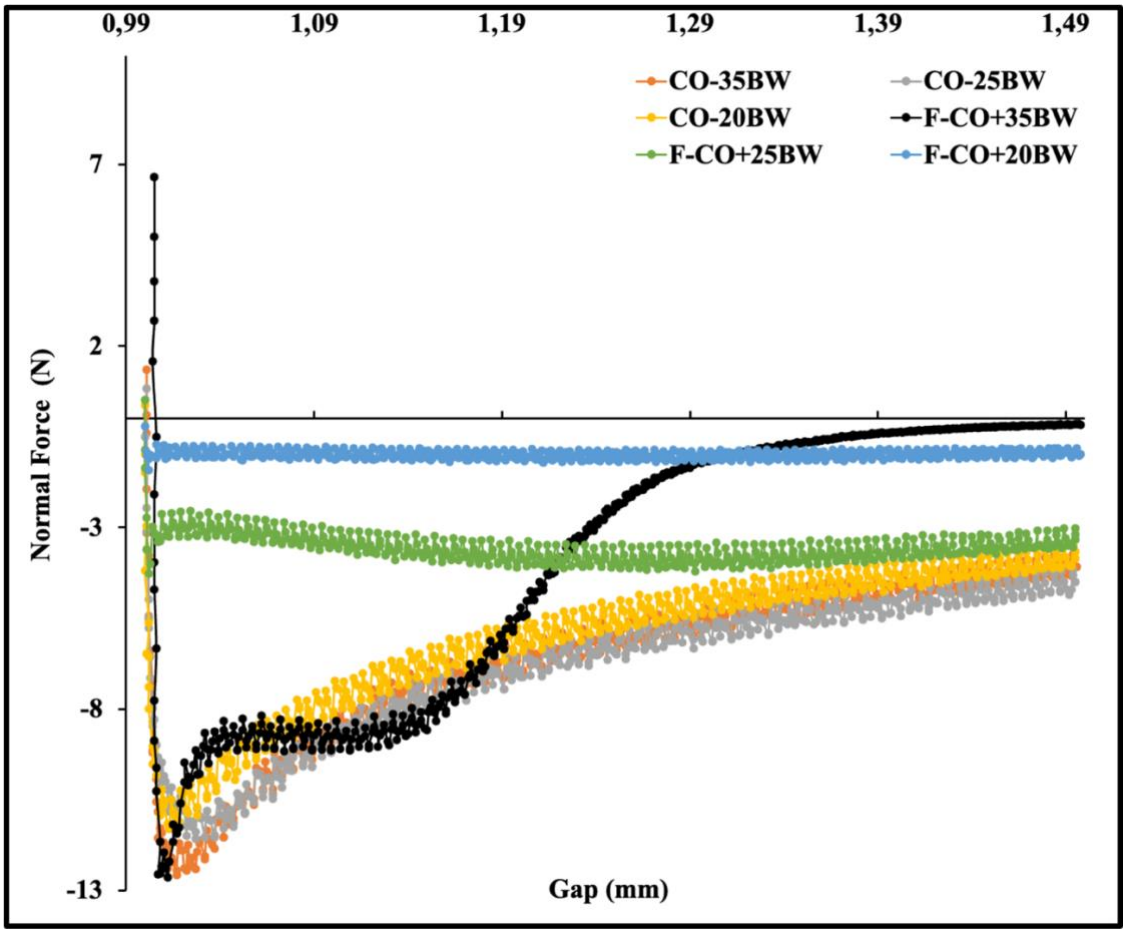


Figure 6-10: Result of tack test of 6 samples of lubricants

6.4.15 Flow test

The flow tests were conducted to investigate the flow behavior of each sample. This property is important for applications where the grease must stay in place without flowing under the force. Three types of flow test were conducted on each sample. The details of each test are given below:

6.4.16 Shear rate vs shear stress

The purpose of the shear rate vs shear stress is the yield stress of all samples, which is the minimum force necessary to cause them to start flowing. The results of all the samples are shown in **Figure 6-11.** Overall, the coconut-based lubricants show higher shear stress as compared to FAME based samples. Furthermore, the samples having higher concentration of BW also shows higher resistance to flow. For example, the CO+35BW sample exhibits the

highest shear stress across all shear rates, indicating a significant resistance to flow due to the triglyceride nature and high beeswax content.

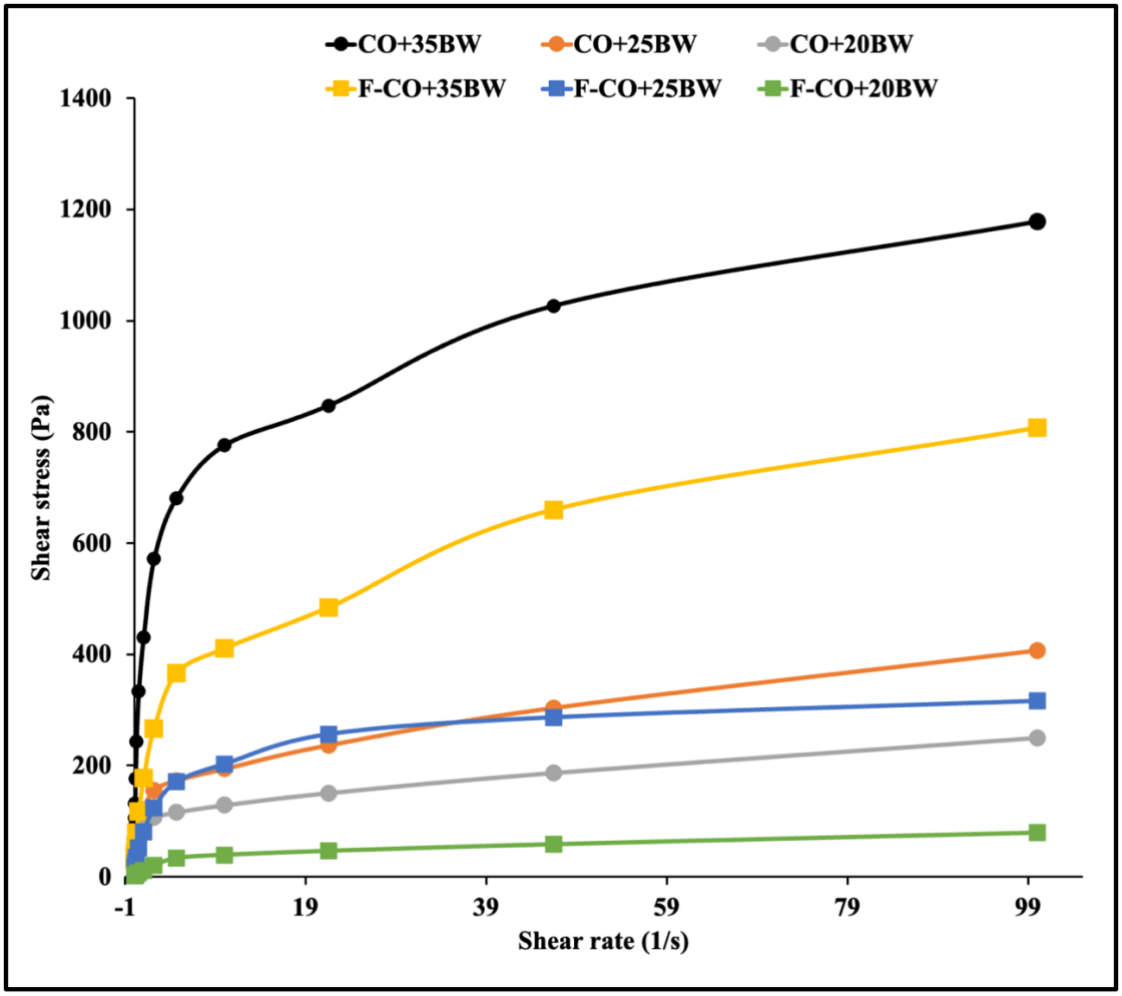


Figure 6-11: Shear rate vs shear stress profile of all the lubricant samples

6.4.17 Viscosity vs Shear rate

This test was conducted to investigate the change in viscosity of a lubricants with the shear rate. **Figure 6-12** shows the viscosity profile against shear rate for the same set of greases. Typically, as the shear rate increases, the viscosity of the greases decreases, exhibiting shear-thinning behavior, which is common in non-newtonian fluids like lubricants. Lubricants based on coconut oil and especially with high BW concentrations shows higher initial viscosities at low shear rates, and then slowly drop down with increase in shear rate. The FAME based lubricants are comparatively shear-thinning, meaning that they are less viscous as they are sheared. These kinds of lubricants are important in applications where the lubricants are needed to be pumped or flow into small spaces under operating conditions.

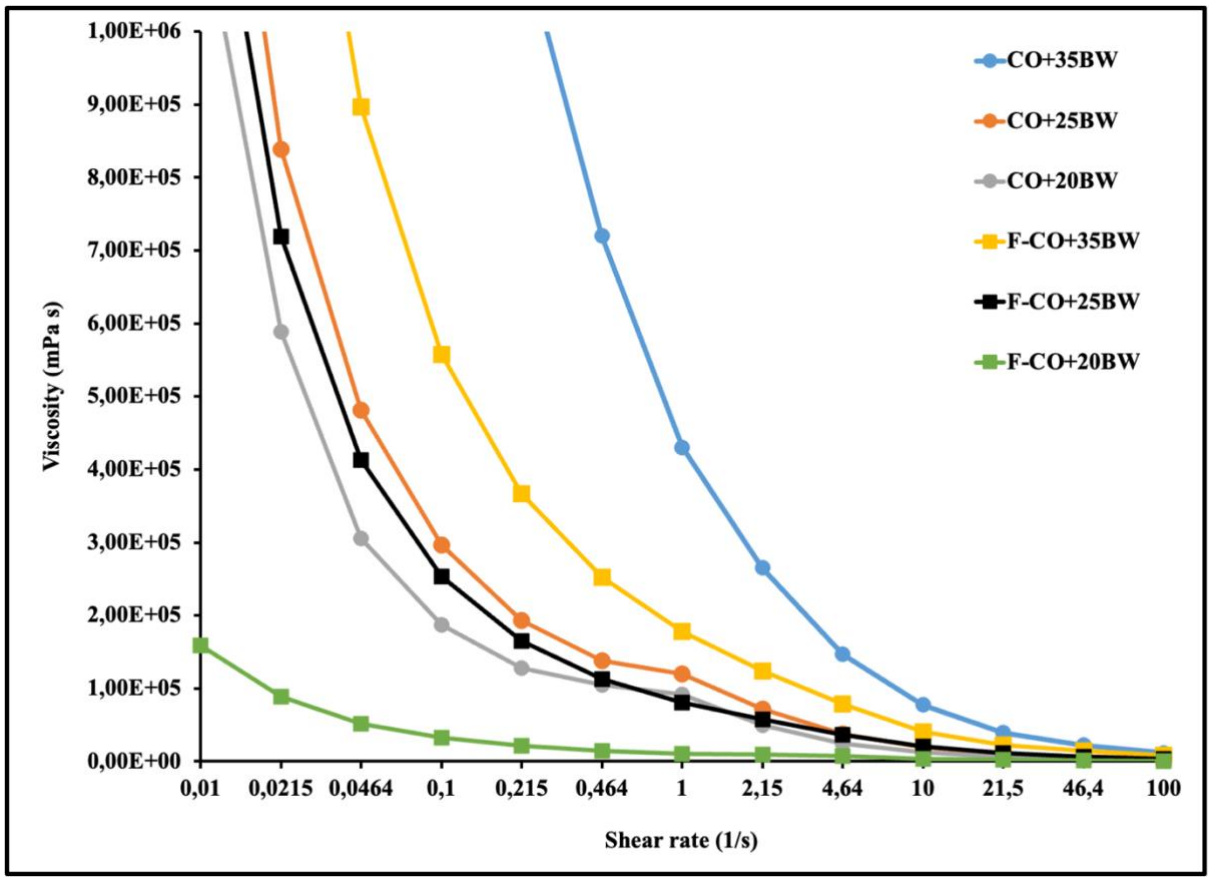


Figure 6-12: Viscosity vs shear rate profile of all the lubricant samples

6.4.18 Storage modulus (G')/loss modulus (G") vs shear stress

The purpose of the storage modulus (G') and loss modulus (G") versus shear stress test was to investigate their ability to store elastic energy (G') and dissipate energy as viscous flow (G") under different shear stresses. This test provides detail information into the balance between the solid and liquid-like properties of the lubricants. **Figure 6-13** represents the result of storage modulus (G') and loss modulus (G") with the increasing shear stress of all the samples. The coconut oil-based samples shows the higher G' and G" values across the shear stress range as compared to FAME based lubricants. Furthermore, the increased BW content through all samples shows the trend of G' dominating over G" at low shear stresses, representing strong elastic behavior. As shear stress increases, G' decreases, transitioning the lubricant to a more liquid like state.

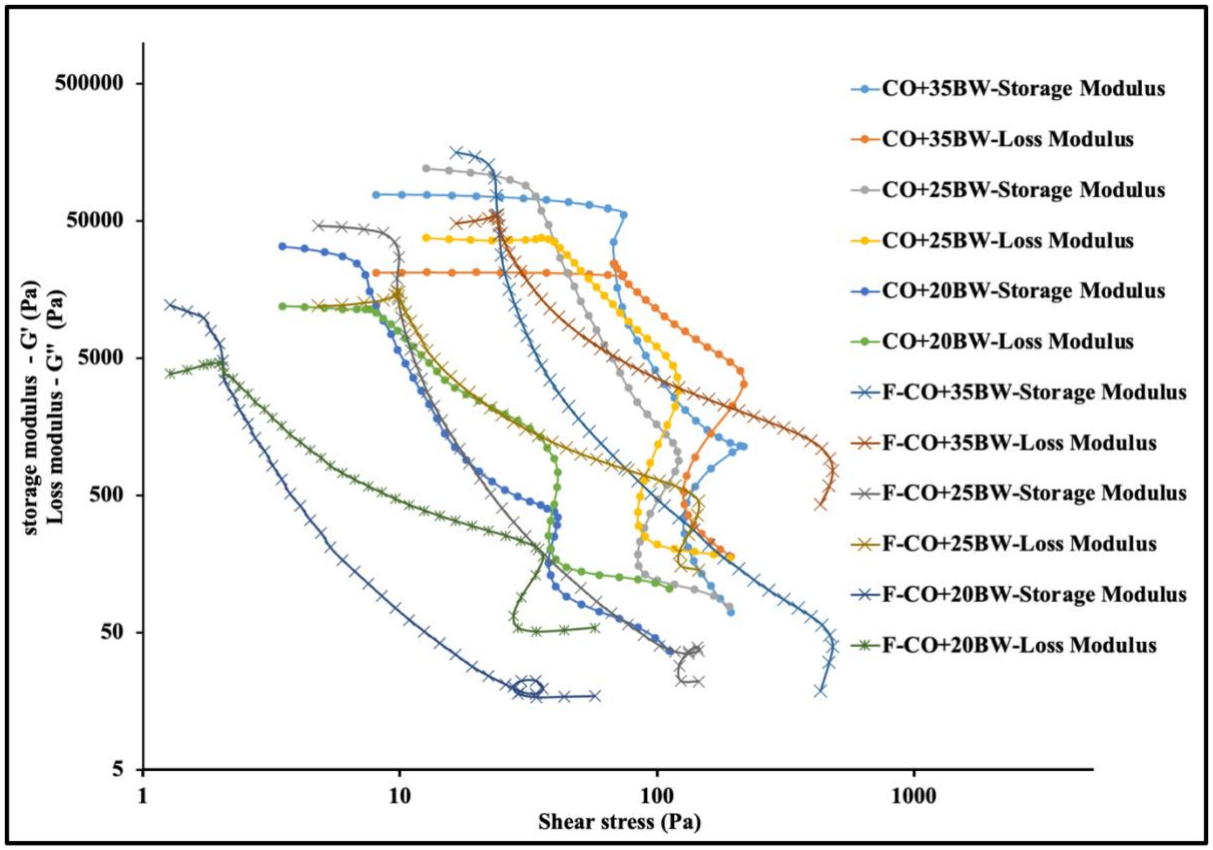


Figure 6-13: Storage modulus (G') and loss modulus (G") versus shear stress profile of all the lubricant samples

6.5 Conclusion

In this study, FAME (biodiesel) production from coconut oil through transesterification and electrolysis techniques are developed. A variety of effecting factors such as MeOH/oil molar ratio, temperature, current intensity and catalyst amount were investigated and concluded that these parameters can be used for controlling and adjusting the yield and quantity of the FAME. Higher MeOH/oil ratio leads to higher product yield, in both transesterification and electrolysis techniques. Using transesterification, 93.5% of yield can be obtained at MeOH/oil molar ratio of 12:1, at temperature of 50 ^{o}C and 1 wt.% of KOH amount. Using electrolysis technique, 96.5% of FAME can be obtained using 6:1 molar ratio of MeOH/oil and 1 wt.% of KOH.

Furthermore, the application of coconut oil and FAME, as a base oil for lubricants formulation concluded that both can be used for the synthesis of bio-lubricants. Both transesterification and electrolysis reactions can be directly used as the starting technique for the synthesis of bio-lubricants. However, coconut oil shows more superior performance in term of high viscosity, adhesive force and high shear stress. Further improvements as investigations of additives role to improve the performance needed to be studied in future.

Chapter 7 Formulation of Bentonite-based greases

In this chapter, the 6-months research activities performed at a lubricant expert company (Bellini S.P.A) are presented. The research project was to formulate biodegradable bentonite-based greased (BBG), having similar properties with the commercial greases (CG). The initial phase of the project was to analyze different commercial greases (CG) to collect extensive data and developing solid understanding of grease properties. Following the analysis of CG, we prepared our own bentonite-based greases (BBG) and compare their rheological behavior, tribometry analysis, oxidation stability and other key parameters with the CG. We also prepared lithium-based greases (LBG) to investigate its wear, friction and extreme pressure (EP) lubricating properties. This in-depth comparative analysis allowed for the assessment of the potential of BBG to serve as effective and environmentally friendly substitutes. The research activities, methodology and results are explained step by step in this chapter, while materials and instrumentation were reported in chapter 3.

Note: It is important to mention that in this chapter, the commercial names of the components are intentionally omitted to respect the confidentiality agreement established with the company involved in this research. This agreement ensures the protection of proprietary information and aligns with the company's privacy policies. As a result, general names are used to represent each component, providing clarity while upholding the terms of the confidentiality arrangement. Also, the name of commercial greases is omitted and the compared results are shown.

6.1 Highlights of research activities

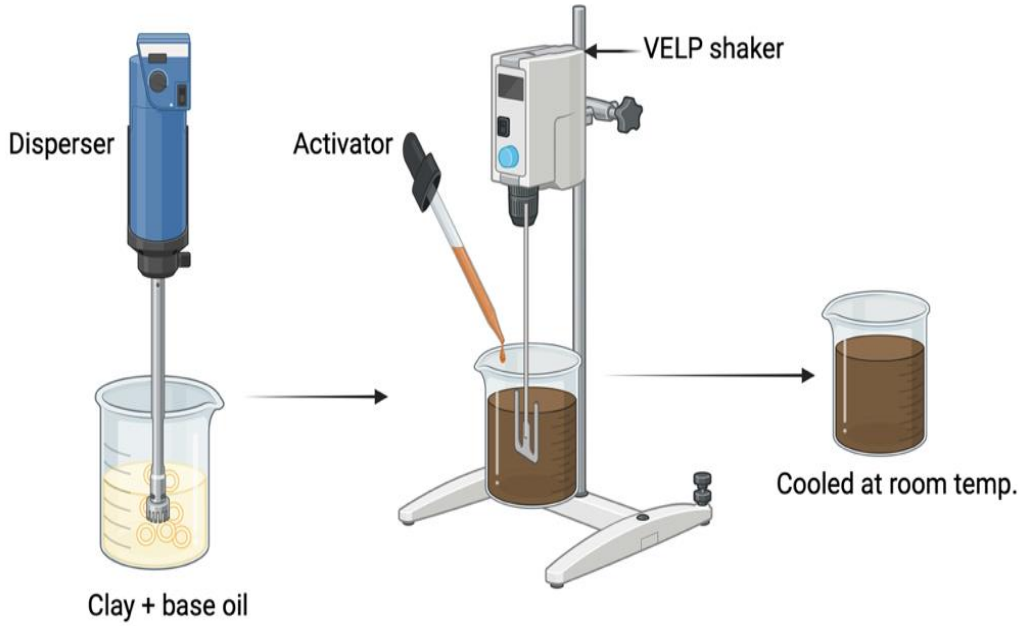
This chapter contains the following research activities.

(h) Analysis of different commercial greases (CG) through different analytical techniques.
(i) Preparation of bentonite-based grease (BBG) and comparison of their properties with commercial greases (CG)
(j) Preparation of lithium-based greases (LBG) to investigate their wear, friction and extreme pressure (EP) lubricating properties

6.2 Experimental part:

6.2.1 Preparation of bentonite-based grease (BBG)

For BBG formulations, three types of components were used i.e., (a) Bentonite clay, (b) saturated vegetable oil as base oil and (c) activator for facilitating dispersion and enhancing thickness. The grease formulation procedure involves a step-by-step mixing to ensure the proper dispersion and to optimize the parameters for obtaining desired consistency/hardness with NLGI 2 **(Scheme 7-1)**. Initially, the bentonite clay and base oil were combined and blended, using a disperser. This mixing step is important to uniform distribution of the clay within the base oil. Following this initial blending, the mixture was transferred to a VELP shaker, where dropwise addition of the activator was carried out. The activator was consisted of a mixture containing 95% propylene carbonate and 5% water. Following changes were applied to optimize the experimental conditions for getting consistency with NLGI 2: concentration of components, disperser duration (5-15 mints), VELP speed (400-1000 rpm), VELP mixing time (5-20 mints).



Scheme 7-1: Schematic representation of formulation of lubricants using coconut oil and their FAME as base oil, and beeswax as thickener

Four types of bentonite clays were used and are named as (1) Clay-1, (2) Clay-2, (3) Clay-3, (4) Clay-4. The clay-1 and clay-2 differ in particle size and surface area, influencing their thickening efficiency and oil absorption capacity. The clay-3 and clay-4 vary in their chemical

modifications, which affect their thermal stability and compatibility with specific base oils. The prepared greases are named based on the number of clays used in the preparation, e.g., grease-1 means that clay-1 is used in the preparation and *vice versa*. All the laboratory prepared greases are collectively named as bentonite-based greases (BBG). After completion, the product was allowed to cool at room temperature and the consistency of the grease was determined using penetrometer and NLGI value was calculated based on the penetration value. The optimized concentrations of each component, penetration value and NLGI are shown in **Table 7-1**.

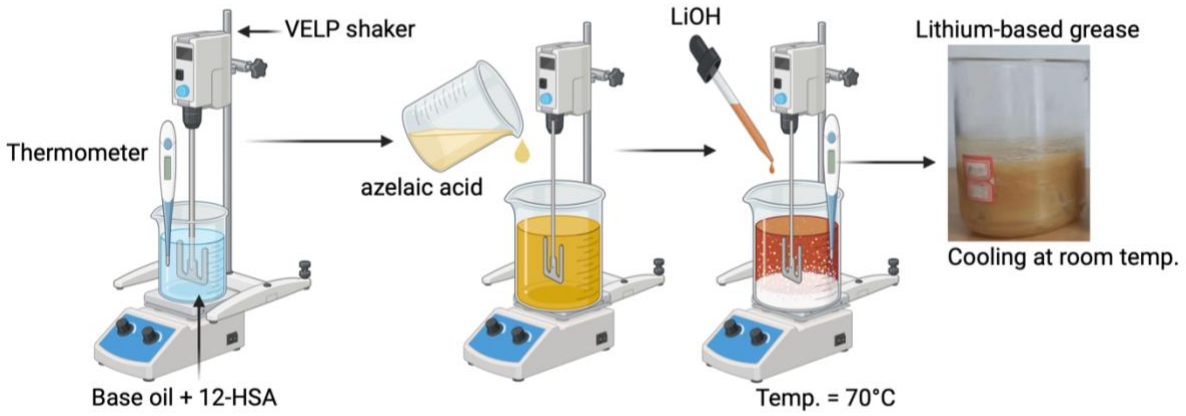
Formulations	**FM1**	**FM2**	**FM3**	**FM4**
Base Oil ((wt. %)	77.0	83.2	86.4	83.2
Clay-1 (wt. %)	19.2	-	-	-
Clay-2 (wt. %)	-	14	-	-
Clay-3 (wt. %)	-	-	11.8	-
Clay-4 (wt. %)		-	-	14.0
Activator (wt. %)	3.8	2.8	1.8	2.8
Penetration	280	273	297	285
NLGI	2	2	2	2

Table 7-1: Optimized concentrations of components for the formulation of bentonite-based greases with NLGI 2

6.2.2 Preparation of lithium-based grease (LBG)

The purpose of the preparation of LBG was to investigate its wear, friction and extreme pressure (EP) lubricating properties. Following materials were used for the preparation of lithium-based grease: (a) mineral oil as base oil, (b) 12-Hydroxistearic acid (12-HSA) (c) azelaic acid, (d) Lithium hydroxide (LiOH). In a detailed procedure, the base oil was mixed with 12-HSA in a beaker using a VELP shaker at 400 rpm and heated at 100°C using a hotplate for 15 minutes. The temperature was recorded using a thermometer. This mixing step was crucial to ensure proper dispersion of the 12-HSA in the base oil. Then the azelaic acid was added to the mixture with continuous stirring. The acid was used to initiate the saponification reaction for the lithium soap. After 5 minutes of mixing, the LiOH was added to the mixture. At this point the reaction starts and impart structure to the grease. The temperature was decreased to 70 °C and the reaction was run for 1 hour with continuous stirring, to complete

saponification reaction, resulting in the formation of the lithium-based grease (**Scheme 7-2)**. After completion, the product was allowed to cool at room temperature for 20 minutes and NLGI was determined using penetrometer test.



Scheme 7-2: Schematic representation of formulation of lubricants using coconut oil and their FAME as base oil, and beeswax as thickener

6.3 Results and discussion

6.3.1 Analysis and comparison of CG and BBG

Different CG were analyzed and compared their properties with BBG. The CG were as follows: (1) Divinol Eco Grease LC 2EP (2) Divinol Lithogrease 2B (3) Aylisynt O EP (4) GR WW EP 0 (5) Complex grease Li/RP B2 (6) Divinol Lithogrease 00 (7) Grease biodegradable (8) X-Draw Bio 40 St (9) Divinol Lithogrease 7000, (10) Arvina EH2 (11) Arvina MB2. The Arvina EH2 and Arvina MB2 are the bentonite-based commercial greases. The results of different test are explained as follows:

6.3.2 Rapid Small Scale Oxidation Test (RSSOT)

The oxidation stability of few commercial grease and bentonite-based greases were investigated by using RapidOxi (RSSOT) apparatus. The results of the test with stopping criteria as 10% pressure drop, are shown in **Table 7-2**. The oxidation stability of commercial greases was much higher as compared to our grease, because it was known in advance that commercial grease contains many kinds of additive for the improved performance. Therefore, we further analyzed the CG by X-ray florescence (XRF) and atomic emission spectrometer (AES) to investigate and confirm the presence of additives and other components.

Commercial grease	Oxidation stability	Bentonite-grease	Oxidation stability
Divinol Lithogrease 00	661.15 mints	Grease-1	38.5 mints
Aylisynt o EP	139.12 mints	Grease-1	41 mints
GR WW EP 2	387.45 mints	Grease-1	37 mints
Divinol litho-grease 2B	930.45 mints	Grease-1	42 mints
Arvina EH2	907.72 mints	-	-
Arvina MB2	347.65 mints	-	-

Table 7-2: Oxidation stability of CG greases and BBG

6.3.3 X-ray florescence (XRF) and atomic emission spectrometer (AES)

Four of the CG (Divinol Lithogrease 2B, GR WW EP2, Arvina EH2 and Arvina MB2) were investigated using atomic emission spectrometer (**Table 7-3**) and X-ray florescence (XRF) (**Table 7-4**), for obtaining information about elemental analysis and additive detection. From the results it is shown that all the CG contains a lot of additives like Ni, Fe, S *etc.*, which improved the oxidation stability and other lubricating properties.

Grease	Elemental parts detected														
GR WW EP 2	**Ag**	**Al**	**B**	**Ba**	**Ca**	**Cd**	**Ce**	**Co**	**Cu**	**Fe**	**Zn**	**H**	**H_2**	**C**	**C_2**
	0.00	0.00	0.02	0.03	146.90	0.02	5.60	0.67	0.07	0.27	0.46	5599	4270	18082	14552
	In	**K**	**Li**	**Mg**	**Mn**	**Mo**	**Na**	**Ni**	**P**	**Pb**	**Si**	**Sn**	**Ti**	**V**	**W**
	0.20	0.28	85.27	7.34	0.00	0.00	0.53	0.05	0.00	0.64	1.18	0.00	0.00	0.16	7.14
Arvina EH2	**Ag**	**Al**	**B**	**Ba**	**Ca**	**Cd**	**Ce**	**Co**	**Cu**	**Fe**	**Zn**	**Sn**	**Ti**	**V**	**W**
	0.01	400.29	0.17	0.31	173.1	0.00	4.99	0.51	0.52	196.63	108.49	8.71	3.74	9.20	0.00
	In	**K**	**Li**	**Mg**	**Mn**	**Mo**	**Na**	**Ni**	**P**	**Pb**	**Si**	**H**	**H_2**	**C**	**C_2**
	0.01	4.09	0.19	71.82	0.19	379.61	23.98	0.00	0.00	0.00	1209	5780	4543	18536	14323
Arvina MB2	**Ag**	**Al**	**B**	**Ba**	**Ca**	**Cd**	**Ce**	**Co**	**Cu**	**Fe**	**Si**	**Sn**	**Ti**	**V**	**W**
	0.01	377.81	0.12	0.19	21.53	0.00	6.69	0.59	4.43	191.74	1208	10.91	3.29	11.53	0.00
	In	**K**	**Li**	**Mg**	**Mn**	**Mo**	**Na**	**Ni**	**P**	**Pb**	**Zn**	**H**	**H_2**	**C**	**C_2**
	0.11	6.10	0.15	66.46	0.30	509.62	16.28	0.07	0.00	2.40	111.46	5818	4601	18708	14933
Divinol lithogreas 2B	**Ag**	**Al**	**B**	**Ba**	**Ca**	**Cd**	**Ce**	**Co**	**Cu**	**Fe**	**Si**	**Sn**	**Ti**	**V**	**W**
	0.00	0.00	33.67	0.06	7.23	0.00	8.73	0.82	0.05	0.11	0.16	0.00	0.00	0.28	7.39
	In	**K**	**Li**	**Mg**	**Mn**	**Mo**	**Na**	**Ni**	**P**	**Pb**	**Zn**	**H**	**H_2**	**C**	**C_2**
	0.29	0.11	132.42	0.11	0.00	6.05	0.63	0.09	13.09	0.04	13.43	5462	4394	17303	13970

Table 7-3: Atomic emission spectroscopy (AES) results of four commercial greases

Grease	Elemental parts %															
Divinol Lithogrease 2B	**Al**	**Si**	**P**	**S**	**Cl**	**Fe**	**Ni**	**Cu**	**Zn**	**Mo**	**Ag**	**Ta**	**-**	**-**	**-**	**-**
	10.3	7.04	10.9	51.8	9.88	2.76	0.47	0.8	4.14	1.14	0.221	0.538	-	-	-	-
GR WW EP2	**Al**	**Si**	**P**	**S**	**Cl**	**Ca**	**Mn**	**Fe**	**Ni**	**Cu**	**Zn**	**Ag**	**Ba**	**Sr**	-	-
	10.1	7.13	8.16	27.5	6.83	31.7	1.33	3.91	0.47	1.23	0.214	0.229	0.812	0.274	-	-
Arvina EH2	**Al**	**Si**	**P**	**S**	**Cl**	**Fe**	**Cu**	**Zn**	**Mo**	**Ag**	**Sr**	**Nb**	**Rh**	-	-	-
	3.5	10.4	1.9	57.7	1.6	4.6	0.07	1.74	7.49	0.029	0.03	0.21	0.06	-	-	-
Arvina MB2	**Al**	**Si**	**P**	**S**	**Cl**	**Ca**	**Fe**	**Ni**	**Cu**	**Zn**	**Mo**	**Ag**	**Cd**	**Sn**	**Ga**	**Nb**
	5.2	15.4	2.07	44.8	2.07	10.3	6.06	0.02	0.118	2.45	10.9	0.04	0.02	0.01	0.018	0.3

Table 7-4: XRF results of four commercial greases

6.3.4 Rheometer tests

Rheometer tests are important tools in the analysis of greases, particularly for understanding the viscoelastic properties and flow behavior of lubricating materials. Three types of tests i.e., (1) viscosity vs temperature (2) tack test and (3) flow tests i.e., (a) shear rate vs shear stress, (b) viscosity vs shear stress and (c) storage modulus/loss modulus vs shear stress of all CG and BBG were conducted in order to gain following information: viscoelastic behavior, yield stress determination, flow behavior and thixotropy, temperature sensitivity and performance under shear. The results of each test are shown below:

6.3.5 Viscosity vs temperature test of CG and BBG

The results of viscoelastic study of different CG, to evaluate the behavior of temperature dependent viscosity are shown in **Figure 7-1**. The viscosity of all the commercial grease samples decreases with increasing temperatures, which is a common behavior of lubricating substance under thermal conditions. In general, different samples show different behavior with increasing temperature. The grease *e.g.*, Lithogrease 7000 and Lithogrease 2B shows initial decline with increasing temperature and then high stability with further increase in temperature. Other grease like Arvina MB2 and Arvina EH2 shows a steep viscosity decline at lower temperature. The samples like GR WW EP 0, GR WW EP 1, GR WW EP 2 and Aylisynt 0 EP etc., shows a strong stability in viscosity with increasing temperatures while some samples like Divinol Eco grease LC 2 EP, Complex grease Li EP3 shows a non-linear relation of viscosity with sudden decrease and then increase indicating a separation of components or phase transition at specific temperature. Overall, the graph shows a different rheological profile of commercial greases which can be attributed to the variation in base oil, thickeners type and additives used in their formulations.

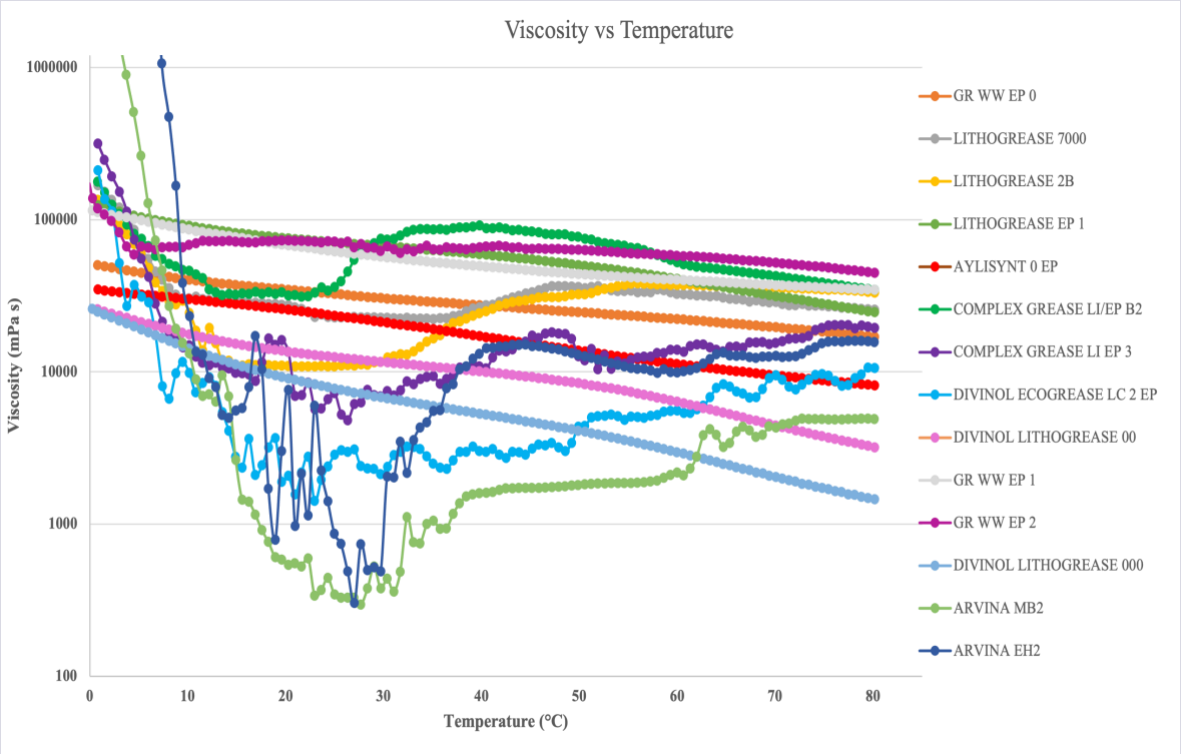


Figure 7-1: Viscosity vs temperature profile of different commercial greases. The temperature range was from 0-80 °C

The viscosity vs temperature profile of BBG were compared with CG especially bentonite-based commercial greases i.e., Arvina MB2 and Arvina EH2. The results revealed striking similarities and share comparable performance characteristics as shown in **Figure 7-2**. For all greases, viscosity decreases as the temperature increases. The decrease is quite steep at lower temperatures and levels off as the temperature rises. Arvina MB2 and Arvina EH2, shows a more stable viscosity over a range of temperatures compared to the BBG. Grease-3, while starting at a lower viscosity than Grease-4, also shows a sharp decrease but seems to stabilize at a higher temperature. The Grease-1 maintains a more consistent viscosity across a wider temperature range. Grease-2 shows the lowest initial viscosity and the least change with temperature increase, which could be indicative of a thinner grease suited for high-temperature applications. At higher temperatures (above 60°C), the viscosities of all greases converge to a narrower range, with BBG showing a similar performance to the commercial products. There is some noise in the data, especially noticeable in the Grease-2 and Grease-4 plots, which could be due to experimental errors or intrinsic properties of the greases causing fluctuations in viscosity.

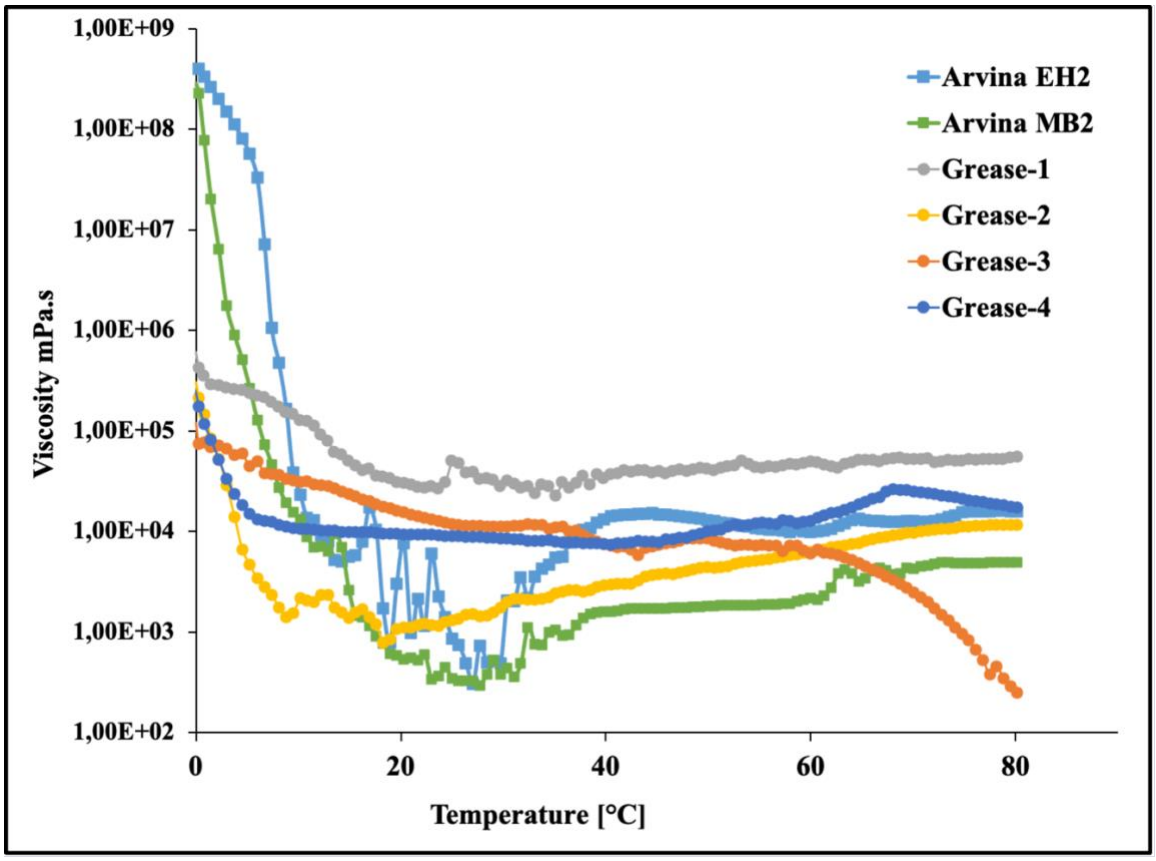


Figure 7-2: Viscosity vs temperature profile of BBG, Arvina MB2 and Arvina EH2

The possible reason for the inconsistency in the viscosity might be because of the following reasons.

(a) **Inhomogeneity:** If the grease isn't mixed well, it can lead to variations in the thickener distribution in different parts of the sample.

(b) **Thermal breakdown or oxidation:** At higher temperatures, some components of the grease, like the thickener might undergo thermal breakdown or chemical reactions that could temporarily increase viscosity before it continues to decrease with further temperature rise.

(c) **Evaporation:** The base oil may contain light fractions that evaporate at high temperatures, leaving behind a more viscous mixture.

(d) **Reversible Changes:** Some thickeners in greases can exhibit reversible changes due to temperature that affect viscosity.

6.3.6 Tack test

Tack test was conducted to investigate the ability of grease to adhere to surfaces under separation, where motion can cause lubricant displacement. **Figure 7-3** illustrating the result of tack test of different CG as measured by response of separation gap with the applied normal force. The data provides a detailed explanation of how each sample responds for tackiness as the gap increases. A general trend shows that some samples show a gentle slope indicating a minimum tackiness level, suggesting a minimum sticky nature. In comparison other samples exhibits a sharp increase in tackiness, representing sharp slopes. These samples show a significant adhesive force in comparison, exhibiting more sticky behavior.

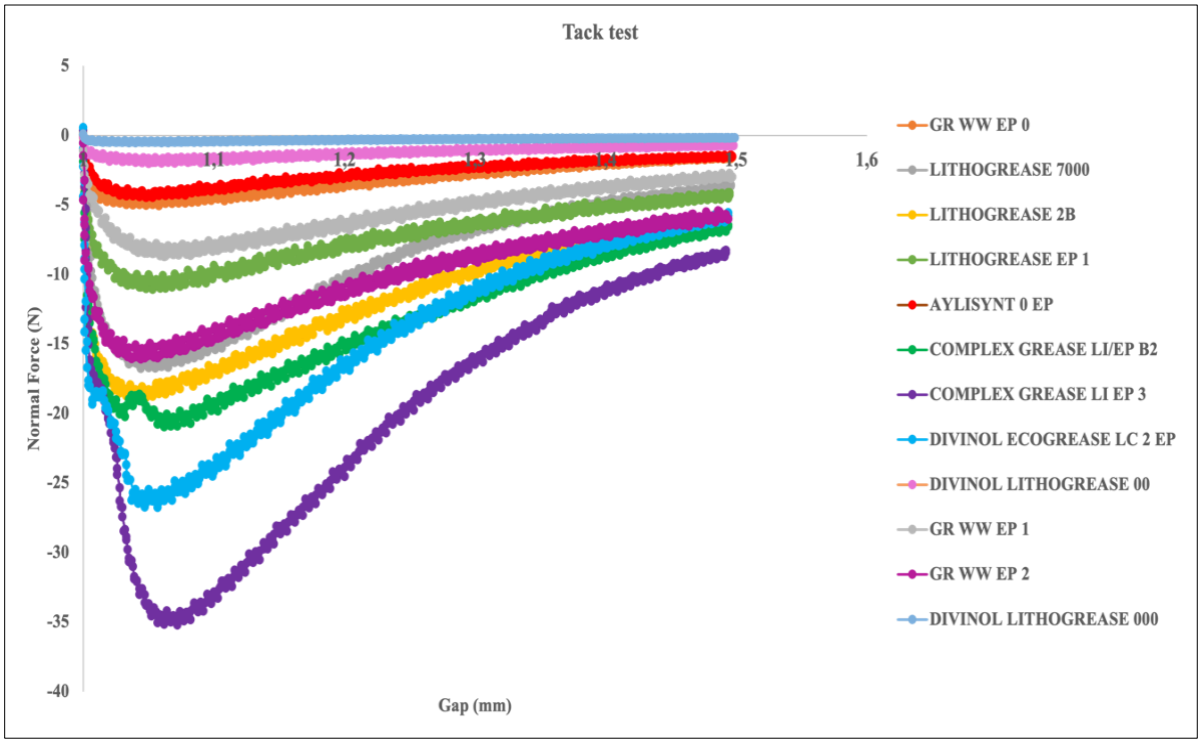


Figure 7-3: Tack test result of different commercial greases

The tack test comparison (**Figure 7-4)** revealed that BBG shows performance levels comparable to those of CG. This shows that the formulations effectively meet the desired adhesiveness and cohesion requirement.

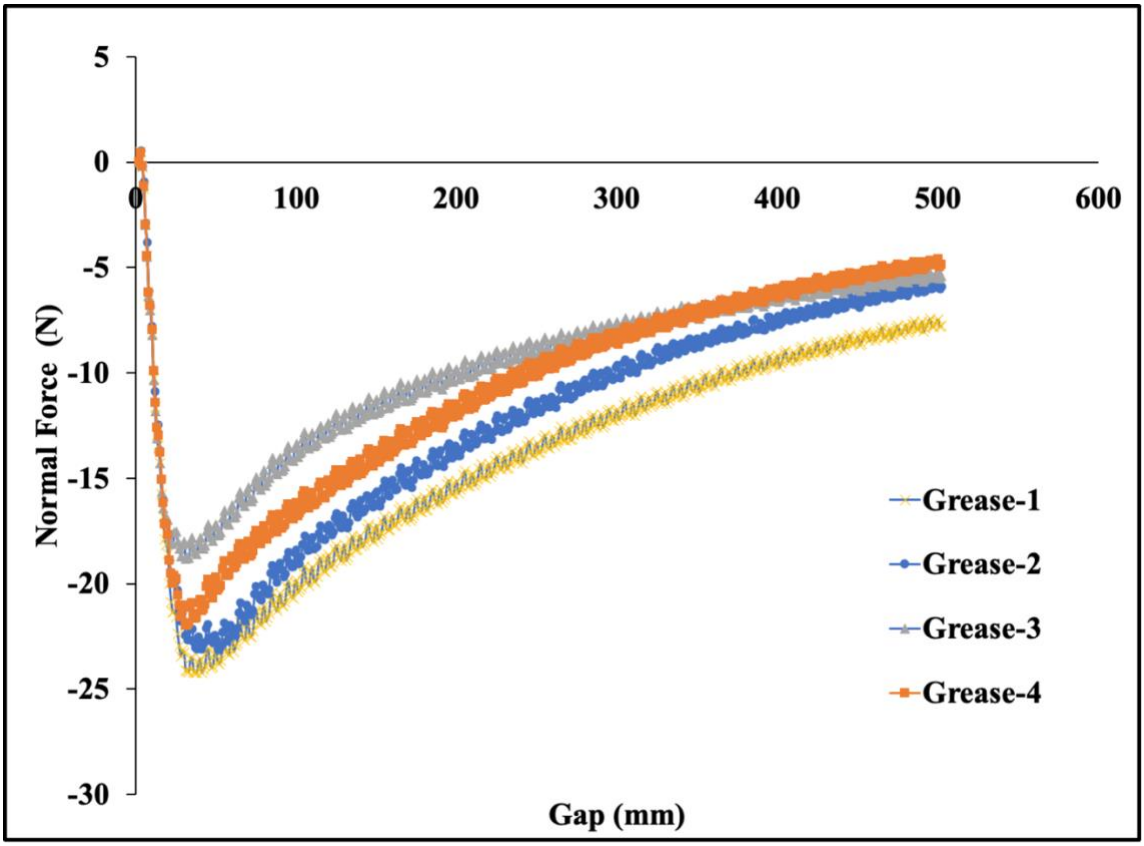


Figure 7-4: Result of tack test of four BBG

6.3.7 Storage modulus (G')/loss modulus (G'') vs shear stress

The result of storage modulus (G') and loss modulus (G") with the increasing shear stress of different CG are shown in **Figure 7-5**. The y-axis represents both G' and G" while the x-axis represents the shear stress. The G' is the elastic portion and G" is the permanent deformation. Different commercial greases show different behavior with the increasing stress. The G' normally starts from higher values followed by initial stability and then decreases as the shear stress increases depending on the composition of grease. The G" of all the commercial greases initially shows stability and then little increase showing energy dissipation as the stress increases.

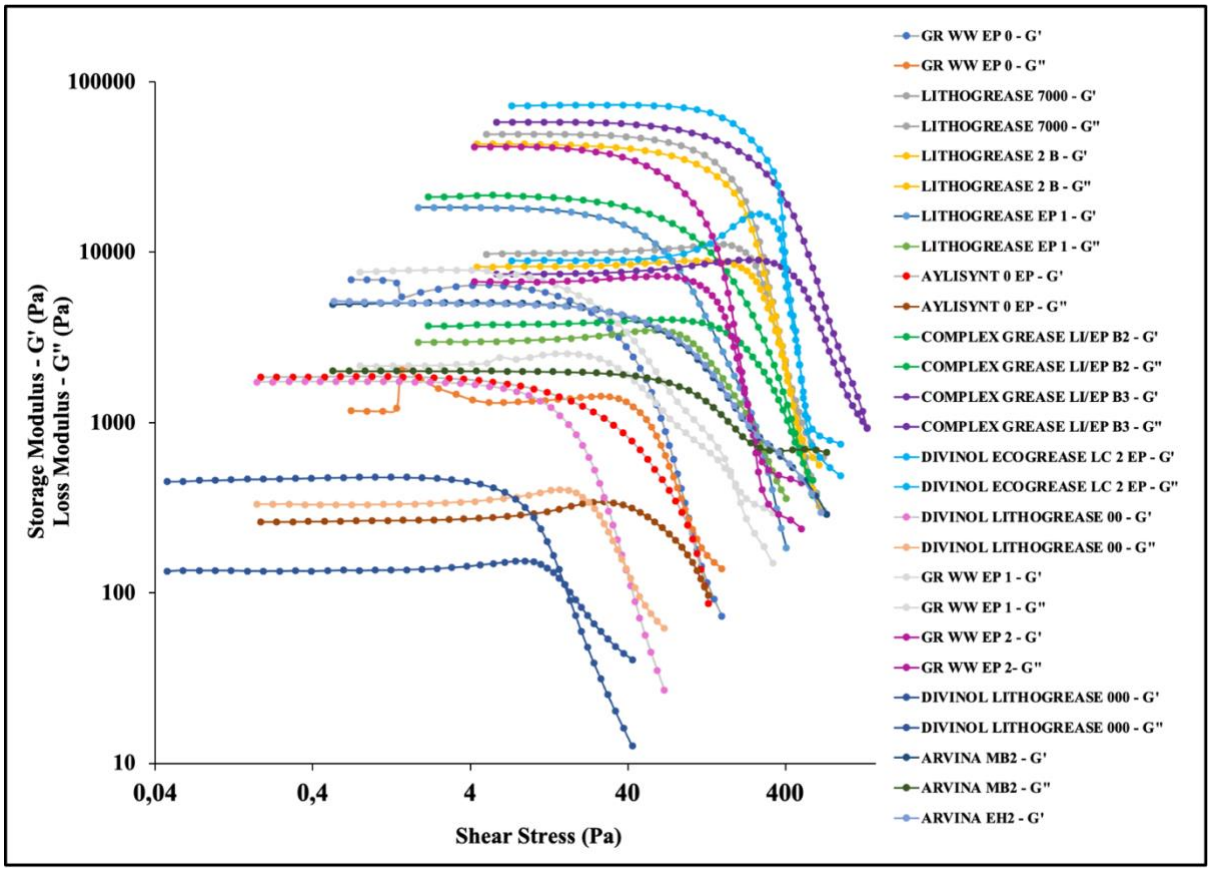


Figure 7-5: Storage modulus (G')/loss modulus (G'') vs shear stress of different commercial greases

The result of Storage modulus (G') and Loss modulus (G") trends for BBG are shown in **Figure 7-6**. For all greases, G' generally decreases with increasing shear stress. This is expected as the grease structure breaks down under shear, it becomes fluid like. The Grease-1 and Grease-3 shows an initial upward trend in the G" and then starts decreasing which is unusual behavior indicate an error due to breakdown of the structure. G" typically stays constant with shear stress initially, indicating an increase in energy dissipation as the grease structure starts to yield. After reaching a peak, it decreases, suggesting that the grease is flowing more and thus less energy is lost to internal friction. Overall, the BBG shows similar behavior of storage and loss modulus against increasing shear stress like CG.

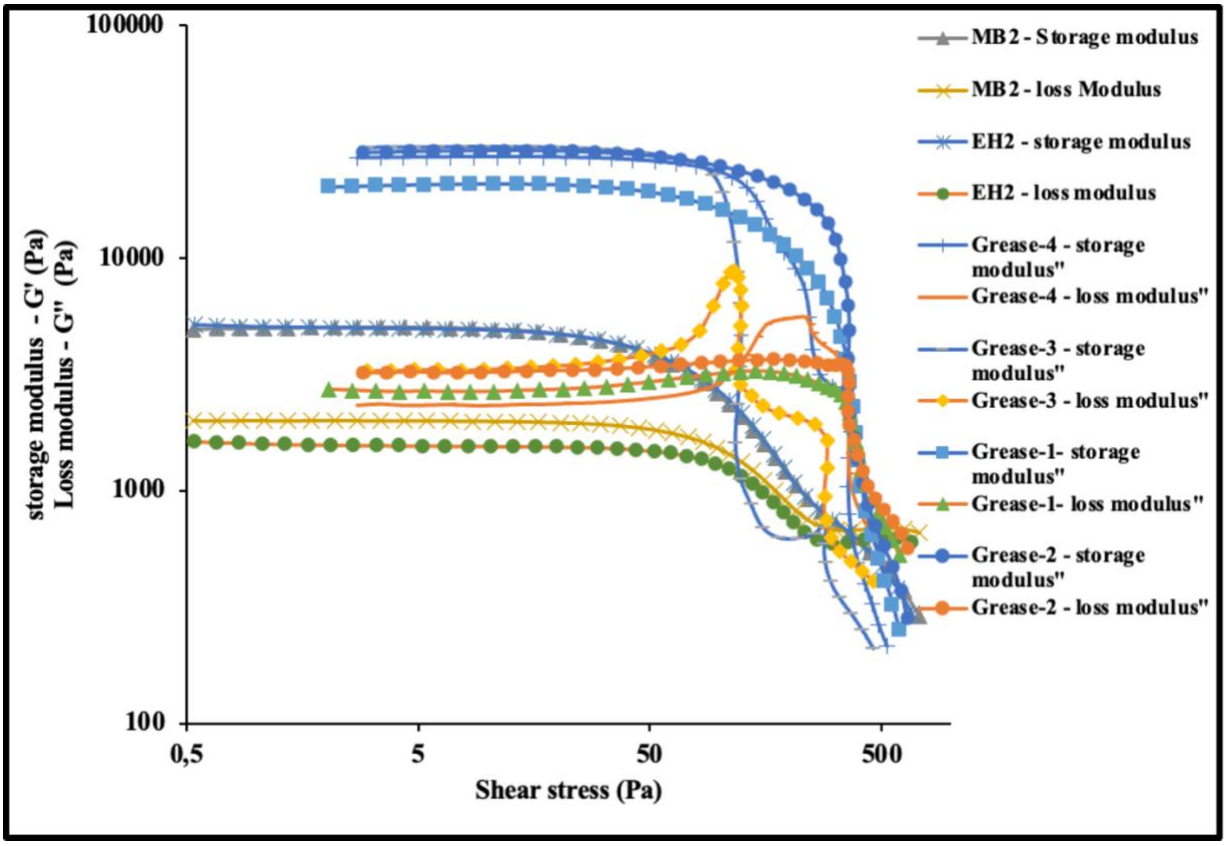


Figure 7-6: Storage modulus (G')/loss modulus (G'') vs shear stress of bentonite-based greases

6.3.8 Shear stress vs Shear rate

The purpose of the shear rate vs shear stress is to investigate the yield stress of lubricating substance, which is the minimum force necessary to cause them to start flow. As shown in **Figure 7-7**, the greases such as Lithogrease 7000, Lithogrease 2B, and Divinol ECO Grease LC 2 EP exhibit higher shear stress at given shear rates, indicating they might be thicker or more resistant to flow under stress. Others like Aylisynt 0 EP and Divinol Lithogrease 00 have lower shear stress values, possibly indicating a softer or less resistant consistency.

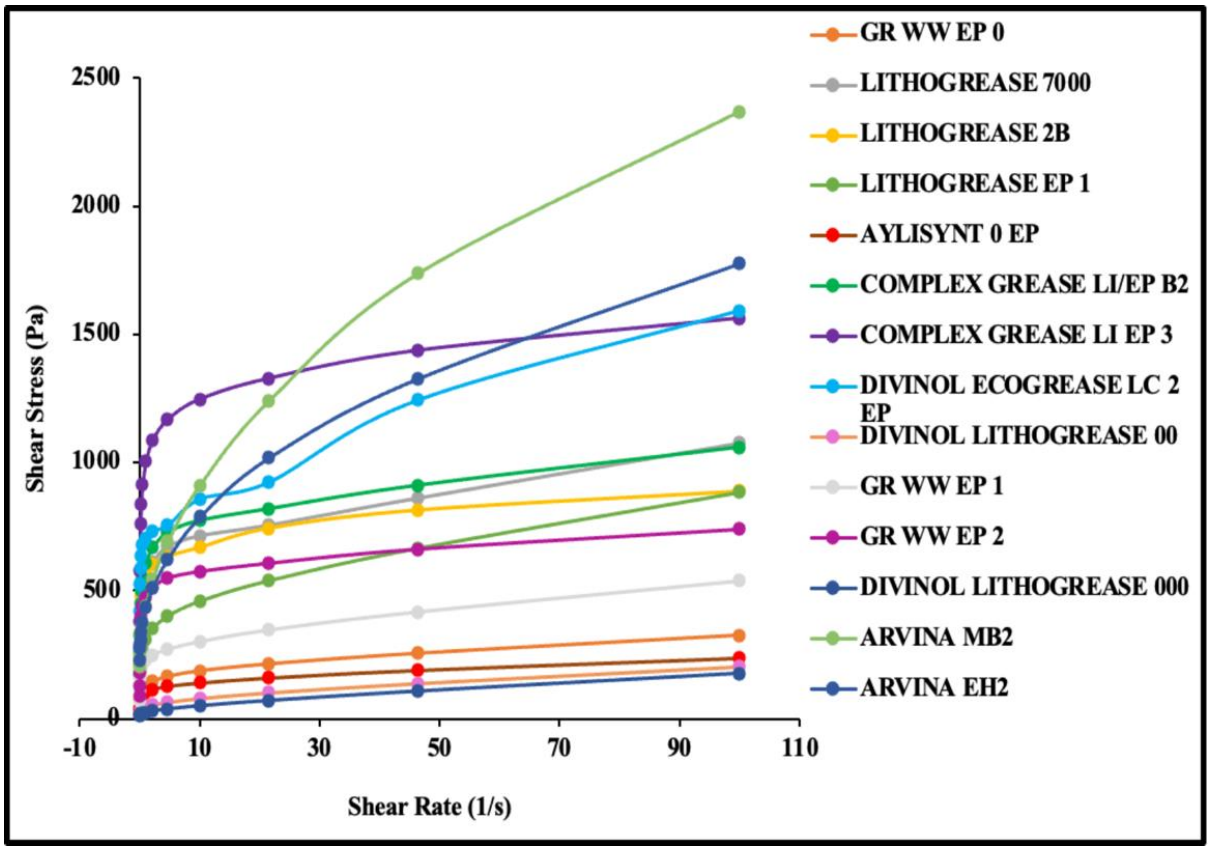


Figure 7-7: Flow test (shear stress vs shear rate) test of different commercial grease

The result of shear rate vs shear stress of BBG shown in **Figure7-8**, shows a similar behavior with the CG. The Arvina Mb2 and Arvina EH2 commercial greases shows higher shear stress with the increasing shear rate as compared to BBG which might be because of presence of different additives.

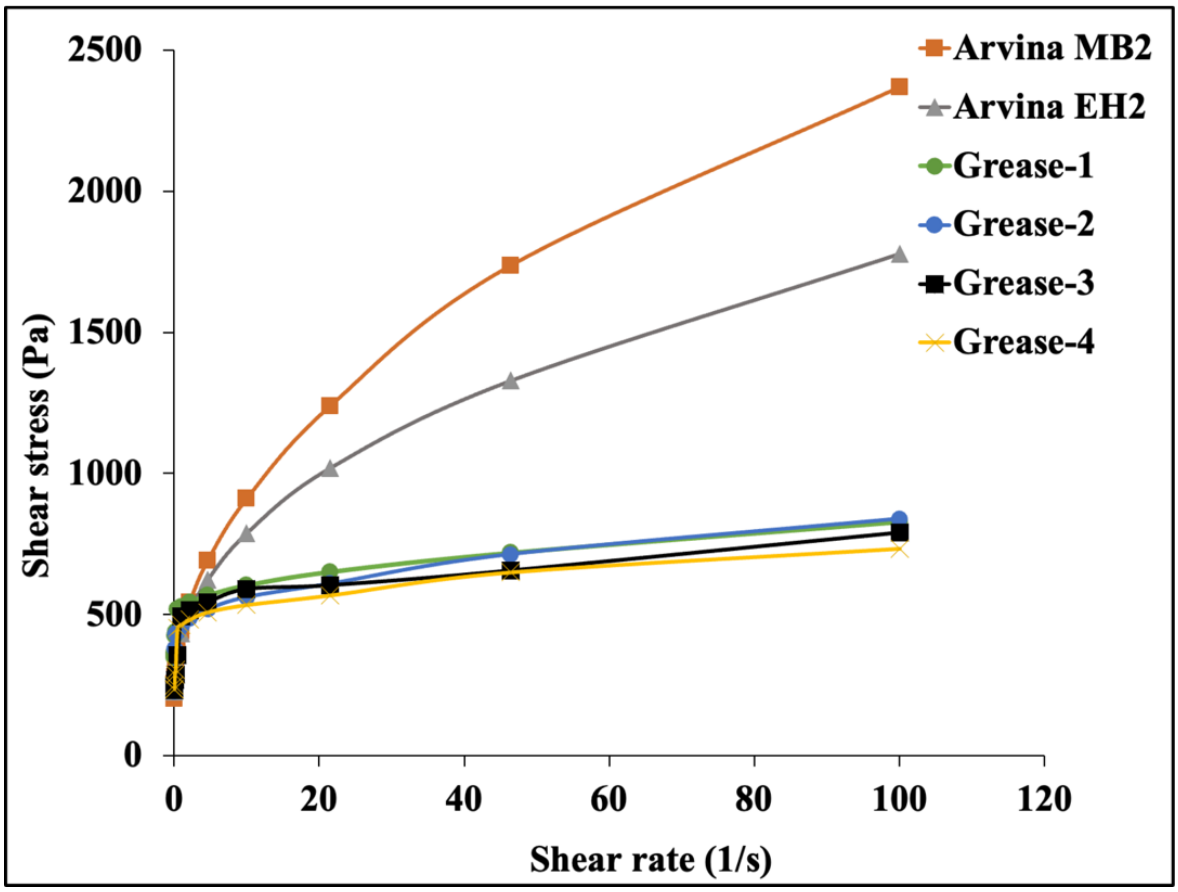


Figure 7-8: Flow test (shear stress vs shear rate) test of BBG, Arvina MB2 and Arvina EH2

6.3.9 Viscosity vs Shear rate

The viscosity profile against shear rate of BBG and CG are shown in **Figure 7-9 and 7-10**. The results shows quite similar behavior of both BBG and CG. Typically, as the shear rate increases, the viscosity of the greases decreases, indicating shear-thinning behavior, which is common in non-newtonian fluids like greases. Greases such as Lithogrease 7000 and ARVINA MB2 show high initial viscosity at low shear rates, which significantly drops as shear rate increases.

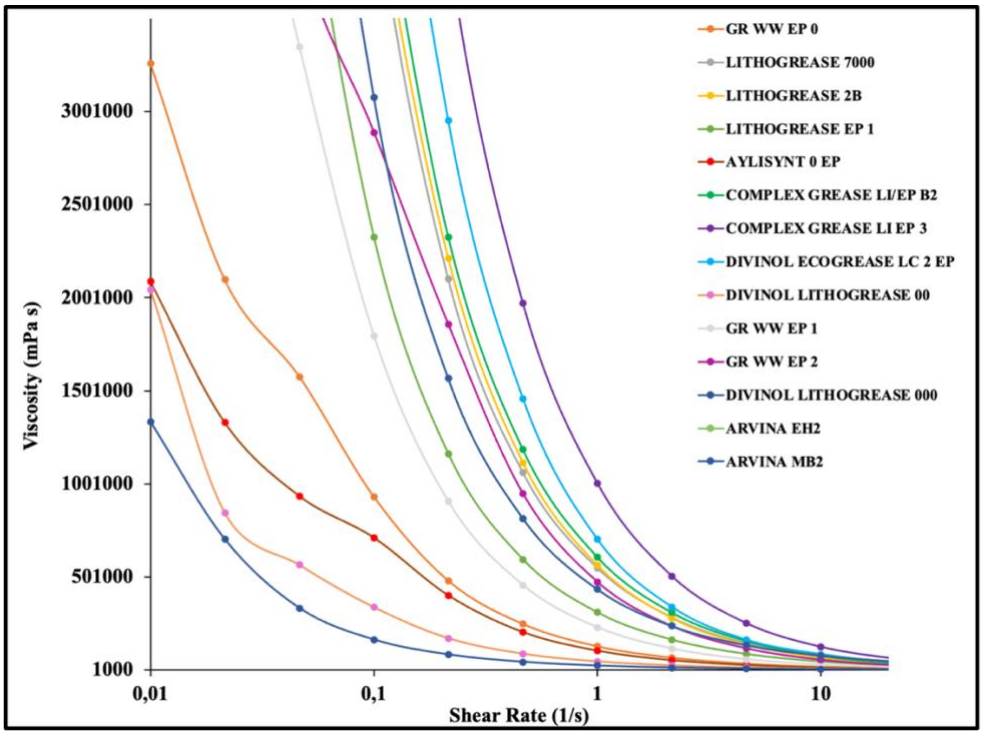


Figure 7-9: Flow test (Viscosity vs Shear rate) of different commercial greases

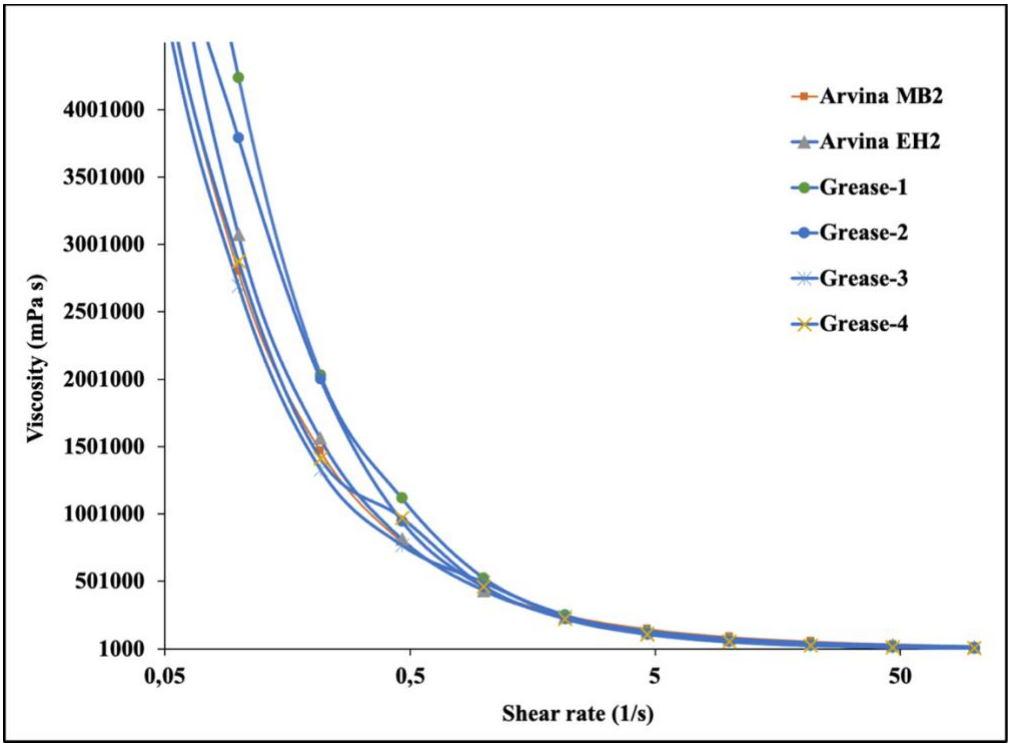


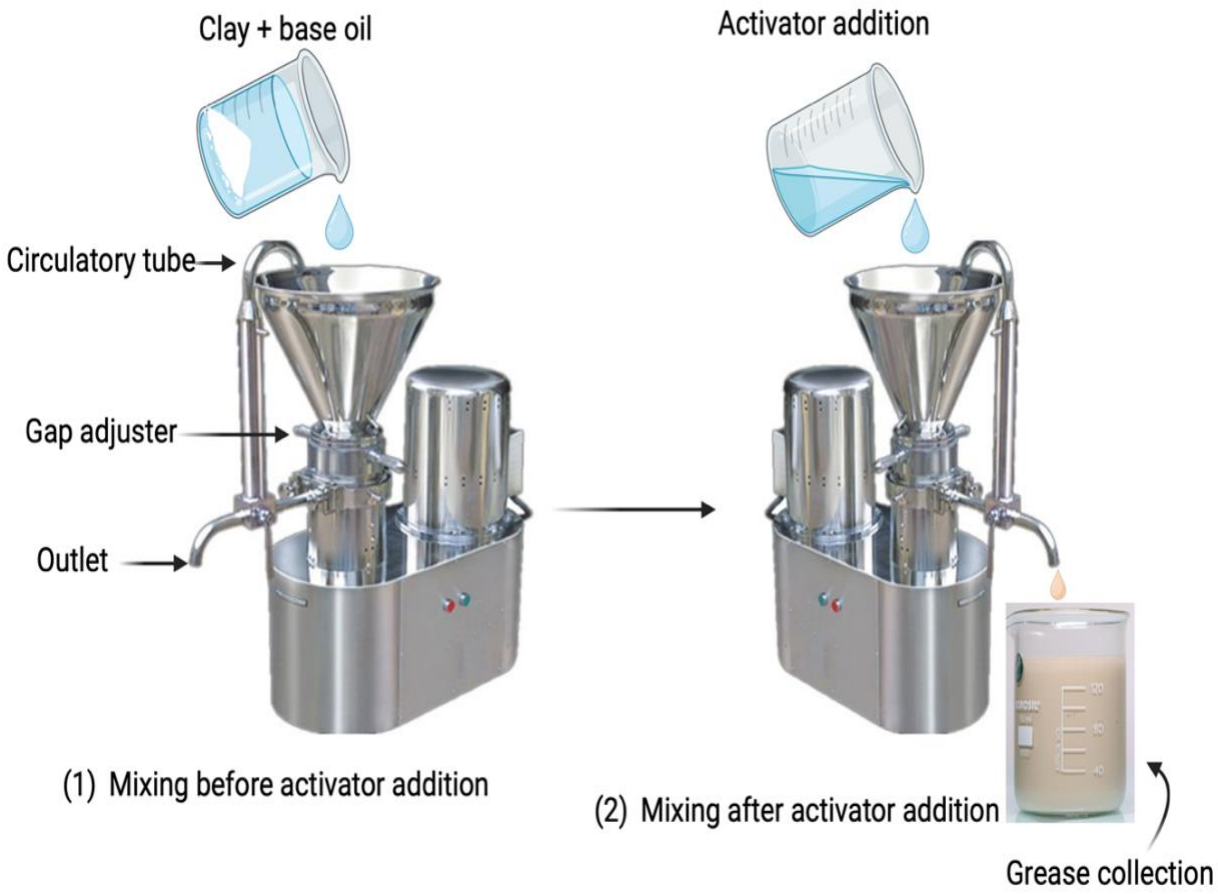
Figure 7-10: Flow test (Viscosity vs Shear rate) profile of BBG, Arvina MB2 and Arvina EH2

6.4 Colloidal mill for the production of greases

After preparation of greases on 100-gram level and obtaining similar properties like commercial greases, the aim was to upscale the procedure to 1-kilogram level using colloidal mil machine, for marketing purposes. The use of the colloidal mill provided enhanced mixing and homogenization capabilities, ensuring the uniform dispersion of the bentonite clay within the base oil and with the activator.

A colloidal mill works by using high speed shearing between a rotating rotor and a stationary stator to mix and grind materials. The gap adjuster controls the gap between the rotor and stator to regulate the fineness of the mixture. The material is fed into the hopper and enters the narrow gap between the rotor and stator and the processed material comes out through the outlet. The circulatory tube recirculates the material back to the hopper for further processing, if needed (**Scheme 7-3**).

A total of 11 experiments were conducted using clay-1 as clay, base oil and activator in the standard amount **(shown in Table 7-5)** The purpose of these trails was to optimize the concentration of components and instrumental conditions to achieve best results. The instrumental conditions like gap adjustment between the rotor and stator ranging from 0 to 3 cm, speed of rotor from 1000 to 4000 rpm, were systematically tested before and after activator addition **(Scheme 7-3)**. Through these experiments, we were able to adjust the colloidal mill's operating conditions to ensure efficient and consistent mixing, leading to a well-dispersed and homogenized grease formulation.



Scheme 7-3: Schematic representation of preparation of bentonite-based greases using colloidal mill

The details of all 11 formulations i.e., concentrations of components, colloidal mill conditions before and after activator addition and their consistencies are shown in the **Table 7-5**. Subsequently, as the instrumental conditions were optimized **(FM1-FM6)**, further experiments were conducted to assess the effect of different clay concentrations on the grease's consistency. Specifically, attempts were made to produce bentonite-based greases with lower clay content than the standard formulation while still achieving NLGI 2 consistency **(FM7-FM11, Table 7-5)**. These experiments aimed to find an optimal balance between reducing the amount of clay required, which can be cost-effective, and maintaining the desired grease consistency. In all formulations, the time was adjusted by the visual observation of the grease thickness.

	Formulations (FM)										
Component	**1**	**2**	**3**	**4**	**5**	**6**	**7**	**8**	**9**	**10**	**11**
Base Oil	77.0	85.6	83.2	77.0	77.0	77.0	85.6	83.2	77.0	83.2	80.8
Clay-1	19.2	12.0	14.0	19.2	19.2	19.2	12.0	14.0	19.2	14.0	16.0
Before activator addition:											
Parameters											
Speed	2000	3000	4000	4000	4000	4000	4000	4000	3000	3000	3000
Gap	0	0	0	0	2	3	3	3	3	3	3
Time (mint)	5	10	10	10	10	10	20	10	10	30	10
After activator addition:											
Activator	3.8	2.4	2.8	3.8	3.8	3.8	2.4	2.8	3.8	2.8	3.2
Speed	4000	4800	4000	4000	4000	4000	4000	4000	3000	3000	4000
Gap	0	0	0	0	2	3	4	3	3	3	0
Time (mint)	10	10	10	25	5	2-3	10	10	10	15	10
Penetration	317	327	323	297	291	287	353	323	265	331	294
NLGI	1	1	1	2	2	2	0	1	2	1	2

Table 7-5: Experimental conditions and parameters of different formulations

6.5 Preparation of lithium-based grease and fixing NLGI 2

The purpose of the preparation of lithium-based grease were to investigate the effect of Brugger test and ball-on-plate tribometer test on the greases. Both tests are normally used for investigating the load bearing or extreme pressure (EP) properties of base oil of lubricating substances.

Brugger test is designed to determine the ability of a lubricant to provide effective lubrication and protection against excessive wear and friction under high-load conditions. After completion of the test, the scar diameter or wear that develops on the specimen due to the extreme pressure and

sliding contact with the rotating steel surface is measured which indicates the lubricant's load carrying capacity or EP capability. The Brugger values below 30 N/mm^2 represents light duty lubricants, the medium value ranges from 30-50 N/mm^2, represents general or industrial lubricants and high Brugger values above 50 N/mm^2 represents heavy duty or extreme pressure lubricants. The final Brugger value is determined by the following equation:

$$\textbf{Brugger value} = \frac{4F}{\pi d^2} \qquad \textbf{Equation (3)}$$

Where, F = applied force (N)
d = diameter of the wear scar (mm)

Four different formulations of lithium-based greases (named Bellini lithium greases) were formulated based on different concentrations of components as shown in **Table 7-6**. The formulation 4 (FM4) were treated with 5% Sulphurized extreme pressure additive and their Brugger's values were determined.

Component	**FM1**	**FM2**	**FM3**	**FM4**	**FM4+ (S-EP)**
Base oil (wt. %)	83.7	87	80.4	79.8	80.4
12-HAS (wt. %)	9	7.2	10.8	10.8	10.8
Azelaic acid (wt. %)	3.1	2.5	3.7	3.7	3.7
LiOH (wt. %)	4.2	3.3	5.1	5.7	5.7
Sulphurized EP additive (S-EP) (%)					5.0
Penetration	309	380	315	284	
NLGI	1	0	1	2	
Brugger (N/mm^2)	27.5	28.6	26.6	23.7	63.6

Table 7-6: Formulation of lithium-based greases using different concentration of components, addition of Sulphurized EP additive and their NLGI and Brugger values

Ball on plate tribometer tests is a type of tribological test commonly used to access the friction, wear and extreme pressure characteristics of lubricating materials. In these tests a spherical ball is brought into contact with a flat plate, simulating the sliding contact between two surfaces typically

under controlled conditions of force, speed, and temperature as shown in **Figure 7-11**. In our experiments, the samples were checked under specified condition including steel plate, test run of 1 hour, an applied force of 23 N, rotation of 200 and 500 rpm and a temperature of 75 C.

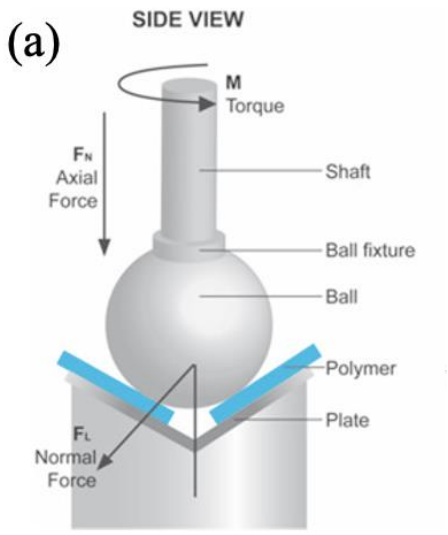


Figure 7-11: Schematic representation of Ball on plate tribometer tests

Three formulations of Bellini lithium greases i.e., grease with NLGI 0, NLGI 2 and NLGI 2 with 5% (S-EP) additive and 1 commercial grease (Divinol Lithogrease 7000) were selected to investigate their COF and scar diameter. **Table 7-7** represents the result of tribometer test of each sample on two rotation speeds (200, 500 rpm), their coefficient of friction values and scar diameters. The scar diameter was analyzed using optical microscope (**Figure 7-12**).

Sample	rpm	COF	Scar diameter (µm)
Bellini Lithium grease NLGI 2	200	0.114	590
Bellini Lithium grease NLGI 2	500	0.098	508
Bellini Lithium grease NLGI 2 + 5% (S-EP) additive	200	0.138	642
Bellini Lithium grease NLGI 2 + 5% (S-EP) additive	500	0.135	864
Bellini Lithium grease NLGI 0	200	0.128	2018
Bellini Lithium grease NLGI 0	500	0.175	2948
Divinol Lithogrease 7000	200	0.124	298
Divinol Lithogrease 7000	500	0.105	354

Table 7-7: Results of ball on plate tribometer test of different grease samples, using two rotation speeds (200, 500 rpm), values of coefficient of friction and scare diameter after test

From the Brugger test results it was determined that the (S-EP) additive effectively enahance the extreme pressure and load bearing properties of greases. It was expected that (S-EP) will also decrease the COF and scare diameter in tribometer test as compared to the samples witout (S-EP) additive. The observed result was opposite and revealed that the limitations of tribometer test for greases samples, because the tribometer test is used for base oil characterizations. Furthermore, other possibilities can be the concentration and nature of additive or the operational conditions. The possible suggestions to overcome this problem is to use varying additive concentrations and microstructure analysis of greases before and after testing to observe grease degradation.

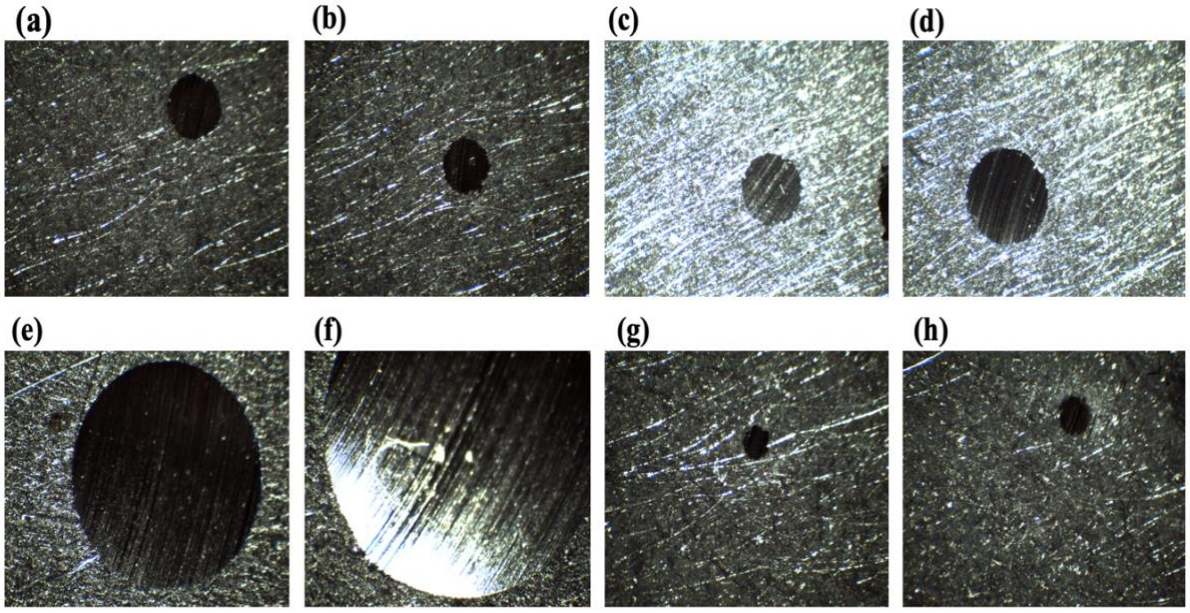


Figure 7-12: Images of scar diameters of (a) Bellini Lithium grease NLGI 2 (200 rpm), (b) Bellini Lithium grease NLGI 2 (500 rpm), (c) Bellini Lithium grease NLGI 2 + 5% (S-EP) additive (200 rpm), (d) Bellini Lithium grease NLGI 2 + 5% (S-EP) additive (500 rpm), (e) Bellini Lithium grease NLGI 0 (200 rpm), (f) Bellini Lithium grease NLGI 0 (500 rpm), (g) Divinol Lithogrease 7000 (200 rpm), and (h) Divinol Lithogrease 7000 (500 rpm)

6.6 Conclusion

In this study, biodegradable bentonite-based grease (BBG) formulations, as a sustainable alternative to traditional lithium-based greases are presented. The reaction parameters and concentration of components were optimized to formulate greases with consistency of NLGI 2. The rheological study demonstrates that BBG shows comparable properties to CG. Viscoelastic characteristics and adhesive properties of BBG strongly matched with commercially greases. The shear stress vs shear rate and viscosity vs shear rate profile indicated analogous properties of BBG and CG.

Furthermore, the lithium-based grease was also formulated, and their extreme pressure and load bearing properties were investigated by Brugger and tribometer tests. The Brugger and tribometer tests were found unsuitable for analyzing extreme pressure (EP) properties of greases and can only be used for analyzing lubricating base oils.

The scalability of BBG production using a colloidal mill, and optimization of parameters was also successfully demonstrated with lower clay amount than the standard amount, to be more economical. This work is performed in a lubricants expert company (Bellini S.P.A), from starting point till the scalability, but the incorporation of suitable additives to enhance oxidation stability, lifetime and load bearing properties are still in progress.

Conclusion and future perspective

As the world population becomes more environmentally conscious, there has been a lot of investment in the research for the development of new technologies that could enhance productivity while decreasing the amount of raw material and energy needed during the process. Among many types of technologies developed in the last decade, Kolbe electrolysis, one of the prominent electrochemical technologies, has gained a lot of attention due to its efficiency, sustainability, and ability to produce valuable products like green fuels and chemicals from bio-based feedstocks.

In the start, Kolbe electrolysis was utilized for producing small quantities of hydrocarbons at laboratorial scales. However, with further advancements in electrochemical technologies and optimization of processes, its applications are level upped in various industrial sectors, especially for the production of renewable fuels and chemicals. Moreover, thanks to scientific research, Kolbe electrolysis has been integrated with other renewable energy systems, such as solar and wind-powered energy setups, enhancing its efficiency and sustainability. This is especially valuable for green chemistry applications, where sustainable processes are essential for minimizing environmental concerns. In order to keep with the advances of Kolbe electrolysis, its application on complex systems also needed to be developed. Particular focus needs to be placed on utilization of animal fats, vegetable oils and bio-waste, as most of the research until now is concentrated on single fatty acids system. This side required significant advancements in understanding the reaction mechanisms, optimization of parameters like temperature, current density, and electrolyte composition, and addressing difficulties associated with handling multi-component systems.

Coconut oil as a substrate due to its diverse composition of fatty acids, including medium-chain and long-chain fatty acids with both saturated and unsaturated types make it an ideal candidate for demonstrating the utility of Kolbe electrolysis on complex systems. Similarly, utilization of Kolbe electrolysis on palm oil with two long chain saturated and unsaturated fatty acids can pave the way for future applications in the efficient conversion of complex renewable substrates.

The work starts with an in-depth exploration of Kolbe electrolysis applied to both single (lauric acid and palmitic acids) and mixture of two fatty acids. In different electrodes usage, the non-commercial platinum electrodes give good conversion rate, while other two electrodes i.e., commercial Pt-coated copper and Au-coated copper electrodes shows surface corrosion after (< 30 h) of usage. The study

also shows that Pt-coated copper electrode and Au-coated copper electrodes with a layer thickness of 400-600 µm might not be useful for electrosynthesis experiments using high current intensities. In comparison of the effect of different solvent environments on the Kolbe electrolysis of mixture of two fatty acids, the MeOH:EtOH:H_2O (16.67:16.67:66.67%) system gives highest total hydrocarbons yield of 62.7%, with nearly fully dissociation of substrate acids.

Prior to Kolbe electrolysis, the saponification reaction of coconut and palm oil can convert all the triglycerides into fatty acids by using 11% w/v of KOH and refluxing at 600 rpm and 110 ^oC for 1.5-2 hours, which is cheap and easy handling technique as compared to other technologies. On the electrolysis of mixture of fatty acids, different solvent environments were applied and the best result in terms of hydrocarbon production was observed in MeOH:EtOH:water (41.66 :41.66 :16.67%) system, with 73.55 % and 73.25 %, for fatty acids mixtures derived from coconut and palm oil, respectively. Although, the number and percentage of fatty acids were different in both oils, and hence solubility was also different, but the hydrocarbon yield was nearly same. These results strengthen the statement of the literature that the solubility of carboxylate anions does not significantly impact hydrocarbon yields in Kolbe electrolysis, and water-insoluble long-chain fatty acid salts (like C16 and C18:1), can also lead to the substantial hydrocarbon production.

The study further confirmed the application of electrolysis technique for the production of biodiesel (FAME) from coconut oil. The results concluded that electrolysis technique can yield 96.5 % of biodiesel using cheap conditions like MeOH/oil of 6:1 and 1 wt.% of KOH, as compared to conventional transesterification technique with same experimental conditions. The coconut oil and their synthesized FAME was also used base oil to investigate their lubricating properties. However, the rheometer analysis proved that coconut oil containing triglyceride structure shows more superior performance in term of high viscosity, adhesive force and high shear stress.

The study also explores the formulation of fully green and biodegradable bentonite-based greases as an alternative to lithium-based greases, which are widely used but not very environment friendly. The formulation and experimental parameters such as concentrations of components, temperature and time of experiments were all optimized after series of experiments, to obtained the greases of required consistency. By making comparison of formulated bentonite-based greases with commercial greases, the results concluded that bentonite-based grease shows very similar and sometimes improved performance then the commercial greases. The viscoelastic characteristics and adhesive properties of bentonite-based greases strongly matched with commercially greases. The shear stress vs shear rate and viscosity vs shear rate profile indicated analogous properties with commercial properties. The

optimization of instrumental conditions of colloidal mill demonstrate that grease production can be scaled up from 1 kilogram to 10 kilogram for marketing.

Overall, this research underscores the importance of integrating sustainable practices into industrial processes. It highlights the potential for biodegradable hydrocarbons and biodegradable lubricants to replace their petroleum-based counterparts. The findings provide a foundation for further development and optimization of bio-based hydrocarbons, paving the way for more sustainable industrial practices in the future. Despite the progress made, future work should concentrate on further improvement of electrode materials designed for the complex fatty acid mixtures, process parameter optimization, and techniques to increase yield and selectivity. This process needs to be further explored to see how scalable it is, especially in integrating mixed and industrial grade feedstocks, in order to make Kolbe electrolysis a realistic, sustainable fuel production process.

References

[1] C. K. Ho, K. B. McAuley, and B. A. Peppley, “Biolubricants through renewable hydrocarbons: A perspective for new opportunities,” *Renewable and Sustainable Energy Reviews*, vol. 113, p. 109261, 2019.

[2] S. M. Santos, D. C. Nascimento, M. C. Costa, A. M. Neto, and L. V. Fregolente, “Flash point prediction: Reviewing empirical models for hydrocarbons, petroleum fraction, biodiesel, and blends,” *Fuel*, vol. 263, p. 116375, 2020.

[3] X. Zhang *et al.*, “Vegetable oil-based nanolubricants in machining: from physicochemical properties to application,” *Chinese Journal of Mechanical Engineering*, vol. 36, no. 1, p. 76, 2023.

[4] A. Burnham, J. Han, C. E. Clark, M. Wang, J. B. Dunn, and I. Palou-Rivera, “Life-cycle greenhouse gas emissions of shale gas, natural gas, coal, and petroleum,” *Environmental science & technology*, vol. 46, no. 2, pp. 619–627, 2012.

[5] A. Sailaja, “Emerging Technologies in Chemical Engineering: Advancements in Process Optimization, Sustainable Practices, and Future Innovations,” *International Journal for Multidimensional Research Perspectives*, vol. 2, no. 5, pp. 59–71, 2024.

[6] G. A. Olah and Á. Molnár, *Hydrocarbon chemistry*. John Wiley & Sons, 2003.

[7] Y. J. Zhou, E. J. Kerkhoven, and J. Nielsen, “Barriers and opportunities in bio-based production of hydrocarbons,” *Nature Energy*, vol. 3, no. 11, pp. 925–935, 2018.

[8] S. Sadrameli, “Thermal/catalytic cracking of hydrocarbons for the production of olefins: A state-of-the-art review I: Thermal cracking review,” *Fuel*, vol. 140, pp. 102–115, 2015.

[9] W.-C. Wang, Y.-C. Liu, and R. A. A. Nugroho, “Techno-economic analysis of renewable jet fuel production: The comparison between Fischer-Tropsch synthesis and pyrolysis,” *Energy*, vol. 239, p. 121970, 2022.

[10] K. A. Shukla and T. P. Kumar, “Pillars of modern electrochemistry: a brief history,” *source: http://electrochem. cwru. edu/ed/encycl/art-p05-pillars-of-ec. htm*, 2008.

[11] P. Anastas and N. Eghbali, “Green chemistry: principles and practice,” *Chemical Society Reviews*, vol. 39, no. 1, pp. 301–312, 2010.

[12] K. Wang and L. Tan, “Electrochemical synthesis to produce lube stock from renewable feeds,” Aug. 2015.

[13] C. Urban *et al.*, “Production of drop-in fuels from biomass at high selectivity by combined microbial and electrochemical conversion,” *Energy & Environmental Science*, vol. 10, no. 10, pp. 2231–2244, 2017.

[14] A. Goldmann *et al.*, “A study on electrofuels in aviation,” *Energies*, vol. 11, no. 2, p. 392, 2018.

[15] K. M. B. Karthikeyan, J. Vijayanand, K. Arun, and V. Seshagiri Rao, “Thermophysical and wear properties of eco-friendly nano lubricants,” *Materials Today: Proceedings*, vol. 39, pp. 285–291, 2021, doi: 10.1016/j.matpr.2020.07.128.

[16] E. J. Beckman, “Supercritical and near-critical CO2 in green chemical synthesis and processing,” *The Journal of Supercritical Fluids*, vol. 28, no. 2–3, pp. 121–191, Mar. 2004, doi: 10.1016/S0896-8446(03)00029-9.

[17] F. Delvigne *et al.*, “Green fluorescent protein (GFP) leakage from microbial biosensors provides useful information for the evaluation of the scale-down effect,” *Biotechnology Journal*, vol. 6, no. 8, pp. 968–978, Aug. 2011, doi: 10.1002/biot.201000410.

[18] N. Winterton, “The green solvent: a critical perspective,” *Clean Techn Environ Policy*, vol. 23, no. 9, pp. 2499–2522, Nov. 2021, doi: 10.1007/s10098-021-02188-8.

[19] S. N. M. Zainon and W. H. Azmi, “Stability and thermo-physical properties of green bio-glycol based TiO2-SiO2 nanofluids,” *International Communications in Heat and Mass Transfer*, vol. 126, p. 105402, Jul. 2021, doi: 10.1016/j.icheatmasstransfer.2021.105402.

[20] Y. Kang, Y. Hu, C. Zhang, K. Yang, and Q. Zhang, “Application of Refrigerant Cooling in a Battery Thermal Management System under High Temperature Conditions: A Review,” *ACS Omega*, vol. 9, no. 24, pp. 25591–25609, Jun. 2024, doi: 10.1021/acsomega.4c02902.

[21] S. M. R. Bantillo, G. A. C. Callejo, S. M. K. G. Camacho, M. A. Montalban, R. E. Valderin, and R. V. C. Rubi, “Future Trends of Natural Refrigerants: Selection, Preparation, and Evaluation,” in *The 3rd International Electronic Conference on Processes*, MDPI, Aug. 2024, p. 9. doi: 10.3390/engproc2024067009.

[22] R. Sirohi *et al.*, “Green processing and biotechnological potential of grape pomace: Current trends and opportunities for sustainable biorefinery,” *Bioresource Technology*, vol. 314, p. 123771, Oct. 2020, doi: 10.1016/j.biortech.2020.123771.

[23] J. L. Lee, G. H. Chong, M. Ota, H. Guo, and R. L. Smith, “Solvent Replacement Strategies for Processing Pharmaceuticals and Bio-Related Compounds—A Review,” *Liquids*, vol. 4, no. 2, pp. 352–381, Apr. 2024, doi: 10.3390/liquids4020018.

[24] S. A. Lawal, I. A. Choudhury, and Y. Nukman, “Application of vegetable oil-based metalworking fluids in machining ferrous metals—A review,” *International Journal of Machine Tools and Manufacture*, vol. 52, no. 1, pp. 1–12, Jan. 2012, doi: 10.1016/j.ijmachtools.2011.09.003.

[25] S. A. Lawal, I. A. Choudhury, I. O. Sadiq, and A. Oyewole, “Vegetable-oil based metalworking fluids research developments for machining processes: survey, applications and challenges,” *Manufacturing Rev.*, vol. 1, p. 22, 2014, doi: 10.1051/mfreview/2014021.

[26] M. P. Schneider, “Plant-oil-based lubricants and hydraulic fluids,” *J Sci Food Agric*, vol. 86, no. 12, pp. 1769–1780, Sep. 2006, doi: 10.1002/jsfa.2559.

[27] C. Kajdas, A. Karpińska, and A. Kulczycki, “Industrial Lubricants,” in *Chemistry and Technology of Lubricants*, R. M. Mortier, M. F. Fox, and S. T. Orszulik, Eds., Dordrecht: Springer Netherlands, 2009, pp. 239–292. doi: 10.1023/b105569_8.

[28] N. A. Zainal, N. W. M. Zulkifli, M. Gulzar, and H. H. Masjuki, “A review on the chemistry, production, and technological potential of bio-based lubricants,” *Renewable and Sustainable Energy Reviews*, vol. 82, pp. 80–102, Feb. 2018, doi: 10.1016/j.rser.2017.09.004.

[29] H. Balat and E. Kırtay, “Hydrogen from biomass – Present scenario and future prospects,” *International Journal of Hydrogen Energy*, vol. 35, no. 14, pp. 7416–7426, Jul. 2010, doi: 10.1016/j.ijhydene.2010.04.137.

[30] Y. Yang, Z. Tian, Y. Lan, S. Wang, and H. Chen, “An overview of biofuel power generation on policies and finance environment, applied biofuels, device and performance,” *Journal of Traffic and Transportation Engineering (English Edition)*, vol. 8, no. 4, pp. 534–553, Aug. 2021, doi: 10.1016/j.jtte.2021.07.002.

[31] S. Mahapatra, D. Kumar, B. Singh, and P. K. Sachan, “Biofuels and their sources of production: A review on cleaner sustainable alternative against conventional fuel, in the framework of the food and energy nexus,” *Energy Nexus*, vol. 4, p. 100036, Dec. 2021, doi: 10.1016/j.nexus.2021.100036.

[32] M. C. Rulli, D. Bellomi, A. Cazzoli, G. De Carolis, and P. D’Odorico, “The water-land-food nexus of first-generation biofuels,” *Sci Rep*, vol. 6, no. 1, p. 22521, Mar. 2016, doi: 10.1038/srep22521.

[33] S. Manikandan, R. Subbaiya, M. Biruntha, R. Y. Krishnan, G. Muthusamy, and N. Karmegam, “Recent development patterns, utilization and prospective of biofuel production: Emerging nanotechnological intervention for environmental sustainability – A review,” *Fuel*, vol. 314, p. 122757, Apr. 2022, doi: 10.1016/j.fuel.2021.122757.

[34] P. T. Aakko-Saksa *et al.*, “Reduction in greenhouse gas and other emissions from ship engines: Current trends and future options,” *Progress in Energy and Combustion Science*, vol. 94, p. 101055, Jan. 2023, doi: 10.1016/j.pecs.2022.101055.

[35] T. Chowdhury *et al.*, “Latest advancements on livestock waste management and biogas production: Bangladesh’s perspective,” *Journal of Cleaner Production*, vol. 272, p. 122818, Nov. 2020, doi: 10.1016/j.jclepro.2020.122818.

[36] Y. Yang *et al.*, “Status and challenges of applications and industry chain technologies of hydrogen in the context of carbon neutrality,” *Journal of Cleaner Production*, vol. 376, p. 134347, Nov. 2022, doi: 10.1016/j.jclepro.2022.134347.

[37] A. K. Vuppaladadiyam *et al.*, “Biomass pyrolysis: A review on recent advancements and green hydrogen production,” *Bioresource Technology*, vol. 364, p. 128087, Nov. 2022, doi: 10.1016/j.biortech.2022.128087.

[38] M. V. L. Chhandama, J. V. L. Ruatpuia, S. Ao, A. C. Chetia, K. B. Satyan, and S. L. Rokhum, “Microalgae as a sustainable feedstock for biodiesel and other production industries: Prospects and challenges,” *Energy Nexus*, vol. 12, p. 100255, Dec. 2023, doi: 10.1016/j.nexus.2023.100255.

[39] S. M. Farouk, A. M. Tayeb, S. M. S. Abdel-Hamid, and R. M. Osman, “Recent advances in transesterification for sustainable biodiesel production, challenges, and prospects: a comprehensive review,” *Environ Sci Pollut Res*, vol. 31, no. 9, pp. 12722–12747, Jan. 2024, doi: 10.1007/s11356-024-32027-4.

[40] K. F. Chai, K. R. Ng, M. Samarasiri, and W. N. Chen, “Precision fermentation to advance fungal food fermentations,” *Current Opinion in Food Science*, vol. 47, p. 100881, Oct. 2022, doi: 10.1016/j.cofs.2022.100881.

[41] B. L. Salvi, “Transesterification methods,” in *Production of Biodiesel from Non-Edible Sources*, Elsevier, 2022, pp. 117–151. doi: 10.1016/B978-0-12-824295-7.00005-X.

[42] Monika, S. Banga, and V. V. Pathak, “Biodiesel production from waste cooking oil: A comprehensive review on the application of heterogenous catalysts,” *Energy Nexus*, vol. 10, p. 100209, Jun. 2023, doi: 10.1016/j.nexus.2023.100209.

[43] A. I. Osman *et al.*, “Optimizing biodiesel production from waste with computational chemistry, machine learning and policy insights: a review,” *Environmental Chemistry Letters*, vol. 22, no. 3, pp. 1005–1071, 2024.

[44] Ravindra B. Malabadi, Sadiya Mr, Kiran P. Kolkar, and Raju K. Chalannavar, “Biodiesel production via transesterification reaction,” *Open Access Res. J. Sci. Technol.*, vol. 9, no. 2, pp. 010–020, Nov. 2023, doi: 10.53022/oarjst.2023.9.2.0064.

[45] B. Aregawi, C.-H. Su, and F.-M. Wang, “Electrolysis Approach of Fatty Acid Methyl Ester Production Using Alkali Hydroxides and Their Alkoxides,” *Meet. Abstr.*, vol. MA2024-01, no. 48, pp. 3042–3042, Aug. 2024, doi: 10.1149/MA2024-01483042mtgabs.

[46] B. H. Aregawi *et al.*, “Biodiesel Production through Electrolysis Using an Ionic Liquid, 1-Ethyl-3-Methylimidazolium Chloride as a Supporting Electrolyte,” *International Journal of Energy Research*, vol. 2023, pp. 1–11, Mar. 2023, doi: 10.1155/2023/4719589.

[47] M. Dhafir, D. Darwin, M. A. Al Fayed, and S. Suharyatun, “Quantity and Physicochemical Analysis of Biodiesel from CPO Processed by Electrolysis Method,” *JTEP-L*, vol. 12, no. 2, p. 384, May 2023, doi: 10.23960/jtep-l.v12i2.384-396.

[48] H. Zabed, J. N. Sahu, A. Suely, A. N. Boyce, and G. Faruq, “Bioethanol production from renewable sources: Current perspectives and technological progress,” *Renewable and Sustainable Energy Reviews*, vol. 71, pp. 475–501, May 2017, doi: 10.1016/j.rser.2016.12.076.

[49] D. P. Ho, H. H. Ngo, and W. Guo, “A mini review on renewable sources for biofuel,” *Bioresource Technology*, vol. 169, pp. 742–749, Oct. 2014, doi: 10.1016/j.biortech.2014.07.022.

[50] B. Reis *et al.*, “Long-term feeding of vegetable oils to Senegalese sole until market size: Effects on growth and flesh quality. Recovery of fatty acid profiles by a fish oil finishing diet,” *Aquaculture*, vol. 434, pp. 425–433, Oct. 2014, doi: 10.1016/j.aquaculture.2014.09.002.

[51] D. Neupane, “Biofuels from Renewable Sources, a Potential Option for Biodiesel Production,” *Bioengineering*, vol. 10, no. 1, p. 29, Dec. 2022, doi: 10.3390/bioengineering10010029.

[52] N. Asikin-Mijan *et al.*, “Vegetable oil-based feedstocks for biofuel production: Physicochemical properties and chemical compositions,” in *Innovations in Thermochemical Technologies for Biofuel Processing*, Elsevier, 2022, pp. 197–219. doi: 10.1016/B978-0-323-85586-0.00002-0.

[53] P. R. Ghosh, D. Saha, S. Chowdhury, and R. D. Mitra, “Home Archives Vol. 44 No. S5 (2023) Articles Waste To Wonder: Production Of Bio-Diesel From Agri-Waste- A Comprehensive Review,” *JAZ*, Nov. 2023, doi: 10.53555/jaz.v44iS5.3278.

[54] R. Singh, A. Arora, and V. Singh, “Biodiesel from oil produced in vegetative tissues of biomass – A review,” *Bioresource Technology*, vol. 326, p. 124772, Apr. 2021, doi: 10.1016/j.biortech.2021.124772.

[55] R. N. Vilas Bôas and M. F. Mendes, “A REVIEW OF BIODIESEL PRODUCTION FROM NON-EDIBLE RAW MATERIALS USING THE TRANSESTERIFICATION PROCESS WITH A FOCUS ON INFLUENCE OF FEEDSTOCK COMPOSITION AND FREE FATTY ACIDS,” *J. Chil. Chem. Soc.*, vol. 67, no. 1, pp. 5433–5444, Jan. 2022, doi: 10.4067/S0717-97072022000105433.

[56] S. M. Alves, B. S. Barros, M. F. Trajano, K. S. B. Ribeiro, and E. Moura, “Tribological behavior of vegetable oil-based lubricants with nanoparticles of oxides in boundary lubrication conditions,” *Tribology International*, vol. 65, pp. 28–36, Sep. 2013, doi: 10.1016/j.triboint.2013.03.027.

[57] R. Uppar, P. Dinesha, and S. Kumar, “A critical review on vegetable oil-based bio-lubricants: preparation, characterization, and challenges,” *Environ Dev Sustain*, vol. 25, no. 9, pp. 9011–9046, Sep. 2023, doi: 10.1007/s10668-022-02669-w.

[58] N. Salih, J. Salimon, and E. Yousif, “Synthetic biolubricant basestocks based on environmentally friendly raw materials,” *Journal of King Saud University - Science*, vol. 24, no. 3, pp. 221–226, Jul. 2012, doi: 10.1016/j.jksus.2011.02.003.

[59] C. J. Reeves, A. Siddaiah, and P. L. Menezes, “A Review on the Science and Technology of Natural and Synthetic Biolubricants,” *J Bio Tribo Corros*, vol. 3, no. 1, p. 11, Mar. 2017, doi: 10.1007/s40735-016-0069-5.

[60] L. Catani *et al.*, “Essential oils and their applications in agriculture and agricultural products: A literature analysis through VOSviewer,” *Biocatalysis and Agricultural Biotechnology*, vol. 45, p. 102502, Oct. 2022, doi: 10.1016/j.bcab.2022.102502.

[61] H. Wagner, R. Luther, and T. Mang, “Lubricant base fluids based on renewable raw materials,” *Applied Catalysis A: General*, vol. 221, no. 1–2, pp. 429–442, Nov. 2001, doi: 10.1016/S0926-860X(01)00891-2.

[62] J. A. Cecilia, D. Ballesteros Plata, R. M. Alves Saboya, F. M. Tavares De Luna, C. L. Cavalcante, and E. Rodríguez-Castellón, “An Overview of the Biolubricant Production Process: Challenges and Future Perspectives,” *Processes*, vol. 8, no. 3, p. 257, Feb. 2020, doi: 10.3390/pr8030257.

[63] M. R. Islam Sazzad *et al.*, “Advancing sustainable lubricating oil management: Re-refining techniques, market insights, innovative enhancements, and conversion to fuel,” *Heliyon*, vol. 10, no. 20, p. e39248, Oct. 2024, doi: 10.1016/j.heliyon.2024.e39248.

[64] B. K. Barnwal and M. P. Sharma, “Prospects of biodiesel production from vegetable oils in India,” *Renewable and Sustainable Energy Reviews*, vol. 9, no. 4, pp. 363–378, Aug. 2005, doi: 10.1016/j.rser.2004.05.007.

[65] P. Nakpong and S. Wootthikanokkhan, “High free fatty acid coconut oil as a potential feedstock for biodiesel production in Thailand,” *Renewable Energy*, vol. 35, no. 8, pp. 1682–1687, Aug. 2010, doi: 10.1016/j.renene.2009.12.004.

[66] A. Abollé, L. Kouakou, and H. Planche, “The viscosity of diesel oil and mixtures with straight vegetable oils: Palm, cabbage palm, cotton, groundnut, copra and sunflower,” *Biomass and Bioenergy*, vol. 33, no. 9, pp. 1116–1121, Sep. 2009, doi: 10.1016/j.biombioe.2008.01.012.

[67] M. Mofijur *et al.*, “Prospects of biodiesel from Jatropha in Malaysia,” *Renewable and Sustainable Energy Reviews*, vol. 16, no. 7, pp. 5007–5020, Sep. 2012, doi: 10.1016/j.rser.2012.05.010.

[68] X. Wu, X. Zhang, S. Yang, H. Chen, and D. Wang, “The study of epoxidized rapeseed oil used as a potential biodegradable lubricant,” *J Americ Oil Chem Soc*, vol. 77, no. 5, pp. 561–563, May 2000, doi: 10.1007/s11746-000-0089-2.

[69] V. Scholz and J. N. Da Silva, “Prospects and risks of the use of castor oil as a fuel,” *Biomass and Bioenergy*, vol. 32, no. 2, pp. 95–100, Feb. 2008, doi: 10.1016/j.biombioe.2007.08.004.

[70] L. A. Quinchia, M. A. Delgado, C. Valencia, J. M. Franco, and C. Gallegos, “Viscosity Modification of High-Oleic Sunflower Oil with Polymeric Additives for the Design of New Biolubricant Formulations,” *Environ. Sci. Technol.*, vol. 43, no. 6, pp. 2060–2065, Mar. 2009, doi: 10.1021/es803047m.

[71] D. Ogunniyi, “Castor oil: A vital industrial raw material,” *Bioresource Technology*, vol. 97, no. 9, pp. 1086–1091, Jun. 2006, doi: 10.1016/j.biortech.2005.03.028.

[72] M. Molefe, D. Nkazi, and H. E. Mukaya, “Method Selection for Biojet and Biogasoline Fuel Production from Castor Oil: A Review,” *Energy Fuels*, vol. 33, no. 7, pp. 5918–5932, Jul. 2019, doi: 10.1021/acs.energyfuels.9b00384.

[73] J. C. Juan, D. A. Kartika, T. Y. Wu, and T.-Y. Y. Hin, “Biodiesel production from jatropha oil by catalytic and non-catalytic approaches: An overview,” *Bioresource Technology*, vol. 102, no. 2, pp. 452–460, Jan. 2011, doi: 10.1016/j.biortech.2010.09.093.

[74] N. H. Jayadas, K. Prabhakaran Nair, and A. G, “Tribological evaluation of coconut oil as an environment-friendly lubricant,” *Tribology International*, vol. 40, no. 2, pp. 350–354, Feb. 2007, doi: 10.1016/j.triboint.2005.09.021.

[75] M. Li *et al.*, “Experimental evaluation of an eco-friendly grinding process combining minimum quantity lubrication and graphene-enhanced plant-oil-based cutting fluid,” *Journal of Cleaner Production*, vol. 244, p. 118747, Jan. 2020, doi: 10.1016/j.jclepro.2019.118747.

[76] N. Salih, J. Salimon, and E. Yousif, “The physicochemical and tribological properties of oleic acid based triester biolubricants,” *Industrial Crops and Products*, vol. 34, no. 1, pp. 1089–1096, Jul. 2011, doi: 10.1016/j.indcrop.2011.03.025.

[77] E. K. Heikal, M. S. Elmelawy, S. A. Khalil, and N. M. Elbasuny, “Manufacturing of environment friendly biolubricants from vegetable oils,” *Egyptian Journal of Petroleum*, vol. 26, no. 1, pp. 53–59, Mar. 2017, doi: 10.1016/j.ejpe.2016.03.003.

[78] J. C. De Haro, M. D. P. Garrido, Á. Pérez, M. Carmona, and J. F. Rodríguez, “Full conversion of oleic acid to estolides esters, biodiesel and choline carboxylates in three easy steps,” *Journal of Cleaner Production*, vol. 184, pp. 579–585, May 2018, doi: 10.1016/j.jclepro.2018.02.190.

[79] J. Greco-Duarte *et al.*, “Understanding the degree of estolide enzymatic polymerization and the effects on its lubricant properties,” *Fuel*, vol. 245, pp. 286–293, Jun. 2019, doi: 10.1016/j.fuel.2019.02.004.

[80] T. M. Panchal, A. Patel, D. D. Chauhan, M. Thomas, and J. V. Patel, “A methodological review on bio-lubricants from vegetable oil based resources,” *Renewable and Sustainable Energy Reviews*, vol. 70, pp. 65–70, Apr. 2017, doi: 10.1016/j.rser.2016.11.105.

[81] A. K. R. Somidi, U. Das, and A. K. Dalai, “One-pot synthesis of canola oil based biolubricants catalyzed by MoO 3 /Al 2 O 3 and process optimization study,” *Chemical Engineering Journal*, vol. 293, pp. 259–272, Jun. 2016, doi: 10.1016/j.cej.2016.02.076.

[82] R. Tesser, V. Russo, R. Turco, R. Vitiello, and M. Di Serio, “Bio-lubricants synthesis from the epoxidized oil promoted by clays: Kinetic modelling,” *Chemical Engineering Science*, vol. 214, p. 115445, Mar. 2020, doi: 10.1016/j.ces.2019.115445.

[83] F. M. Baena-Moreno, E. Le Saché, L. Pastor-Pérez, and T. R. Reina, “Membrane-based technologies for biogas upgrading: a review,” *Environ Chem Lett*, vol. 18, no. 5, pp. 1649–1658, Sep. 2020, doi: 10.1007/s10311-020-01036-3.

[84] C. S. Osorio-González, N. Gómez-Falcon, F. Sandoval-Salas, R. Saini, S. K. Brar, and A. A. Ramírez, “Production of Biodiesel from Castor Oil: A Review,” *Energies*, vol. 13, no. 10, p. 2467, May 2020, doi: 10.3390/en13102467.

[85] A. Chowdhury, D. Sarkar, and D. Mitra, “Esterification of Free Fatty Acids Derived from Waste Cooking Oil with Octanol: Process Optimization and Kinetic Modeling,” *Chem Eng & Technol*, vol. 39, no. 4, pp. 730–740, Apr. 2016, doi: 10.1002/ceat.201400745.

[86] M. Bahadi, M. F. Yusoff, J. Salimon, and D. Derawi, “Optimization of Response Surface Methodology by D-Optimal Design for Alkaline Hydrolysis of Crude Palm Kernel Oil,” *JSM*, vol. 49, no. 1, pp. 29–41, Jan. 2020, doi: 10.17576/jsm-2020-4901-04.

[87] N. Salih and J. Salimon, “A Review on New Trends, Challenges and Prospects of Ecofriendly Friendly Green Food-Grade Biolubricants,” *Biointerface Res Appl Chem*, vol. 12, no. 1, pp. 1185–1207, Apr. 2021, doi: 10.33263/BRIAC121.11851207.

[88] N. Mahmud, J. Islam, W. Oyom, K. Adrah, S. C. Adegoke, and R. Tahergorabi, “A review of different frying oils and oleogels as alternative frying media for fat-uptake reduction in deep-fat fried foods,” *Heliyon*, vol. 9, no. 11, p. e21500, Nov. 2023, doi: 10.1016/j.heliyon.2023.e21500.

[89] M. Plourde, K. Belkacemi, and J. Arul, “Hydrogenation of Sunflower Oil with Novel Pd Catalysts Supported on Structured Silica,” *Ind. Eng. Chem. Res.*, vol. 43, no. 10, pp. 2382–2390, May 2004, doi: 10.1021/ie030708x.

[90] C. K. Ho, K. B. McAuley, and B. A. Peppley, “Biolubricants through renewable hydrocarbons: A perspective for new opportunities,” *Renewable and Sustainable Energy Reviews*, vol. 113, p. 109261, Oct. 2019, doi: 10.1016/j.rser.2019.109261.

[91] P. Roy, T. Rahman, R. L. Jackson, H. Jahromi, and S. Adhikari, “Hydrocarbon biolubricants from hydrotreated renewable and waste derived liquid intermediates,” *Journal of Cleaner Production*, vol. 409, p. 137120, Jul. 2023, doi: 10.1016/j.jclepro.2023.137120.

[92] S. M. Santos, D. C. Nascimento, M. C. Costa, A. M. B. Neto, and L. V. Fregolente, “Flash point prediction: Reviewing empirical models for hydrocarbons, petroleum fraction, biodiesel, and blends,” *Fuel*, vol. 263, p. 116375, Mar. 2020, doi: 10.1016/j.fuel.2019.116375.

[93] H.-J. Lee, I.-H. Choi, S.-W. Kim, and K.-R. Hwang, “Selective Production of Bio-Based Linear Alpha-Olefin from Wasted Fatty Alcohol on Al2O3 for Bio-Based Chemicals,” *Polymers*, vol. 13, no. 17, p. 2850, Aug. 2021, doi: 10.3390/polym13172850.

[94] R. Narayana Sarma and R. Vinu, “Current Status and Future Prospects of Biolubricants: Properties and Applications,” *Lubricants*, vol. 10, no. 4, p. 70, Apr. 2022, doi: 10.3390/lubricants10040070.

[95] D. Klüh, W. Waldmüller, and M. Gaderer, “Kolbe Electrolysis for the Conversion of Carboxylic Acids to Valuable Products—A Process Design Study,” *Clean Technol.*, vol. 3, no. 1, pp. 1–18, Jan. 2021, doi: 10.3390/cleantechnol3010001.

[96] S. Liu, N. Govindarajan, H. Prats, and K. Chan, “Understanding the reaction mechanism of Kolbe electrolysis on Pt anodes,” *Chem Catalysis*, vol. 2, no. 5, pp. 1100–1113, May 2022, doi: 10.1016/j.checat.2022.02.014.

[97] T. Ashraf, A. P. Rodriguez, B. T. Mei, and G. Mul, “Electrochemical decarboxylation of acetic acid on boron-doped diamond and platinum-functionalised electrodes for pyrolysis-oil treatment,” *Faraday Discuss.*, vol. 247, pp. 252–267, 2023, doi: 10.1039/D3FD00066D.

[98] M. Olde Nordkamp *et al.*, “Investigating the platinum electrode surface during Kolbe electrolysis of acetic acid,” *Surfaces and Interfaces*, vol. 44, p. 103684, Jan. 2024, doi: 10.1016/j.surfin.2023.103684.

[99] J. Ying, Y. Yuan, and S. Xin, “The impact of different types of wastewaters on electrode passivation in electrical coagulation systems,” *ACE*, vol. 85, no. 1, pp. 212–218, Jul. 2024, doi: 10.54254/2755-2721/85/20240944.

[100] J. Zhang, X. Wen, W. Chen, L. Zhang, F. Mo, and S. Xu, “First-Principles Investigation of the Unique Role of Anode Surfaces in Organic Electrochemical Reactions,” *J. Phys. Chem. C*, vol. 127, no. 31, pp. 15215–15226, Aug. 2023, doi: 10.1021/acs.jpcc.3c03221.

[101] K. Neubert, M. Schmidt, and F. Harnisch, “Platinized Titanium as Alternative Cost-Effective Anode for Efficient Kolbe Electrolysis in Aqueous Electrolyte Solutions,” *ChemSusChem*, vol. 14, no. 15, pp. 3097–3109, 2021, doi: 10.1002/cssc.202100854.

[102] “Amorphous RuO2 Catalyst for Medium Size Carboxylic Acid to Alkane Dimer Selective Kolbe Electrolysis in an Aqueous Environment.,” *Chemsuschem*, pp. e202300222–e202300222, Jul. 2023, doi: 10.1002/cssc.202300222.

[103] G. Yuan *et al.*, “Kolbe Electrolysis of Biomass-Derived Fatty Acids Over Pt Nanocrystals in an Electrochemical Cell,” *ChemCatChem*, vol. 12, no. 2, pp. 642–648, Jan. 2020, doi: 10.1002/cctc.201901443.

[104] T. Ashraf, G. Mul, and B. Mei, “Investigating the Effect of Alkali Metal Cations on Kolbe Electrolysis,” *Meet. Abstr.*, vol. MA2023-02, no. 27, pp. 1429–1429, Dec. 2023, doi: 10.1149/MA2023-02271429mtgabs.

[105] Z. Sun, C. Liu, G. Lu, X. Song, and J. Yu, “Effects of operational and structural parameters on cell voltage of industrial magnesium electrolysis cells,” *Front. Chem. Sci. Eng.*, vol. 9, no. 4, pp. 522–531, Dec. 2015, doi: 10.1007/s11705-015-1539-x.

[106] Bethany Halford, “Switching up the Kolbe reaction,” *C&EN Global Enterp*, vol. 101, no. 12, pp. 5–5, Apr. 2023, doi: 10.1021/cen-10112-scicon2.

[107] Y. Hioki *et al.*, “Overcoming the limitations of Kolbe coupling with waveform-controlled electrosynthesis,” *Science*, vol. 380, no. 6640, pp. 81–87, Apr. 2023, doi: 10.1126/science.adf4762.

[108] L. Forschner, E. Artmann, T. Jacob, and A. K. Engstfeld, “Electric Potential Distribution Inside the Electrolyte during High Voltage Electrolysis,” *J. Phys. Chem. C*, vol. 127, no. 9, pp. 4387–4394, Mar. 2023, doi: 10.1021/acs.jpcc.2c07873.

[109] Z. Zhang *et al.*, “Electrolyte dependence for the electrochemical decarboxylation of medium-chain fatty acids (n-octanoic acid) into fuel on Pt electrode,” *Materials Reports: Energy*, vol. 4, no. 2, p. 100244, May 2024, doi: 10.1016/j.matre.2023.100244.

[110] V. Hessel, C. Hofmann, P. Löb, J. Löhndorf, H. Löwe, and A. Ziogas, “Aqueous Kolbe−Schmitt Synthesis Using Resorcinol in a Microreactor Laboratory Rig under High-p,T Conditions,” *Org. Process Res. Dev.*, vol. 9, no. 4, pp. 479–489, Jul. 2005, doi: 10.1021/op050045q.

[111] X. Li *et al.*, “Sustainable separation of petroleum hydrocarbons pollutant using hydrophobic deep eutectic solvents regulated by CO2,” *Journal of Environmental Chemical Engineering*, vol. 9, no. 5, p. 106280, Oct. 2021, doi: 10.1016/j.jece.2021.106280.

[112] L. Lang, Y. Li, J. C.-H. Lam, Y. Ding, X. Yin, and C. Wu, “Enhancing the selectivity of hydrocarbons during the Kolbe electrolysis of biomass-derived short-chain carboxylic acids by

anionic surfactants," *Sustainable Energy Fuels*, vol. 6, no. 11, pp. 2797–2804, 2022, doi: 10.1039/D1SE02067F.

[113] O. N. Chechina, A. P. Tomilov, and S. V. Sokolov, "A Voltammetric Study of the Kolbe Synthesis with Perfluorinated Oxa Acids: Influence of the Structure of the Fluorocarbon Residue," *Russ J Gen Chem*, vol. 75, no. 5, pp. 719–723, May 2005, doi: 10.1007/s11176-005-0306-y.

[114] I. Stanescu, R. R. Gupta, and L. E. K. Achenie, "An *in-silico* study of solvent effects on the Kolbe–Schmitt reaction using a DFT method," *Molecular Simulation*, vol. 32, no. 3–4, pp. 279–290, Mar. 2006, doi: 10.1080/08927020600615000.

[115] L. Schulz and S. Waldvogel, "Solvent Control in Electro-Organic Synthesis," *Synlett*, vol. 30, no. 03, pp. 275–286, Feb. 2019, doi: 10.1055/s-0037-1610303.

[116] Y. Luo *et al.*, "Investigating the effect of polarity reversal of the applied current on electrochemical degradation of per-and polyfluoroalkyl substances," *Journal of Cleaner Production*, vol. 433, p. 139691, Dec. 2023, doi: 10.1016/j.jclepro.2023.139691.

[117] M. O. Nordkamp, B. Mei, R. Venderbosch, and G. Mul, "Study on the Effect of Electrolyte pH during Kolbe Electrolysis of Acetic Acid on Pt Anodes," *ChemCatChem*, vol. 14, no. 16, p. e202200438, Aug. 2022, doi: 10.1002/cctc.202200438.

[118] S.-L. Lee *et al.*, "Enhanced electricity generation and degradation of the azo dye Reactive Green 19 in a photocatalytic fuel cell using ZnO/Zn as the photoanode," *Journal of Cleaner Production*, vol. 127, pp. 579–584, Jul. 2016, doi: 10.1016/j.jclepro.2016.03.169.

[119] S. Ahmadpour, J. Tashkhourian, and B. Hemmateenejad, "A chemometric investigation on the influence of the nature and concentration of supporting electrolyte on charging currents in electrochemistry," *Journal of Electroanalytical Chemistry*, vol. 871, p. 114296, Aug. 2020, doi: 10.1016/j.jelechem.2020.114296.

[120] T. Ashraf, B. T. Mei, and G. Mul, "The Influence of Alkali Cations on the Performance of Pt Electrodes in Kolbe Electrolysis of Acetic Acid," *ChemElectroChem*, vol. 11, no. 14, p. e202400274, Jul. 2024, doi: 10.1002/celc.202400274.

[121] H. Kolbe, "Umwandlung der Monocarbonsäuren in die zugehörenden kohlenstoffreicheren Dicarbonsäuren," *Justus Liebigs Annalen der Chemie*, vol. 131, no. 3, pp. 348–349, 1864.

[122] S. Wang *et al.*, "A review of anodic catalysts and their application in (non-) Kolbe electrocatalytic decarboxylation of carboxylic acids," *Carbon Resources Conversion*, vol. 6, no. 4, pp. 287–297, 2023.

[123] T. R. dos Santos, F. Harnisch, P. Nilges, and U. Schröder, "Electrochemistry for Biofuel Generation: Transformation of Fatty Acids and Triglycerides to Diesel-Like Olefin/Ether Mixtures and Olefins," *ChemSusChem*, vol. 8, no. 5, pp. 886–893, 2015, doi: 10.1002/cssc.201403249.

[124] J. Meyers *et al.*, “Electrochemical conversion of a bio-derivable hydroxy acid to a drop-in oxygenate diesel fuel,” *Energy & Environmental Science*, vol. 12, no. 8, pp. 2406–2411, 2019.

[125] F. J. Holzhäuser *et al.*, “Electrochemical cross-coupling of biogenic di-acids for sustainable fuel production,” *Green chemistry*, vol. 21, no. 9, pp. 2334–2344, 2019.

[126] P. Nilges, T. R. dos Santos, F. Harnisch, and U. Schröder, “Electrochemistry for biofuel generation: Electrochemical conversion of levulinic acid to octane,” *Energy & Environmental Science*, vol. 5, no. 1, pp. 5231–5235, 2012, doi: 10.1039/C1EE02685B.

[127] C. Urban *et al.*, “Production of drop-in fuels from biomass at high selectivity by combined microbial and electrochemical conversion,” *Energy Environ. Sci.*, vol. 10, no. 10, pp. 2231–2244, Oct. 2017, doi: 10.1039/C7EE01303E.

[128] K. Neubert, M. Hell, M. Chávez Morejón, and F. Harnisch, “Hetero-Coupling of Bio-Based Medium-Chain Carboxylic Acids by Kolbe Electrolysis Enables High Fuel Yield and Efficiency,” *ChemSusChem*, vol. 15, no. 21, p. e202201426, 2022, doi: 10.1002/cssc.202201426.

[129] A. H. Johnstone, “CRC Handbook of Chemistry and Physics—69th Edition Editor in Chief R. C. Weast, CRC Press Inc., Boca Raton, Florida, 1988, pp. 2400, price £57.50. ISBN 0–8493–0369–5,” *Journal of Chemical Technology & Biotechnology*, vol. 50, no. 2, pp. 294–295, 1991, doi: 10.1002/jctb.280500215.

[130] J. Ranninger, P. Nikolaienko, K. J. Mayrhofer, and B. B. Berkes, “On-line Electrode Dissolution Monitoring during Organic Electrosynthesis: Direct Evidence of Electrode Dissolution during Kolbe Electrolysis,” *ChemSusChem*, vol. 15, no. 5, p. e202102228, 2022.

[131] H. Ding and M. Orazov, “Anodically-Generated Alkyl Radicals Derived from Carboxylic Acids as Reactive Intermediates for Addition to Alkenes,” *ChemElectroChem*, vol. 10, no. 10, p. e202201099, 2023.

[132] Y. Zhang, G. Liu, and J. Wu, “Electrochemical conversion of palmitic acid via Kolbe electrolysis for synthesis of n-triacontane,” *Journal of Electroanalytical Chemistry*, vol. 822, pp. 73–80, 2018.

[133] K. Neubert, M. Hell, M. Chávez Morejón, and F. Harnisch, “Hetero-Coupling of Bio-Based Medium-Chain Carboxylic Acids by Kolbe Electrolysis Enables High Fuel Yield and Efficiency,” *ChemSusChem*, vol. 15, no. 21, p. e202201426, 2022.

[134] D. Yue, F. You, and S. W. Snyder, “Biomass-to-bioenergy and biofuel supply chain optimization: Overview, key issues and challenges,” *Computers & Chemical Engineering*, vol. 66, pp. 36–56, 2014.

[135] R. Singh, A. Shukla, S. Tiwari, and M. Srivastava, “A review on delignification of lignocellulosic biomass for enhancement of ethanol production potential,” *Renewable and Sustainable Energy Reviews*, vol. 32, pp. 713–728, 2014.

[136] J. M. Perez, H. Richter, S. E. Loftus, and L. T. Angenent, “Biocatalytic reduction of short-chain carboxylic acids into their corresponding alcohols with syngas fermentation,” *Biotechnology and bioengineering*, vol. 110, no. 4, pp. 1066–1077, 2013.

[137] K. Kuruti *et al.*, “Generation of bioethanol and VFA through anaerobic acidogenic fermentation route with press mud obtained from sugar mill as a feedstock,” *Bioresource technology*, vol. 192, pp. 646–653, 2015.

[138] C. Stang and F. Harnisch, “The dilemma of supporting electrolytes for electroorganic synthesis: a case study on Kolbe electrolysis,” *ChemSusChem*, vol. 9, no. 1, pp. 50–60, 2016.

[139] J. Mikulec, J. Cvengroš, Ľ. Joríková, M. Banič, and A. Kleinová, “Second generation diesel fuel from renewable sources,” *Journal of Cleaner Production*, vol. 18, no. 9, pp. 917–926, 2010.

[140] F. A. Twaiq, N. A. Zabidi, and S. Bhatia, “Catalytic conversion of palm oil to hydrocarbons: performance of various zeolite catalysts,” *Industrial & Engineering Chemistry Research*, vol. 38, no. 9, pp. 3230–3237, 1999.

[141] H. Tani, M. Shimouchi, H. Haga, and K. Fujimoto, “Development of direct production process of diesel fuel from vegetable oils,” *Journal of the Japan Institute of Energy*, vol. 90, no. 5, pp. 466–470, 2011.

[142] S. P. Katikaneni, J. D. Adjaye, and N. N. Bakhshi, “Catalytic conversion of canola oil to fuels and chemicals over various cracking catalysts,” *The Canadian Journal of Chemical Engineering*, vol. 73, no. 4, pp. 484–497, 1995.

[143] E. Santillan-Jimenez, T. Morgan, J. Lacny, S. Mohapatra, and M. Crocker, “Catalytic deoxygenation of triglycerides and fatty acids to hydrocarbons over carbon-supported nickel,” *Fuel*, vol. 103, pp. 1010–1017, 2013.

[144] J. Satyarthi, D. Srinivas, and P. Ratnasamy, “Hydrolysis of vegetable oils and fats to fatty acids over solid acid catalysts,” *Applied Catalysis A: General*, vol. 391, no. 1–2, pp. 427–435, 2011.

[145] A. Kubátová *et al.*, “New path in the thermal cracking of triacylglycerols (canola and soybean oil),” *Fuel*, vol. 90, no. 8, pp. 2598–2608, 2011.

[146] C. Ratledge and C. Lippmeier, “Microbial production of fatty acids,” in *Fatty Acids*, Elsevier, 2017, pp. 237–278.

[147] M. Zan, X. Wang, A. Amuti, Z. Wang, and L. Dang, “Saponification of peony seed oil using response surface methodology,” *Industrial Crops and Products*, vol. 173, p. 114134, 2021.

[148] B. N. Alum, “Saponification Process and Soap Chemistry,” *INOSR Appl Sci*, vol. 12, no. 2, pp. 51–56, 2024.

[149] J. Jumina, W. Lavendi, T. Singgih, S. Triono, Y. Steven Kurniawan, and M. Koketsu, “Preparation of monoacylglycerol derivatives from Indonesian edible oil and their antimicrobial assay against Staphylococcus aureus and Escherichia coli,” *Scientific reports*, vol. 9, no. 1, p. 10941, 2019.

[150] G. C. Gervajio, “Fatty acids and derivatives from coconut oil,” *Kirk-Othmer Chemical Technology of Cosmetics*, pp. 445–482, 2013.

[151] S. Rachman, L. Komariah, A. Andwikaputra, and N. Umbara, “High conversion and yield of biodiesel using electrolysis method,” presented at the Journal of Physics: Conference Series, IOP Publishing, 2018, p. 012040.

[152] L. Schulz and S. R. Waldvogel, “Solvent control in electro-organic synthesis,” *Synlett*, vol. 30, no. 03, pp. 275–286, 2019.

[153] H. Ahmad, B. Bertolotti, and I. N. Sora, “Innovative Application of Kolbe Reaction on Constituents of Plant Oils,” *Chemical Engineering Transactions*, vol. 109, pp. 661–666, 2024.

[154] C. Taube, A. Fischer, and M. Beyer, “Kolbe Electrolysis of Long-Chain Fatty Acids for Efficient Production of Bio-Based Hydrophobic Paraffin Waxes,” *ChemCatChem*, vol. 16, no. 18, p. e202400628, 2024.

[155] K. Hiromori, Y. Konno, K. Katagami, A. Takahashi, and N. Shibasaki-Kitakawa, “Kolbe Electrolysis for Recycling Non-Aqueous Fatty Acid Salts,” *Journal of Chemical Engineering of Japan*, vol. 57, no. 1, p. 2332621, 2024.

[156] S. Shaldar, D. Athith, and H. Abhishek, “Biodiesel production, optimization and fuel properties characterization of waste fish oil,” *Int Res J Eng Technol*, vol. 6, no. 7, pp. 947–952, 2019.

[157] R. Z. Hussein, N. K. Attia, M. K. Fouad, and S. T. ElSheltawy, “Experimental investigation and process simulation of biolubricant production from waste cooking oil,” *Biomass and Bioenergy*, vol. 144, p. 105850, 2021.

[158] S. Sukirno, A. S. Triana, and M. Rifqi, “Biolubricant from spent bleaching earth oil through propylene glycol ester synthesis,” presented at the AIP Conference Proceedings, AIP Publishing, 2020.

[159] R. Garcés, E. Martínez-Force, and J. J. Salas, “Vegetable oil basestocks for lubricants,” *Grasas y aceites*, vol. 62, no. 1, pp. 21–28, 2011.

[160] J. McNutt, “Development of biolubricants from vegetable oils via chemical modification,” *Journal of industrial and Engineering Chemistry*, vol. 36, pp. 1–12, 2016.

[161] J. H. Urbanus, R. C. Lobo, and A. J. Riley, “European Hazard classification advice for crude oil–derived lubricant base oils compared with the proposed mineral oil mist TLV®,” *Applied occupational and environmental hygiene*, vol. 18, no. 11, pp. 815–817, 2003.

[162] K. Wickramasinghe, H. Sasahara, E. Abd Rahim, and G. Perera, “Green Metalworking Fluids for sustainable machining applications: A review,” *Journal of Cleaner Production*, vol. 257, p. 120552, 2020.

[163] J. A. Cecilia, D. Ballesteros Plata, R. M. Alves Saboya, F. M. Tavares de Luna, C. L. Cavalcante Jr, and E. Rodríguez-Castellón, “An overview of the biolubricant production process: Challenges and future perspectives,” *Processes*, vol. 8, no. 3, p. 257, 2020.

[164] F. Ma and M. A. Hanna, “Biodiesel production: a review,” *Bioresource technology*, vol. 70, no. 1, pp. 1–15, 1999.

[165] M. Page Bailey, “Defining Sustainability in the Chemical Process Industries.,” *Chemical Engineering*, vol. 123, no. 7, 2016.

[166] E. Oleochemicals, “Bio-Lubricants Product Brochure,” 2013.

[167] S. Rakesh, J. Tharunkumar, B. Sri, K. Jothibasu, and S. Karthikeyan, “Sustainable cost-effective microalgae harvesting strategies for the production of biofuel and oleochemicals,” *Highlights in bioscience*, vol. 3, no. July, pp. 1–8, 2020.

[168] E. Suyenty, H. Sentosa, M. Agustine, S. Anwar, A. Lie, and E. Sutanto, “Catalyst in basic oleochemicals,” *Bulletin of Chemical Reaction Engineering and Catalysis*, vol. 2, no. 2–3, pp. 22–31, 2007.

[169] J. F. Sierra-Cantor and C. A. Guerrero-Fajardo, “Methods for improving the cold flow properties of biodiesel with high saturated fatty acids content: A review,” *Renewable and Sustainable Energy Reviews*, vol. 72, pp. 774–790, 2017.

[170] F. Ma and M. A. Hanna, “Biodiesel production: a review,” *Bioresource technology*, vol. 70, no. 1, pp. 1–15, 1999.

[171] J.-S. Lee and S. Saka, “Biodiesel production by heterogeneous catalysts and supercritical technologies,” *Bioresource technology*, vol. 101, no. 19, pp. 7191–7200, 2010.

[172] X. Miao and Q. Wu, “Biodiesel production from heterotrophic microalgal oil,” *Bioresource technology*, vol. 97, no. 6, pp. 841–846, 2006.

[173] P. D. Patil and S. Deng, “Optimization of biodiesel production from edible and non-edible vegetable oils,” *Fuel*, vol. 88, no. 7, pp. 1302–1306, 2009.

[174] E. Abbah, G. Nwandikom, C. Egwuonwu, and N. Nwakuba, “Effect of reaction temperature on the yield of biodiesel from neem seed oil,” *American Journal of Energy Science*, vol. 3, no. 3, pp. 16–20, 2016.

[175] R. B. Istiningrum, T. Aprianto, and F. L. U. Pamungkas, “Effect of reaction temperature on biodiesel production from waste cooking oil using lipase as biocatalyst,” presented at the AIP Conference Proceedings, AIP Publishing, 2017.

[176] R. Z. Hussein, N. K. Attia, M. K. Fouad, and S. T. ElSheltawy, “Experimental investigation and process simulation of biolubricant production from waste cooking oil,” *Biomass and Bioenergy*, vol. 144, p. 105850, 2021.

[177] J. Padgurskas *et al.*, “Tribological study of beeswax-thickened biogrease and its modification with carbon nanoparticles,” *Tribology International*, vol. 184, p. 108465, 2023.

[178] L. J. Lee JinSuk and S. Saka, “Biodiesel production by heterogeneous catalysts and supercritical technologies.,” 2010.

[179] O. Alamu, M. Waheed, and S. Jekayinfa, “Biodiesel production from Nigerian palm kernel oil: effect of KOH concentration on yield,” *Energy for Sustainable Development*, vol. 11, no. 3, pp. 77–82, 2007.

[180] L. de Castro Barboza, V. S. Oliveira, J. de O. N. Ribeiro, and C. E. C. Alvarez, “Influence of temperature in the transesterification process for biodiesel production from residual cooking oil,” SAE Technical Paper, 0148–7191, 2021.

[181] E. Abbah, G. Nwandikom, C. Egwuonwu, and N. Nwakuba, “Effect of reaction temperature on the yield of biodiesel from neem seed oil,” *American Journal of Energy Science*, vol. 3, no. 3, pp. 16–20, 2016.

[182] M. A. Asl, K. Tahvildari, and T. Bigdeli, “Eco-friendly synthesis of biodiesel from WCO by using electrolysis technique with graphite electrodes,” *Fuel*, vol. 270, p. 117582, 2020.

[183] L. Fereidooni, K. Tahvildari, and M. Mehrpooya, “Trans-esterification of waste cooking oil with methanol by electrolysis process using KOH,” *Renewable Energy*, vol. 116, pp. 183–193, 2018.